General Strategies for Visible-Light Decaging Based on Quinone Photochemistry

Thesis by

David P. Walton

In Partial Fulfillment of the Requirements for

the degree of

Doctor of Philosophy

CALIFORNIA INSTITUTE OF TECHNOLOGY

Pasadena, California

2019

(Defended 30 January 2019)

David P. Walton
ORCID: 0000-0002-9557-6461

For Ellen and Dennis,

Edward Rajaseelan,

The San Gabriel Mountains,

and my favorite sister

Acknowledgements

I would like to first thank my adviser, Prof. Dennis Dougherty who has been an inspiration and role model. I would also like to thank Ellen Dougherty, a fellow Millersville alum. It is clear that the Doughertys genuinely care about members of the lab, and I am grateful for both of their support.

I thank my thesis committee, Prof. Brian Stoltz, Prof. Sarah Reisman, and Prof. Robert Grubbs for their patience and valuable advice. Thank you all for your time, I have learned a lot from our meetings. I would also like to thank Bob for getting me hooked on hiking in the San Gabriels when I first came to Caltech.

I thank my undergraduate adviser, Prof. Edward Rajaseelan, for inspiring me to love chemistry and research. I thank my mom, dad, and three sisters for their support.

I worked closely with Clint Regan, who I am indebted to for insightful chemistry discussions and tireless efforts on the mechanistic studies. Clint was a constant source of good ideas and a master of chromatography. Oliver taught me everything I know about lasers and has a gift for instruments. Chris Marotta taught me how to use the Opus and helped with $GABA_A$ experiments for which I am very grateful. I have gone on many hiking adventures with Noah Duffy, Mathew Rienzo and Tim Miles - and hope to continue to do so. I have been roommates with Noah Duffy for the past year, and he has endured that well. I thank him for his support and for not talking me out of buying the Miata.

Kayla Busy is awesome and her husband Shannon is really good at basketball - together they are unstoppable. *Xenopus Daevis* is an accomplished Jazz musician. Catriona Blunt is an excellent skier. Stephen Grant is a faster rower than Brandon. Annett Holland is an international dancing star. Richard is a righteous dude. I have collaborated with Bryce Jarman on several chemical biology projects and thank him for the time and effort. As we have shared a bay for the last few years, I have enjoyed our talks on chemistry and the science of beverages. The Grubbs group down the hallway have been good friends. Nicholas Swisher in particular is a karaoke master. William Wolf shreds a mean guitar. Ben Matson*, Trevor Del Castillo*, Mark Nesbit*, Josh Buss, Taryn Campbell, Tanvi Ratani, Liz O'Brien, Kareem Hannoun, Adam Boyton, Matt Chalkley. *Lake House members; can't say enough good things about these guys. Lastly, I thank Jenna Bush for her friendship and support over the past 11 years.

Abstract.

The design, synthesis, and photochemistry of several quinone based photoremovable protecting groups is reported. A visible light (400-600 nm) intramolecular photoreduction of 1,4-benzoquinones and 1,4-naphthoquinones mediated by amine and sulfide substituents was employed to launch a fast thermal lactonization step. Both the trimethyl lock and *o*-coumarinic acid lactonizations were incorporated into these designs. Quantum yields in air equilibrated solvents are moderate (Φ = 0.01-0.10), and chemical yields are generally quantitative. Detailed mechanistic studies reveal a mechanism distinct from typical n,π^* quinone photochemistry. Biological applications and longer wavelength derivatives were further explored.

PUBLISHED CONTENT AND CONTRIBUTIONS

- Walton, D. P.; Dougherty, D. A. "A General Strategy for Visible-Light Decaging Based on the Quinone Trimethyl Lock." *J. Am. Chem. Soc.* **2017**, *139* (13), 4655–4658. https://doi.org/10.1021/jacs.7b01548.

  D.P.W. participated in the conception of the project, synthesized and characterized compounds and their photolysis products, and participated in manuscript writing.

- Regan, C. J.; Walton, D. P.; Shafaat, O. S.; Dougherty, D. "A. Mechanistic Studies of the Photoinduced Quinone Trimethyl Lock Decaging Process." *J. Am. Chem. Soc.* **2017**, *139* (13), 4729–4736. https://doi.org/10.1021/jacs.6b12007.

  D.P.W. participated in the conception of the project, synthesized and characterized compounds and their photolysis products, and participated in manuscript writing. (C.J.R. prepared several key compounds and conducted mechanistic studies including quantum yields, sensitization, and quenching experiments required to determine the mechanism. O.S.S. obtained laser flash photolysis data. Both C.J.R. and O.S.S. participated in manuscript preparation).

Table of Contents

Chapter 1. Introduction

1.1 Motivation

The ability to non-invasively influence a system with high spatiotemporal control has applications in chemistry and chemical biology.[1] That UV light is absorbed and causes damage to skin, for example, is common knowledge.[2] A lesser appreciated fact is that 810 nm light penetrates a human skull.[3] The development of molecules that are activated by inert and deeper tissue penetrating visible to near-infra red light is necessary to exploit this observation for applications in biology and medicine.[4,5] The window of relative tissue transparency between 600 and 810 nm, as depicted in **Figure 1.1** for rat skin,[6] is promisingly close to known visible light photochemistry. There is an intense interest in designing new photoremovable protecting groups, or photocages, that are activated by visible to near-infrared light for this purpose.[1] Coumarins[7–11], BODIPY[5,12–15], and cyanine[16–19] dyes have shown promise in this regard, but there are still relatively few photocages that are activated at longer wavelengths than 450 nm.[1,5] The challenge in designing such compounds is exemplified by considering a hypothetical photocage operating by 810 nm light. The photocage must first absorb 850 nm light, which is non-trivial for most organic molecules, and then a reaction must occur with the available 35 kcal/mol excitation energy. While this is a tall order, it is an interesting challenge that if solved would benefit many areas of science and medicine.

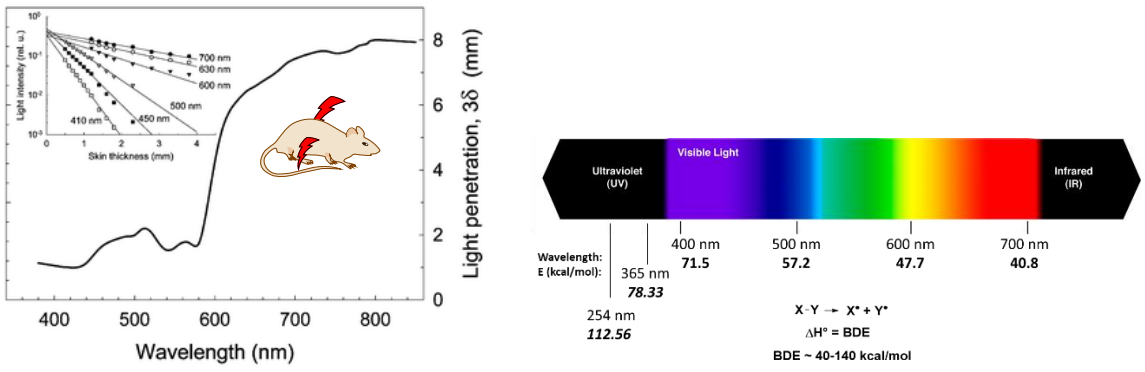

Figure 1.1 Wavelength of light vs. penetration depth for rat skin, adapted from reference,[6] and E (kcal/mol) vs λ (nm) in the context of common bond strengths.

1.2 Visible Light Quinone Photochemistry

We identified the visible light photochemistry of quinones as a relatively underutilized area for the development of visible light protecting groups (**Scheme 1.1**). We were particularly interested in the photochemistry of amine substituted quinones, as these display both the longest red-shifted absorbances and efficient photoreactivity in many cases even at 540-600 nm. The effects of substitution on absorbance[20–24] and photochemistry[25–31] have been thoroughly studied for 2-amino-1,4-napthoquinone and 2,5-diamino-1,4-benzoquinones. On exposure to visible light, a formal hydrogen shift from the amine substituent to the quinone core occurs, oxidizing the amine substituent and reducing the quinone. [31–34] The cyclized benzoxazoline product (**2a** and **4a**) is formed[31,33] with few exceptions[35,36] (such as **2b**, and **4b**). The reaction has been found to also occur by thermolysis.[37]

The primary photochemical reaction in either case is an isomerization in which the amine substituent is oxidized and the quinone core is reduced. Interestingly, **1** is stable to photolysis in the case of aziridino or azetidino, or primary amine substituents.[33] For the small rings, unfavorable O---H distances may account for the lack of reactivity. The hydrogen bonding of primary amines orients the alkyl substituent away from the quinone carbonyl, prohibiting the photoreaction, but reactivity is regained by introduction of an intramolecular hydrogen bond to an adjacent acetyl group (**1d)**.[38] This could also be a pK_a effect, as N-H deprotonation is faster than C-H deprotonation.

The addition of electron donors to the quinone core results in broad charge-transfer type bands in the visible spectrum.[23] Although 2-amino-1,4-naphthoquinones (and 2-amino-1,4-anthraquinones) appear to have a larger extended π system than comparable 1,4-benzoquinones, a blue-shifted absorbance of approximately 50 nm is instead observed for each fused ring.[25] In this way, simple naphthoquinone and anthraquinone derivatives appear to behave more as benzoquinones with aryl substituents. Incorporation of electron donors and acceptors into the distal ring, however, produces substantial shifts in absorbance out to the near-infrared (**Scheme 1c**).[39]

Detailed mechanistic work has been carried out for dialkylamino-1,4-naphthoquinones.[29,30] The efficiency of visible light photolysis was found to be highly influenced

by both substituent and solvent effects (**Table 1**).[25,27,28,30] In particular, the amine and *ortho*-substituent should be considered as a pair, because quantum yields vary with both. The solvent effect is pronounced for both benzoquinones and naphthoquinones, with quantum yields decreasing with solvent polarity (**Table 1**).[25,30,40] The solvent effect on quantum yield is attributed to changes in dielectric constant and hydrogen bonding, as a consequence of a charge transfer excited state.[30]

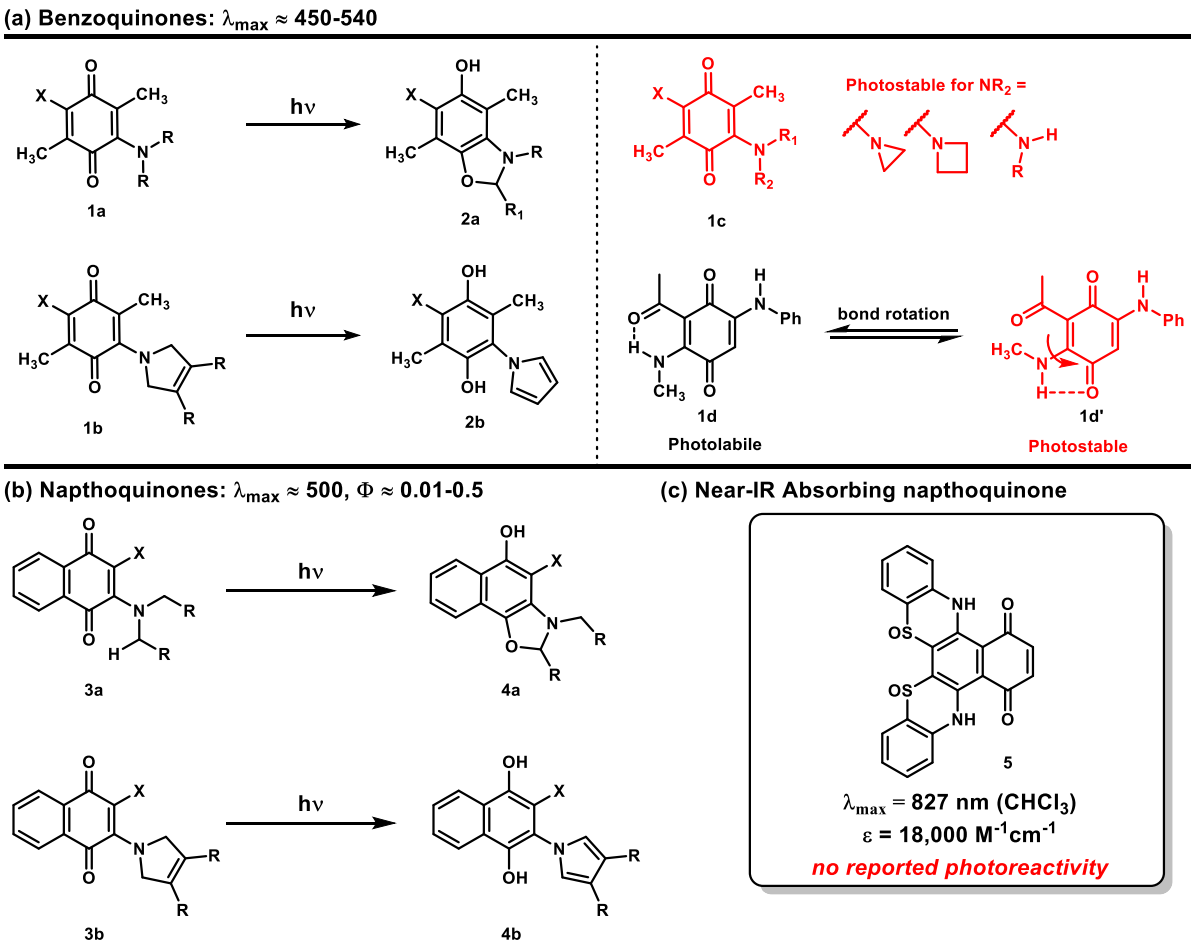

Scheme 1.1 2-Aminoquinone photochemistry and an inspiring near-IR absorbing quinone dye

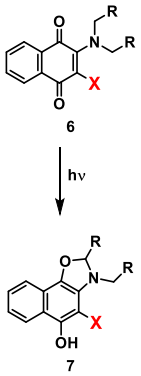

	Φ (PhMe) vs. Substituent (X)			
R	**X = H**	**OMe**	**Cl**	**CH_3**
H	0.092	0.145	0.11	0.46
CH_3	0.24	---	0.092	0.48
$-CH_2-CH_2-$	0.054	---	0.19	0.35
$-(CH_2)_3-$	0.073	0.056	0.081	0.21
$-CH_2-O-CH_2-$	0.065	0.061	0.092	0.19
Φ vs. Solvent (X = H)				
R	**PhMe**	**iPrOH**	**EtOH**	
CH_2-O-CH_2-	0.076	0.023	0.007	
E_a (kcal/mol)	2.8	1.9	1.9	

Table 1. Substituent and solvent effects on quantum yields for 2-amino-1,4-naphthoquinones[28,30,41]

Gritsan and Bazhin assigned the UV-visible bands and investigated the photolysis in different solvents and temperatures to propose the mechanism outlined in **Scheme 2a** for 2-amino-1,4-naphthoquinones.[29,30] The long-wavelength band was assigned as a charge transfer state, with energy levels ordered as S_0, T_{CT}, S_{CT}, T_{n,π^*}, S_{n,π^*} with a singlet-triplet CT splitting between 5,600-7,500 cm^{-1} depending on the amine.[29] On excitation, considerable charge transfer from the amine to carbonyl oxygen occurs, and it is this polar state that undergoes a proton transfer as the primary photochemical step.[30]

Photolysis (λ > 400 nm) at 77 K generates no radical products but at least two intermediates that produce the photolysis product when warmed.[30] Oxygen has little to no effect on the quantum yield and fluorescence is not observed, indicating rapid deactivation from the excited triplet and singlet states.[29] An energy of activation for 2-morpholino-1,4-naphthoquinone of 1.9-2.8 kcal/mol was measured in toluene and alcohols (**Table 1**.).[30] It reasonable to assume that the findings are applicable to 2-amino-1,4-benzoquinones as well.

The superficially similar α-dimethylaminoacetophenone photoelimination reaction has been studied in detail[43] where the excited n,π^* singlet ketone is quenched by extraordinarily fast charge transfer from the amine followed by proton transfer (**scheme 2b**).

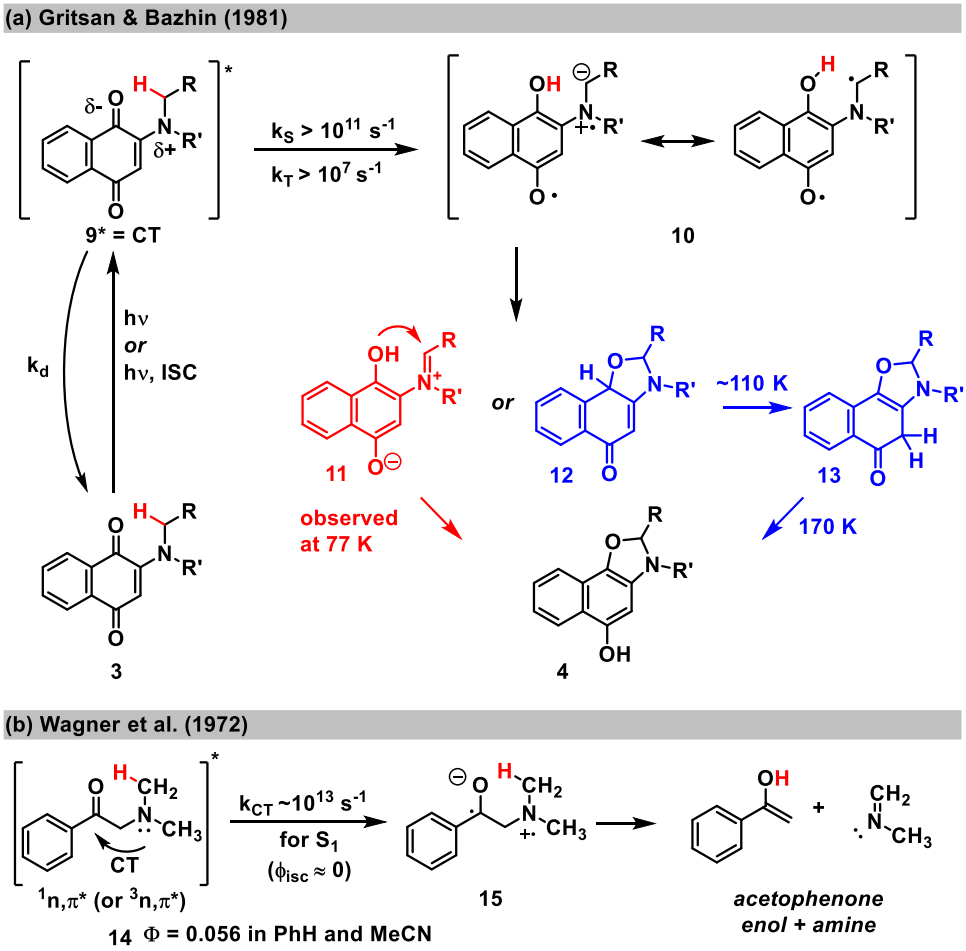

Scheme 1.2 Mechanism of α-dimethylaminoacetophenone[43] aminoquinone photoisomerization[29,30] Photochemistry of alkyl-amine substituted quinones

Given the caveat that direct conjugation allows *excitation and electron transfer to be the same step*, this mechanism of hydrogen atom transfer (HAT) to an excited n,π* carbonyl is plausible for amino quinones and should be considered. However, α-dimethylaminoacetophenone displays the opposite solvent effect on quantum yield (**scheme 2b**).[43] The quantum yield for the singlet is nearly constant ($\Phi_S \sim 0.06$) for benzene, acetonitrile, and methanol, but the triplet is only active in methanol which results in an increase of total quantum yield equal to that of the triplet ($\Phi_T = 0.027$).[43] Because there is only total quantum yield data available for 2-aminoquinones, it is possible that the observed solvent effects arise only from the triplet

reactivity. This would resolve the discrepancy, but due to the large difference in excitation energies, it seems likely that the reactions are fundamentally different.

We were encouraged by these results as electron transfer followed by proton transfer is energetically favorable at long wavelengths compared to HAT based on bond energies. We envisioned a system where photochemical reduction of a quinone core via an electron transfer / proton transfer mechanism, launched an energetically decoupled fast thermal reaction. Because the reduction of a quinone core reveals reactive phenols that can be used as nucleophiles in subsequent thermal decaging processes, we turned to fast lactonization reactions already in use via chemical reduction of quinones. Namely, the trimethyl lock and *o*-coumarate esters were investigated (**Scheme 1.3**). We were aware of these two reactions from previous studies in our lab on photoacids, which is another low-energy process suitable for long wavelength decaging investigated in this work.

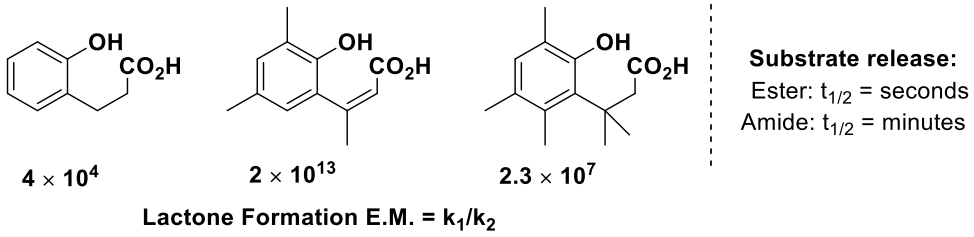

Scheme 1.3 Fast thermal reactions utilizing a phenol nucleophile.

1.3 Summary of the Dissertation

Synthetic challenges initially encountered with amine derivatives of the trimethyl lock inadvertently directed our efforts to sulfide substituted quinones. This was a fortuitous direction of study as little was previously known about the intramolecular photoreduction of sulfide appended quinones. The first generation of quinone based photocages were these sulfide derivatives, which are activated above 450 nm. Subsequent designs circumvented the initial synthetic challenges associated with amines, and which achieved photolysis above 600 nm. Although derivatives with visible bands tailing out to 800 nm were prepared, they proved photostable. The synthesis and applications of these quinone cages is described in **Chapter 2**. Detailed mechanistic studies are described in **Chapter 3**. The development of quinone

photocages incorporating an alternative thermal reaction is detailed in **Chapter 4**. Finally, **Chapter 5** describes some of our earlier work with photoacids.

1.4 References

1. Klán, P.; Šolomek, T.; Bochet, C. G.; Blanc, A.; Givens, R.; Rubina, M.; Popik, V.; Kostikov, A.; Wirz, J. Photoremovable Protecting Groups in Chemistry and Biology: Reaction Mechanisms and Efficacy. *Chem. Rev.* **2013**, *113* (1), 119–191. https://doi.org/10.1021/cr300177k.
2. Sambandan, D. R.; Ratner, D. Sunscreens: An Overview and Update. *Journal of the American Academy of Dermatology* **2011**, *64* (4), 748–758. https://doi.org/10.1016/j.jaad.2010.01.005.
3. Henderson, T. Multi-Watt near-Infrared Light Therapy as a Neuroregenerative Treatment for Traumatic Brain Injury. *Neural Regeneration Research* **2016**, *11* (4), 563. https://doi.org/10.4103/1673-5374.180737.
4. König, K. Multiphoton Microscopy in Life Sciences. *Journal of Microscopy* **2000**, *200* (2), 83–104. https://doi.org/10.1046/j.1365-2818.2000.00738.x.
5. Slanina, T.; Shrestha, P.; Palao, E.; Kand, D.; Peterson, J. A.; Dutton, A. S.; Rubinstein, N.; Weinstain, R.; Winter, A. H.; Klán, P. In Search of the Perfect Photocage: Structure–Reactivity Relationships in Meso-Methyl BODIPY Photoremovable Protecting Groups. *J. Am. Chem. Soc.* **2017**, *139* (42), 15168–15175. https://doi.org/10.1021/jacs.7b08532.
6. Juzenas, P.; Juzeniene, A.; Kaalhus, O.; Iani, V.; Moan, J. Noninvasive Fluorescence Excitation Spectroscopy during Application of 5-Aminolevulinic Acid in Vivo. *Photochem. Photobiol. Sci.* **2002**, *1* (10), 745–748. https://doi.org/10.1039/B203459J.
7. Fournier, L.; Gauron, C.; Xu, L.; Aujard, I.; Le Saux, T.; Gagey-Eilstein, N.; Maurin, S.; Dubruille, S.; Baudin, J.-B.; Bensimon, D.; et al. A Blue-Absorbing Photolabile Protecting Group for in Vivo Chromatically Orthogonal Photoactivation. *ACS Chem. Biol.* **2013**, *8* (7), 1528–1536. https://doi.org/10.1021/cb400178m.
8. Fournier, L.; Aujard, I.; Le Saux, T.; Maurin, S.; Beaupierre, S.; Baudin, J.-B.; Jullien, L. Coumarinylmethyl Caging Groups with Redshifted Absorption. *Chem. Eur. J.* **2013**, *19* (51), 17494–17507. https://doi.org/10.1002/chem.201302630.
9. Amatrudo, J. M.; Olson, J. P.; Lur, G.; Chiu, C. Q.; Higley, M. J.; Ellis-Davies, G. C. R. Wavelength-Selective One- and Two-Photon Uncaging of GABA. *ACS Chem. Neurosci.* **2014**, *5* (1), 64–70. https://doi.org/10.1021/cn400185r.
10. Hansen, M. J.; Velema, W. A.; Lerch, M. M.; Szymanski, W.; Feringa, B. L. Wavelength-Selective Cleavage of Photoprotecting Groups: Strategies and

Applications in Dynamic Systems. *Chem. Soc. Rev.* **2015**, *44* (11), 3358–3377. https://doi.org/10.1039/C5CS00118H.

11. Lin, Q.; Yang, L.; Wang, Z.; Hua, Y.; Zhang, D.; Bao, B.; Bao, C.; Gong, X.; Zhu, L. Coumarin Photocaging Groups Modified with an Electron-Rich Styryl Moiety at the 3-Position: Long-Wavelength Excitation, Rapid Photolysis, and Photobleaching. *Angewandte Chemie International Edition* **2018**, *57* (14), 3722–3726. https://doi.org/10.1002/anie.201800713.
12. Goswami, P. P.; Syed, A.; Beck, C. L.; Albright, T. R.; Mahoney, K. M.; Unash, R.; Smith, E. A.; Winter, A. H. BODIPY-Derived Photoremovable Protecting Groups Unmasked with Green Light. *J. Am. Chem. Soc.* **2015**, *137* (11), 3783–3786. https://doi.org/10.1021/jacs.5b01297.
13. Palao, E.; Slanina, T.; Muchová, L.; Šolomek, T.; Vítek, L.; Klán, P. Transition-Metal-Free CO-Releasing BODIPY Derivatives Activatable by Visible to NIR Light as Promising Bioactive Molecules. *J. Am. Chem. Soc.* **2016**, *138* (1), 126–133. https://doi.org/10.1021/jacs.5b10800.
14. Štacko, P.; Muchová, L.; Vítek, L.; Klán, P. Visible to NIR Light Photoactivation of Hydrogen Sulfide for Biological Targeting. *Org. Lett.* **2018**, *20* (16), 4907–4911. https://doi.org/10.1021/acs.orglett.8b02043.
15. Peterson, J. A.; Wijesooriya, C.; Gehrmann, E. J.; Mahoney, K. M.; Goswami, P. P.; Albright, T. R.; Syed, A.; Dutton, A. S.; Smith, E. A.; Winter, A. H. Family of BODIPY Photocages Cleaved by Single Photons of Visible/Near-Infrared Light. *J. Am. Chem. Soc.* **2018**, *140* (23), 7343–7346. https://doi.org/10.1021/jacs.8b04040.
16. Gorka, A. P.; Nani, R. R.; Zhu, J.; Mackem, S.; Schnermann, M. J. A Near-IR Uncaging Strategy Based on Cyanine Photochemistry. *J. Am. Chem. Soc.* **2014**. https://doi.org/10.1021/ja5065203.
17. Nani, R. R.; Gorka, A. P.; Nagaya, T.; Kobayashi, H.; Schnermann, M. J. Near-IR Light-Mediated Cleavage of Antibody–Drug Conjugates Using Cyanine Photocages. *Angewandte Chemie International Edition* **2015**, *54* (46), 13635–13638. https://doi.org/10.1002/anie.201507391.
18. Nani, R. R.; Gorka, A. P.; Nagaya, T.; Yamamoto, T.; Ivanic, J.; Kobayashi, H.; Schnermann, M. J. In Vivo Activation of Duocarmycin–Antibody Conjugates by Near-Infrared Light. *ACS Cent. Sci.* **2017**. https://doi.org/10.1021/acscentsci.7b00026.
19. Gorka, A. P.; Nani, R. R.; Schnermann, M. J. Harnessing Cyanine Reactivity for Optical Imaging and Drug Delivery. *Acc. Chem. Res.* **2018**, *51* (12), 3226–3235. https://doi.org/10.1021/acs.accounts.8b00384.
20. Wallenfels, K.; Draber, W. Der Einfluss Der Substituenten Auf Elektronen- Und Schwingungsspektren von Aminochinonen. *Tetrahedron* **1964**, *20* (8), 1889–1912. https://doi.org/10.1016/S0040-4020(01)98457-1.
21. Leupold, D.; Dähne, S. On a Herzberg-Teller Mixture in the Case of 2,5-Diaminobenzoquinones-(1,4) and Its Influence on the Molecule Diagram. *Journal of Molecular Spectroscopy* **1965**, *17* (2), 325–333. https://doi.org/10.1016/0022-2852(65)90169-4.

22. Chu, K.-Y.; Griffiths, J. Naphthoquinone Colouring Matters. Part 1. Synthesis and Electronic Absorption Spectra of 1,4-Naphthoquinone Derivatives with Electron-Donating Groups in the Quinonoid Ring. *J. Chem. Soc., Perkin Trans. 1* **1978**, *0* (9), 1083–1087. https://doi.org/10.1039/P19780001083.
23. Perpète, E. A.; Lambert, C.; Wathelet, V.; Preat, J.; Jacquemin, D. Ab Initio Studies of the Λmax of Naphthoquinones Dyes. *Spectrochimica Acta Part A: Molecular and Biomolecular Spectroscopy* **2007**, *68* (5), 1326–1333. https://doi.org/10.1016/j.saa.2007.02.012.
24. Fabian, J.; Nakazumi, H.; Matsuoka, M. Near-Infrared Absorbing Dyes. *Chem. Rev.* **1992**, *92* (6), 1197–1226. https://doi.org/10.1021/cr00014a003.
25. Russkikh, V. V. Synthesis and Efficiency of Photolysis of 2-(Dialkylamino)-1,4-Benzoquinones and 2-(Dialkylamino)-1,4-Anthraquinones. *Zhurnal Organicheskoi Khimii* **1995**, *31* (3), 380–384.
26. Falci, K. J.; Franck, R. W.; Smith, G. P. Approaches to the Mitomycins. Photochemistry of Aminoquinones. *J. Org. Chem.* **1977**, *42* (20), 3317–3319. https://doi.org/10.1021/jo00440a033.
27. Berezhnaya, V. N.; Shishkina, R. P.; Pavlova, N. V.; Trofimov, A. S.; Eroshkin, V. I. Synthesis, Photolysis, and Redox Properties of 2-Dialkylamino-3-Methoxy-1,4-Naphthoquinones. *Russ Chem Bull* **1990**, *39* (3), 578–583. https://doi.org/10.1007/BF00959587.
28. Stavitskaya, T. A.; Bukhtoyarova, A. D.; Shishkina, R. P.; Berezhnaya, V. N.; Shchegoleva, L. N.; Eroshkin, V. I. Influence of the Structure of 2-Dialkyl(Cycloalkyl)Amino-1,4-Naphthoquinones on Their Photochemical Activity. *Khimiya Vysokikh Energii* **1991**, *25* (3), 262–267.
29. Gritsan, N. P.; Bazhin, N. M. Nature and Properties of the Reaction State in the Photolysis of 2-Amino-1,4-Naphthoquinone Derivatives. *Russ Chem Bull* **1980**, *29* (6), 897–902. https://doi.org/10.1007/BF00958803.
30. Gritsan, N. P.; Bazhin, N. M. The Mechanism of Photolysis of 2-Amino-1,4-Naphthoquinone Derivatives. *Russ Chem Bull* **1981**, *30* (2), 210–214. https://doi.org/10.1007/BF00953566.
31. Shishkina, R. P.; Berezhnaya, V. N. Photochemistry of 2-Dialkylamino-1,4-Naphthoquinones. *Russ. Chem. Rev.* **1994**, *63* (2), 139. https://doi.org/10.1070/RC1994v063n02ABEH000076.
32. Cameron, D. W.; Giles, R. G. F. A Photochemical Rearrangement Involving Aminated Quinones. *Chem. Commun. (London)* **1965**, No. 22, 573–574. https://doi.org/10.1039/C19650000573.
33. Cameron, D. W.; Giles, R. G. F. Photochemical Formation of Benzoxazoline Derivatives from Aminated Quinones. *J. Chem. Soc. C* **1968**, No. 0, 1461–1464. https://doi.org/10.1039/J39680001461.
34. Giles, R. G. F. The Photochemistry of an Aminated 1,4-Benzoquinone. *Tetrahedron Letters* **1972**, *13* (22), 2253–2254. https://doi.org/10.1016/S0040-4039(01)84819-X.

35. Maruyama, K.; Kozuka, T.; Otsuki, T. The Intramolecular Hydrogen Abstraction Reaction in the Photolysis of Aminated 1,4-Naphthoquinones. *Bulletin of the Chemical Society of Japan* **1977**, *50* (8), 2170–2173. https://doi.org/10.1246/bcsj.50.2170.
36. Aponick, A.; Dietz, A. L.; Pearson, W. H. 2-(3-Pyrrolin-1-Yl)-1,4-Naphthoquinones: Photoactivated Alkylating Agents. *Eur. J. Org. Chem.* **2008**, *2008* (25), 4264–4276. https://doi.org/10.1002/ejoc.200800482.
37. Akiba, M.; Kosugi, Y.; Takada, T. Reactions of Acylaminoquinone Tosylhydrazones. 4. A New Synthesis of Pyrrolo[1,2-a]Indoloquinone and Related Compounds via Benzoxazoline by Thermolysis and Photolysis. *The Journal of Organic Chemistry* **1978**, *43* (23), 4472–4475. https://doi.org/10.1021/jo00417a017.
38. Giles, R. G. F.; Mitchell, P. R. K.; Roos, G. H. P.; Baxter, I. A Photochemical Reaction of 2-Acetyl-3-Alkylamino-1,4-Benzoquinones: Formation of Benzoxazoles. *J. Chem. Soc., Perkin Trans. 1* **1973**, No. 0, 493–496. https://doi.org/10.1039/P19730000493.
39. Takagi, K.; Kawabe, M.; Matsuoka, M.; Kitao, T. Syntheses of Deep Coloured Aminonaphthoquinonoid Dyes. Reaction of Dichloronaphthazarins with 2-Aminobenzenethiol and Related Compounds. *Dyes and Pigments* **1985**, *6* (3), 177–188. https://doi.org/10.1016/0143-7208(85)80016-4.
40. Chen, Y.; Steinmetz, M. G. Photoactivation of Amino-Substituted 1,4-Benzoquinones for Release of Carboxylate and Phenolate Leaving Groups Using Visible Light. *J. Org. Chem.* **2006**, *71* (16), 6053–6060. https://doi.org/10.1021/jo060790g.
41. Bukhtoyarova, A.; Berezhnaya, V.; Shishkina, R.; Vetchinov, V.; Eroshkin, V.; Stavitskaya, T. Photolysis of 2-Dialkylamino-3-Methyl-1,4-Naphthoquinones. *Bulletin of the Academy of Sciences of the Ussr Division of Chemical Science* **1991**, *40* (10), 2094–2098. https://doi.org/10.1007/BF00963513.
42. Regan, C. J.; Walton, D. P.; Shafaat, O. S.; Dougherty, D. A. Mechanistic Studies of the Photoinduced Quinone Trimethyl Lock Decaging Process. *J. Am. Chem. Soc.* **2017**, *139* (13), 4729–4736. https://doi.org/10.1021/jacs.6b12007.
43. Wagner, P. J.; Kemppainen, A. E.; Jellinek, T. Type II Photoreactions of Phenyl Ketones. Competitive Charge Transfer in .Alpha.-, .Gamma.-, and .Delta.-Dialkylamino Ketones. *J. Am. Chem. Soc.* **1972**, *94* (21), 7512–7519. https://doi.org/10.1021/ja00776a038.

Chapter 2. A General Strategy for Visible-Light Decaging Based on the Quinone Trimethyl Lock*

* Parts of this chapter are adapted with permission from: Walton, D. P.; Dougherty, D. A. A General Strategy for Visible-Light Decaging Based on the Quinone Trimethyl Lock. *J. Am. Chem. Soc.* **2017**, *139* (13), 4655–4658.

2.1 Abstract

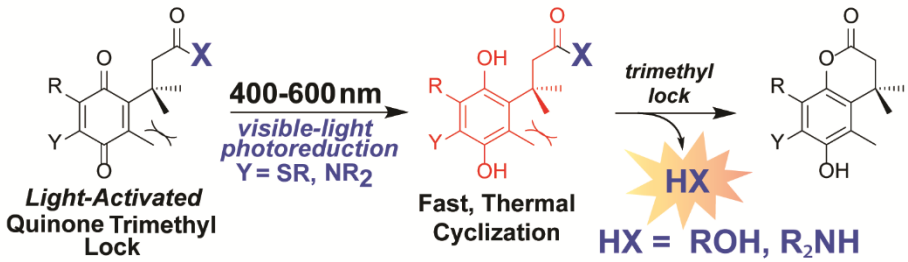

Visible-light triggered quinone trimethyl locks are reported as a general design for long-wavelength photoremovable protecting groups for alcohols and amines. Intramolecular photoreduction unmasks a reactive phenol that undergoes fast lactonization to release alcohols and amines. Model substrates are released in quantitative yield along with well-defined, colorless hydroquinone byproducts. Substituent modifications of the quinone core allow absorption from 400-600 nm. The synthesis and evaluation of photoreactivity for various quinone dyes absorbing past 600 nm is described in an effort to rationally design longer wavelength absorbing photocages. Finally, the sensitized photoreduction of a quinone trimethyl lock derivative with 660 nm light is reported.

2.2 Introduction

The trimethyl lock (TML) is a highly modular motif that has found many applications[1] as a protecting group for alcohols and amines (**Figure 2.1**). Once a phenolic oxygen is revealed, rapid cyclization of the propionic ester or amide occurs, releasing **HX** in seconds (HX = HOR) to minutes (HX = HNR_2) in a process often referred to as decaging.[2] The reaction is quite general, and scores of examples are found in the literature. The phenol is frequently part of a hydroquinone, and chemical, enzymatic, and electrochemical reductions of the corresponding quinone have been used to initiate the trimethyl lock (**Figure 2.1**). Photochemical initiation of

the trimethyl lock, however, has not been reported, except for the trivial case of nitrobenzyl decaging of a phenol using UV light.[1-18]

We describe here a photochemically-initiated trimethyl lock system that operates well into the visible range and has the potential for extension into the near-infrared. Decaging reactions at longer wavelengths are rare and would be useful in many contexts.[19-29] Importantly, *the photochemical step and the trimethyl lock decaging are completely distinct processes.* An intramolecular photochemical quinone reduction is followed by a *thermal* trimethyl lock reaction. As such, this system innately spans the broad substrate applicability of the trimethyl lock reaction. In addition, the photochemical step can be optimized separately regarding quantum yields, wavelength, etc. without impacting the decaging step.

There are numerous examples of intermolecular photochemical reductions of quinones[30-34], and several variants where an appended amine[28, 35-41] or sulfide[42-44] mediates the photochemical reduction. As such, we considered compounds such as **1**, in which a photochemical reduction would launch the trimethyl lock process. We describe here the synthesis and photochemistry of variants of **1**.

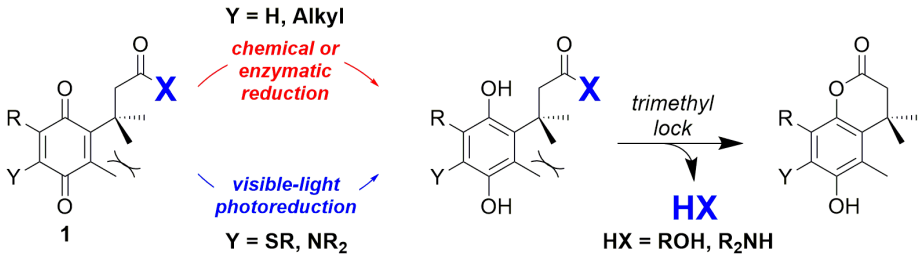

Figure 2.1. Decaging strategies for the quinone trimethyl lock.

2.3 Results and Discussion

2.3.1 Sulfide and Dialkylamine Photocages

Our initial approach to compounds such as 1 is outlined in scheme 2.1. The bromoquinone acid intermediate 4 is quickly obtainable in gram quantities as a crystalline solid without the need for chromatography. Sulfide substituents were then introduced by conjugate addition to 4 (or esters of 4) in a reaction that is rapid at room temperature under mild conditions and is

highly selective for displacement of the bromine. Immediate Steglich esterification affords the methyl, ethyl, and N-hydroxysuccinimide (NHS) esters. Chromatography is only required after esterification, and simply involves collecting the yellow band that elutes. γ-Aminobutyric acid was caged by reaction of the NHS ester in acetonitrile - bicarbonate buffer with the free amino acid.

Scheme 2.1 Synthesis of Quinone TML Derivatives.

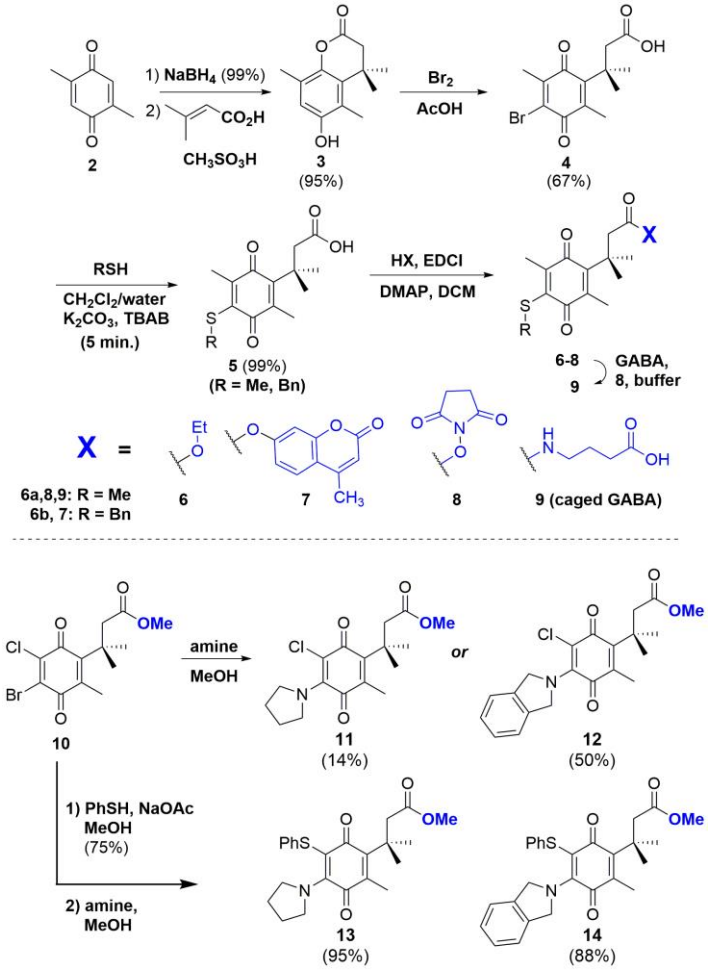

Surprisingly, conjugate addition of amines was unsuccessful for substrate **4** or **5**. Amine derivatives **11-14** were instead synthetized from **10**, prepared from 2-chloro-5-methylphenol (see SI). Yields of the desired substitution pattern, with the amine para to the trimethyl lock chain, were increased by first treating **10** with thiophenol before addition of amine to give **13** and **14**.

The UV-vis spectra of compounds **6-9** and **11-14** are similar, with charge transfer absorptions in the visible (**Figure 2.2**). In both systems, the absorption bands are broad enough that efficient and clean photolysis is possible at wavelengths both below and well beyond λ_{max}. Irradiation with visible light (300 W Hg arc lamp with >400 nm glass filter) leads to clean and efficient photolysis for both compounds. In practice, a simple 455 nm 1 watt portable LED is suitable for photolysis of both amine and sulfide derivatives. For the amines, a longer-wavelength, 565 nm, 1 watt LED was also practical, allowing for orthogonal decaging (see below).

Reduction of the quinone core and subsequent trimethyl lock occurs in all cases, releasing caged alcohols in quantitative yield. The reaction is remarkably clean; after removal of the solvent, the crude reaction is pure by NMR and LCMS with few exceptions. Monitoring the reaction by NMR in CD_3OD shows clean conversion and quantitative release of the methanol or ethanol. The hydroquinone byproducts vary depending on the solvent and substituent (**Scheme 2.2**). Irradiation of **6a** in methanol with a 455 nm LED releases ethanol and generates methanol-trapped **16a** (R = CH_3) as the exclusive product (Φ_{420} = 1.2%). Photolysis of **6b** is more efficient (Φ_{420} = 6.3%) and produces **16b** (R = Ph), along with a cyclized product **17** (R = Ph).[45] In aqueous solution, the disulfide **18** is cleanly produced, presumably via aqueous trapping of zwitterionic intermediate **15**, subsequent hydrolysis to release a carbonyl and oxidation. Interestingly, a ketone masked as the thiol substituent can be released simultaneously with an alcohol or amine in water. In aprotic solvents, the sulfides undergo slow photolysis to a complex mixture of products.

In contrast to the sulfides **6-9**, photolysis of amines **11-14** to the hydroquinone not only proceeds smoothly in a range of solvents, but is more efficient in non-polar solvents. Pyrrolidine derivatives **11** and **13** cyclize to form oxazolidines **19** and **21**, whereas isoindoline derivatives **12** and **14** form isoindoles **20** and **22**. For the closely related series **11-14**, the relative rate of reaction is **12** > **11** > **14** > **13**. As with the sulfides, an activated benzylic hydrogen on the substituent facilitates a more rapid reaction. The aryl sulfide substituent of **13** and **14** appears to impede the reaction relative to Cl in **11** and **12**. We estimate the quantum yields in methanol for **11** and **12** to be similar to that of **6a** and **6b**, and that of **13** and **14** to be lower. However, detailed photophysical studies are still in progress.

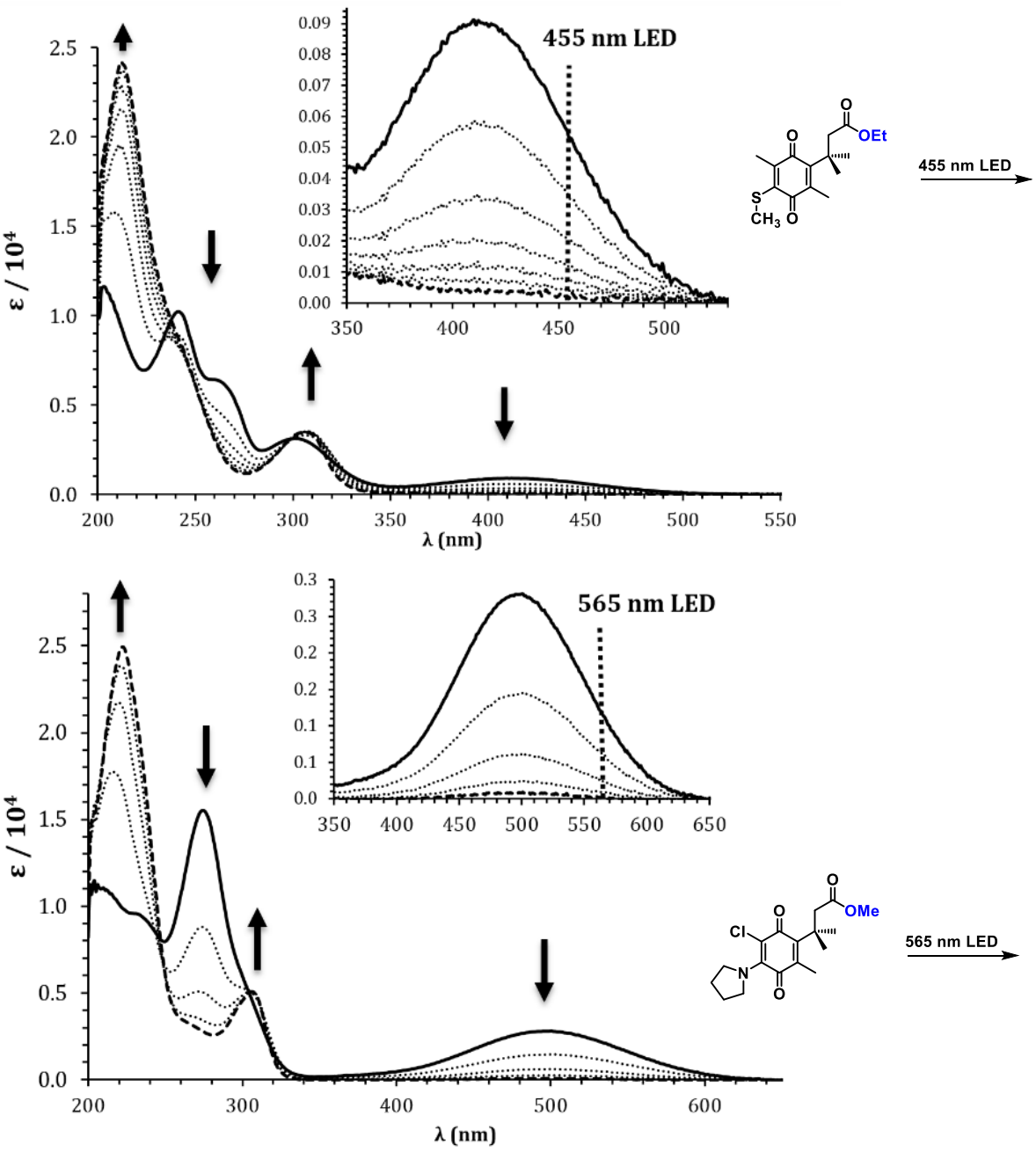

Figure 2.2 Representative time course UV-vis spectra during photolysis for compounds 6a (top) and 11 (bottom) irradiated with 455 nm and 565 nm LEDs, respectively. Expansions of the visible bands are shown as insets. Arrows indicate changes in the spectra over time. Traces are 1 minute apart. For both compounds, 3 mL of 0.1-0.2 mM solutions fully converted in under 5 minutes with a standard 1W mounted LED.

Scheme 2.2. Photolysis of 6-14.

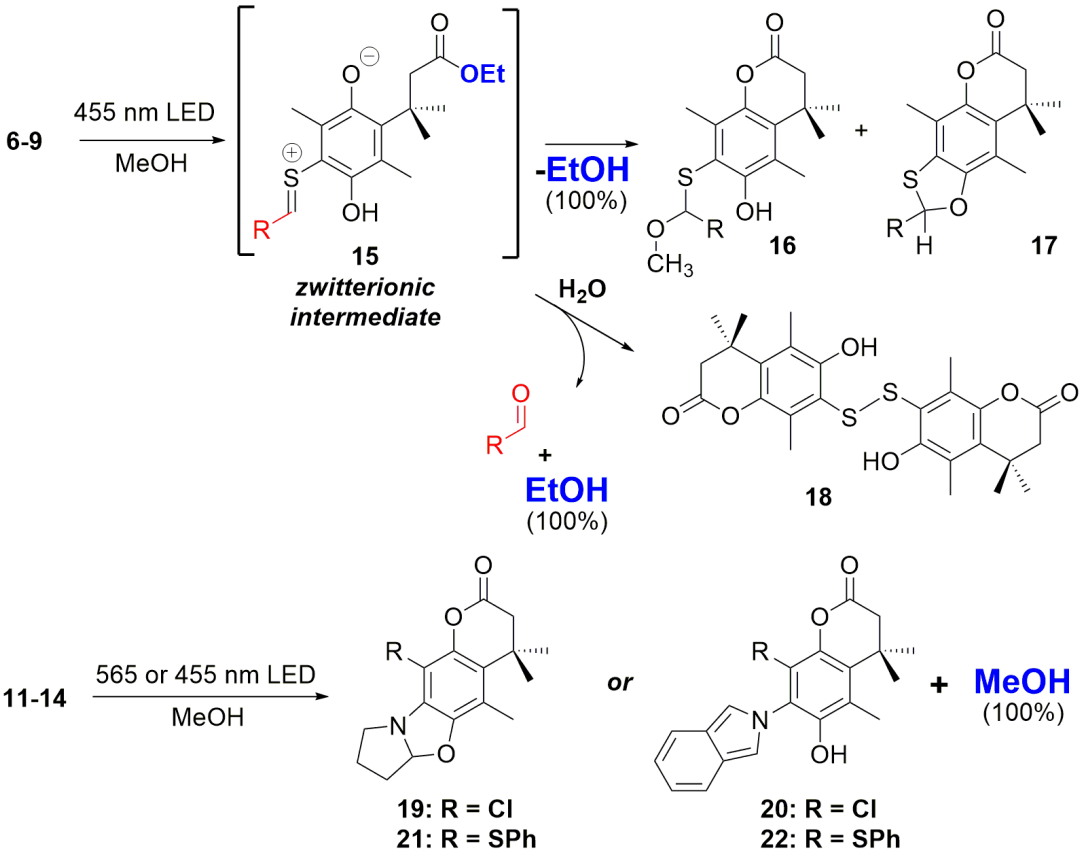

As described in detail elsewhere, we have performed extensive mechanistic studies on the photoreaction of sulfides such as **6**.[45] Based on substituent effects, kinetic isotope effects, stereochemical and radical clock probes, and nanosecond transient-absorption spectroscopy, we consider the reaction to proceed as follows. Photochemically induced electron transfer is followed by a critical and irreversible hydrogen transfer, which leads to a net two-electron intramolecular reduction of the quinone and formation of a zwitterionic intermediate such as **15**. Capture by solvent or the phenolic oxygen, followed by trimethyl lock ring closure completes the decaging. In some cases, the intermediate hydroquinone can be directly observed, and the thermal trimethyl lock ring closure can be monitored (Supporting Information). Given the importance of the hydrogen transfer step, it is not surprising that the benzylic derivative **6b** is more efficient than the methyl derivative, **6a**.

To illustrate the potential usefulness of these compounds, we sought to demonstrate release of a fluorophore, release of a biologically relevant molecule, and the orthogonality of the

two developed systems. **Figure 2.4** shows that irradiation of **7** at 455 nm in aqueous acetonitrile rapidly releases a fluorescence sensor (hymecromone). The uncaged coumarin is selectively excited in aqueous solvents, allowing release to be monitored by fluorescence (**Figure 2.4**).

Decaging is also possible in a biological setting, permitting optical control of protein targets. **Figure 2.5** shows decaging of the neurotransmitter γ-aminobutyric acid (GABA) using precursor **9**. When expressed in *Xenopus* oocytes, $GABA_A$ receptors are activated after incubation with **9** and exposure to a 455 nm LED (see SI for details). For caged amines, such as **9**, photolysis is much faster than trimethyl lock closure, as expected from previously determined reaction rates of redox triggered quinone trimethyl lock amine conjugates.[2] Drug conjugates with 5-HT, choline, and lobeline were also prepared, but GABA gave the best results in ion channels.

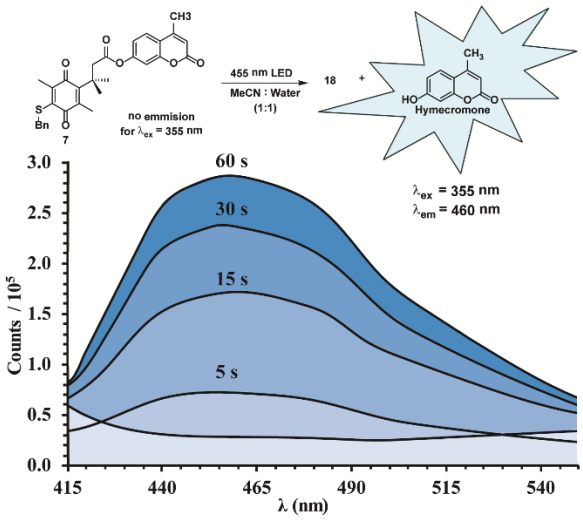

Figure 2.4. Release of 4-Methylumbelliferone (hymecromone) monitored by fluorescence with 355 nm excitation after samples were irradiated with a 1 watt 455 nm LED for 0 s, 5 s, 15 s, 30 s, and 60 s.

Having demonstrated the release of biologically meaningful concentrations of model substrates in seconds to minutes, we sought to demonstrate orthogonality of the amine and sulfide systems.[25] Solutions of **6** and **11** in methanol with matched optical densities were mixed 1:1 to give a solution with a broad absorbance from 360 to 620 nm (**Figure 2.6**). Irradiation with first a 565 nm LED through a 530 nm long-pass filter cleanly released only caged methanol from **11** (red). Subsequent irradiation with a 455 nm LED released ethanol from **6**. LCMS (see SI) and UV-vis indicated that no decaging of **6** occurred with the long-wavelength irradiation, allowing complete conversion of **11** orthogonally to **6**. Irradiating the solution with

a 455 nm LED led to simultaneous release of the two alcohols. The orthogonality of the two similar systems allows for rapid release of two different compounds in quick succession.

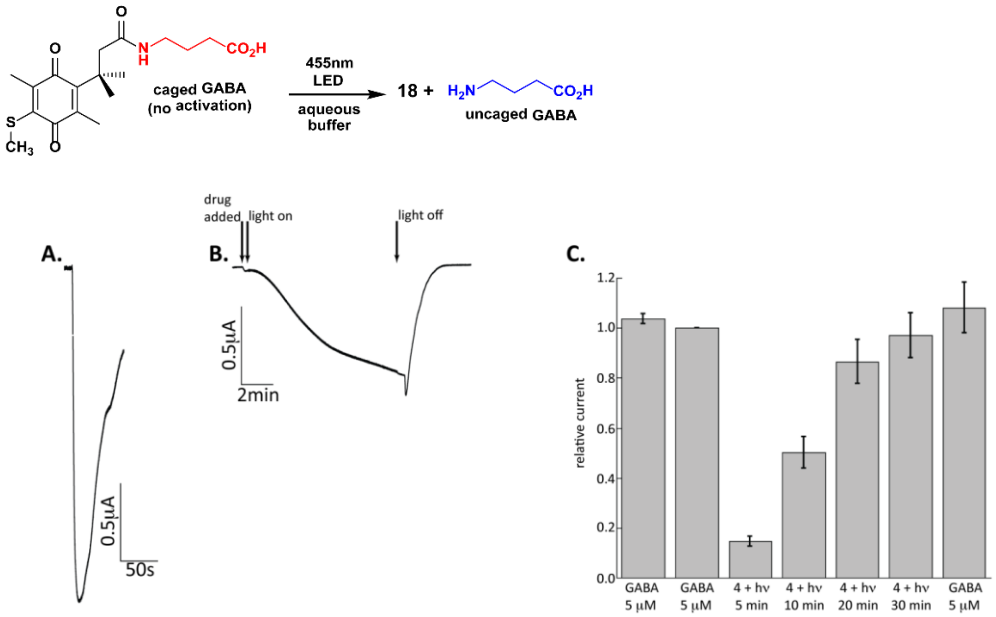

Figure 2.5. Release of the neurotransmitter γ-amminobutyric acid (GABA) to activate $GABA_A$ receptors in *Xenopus* oocytes upon photolysis with a 455 nm LED. Shown is current produced by activation of the receptor, as probed by whole-cell, two-electrode, voltage clamp electrophysiology. **A.** Response from 50 mM GABA. **B.** Response from irradiation of **9** with 455 nm LED. **C.** Dose-response from irradiation of solutions of **9** before application to oocyte

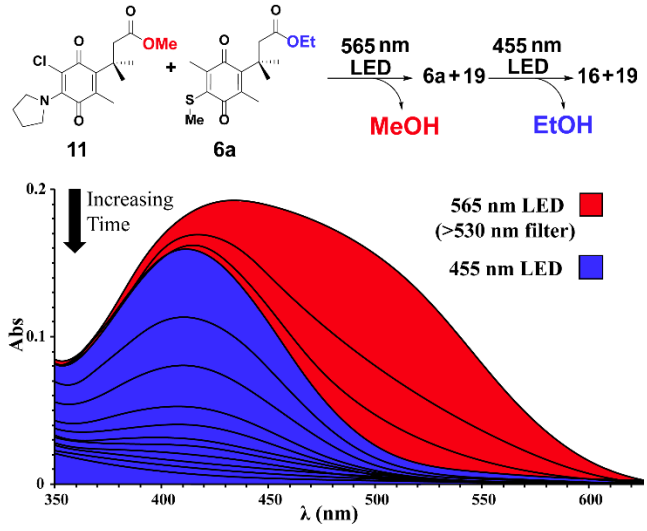

Figure 2.6 Orthogonal photolysis of **11** and **6** in methanol. Photolysis of a solution of **11** and **6** with >530 nm light followed by >420 nm light allows selective decaging.

2.3.2 Efforts Towards Long-Wavelength Quinone Photochemistry:

After demonstrating initial success with alklylamine substituted trimethyl lock compounds, we turned our efforts towards increasing the wavelength of absorption into the near-IR. Compound **10** served as a convenient entry point for disubstituted quinone trimethyl locks depicted in **Scheme 2.3**. The dihalide quinone and other derivatives (X = OMe, F, OH, H, CH_3) were synthesized on multigram scale. Heating 3,3-dimethylacrylic acid and the appropriate phenol (**23**) in methanesulfonic acid yielded lactones **24**. Hydrolysis of **24** followed by Elb's persulfate oxidation installed the distal hydroquinone oxygen in **25**. Brominative oxidation to the dihalide quinone acid **26** and subsequent esterification afforded the ester **10**. Here, the two-step oxidation is preferable to Fremy's salt because Elb's persulfate oxidation occurs at the high pH required to hydrolyze **24**.

Successive conjugate additions to quinone **10** were easily followed by LCMS, where displacement of either bromide or chloride substituent is clear by the isotopic abundance. The regioselectivity of nucleophile addition to **10** depends highly on the nature of the nucleophile, and likely also on the solvent. For thiophenols, only the chloride substitution and disubstitution products are formed, even at sub-stoichiometric amounts of thiophenol. This indicates that monosubstitution either does not occur at bromine from the soft nucleophile PhSH or that if it does the product is more reactive to further substitution. For alkyl thiols both products are formed equally. Amines range from favoring chloride substitution to a 1:1 product mixture. For example, the yield increase from **11** to **12** is at the expense of bromide substitution. A possible charge transfer occuring before addition could explain these observations. An additional complication arose when phenols and alcohols were displaced by thiols or amines over a second halide substitution. The distortion of the quinone carbonyl imparted by the adjacent the trimethyl lock likely suppresses reactivity at the bromide site as well. The amine addition to the methyl ester of **4** (**scheme 2.3**) gave only side-chain amination. This is in stark contrast to the ease of thiol addition to derivatives of **4**. The removal of the problematic methyl group was essential to allow amine addition to occur for **11**-**14**. Phenyl, methoxy, and other substituents were investigated in place of the chloride, but compound **10** proved the most useful. These effects were generally predictive, and given the correct order of addition many compounds were obtainable with the desired substitution. Sequential conjugate additions of various nucleophiles to **10** afforded compounds **27-33** depicted in **Scheme 2.3**.

Scheme 2.3. Extending Wavelength of Absorption for QTMLs

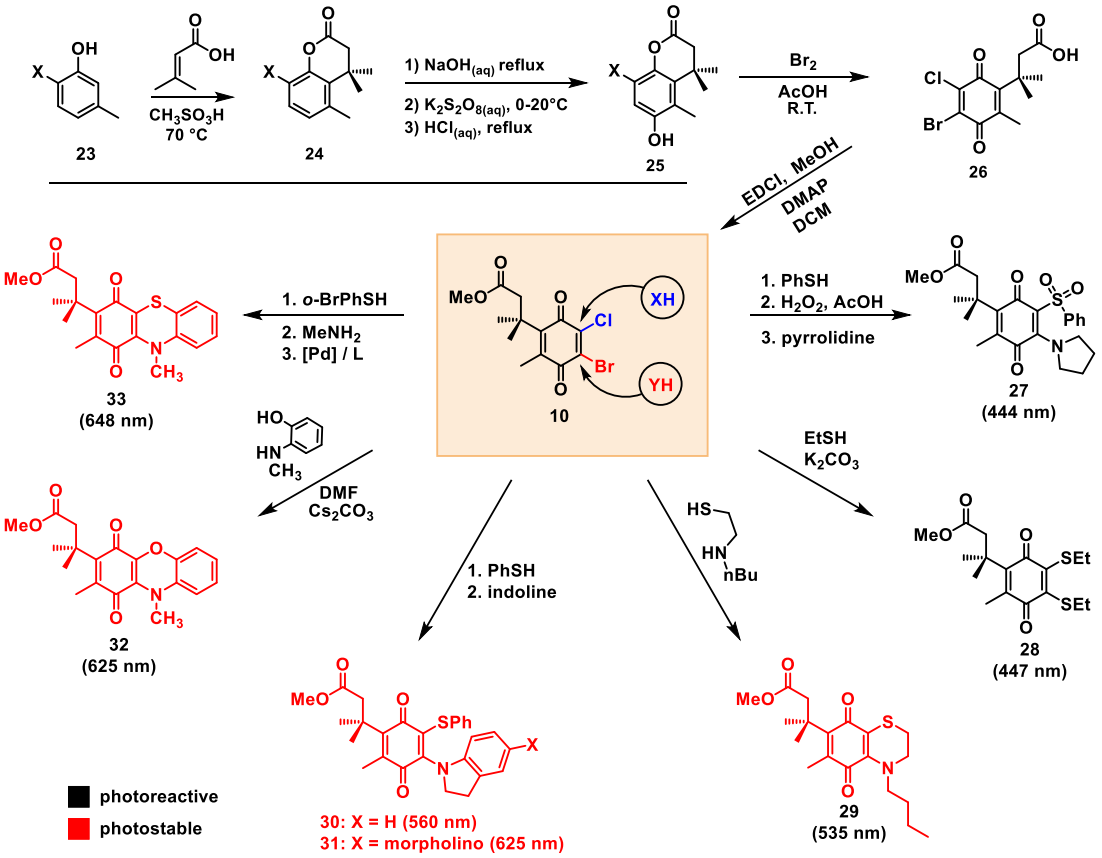

Methyl deprotonation:

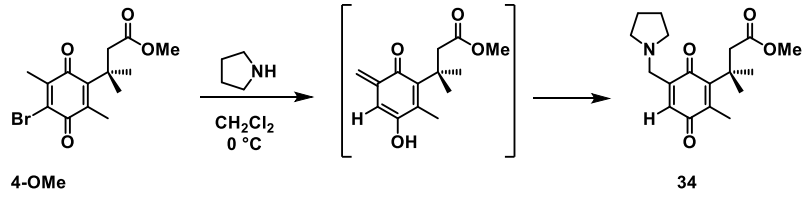

4-OMe 34

Naphthoquinones:

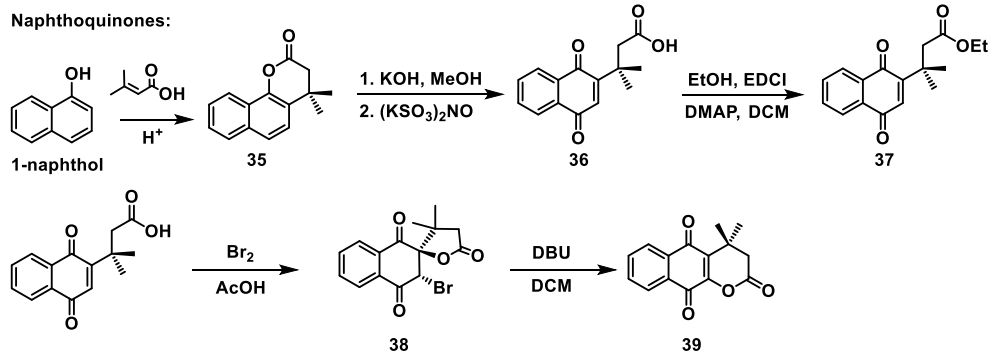

1-naphthol 35 36 37 38 39

Extension of the QTML concept to a 1,4-naphthoquinone scaffold proved challenging. Although the naphthoquinone **36** was readily prepared from 1-naphthol analogously to **26**, amine addition did not occur and thiol addition led to the reduced lactone. Bromination was required to avoid a reoxidation step after conjugate addition. Treating **37** with bromine in acetic acid gave no reaction, but the spiro compound **38** was formed from **36**. A Nuclear Overhauser Effect (NOE) was observed between the gem-dimethyls and quinone proton, confirming the structure as drawn. This is the epimer of the expected product from intramolecular carboxylate trapping of a bromonium ion, and likely forms via acid catalysis as calculations suggest it is the more stable diastereomer. Treating **38** with base quantitatively gives the lawsone lactone derivative **39**, which was difficult to further functionalize.

Unfortunately, many of the derivatives prepared from **10** were unreactive to visible light. Several structural features were identified as problematic for the photoreaction, namely aromatic amines, excessive electron donors, and planar structures. In addition, key comparisons give the picture of N-**C**-**H** bond breaking, competing electron transfer (or otherwise fast deactivation) from electron rich substituents, and quinone-amine **C-N** bond twisting being important aspects of photoreactivity.

From above, isoindoline derivatives **12** and **14** react more efficiently than pyrrolidine, and the thiophenol substituents of **13** and **14** appear to inhibit the photoreaction. We have interpreted this as non-productive electron transfer (ET) that returns the excited state to the ground state unaltered and a rate limiting N-**C-H** bond breaking step. The sulfone **17** was therefore prepared to probe whether oxidation of the sulfide substituent would ablate the deleterious ET to improve quantum yields. While reactivity was improved compared to the sulfide parent, sulfone **27** was blue-shifted by nearly 50 nm. This improved efficiency could stem from the removal of a non-productive ET by sulfoxide oxidation, a steric effect, or the higher excitation energy. The blue shift and intermediate reactivity of sulfoxide **27** compared to **11-14** did not warrant further investigation.

Bis-sulfide **28** was formed when excess thiol was reacted with **10**. Although sulfides do not produce as red-shifted absorbances as amines, the effects of multiple sulfide substitutions are at least partially additive, and **28** absorbs at 447 nm (ε = 4,000 $M^{-1}cm^{-1}$). For **28**, the additional sulfur substituents potentially double the number of reactive hydrogens, yet photolysis is sluggish and proceeds to multiple products. Bis-sulfides were therefore abandoned as an option.

Replacing an alkyl amine substituent with an aromatic one produces a significant red-shift in absorbance for **30** relative to **11-14** of 60 nm. An additional 65 nm red-shift is gained on increasing the electron releasing ability of the indoline substituent. Compound **31** with a *para*-morpholino donor absorbs at 625 nm. Constraining the electron donating substituent to be coplanar with the quinone offers another large red-shift, as demonstrated by **29** (535 nm)**, 32** (625 nm), and **33** (648 nm). Alternatively, the electron accepting ability of the quinone can be increased to enhance the effect of the donor, as in 2-indolino-3,5,6-trichloro-1,4-benzoquinone (λ_{max} = 640 nm). No photoreactivity was observed, however, for planar or aromatic amines when irradiating the visible band.

In the case of thiol substituted **28** and **29**, irradiation with > 500 nm light produced slow bleaching in air equilibrated methanol, and rapid bleaching on irradiation from a 420 nm LED. The related naphthoquinones 2-chloro-3-indolino-1,4-naphthoquinone and 2-(ethanethiol)-3-chloro-1,4-naphthoquinone behaved similarly, although 2-chloro-3-indolino-1,4-naphthoquinone underwent no bleaching at long wavelengths. However, the UV-vis spectra of thiolsubstituted arylamino quinones display an absorbance near 410 nm characteristic of thiol substituted quinones that is absent for 2-chloro-3-indolino-1,4-naphthoquinone. Monitoring the reaction under degassed conditions in both benzene and methanol showed no changes in the NMR spectra. It is therefore likely that the slow bleaching process is oxidation or reaction with solvent, rather than the photoreduction observed with dialkylamines.

Without suitable reactivity above 600 nm, we sought to photosensitize the quinone reduction. The phthalocyanine sensitized photoreduction of quinones by thiols has been reported in chloroform.[46] Following the published procedure, the sensitized photoreduction of quinone trimethyl lock derivative **40** to lactone **41** by aryl thiols in degassed chloroform was possible with the zinc phthalocyanine (**42**, **Zn Pc**) at 660 nm (**scheme 2.5**). The reaction does not proceed in the presence of oxygen or in the absence of light, thiol, or sensitizer. Here, a quinone trimethyl lock that normally undergoes HAT from the trimethyl lock substituent cleanly gave the photoreduced product after 12 h of irradiation. Though this provides proof of principle for sensitized photoreduction, the conditions are far from ideal for applications.

Scheme 2.4 Sensitized Photoreduction of a QTML

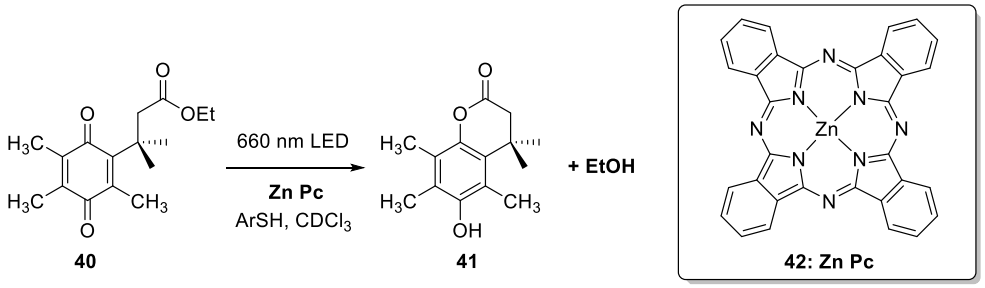

2.2 Conclusions

We believe compounds of the sort described here will be useful in many contexts. Photoremovable protecting groups, or photocages, offer the ability to spatio-temporally control the release (decaging) of molecules with light. The most widely used examples are 2-nitrobenzyl derivatives, which require UV irradiation and generate toxic byproducts. In fact, there are few transition-metal free photoremovable protecting groups that absorb significantly above 450 nm.[19, 21-28] Because of the well-established increase in tissue penetrance as wavelength increases, longer wavelength decaging strategies such as that described here have great potential as chemical biology tools or in a therapeutic setting. The present systems are already well into the visible range, and a great deal is known about photo-induced electron transfer reactions of the sort that initiate this process, providing valuable guidance on how to move to even longer wavelengths.

In summary, we have created a modular system in which a photoinduced electron transfer of a quinone leads to a thermal trimethyl lock release of an alcohol or amine. The reaction works well with visible light in aqueous media to produce non-absorbing products. The entire range of substrates established to be compatible with the trimethyl lock is now available through visible light activation.

In the context of chemical biology and materials chemistry, the developed photocages have excellent potential at substantially longer wavelengths than the ubiquitous nitrobenzyls. The lack of long-wavelength reactivity is unfortunate for clinical applications, but it is not entirely surprising. The electron donors that produced the largest red-shifts in absorbance were delocalized aromatic systems. In the context of the dialkylaminoquinone mechanism, a delocalized charge transfer state would be less likely to undergo proton transfer (k_{H+} is slow).

Alternatively, the charge transfer state of reactive compounds could be energetically close enough to mix with or thermally populate the nearby n,π*, which undergoes HAT. At longer wavelengths, the energy difference between this state and a reactive state is large, which shuts down this pathway. Either way, it seems likely that the structural and electronic changes leading to large red-shifts in absorbance for the quinones investigated also lead to photostability. However, the general strategy of a decoupled photochemical step to reveal a fast thermal reaction such as the trimethyl lock is not inherently tied to quinone photochemistry, and therefore long-wavelength absorbing dyes that undergo photoreduction can be developed around the trimethyl lock.

Finally, the phthalocyanine sensitized photoreduction of a quinone trimethyl lock offers an attractive option for long wavelength photochemistry in degassed chloroform in the presence of thiophenol. Notably, these are not conditions commonly found in chemical biology or a clinical setting. Further, the trimethyl lock is slow to close in aprotic solvents, limiting purely synthetic applications of the sensitized reaction. With careful choice of quinone core and sensitizer, an optimized system in water is feasible, and future efforts may find that avenue more fruitful, albeit less exciting.

2.5 Experimental

Materials and Methods. Unless otherwise stated, reactions were carried out under ambient conditions in air. Commercially available reagents were obtained from Sigma Aldrich, AK Scientific, Alfa Aesar, or Acros Organics and used without further purification. Solvents used for photolysis and UV-vis were EMD Millipore (OmniSolv®) grade. Other solvents were used as received or dried by elution through activated alumina where noted. If a photoproduct was found to be unstable to hydrolysis, methanol was distilled from magnesium. Thin-layer chromatography with Sigma Aldrich silica gel coated plates with fluorescent indicator (0.25 mm) was used to monitor reactions. Silica gel chromatography was conducted as described by Still et al. (W. C. Still, M. Kahn, A. Mitra, *J. Org. Chem.* **1978**, *43*, 2923), with silica gel purchased from Alfa Aesar (60 Å, 230-400 mesh). NMR spectra were recorded on Varian (300, 400, 500, or 600 MHz), or Bruker (400 MHz) spectrometers. HRMS (ESI) were obtained with an Agilent 6200 Series TOF. UV-vis spectra were recorded on a Cary 60 spectrometer. Samples were irradiated with a 300 W Hg arc lamp with glass filter (>400 nm), M455L3 (455 nm, 900 mW), or a M565L3 (565 nm, 880 mW) mounted LED purchased from Thor Labs. Photolysis was

conducted inside the UV-vis spectrometer cavity in a 3 mL cuvette and side on through a glass flask or NMR tube in air-equilibrated methanol, methanol-d_4, or benzene-d_6. Isolated yields are reported except for photolysis yields, which were determined by NMR. Preparatory photolysis was conducted under ambient conditions (air) in glass round bottom flasks with stir bar and side-on illumination. Steady-state luminescence spectra were collected with a Jobin Yvon Spex Fluorolog-3-11 spectrometer. Samples were excited with 355 nm light from a 450 W xenon arc lamp selected with a monochromator. A scanning monochromator was used to collect emission, detecting with a Hamamatsu R928P photomultiplier tube in photon counting mode.

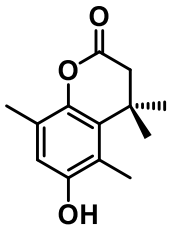

6-hydroxy-4,4,5,8-tetramethylchroman-2-one (3). Compound **3** is conveniently prepared from commercially available 2,5-dimethyl-1,4-benzoquinone via an adapted synthetic route.[4] To a vigorously stirred mixture of 2,5-dimethyl-1,4-benzoquinone (1.0181 g, 7.5 mmol) in ether (20 mL), MeOH (10 mL), and water (40 mL), was added $NaBH_4$ (1.422 g, 37.6 mmol) portion wise, and the yellow mixture turned brown then colorless after 15 min. The mixture was then quickly extracted with ether (3 x 50 mL). The combined ether layers were washed with brine, dried over $MgSO_4$, and evaporated to yield 2,5-dimethyhydroquinone as a white solid 1.033 g (99%). ^{1}H NMR (500 MHz, DMSO-d_6) δ 8.32 (s, 2H), 6.45 (s, 2H), 1.99 (s, 6H). ^{13}C NMR (126 MHz, dmso) δ 147.46, 116.84, 39.52, 15.82. The crude product, 2,5-dimethyhydroquinone (1.033 g, 7.5 mmol), and 3,3-dimethylacrylic acid (0.8453 g, 8.4 mmol) were dissolved in methanesulfonic acid (30 mL) the resulting mixture was heated to 70 °C under argon overnight. The resulting red solution was poured into ice-water and extracted with ethyl acetate (4 x 90mL). The combined organic layers were washed with brine, dried ($MgSO_4$), and the solvent was removed to yield **3** as a tan solid 1.59 g (95%). ^{1}H NMR (500 MHz, DMSO-d_6) δ 9.16 (s, 1H), 6.60 (s, 1H), 2.59 (s, 2H), 2.21 (s, 3H), 2.10 (s, 3H), 1.34 (s, 6H). ^{13}C NMR (126 MHz, dmso) δ 168.15, 151.60, 142.19, 130.98, 122.90, 119.50, 115.10, 44.96, 39.52, 35.17, 27.12, 15.93, 13.86. HRMS (ESI) calculated 219.1027 for $C_{13}H_{15}O_3$ $[M-H]^-$, found 219.1016.

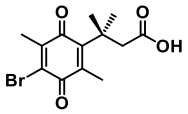

3-(4-bromo-2,5-dimethyl-3,6-dioxocyclohexa-1,4-dien-1-yl)-3-methylbutanoic acid (4). To a solution of lactone **3** (1.59 g, 7.218 mmol) in acetic acid (70 mL) was added bromine (0.817 mL) as a solution in 9.5 mL acetic acid. The resulting red solution was stirred overnight, open to air but protected from light, then poured into water and extracted with dichloromethane until the aqueous solution was colorless. The combined organic layers were then extracted with 10% sodium bicarbonate solution until the bicarbonate layer was colorless. The combined bicarbonate extracts were washed with CH_2Cl_2, then carefully acidified with conc. HCl and extracted with ethyl acetate until colorless. The yellow ethyl acetate extracts were then dried ($MgSO_4$) and concentrated to give a yellow solid. Isolated yield: 1.5301 g (67%). ^{1}H NMR (500 MHz, Chloroform-*d*) δ 10.22 (s, 1H, COOH), 3.02 (s, 2H, CH_2), 2.21 (s, 3H), 2.14 (s, 3H), 1.45 (s, 6H). ^{13}C NMR (126 MHz, cdcl$_3$) δ 187.59, 179.88, 177.66, 152.78, 148.52, 138.72, 131.84, 46.94, 38.07, 28.54, 17.14, 15.15. HRMS (ESI) calculated 313.0081, 315.0060 for $C_{13}H_{14}BrO_4$ [M-H]$^-$, found 313.0060, 315.0051.

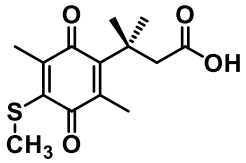

3-(2,5-dimethyl-4-(methylthio)-3,6-dioxocyclohexa-1,4-dien-1-yl)-3-methylbutanoic acid (5a). To a 20 mL scintillation vial charged with **4** (119.9 mg, 0.38 mmol) in a mixture of dichloromethane / water (1:1, 10.8 mL total) was added tetrabutylammonium bromide (5.5 mg; PTC, 4.5%), followed by sodium methanethiolate (53 mg, 0.76 mmol). The vial was capped and vigorously shaken for 2 minutes, then allowed to stand until the layers separated. 1 M HCl was added with stirring until the aqueous layer was colorless, the yellow organic layer was then separated, dried over $MgSO_4$, and evaporated to give **5a** as a yellow solid (106.8 mg, 99%). ^{1}H NMR (300 MHz, Chloroform-*d*) δ 3.59 (s, 2H), 2.97 (s, 2H), 2.47 (s, 3H), 2.17 (s, 2H), 2.13 (s, 2H), 1.42 (s, 5H). ESI-MS(-) calculated for $C_{14}H_{17}O_4S$ [M-H]$^-$ 281.1, found 281.1.

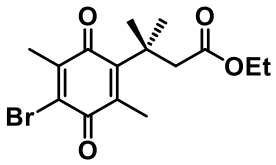

23

ethyl 3-(4-bromo-2,5-dimethyl-3,6-dioxocyclohexa-1,4-dien-1-yl)-3-methylbutanoate. To **4 (**2.6526 g, 8.4 mmol) dissolved in dichloromethane (10 mL) under argon was added ethanol (4.9 mL, 84 mmol), and the solution was cooled to 0 °C under argon. N-(3-dimethylaminopropyl)-N'-ethylcarbodiimide hydrochloride (1.7908 g, 9.3 mmol) and 4-(dimethylamino)pyridine (105.3 mg, 0.86 mmol) were added in one portion, and the resulting solution was stirred for 5 min, then allowed to warm to room temperature. The crude product was diluted in hexanes and purified by flash column chromatography (SiO_2, 10% EtOAc in hexanes), collecting the yellow band to yield 1.5952 g (55%) of the bromoquinone ester **23** as an oil. ^{1}H NMR (400 MHz, Chloroform-*d*) δ 4.04 (q, *J* = 7.1 Hz, 2H), 2.95 (s, 2H), 2.21 (s, 3H), 2.17 (s, 3H), 1.44 (s, 6H), 1.20 (t, *J* = 7.1 Hz, 3H). ^{13}C NMR (101 MHz, $CDCl_3$) δ 187.60, 179.88, 172.70, 153.61, 148.77, 138.04, 131.63, 60.39, 47.50, 38.22, 28.46, 17.23, 15.05, 14.17. HRMS (ESI) calculated for $C_{15}H_{20}BrO_4$ $[M+H]^+$ 343.0539 (100%), 345.0519 (97.3 %), found 343.0536 (100%), 345.0521 (97.1 %).

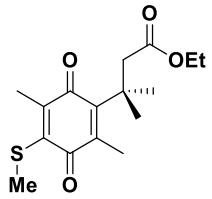

ethyl 3-(2,5-dimethyl-4-(methylthio)-3,6-dioxocyclohexa-1,4-dien-1-yl)-3-methyl-butanoate (6a). To a solution of **4** (40 mg, 0.11 mmol) in dichloromethane (1 mL) was added water (1 mL), tetrabutylammonium bromide (1.8 mg, 5%), and sodium methanethiolate (16 mg, 0.23 mmol). The resulting mixture was shaken vigorously for 2 min, then the organic layer was separated, dried, and concentrated. The crude was purified by flash column chromatography (SiO_2, 10% EtOAc in hexanes) to yield **6a** as a yellow oil (30 mg, 83%). ^{1}H NMR (300 MHz, Chloroform-*d*) δ 4.03 (q, *J* = 7.1 Hz, 2H), 2.95 (s, 2H), 2.47 (s, 2H), 2.16 (s, 3H), 2.13 (s, 2H), 1.42 (s, 6H), 1.19 (t, *J* = 7.1 Hz, 2H). ^{13}C NMR (101 MHz, $CDCl_3$) δ 188.26, 183.32, 172.70, 152.99, 146.36, 141.61, 139.54, 60.26, 47.62, 38.12, 28.64, 17.09, 14.64, 14.51,

14.18. HRMS (ESI) calculated for $C_{16}H_23O_4S$ $[M+H]^+$ 311.1312, found 311.1316. UV/vis: λ_{max} = 413 nm (ε = 903 $M^{-1}cm^{-1}$).

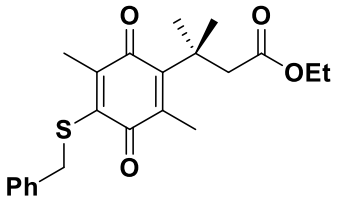

ethyl 3-[4-(benzylsulfanyl)-2,5-dimethyl-3,6-dioxocyclohexa-1,4-dien-1-yl]-3-methyl-butanoate (6b). To a solution of **4** (1 eq) in methanol was added benzyl mercaptan (1.1 eq), followed by K_2CO_3 (1.1 eq), at which point the pale solution turned dark mustard yellow. The resulting solution was stirred, protected from light until LCMS indicated the reaction was complete, then 1 equivalent of acetic acid was added, and the solvent was removed. The crude product was dissolved in a small amount of CH_2Cl_2, then diluted in hexanes and filtered through a cotton plug to remove inorganic salts before purification by flash column chromatography (SiO_2, 10% EtOAc in hexanes) to yield **6b** as a yellow oil (>95%). ^{1}H NMR (300 MHz, Chloroform-*d*) δ 7.36 – 7.14 (m, 5H), 4.18 (s, 2H), 3.98 (q, *J* = 7.1 Hz, 2H), 2.90 (s, 2H), 2.16 (s, 3H), 2.00 (s, 3H), 1.40 (s, 6H), 1.14 (t, *J* = 7.1 Hz, 3H). ^{13}C NMR (126 MHz, cdcl$_3$) δ 188.50, 183.71, 172.44, 153.14, 149.22, 139.47, 139.40, 137.76, 129.01, 128.52, 127.24, 60.21, 47.53, 38.19, 38.16, 28.62, 14.86, 14.59, 14.18. HRMS (ESI) calculated for $C_{22}H_{27}O_4S$ $[M+H]^+$ 387.1625, found 387.1632. UV/vis: λ_{max} = 413 nm (ε = 951 $M^{-1}cm^{-1}$).

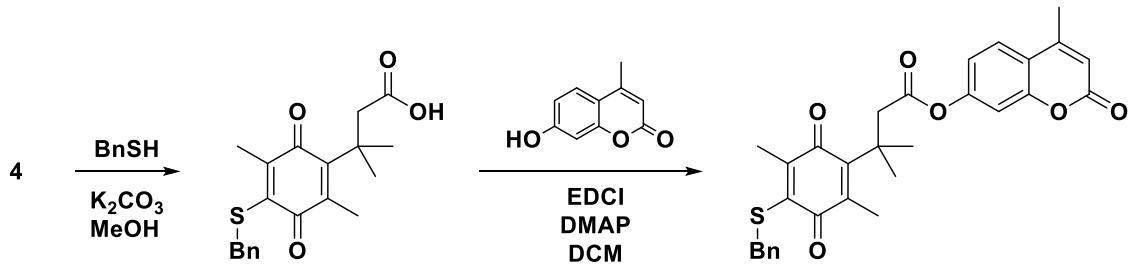

4-methyl-2-oxo-2H-chromen-7-yl 3-(4-(benzylthio)-2,5-dimethyl-3,6-dioxocyclohexa-1,4-dien-1-yl)-3-methylbutanoate (7). To a solution of **4** (250.0 mg, 0.793 mmol) in methanol (50 mL) was added benzyl mercaptan (0.15 mL, 1.3 mmol), followed by K_2CO_3 (219.1 mg, 1.58 mmol). The resulting solution was stirred and protected from light until HPLC indicated the reaction was complete. The solvent was removed, and the mixture was partially purified on silica, removing residual benzyl mercaptan by first eluting with dichloromethane, then eluting **5b** (yellow band) with 1% CH_3CO_2H / 5 % CH_3OH / CH_2Cl_2. Due to a known[5]

intramolecular Michael addition on similar compounds, the pooled yellow fractions were quickly concentrated and used immediately in the next step. To a solution of **5b** (250 mg, 0.7 mmol) in dichloromethane was added 7-hydroxy-4-methyl-2H-chromen-2-one (300 mg, 1.7 mmol). Ethyl acetate was added to solubilize the coumarin, and once the solution was homogenous excess EDCI·HCl and DMAP (14.5 mg, 0.12 mmol) were added. Once TLC indicated the reaction was complete, the crude product was purified by flash chromatography to yield 122 mg of **7** as a yellow solid (34%). ^{1}H NMR (400 MHz, Chloroform-*d*) δ 7.58 (d, *J* = 8.7 Hz, 1H), 7.34 – 7.09 (m, 5H), 7.02 (d, *J* = 2.3 Hz, 1H), 6.95 (dd, *J* = 8.6, 2.3 Hz, 1H), 6.26 (q, *J* = 1.3 Hz, 1H), 4.15 (s, 2H), 3.24 (s, 2H), 2.42 (d, *J* = 1.3 Hz, 3H), 2.20 (s, 3H), 1.97 (s, 3H), 1.51 (s, 6H). ^{13}C NMR (101 MHz, $CDCl_3$) δ 188.41, 183.53, 170.52, 160.38, 154.09, 152.74, 151.90, 151.84, 148.45, 140.35, 140.25, 137.49, 128.97, 128.49, 127.23, 125.39, 117.92, 117.86, 114.55, 110.39, 47.42, 38.30, 38.20, 28.75, 18.73, 14.83, 14.77.

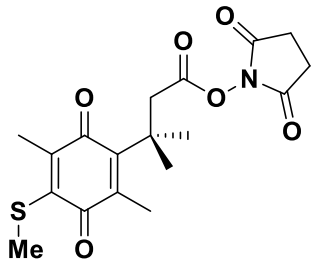

2,5-dioxopyrrolidin-1-yl 3-(2,5-dimethyl-4-(methylthio)-3,6-dioxocyclohexa-1,4-dien-1-yl)-3-methylbutanoate (8). To a solution of **5a** in CH_2Cl_2 (5 mL) was added DMAP (8.4 mg, 0.07 mmol) and NHS (80.8 mg, 0.7 mmol). After cooling to 0 °C, EDCI was added (134.3 mg, 0.7 mmol), and the resulting solution was stirred for 1 h, then allowed to warm to r.t. over 24 h. Solvent was removed, then the crude material was purified by flash chromatography, eluting with 30% Ethyl acetate/Hexanes, collecting the major yellow band. Yield: 72 mg (29%). ^{1}H NMR (400 MHz, Chloroform-*d*) δ 3.26 (s, 2H), 2.79 (s, 4H), 2.47 (d, *J* = 0.9 Hz, 3H), 2.19 (s, 3H), 2.11 (s, 3H), 1.53 (s, 6H). ^{13}C NMR (101 MHz, cdcl$_3$) δ 187.53, 183.31, 168.83, 167.59, 150.17, 145.60, 142.47, 141.49, 44.11, 38.95, 29.70, 29.09, 25.54, 17.10, 14.55.

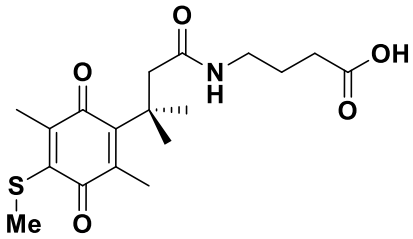

4-(3-(2,5-dimethyl-4-(methylthio)-3,6-dioxocyclohexa-1,4-dien-1-yl)-3-methyl-butanamido)-butanoic acid (9). To a solution of **8** (62.6 mg, 0.16 mmol) in 5 mL MeCN / 5 mL aqueous buffer (pH =7), followed by *gamma*-aminobutryic acid (29 mg, 0.28 mmol). K_2CO_3 was added to adjust the pH (20 mg, 0.14 mmol), and the stirred reaction was monitored by TLC. After 3 hours, removed solvent and flashed (7.5% MeOH, 1% AcOH, DCM), collecting the first eluting yellow bad. ^{1}H NMR (400 MHz, Chloroform-*d*) δ 3.26 (s, 2H), 2.79 (s, 4H), 2.47 (s, 3H), 2.19 (s, 3H), 2.11 (s, 3H), 1.53 (s, 6H). ^{13}C NMR (101 MHz, cdcl$_3$) δ 188.75, 183.54, 177.58, 172.51, 153.56, 147.06, 141.39, 138.88, 49.12, 38.74, 38.43, 31.41, 28.92, 24.72, 17.18, 14.83, 14.49. HRMS (ESI) calculated 366.1380 for $C_{18}H_{24}NO_5S$ [M-H]$^-$, found 366.1389.

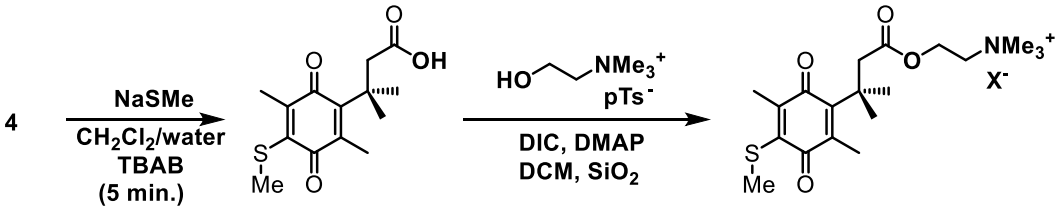

Prepared from **4** (173.3 mg, 0.55 mmol), NaSMe (250 mg), TBAB (23.3 mg), choline tosylate (150.3 mg), DIC (0.1 mL), and DMAP (7.9 mg). The tosylate salt was used for solubility reasons, but the counterion was exchanged on chromatography. The crude product was loaded onto a silica gel column and eluted with 0-10% MeOH / DCM gave 137.8 mg of a yellow solid (65% over two steps). ^{1}H NMR (300 MHz, Chloroform-*d*) δ 4.48 (d, *J* = 5.5 Hz, 2H), 4.22 – 4.00 (m, 2H), 3.56 (s, 9H), 3.03 (s, 2H), 2.50 (s, 3H), 2.19 (s, 3H), 2.09 (s, 2H), 1.43 (s, 6H).

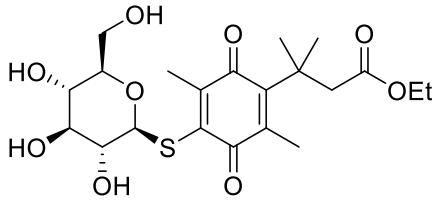

ethyl 3-(2,5-dimethyl-3,6-dioxo-4-(((2S,3R,4S,5S,6R)-3,4,5-trihydroxy-6-(hydroxymethyl)-tetrahydro-2H-pyran-2-yl)thio)cyclohexa-1,4-dien-1-yl)-3-methylbutanoate. To a solution of **4** in methylene chloride / water / acetonitrile with tetrabutylammonium bromide (5%) was added excess sodium 1-thio-β-D-glucose, and the reaction was vigoursly stirred until the complete consumption of **4** was observed by HPLC. The mixture was diluted with methylene chloride and brine to form two layers, then the yellow organic layer was separated, washed with brine, dried, then filtered through a plug of silica gel with 100% ethyl acetate to yield **24** as a pale yellow oil. ^{1}H NMR (500 MHz, Chloroform-*d*) δ

4.78 (dd, *J* = 9.7, 2.9 Hz, 1H), 4.03 (q, *J* = 7.1 Hz, 2H), 3.76 (qd, *J* = 12.4, 3.6 Hz, 2H), 3.60 (dt, *J* = 33.9, 9.0 Hz, 2H), 3.44 – 3.25 (m, 2H), 3.09 (d, *J* = 16.2 Hz, 1H), 2.72 (d, *J* = 16.2 Hz, 1H), 2.18 (d, *J* = 26.3 Hz, 6H), 1.41 (d, *J* = 6.1 Hz, 6H), 1.19 (t, *J* = 7.1 Hz, 3H). ^{13}C NMR (126 MHz, cdcl$_3$) δ 188.76, 184.31, 173.05, 154.45, 153.94, 138.90, 135.65, 85.51, 79.98, 77.64, 73.58, 69.76, 62.10, 60.59, 47.48, 38.09, 28.52, 28.15, 15.84, 14.68, 14.16.

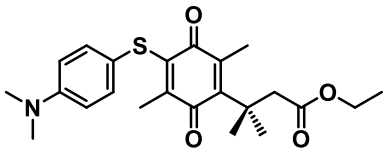

25. 50 mg quinone, 22.3 mg thiphenol, 0.34 mL (0.425 M) NaOAc in MeOH, 7mL MeOH total. P9nb5 Flashed 15-30% EtOAc/Hexanes. ^{1}H NMR (400 MHz, Chloroform-*d*) δ 7.34 – 7.28 (m, 2H), 6.68 – 6.56 (m, 2H), 4.03 (q, *J* = 7.1 Hz, 2H), 2.94 (s, 6H), 2.93 (s, 2H), 2.09 (d, *J* = 3.8 Hz, 6H), 1.42 (s, 6H), 1.18 (t, *J* = 7.1 Hz, 3H). ^{13}C NMR (101 MHz, cdcl$_3$) δ 189.13, 183.64, 172.45, 152.98, 150.03, 147.28, 141.04, 139.38, 134.21, 133.90, 118.08, 112.65, 112.47, 60.20, 47.62, 40.31, 38.23, 28.70, 14.85, 14.58, 14.23. UV-vis: $\lambda_{max(vis)}$: 426 nm (1,000 M^{-1}cm^{-1}), 500 nm (shoulder, ε = 900 M^{-1}cm^{-1}).

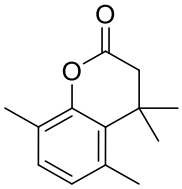

4,4,5,8-tetramethylchroman-2-one (23-Me). Prepared according to a literature procedure.[47] 2,5-Dimethylphenol (14.4066 g, 0.10 mol), 3,3,-dimethylacrylic acid (11.1237 g, 0.11 mol), and methanesulfonic acid (100 mL) were added to a round bottom flask equipped with a magnetic stir bar and the resulting mixture was heated at 70 °C for 48 h. The deep red solution was poured into water and the precipitated oil was extracted with ethylacetate (3 x 100 mL). The organic layer was washed with 5% KOH (5x50 mL), then 5% phosphoric acid (50 mL), and finally brine before drying ($MgSO_4$). The solvent was evaporated to yield an oil, which was recrystallized with ether/hexanes to give **29** as a white solid (3.31g, 14.6%). ^{1}H NMR (300 MHz, Chloroform-*d*) δ 6.98 (d, *J* = 7.7 Hz, 1H), 6.81 (d, *J* = 7.7 Hz, 1H), 2.59 (s, 2H), 2.46 (s, 3H), 2.26 (s, 3H), 1.45 (s, 6H). ^{13}C NMR (101 MHz, $CDCl_3$) δ 168.32, 149.78, 133.53, 129.51, 129.10, 127.98, 124.55, 45.64, 35.36, 27.65, 23.07, 16.25. HRMS (ESI) calculated for $C_{13}H_{17}O_2^+$ requires 205.1223, found 205.1231.

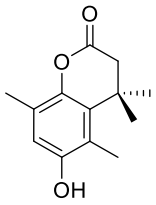

6-hydroxy-4,4,5,8-tetramethylchroman-2-one (24-Me). The Elbs persulfate oxidation of **29** to **3** was carried out following general methods.[48,49] A mixture of **29** (10.070 g, 49 mmol) and NaOH (9.78 g, 244 mmol) in 100 mL water and 75 mL methanol was refluxed for 12 h under argon to hydrolyze the lactone, then cooled to 15 °C. Ammonium persulfate (11.249 g, 49 mmol) was added as a solution in 150 mL of water slowly while keeping the temperature below 20 °C. The resulting dark brown solution was carefully acidified to pH = 5 and filtered to recover unreacted starting material. The aqueous solution was then extracted twice with ether to further recover starting material, then strongly acidified to pH = 0 with HCl (aq) and refluxed until LCMS indicated complete conversion of the intermediate sulfate to the product. The resulting orange solution was cooled to precipitate the **3** as a yellow solid (3.8 g, 35 %) collected by filtration.

Synthesis of amine derivatives. An alternative approach was developed to allow incorporation of more diverse substituents, such as amines (**Scheme S1**). The procedure is general can be carried out in large scale reactions from commercially available 2-R-5-methylphenols and inexpensive reagents. For 2,5-dimethylphenol, the procedure is equally applicable and intercepts the synthesis of **6-9** at compound **3**.

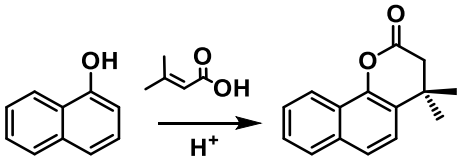

4,4-dimethyl-3,4-dihydro-2H-benzo[h]chromen-2-one (35). 1-Napthol (10 g, 69 mmol) and 3,3-dimethylacrylic acid (13.9 g, 139 mmol) were refluxed in 140 mL of toluene over amberlyst 15 catalyst (1 g). After 2 d, the mixture was filtered through celite while hot, then concentrated. Crude NMR indicated a 75:25 mixture of lactone:ether. Purification by double extraction as with **4** followed by column chromatography afforded the lactone.

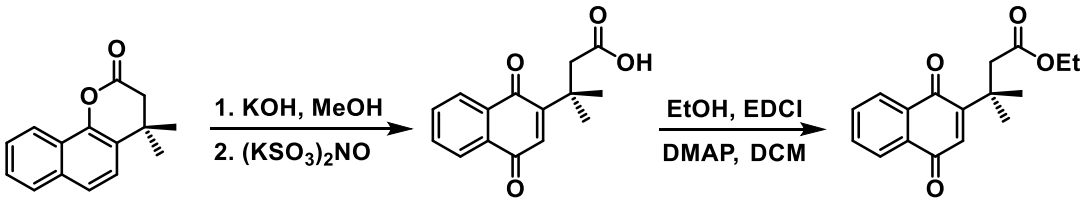

3-(1,4-dioxo-1,4-dihydronaphthalen-2-yl)-3-methylbutanoic acid (36). The naphthoquinone lactone (446.8 mg KOH, 8 mmol) was heated in methanol with KOH (811.6 mg, 3.6 mmol), before oxidation with Fremy's salt (2.3929 g, 8.92 mmol) in buffer (760 mg NaH_2PO_4 in 200 mL water) to give the naphthoquinone acid in 70% yield: ^{1}H NMR (400 MHz, Chloroform-*d*) δ 8.13 – 7.92 (m, 2H), 7.81 – 7.61 (m, 2H), 6.81 (d, *J* = 1.4 Hz, 1H), 3.04 (d, *J* = 1.7 Hz, 2H), 1.38 (d, *J* = 1.7 Hz, 6H).

ethyl 3-(1,4-dioxo-1,4-dihydronaphthalen-2-yl)-3-methylbutanoate (37). The crude product was immediately treated with ethanol and EDCI/DMAP in dichloromethane to give the ethyl ester. ^{1}H NMR (600 MHz, Chloroform-*d*) δ 8.12 – 8.07 (m, 1H), 8.07 – 8.00 (m, 1H), 7.78 – 7.67 (m, 2H), 6.82 (s, 1H), 3.96 (q, *J* = 7.1 Hz, 2H), 3.02 (s, 2H), 1.41 (s, 6H), 1.05 (t, *J* = 7.1 Hz, 3H). ^{13}C NMR (126 MHz, Chloroform-*d*) δ 185.52, 185.13, 171.61, 156.23, 134.46, 133.72, 133.37, 131.60, 126.87, 125.68, 60.15, 45.47, 37.71, 28.24, 14.04.

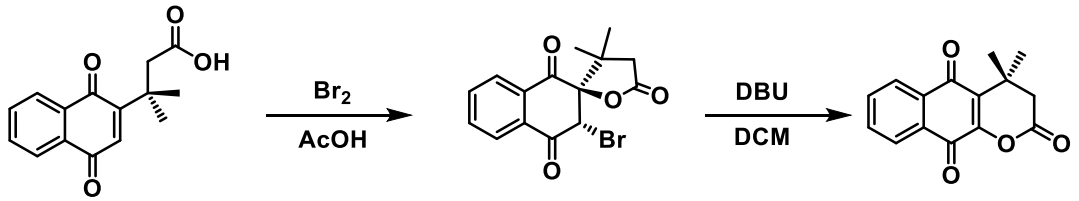

(2R,3'S)-3'-bromo-3,3-dimethyl-3,4-dihydro-1'H,5H-spiro[furan-2,2'-naphthalene]-1',4',5(3'H)-trione (38). To a solution of naphthoquinone (500 mg, 1.9 mmol) in glacial acetic acid was added bromine (0.11 mL). After TLC indicated complete conversion, the solvent was removed via rotovap with heating (40 °C). The crude product was recrystallized to give 226.4 mg (35%). of the product as white needles. Stereochemistry is assigned based on an NOE data. ^{1}H NMR (500 MHz, Chloroform-*d*) δ 8.19 (d, *J* = 7.2 Hz, 1H), 8.11 (d, *J* = 7.4 Hz, 1H), 7.92 – 7.79 (m, 2H), 5.03 (s, 1H), 2.73 (d, *J* = 17.2 Hz, 1H), 2.43 (d, *J* = 17.2 Hz, 1H), 1.30 (s, 3H), 0.81 (s, 3H). MS(ESI$^+$): [M+Na$^+$] = 360.9, 358.9 (1:1).

4,4-dimethyl-3,4-dihydro-2H-benzo[g]chromene-2,5,10-trione (39). Treating the spirocycle with DBU in methylene chloride gave the lawsone lactone. ^{1}H NMR (600 MHz,

Chloroform-*d*) δ 8.14 – 8.11 (m, 1H), 8.09 – 8.06 (m, 1H), 7.80 – 7.76 (m, 1H), 7.76 – 7.72 (m, 1H), 2.66 (s, 2H), 1.53 – 1.49 (m, 6H).

8-chloro-4,4,5-trimethylchroman-2-one (25). Prepared according to literature procedure.[4] 2-Chloro-5-methylphenol (14.4066 g, 0.10 mol) and 3,3,-dimethylacrylic acid (11.1237 g, 0.11 mol) were dissolved in methanesulfonic acid (100 mL), and the resulting mixture was heated at 70 °C for 48 h. The resulting solution was poured into water and extracted with ethylacetate (3 x 100 mL). The organic layer was washed with 5% KOH (5x50 mL), then 5% phosphoric acid (50 mL), and finally brine before drying ($MgSO_4$). The solvent was evaporated to yield an oil, which was recrystallized with ether/hexanes to give **25** as a white solid (3.31g, 14.6%). ^{1}H NMR (500 MHz, Chloroform-*d*) δ 7.19 (d, *J* = 8.3 Hz, 1H), 6.85 (dd, *J* = 8.2, 0.8 Hz, 1H), 2.63 (s, 2H), 2.48 (d, *J* = 0.7 Hz, 3H), 1.46 (s, 6H). ^{13}C NMR (126 MHz, cdcl$_3$) δ 166.77, 147.16, 134.83, 131.53, 128.60, 128.26, 120.35, 45.27, 35.90, 27.40, 27.39, 23.04.

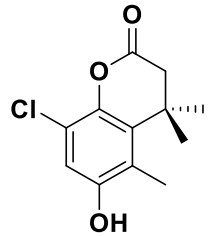

8-chloro-6-hydroxy-4,4,5-trimethylchroman-2-one (26). The Elbs persulfate oxidation of **25** to **26** was carried out following general methods.[2,3] A mixture of **25** (2.2473 g, 10 mmol) and NaOH (2.0549 g, 51 mmol) in 20 mL water and 20 mL methanol was refluxed for 12 h under argon to hydrolyze the lactone, then cooled to 15 °C. Ammonium persulfate (2.2827 g, 10 mmol) was added as a solution in 60 mL of water slowly over 5 h while keeping the temperature below 20 °C. The resulting dark brown solution was carefully acidified to pH = 5 and filtered to recover unreacted starting material. The aqueous solution was then extracted twice with ether to further recover starting material, then strongly acidified to pH = 0 with HCl (aq) and refluxed until LCMS indicated complete conversion of the intermediate sulfate to the product (1 h). The resulting orange solution was cooled to precipitate **26** as a yellow solid (0.9296 g, 38.6%) collected by filtration. ^{1}H NMR (500 MHz, Chloroform-*d*) δ 6.83 (d, *J* = 0.5 Hz, 1H), 5.08 (s, 1H), 2.60 (s, 2H), 2.34 (d, *J* = 0.5 Hz, 3H), 1.48 (s, 6H). ^{1}H NMR (500 MHz, DMSO-d_6) δ 9.75 (s, 1H), 6.85 (s, 1H), 2.69 (s, 2H), 2.23 (s, 3H), 1.37 (s, 6H). ^{13}C NMR (126 MHz, DMSO-d_6) δ 167.20, 152.23, 139.52, 133.15, 121.92, 117.63, 113.74, 44.47, 35.81, 26.87, 13.88. HRMS (ESI) calculated 239.0480 for $C_{12}H_{12}ClO_3$ [M-H]$^-$, found 239.0485.

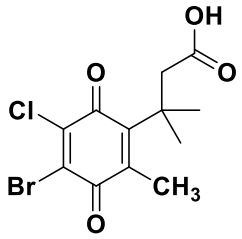

3-(4-bromo-5-chloro-2-methyl-3,6-dioxocyclohexa-1,4-dien-1-yl)-3-methylbutanoic acid (27). To a solution of **26** (1.0531 g, 4.38 mmol) dissolved in glacial acetic acid (50 mL) was added Br_2 (0.5 mL, 9.6 mmol). The resulting solution was stirred in the dark overnight, then diluted with water and extracted with ethyl acetate. The combined organic layers were washed with brine, dried ($MgSO_4$) and concentrated to give a 1.47 g (100%) of **27** as a yellow solid. The crude product was used without further purification. ^{1}H NMR (500 MHz, Chloroform-*d*) δ 3.04 (s, 2H), 2.25 (s, 3H), 1.47 (s, 6H). ^{13}C NMR (126 MHz, cdcl$_3$) δ 180.26, 178.66, 178.30, 152.91, 145.20, 139.60, 132.38, 47.15, 38.66, 28.58, 15.41. HRMS (ESI) calculated 332.9535 for $C_{12}H_{11}BrClO_4^-$, found 334.9517.

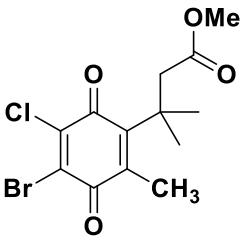

methyl 3-(4-bromo-5-chloro-2-methyl-3,6-dioxocyclohexa-1,4-dien-1-yl)-3-methyl-butanoate (10). To a solution of **27** (1.5241 g, 4.5 mmol) in 5 mL dichloromethane at 0 °C was added anhydrous methanol (0.73 mL, 18 mmol) followed by N-(3-dimethylaminopropyl)-N'-ethylcarbodiimide hydrochloride (877.4 mg, 4.5 mmol) and 4-(dimethylamino)pyridine (56.8 mg, 10%) in one portion. The resulting solution was protected from light and stirred for 5 min, then allowed to warm to room temperature overnight. The solvent was removed, and the crude product was taken up in a minimal amount of dichloromethane, diluted with hexanes and purified by flash chromatography (10% ethylacetate / hexanes), with the product eluting as a yellow band. The combined fractions were concentrated to give a yellow oil (0.9686 g, 61%). ^{1}H NMR (500 MHz, Chloroform-*d*) δ 3.60 (s, 3H), 2.98 (s, 2H), 2.24 (s, 3H), 1.45 (s, 6H). ^{13}C NMR (126 MHz, cdcl$_3$) δ 180.43, 178.82, 173.21, 153.69, 145.48, 139.27, 132.50, 51.81, 47.47, 39.02, 28.70, 15.50.

General reaction conditions for addition to dihalidequinone 10: To a solution of quinone in methanol was added 1 equivalent of nucleophile, and 1 equivalent of base (NaOAc or K_2CO_3). The mixture was stirred under air, protected from light, until TLC indicated complete conversion. Solvent was removed and the residue was taken up in a minimal amount of dichloromethane, which was diluted with hexanes before purification by flash chromatography, eluting with ethyl acetate/hexanes. In general, the amount of hexanes used to load the column does not matter because the quinone will not elute without ethyl acetate in the solvent mixture. Reaction progress and purification are greatly facilitated by knowing the expected color of the desired product: pale yellow (quinone), mustard-dark yellow (sulfides), orange-red (disulfide), red-purple (amine), purple-blue (arylamines / phenothiazines).

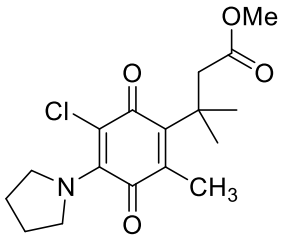

methyl 3-(5-chloro-2-methyl-3,6-dioxo-4-(pyrrolidin-1-yl)-cyclohexa-1,4-dien-1-yl)-3-methyl-butanoate (11). To a solution of **10** (471 mg, 1.35 mmol) in methanol (50 mL) was added 0.25 mL pyrrolidine, and the resulting solution was stirred, protected from light, until TLC indicated the reaction was complete. The desired product **(11;** cherry-red band) was carefully separated from the other substitution product (orange-red band) by flash chromatography (30% ether / hexanes) as a red solid (14% yield by NMR). ^{1}H NMR (500 MHz, Chloroform-*d*) δ 3.85 – 3.78 (m, 4H), 3.60 (s, 3H), 3.09 (s, 2H), 2.13 (s, 3H), 1.93 – 1.84 (m, 4H), 1.45 (s, 6H). ^{13}C NMR (126 MHz, Chloroform-*d*) δ 186.05, 181.00, 173.12, 152.46, 147.88, 135.08, 106.40, 52.94, 51.29, 47.88, 38.92, 29.32, 25.50, 13.95. HRMS (ESI) calculated 340.1310 for $C_{17}H_{23}ClNO_4$ $[M+H]^+$, found 340.1311. UV/vis: λ_{max} = 497 nm (ε = 2,800 $M^{-1}cm^{-1}$).

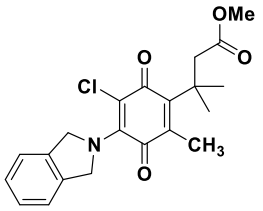

methyl 3-(5-chloro-4-(isoindolin-2-yl)-2-methyl-3,6-dioxocyclohexa-1,4-dien-1-yl)-3-methyl-butan-oate (12). To a solution of **10** (359 mg) in methanol (20 mL) was added 0.26 mL isoindoline, and the resulting solution was stirred, protected from light, until TLC indicated the reaction was complete. The desired product, **12**, (cherry-red band) was carefully separated from the other substitution product (orange-red band) by flash chromatography (30% ether / hexanes) as a red solid (50% yield by NMR). ^{1}H NMR (400 MHz, Chloroform-*d*) δ 7.38 – 7.27 (m, 4H), 5.22 (s, 4H), 3.59 (s, 3H), 3.07 (s, 2H), 2.17 (s, 3H), 1.45 (s, 6H). HRMS calculated 388.1310, found 388.1311. UV/vis: λ_{max} = 483 nm.

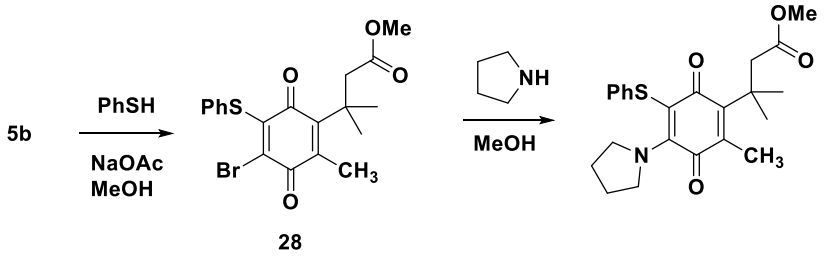

methyl 3-methyl-3-(2-methyl-3,6-dioxo-5-(phenylthio)-4-(pyrrolidin-1-yl)cyclohexa-1,4-dien-1-yl)-butanoate (13). To a 25 mL round bottom flask equipped with stirbar under argon was added **10** (351 mg, 1 mmol), thiophenol (122 mg, 1.1 mmol), and methanol (15 mL), and the resulting solution was cooled to -78 °C. Sodium acetate (180 mg, 2.2 mmol) was added dropwise as a 0.845 M solution in methanol, and the resulting mixture was allowed to warm to room temperature. When TLC indicated the reaction was complete, the solvent was removed and the crude product was purified on silica gel (7.5 % ethyl acetate / hexanes). The first band (yellow) eluted was starting material, the second band (orange) was product, and the third band (red-orange) is the disubstituted byproduct. The pure fractions from the orange band were pooled and concentrated to yield **28** as an orange oil (319.8 mg, 75%). ^{1}H NMR (500 MHz, Chloroform-*d*) δ 7.58 – 7.51 (m, 2H), 7.36 – 7.25 (m, 3H), 3.61 (s, 3H), 2.60 (s, 2H), 2.20 (s, 3H), 1.29 (s, 6H). ^{13}C NMR (126 MHz, cdcl$_3$) δ 183.21, 177.86, 172.60, 154.91, 152.44, 138.34, 133.97, 130.86, 129.04, 128.93, 128.90, 77.41, 77.16, 76.91, 51.62, 46.73, 38.80, 28.61, 15.04. To a solution of **28** (57 mg, 0.135 mmol) in methanol (5mL) was added pyrroldine (20.8 mg, 0.292 mmol) as a 10% (v/v) solution in methanol. The resulting solution was stirred,

protected from light, as it turned from orange to red. Once TLC indicated the reaction was complete, the solvent was evaporated, and the crude residue was purified on silica (10% EtOAc / Hexanes) to yield 53 mg of **13** as a red solid (95%). ^{1}H NMR (500 MHz, Chloroform-*d*) δ 7.17 (tt, *J* = 7.4, 1.8 Hz, 2H), 7.14 – 7.07 (m, 2H), 7.06 – 6.98 (m, 1H), 3.86 – 3.71 (m, 4H), 3.59 (s, 3H), 3.04 (s, 2H), 2.17 (s, 3H), 1.85 – 1.75 (m, 4H), 1.44 (s, 6H). ^{13}C NMR (126 MHz, cdcl$_3$) δ 187.53, 183.74, 173.27, 156.18, 155.25, 139.77, 134.71, 128.60, 125.32, 124.38, 97.41, 52.71, 51.20, 47.69, 38.81, 29.05, 25.22, 13.68. HRMS: Calculated 414.1734 for $C_{23}H_{28}NO_4S$ $[M+H]^+$, found 414.1753. UV/vis: λ_{max} = 476 nm (ε = 2,700 $M^{-1}cm^{-1}$).

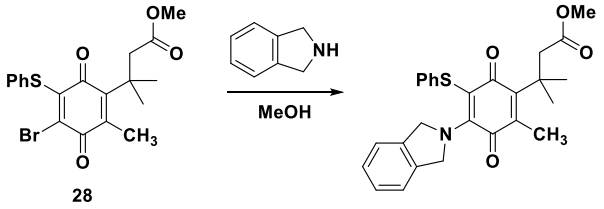

methyl 3-(4-(isoindolin-2-yl)-2-methyl-3,6-dioxo-5-(phenylthio)cyclohexa-1,4-dien-1-yl)-3-methyl-butanoate (14). To a solution of **28** (114 mg, 0.27 mmol) in methanol (20 mL), was added 70 μL isoinodoline. The solution was stirred in the dark until TLC indicated the reaction was complete. The solvent was removed and the crude material was purified by silica gel (10% ethylacetate / hexanes) to yield **14** as a red solid (110 mg, 88%). ^{1}H NMR (400 MHz, Chloroform-*d*) δ 7.29 – 7.16 (m, 9H), 7.12 – 7.04 (m, 1H), 5.21 (s, 4H), 3.62 (s, 3H), 3.04 (s, 2H), 2.24 (s, 3H), 1.46 (s, 6H). ^{13}C NMR (101 MHz, $CDCl_3$) δ 187.34, 183.85, 173.17, 156.50, 155.54, 139.37, 135.43, 134.63, 128.79, 127.57, 125.51, 124.71, 122.00, 98.00, 58.33, 51.27, 47.60, 38.83, 28.95, 13.59. HRMS (ESI) calculated 462.1734 for $C_{27}H_{28}NO_4S$ $[M+H]^+$, found 462.1763. UV/vis: λ_{max} = 467 nm (ε = 3,000 $M^{-1}cm^{-1}$).

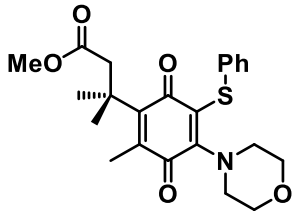

methyl 3-methyl-3-(2-methyl-4-morpholino-3,6-dioxo-5-(phenylthio)cyclohexa-1,4-dien-1-yl)butanoate. To a solution of quinone (39.5 mg, 0.09 mmol) in methanol was added morpholine (0.03 mL, 0.34 mmol). The resulting solution was slow to change color, and therefore stirred overnight in the dark. Removing solvent and purification by flash chromatography (SiO_2, 15% EtOAc / Hexanes) collecting the red band gave 32.2 mg (80%) of the desired product. ^{1}H NMR (600 MHz, Chloroform-*d*) δ 7.25 – 7.20 (m, 5H), 7.16 –

7.11 (m, 1H), 3.68 – 3.64 (m, 4H), 3.55 (s, 3H), 3.48 – 3.41 (m, 4H), 2.94 (s, 2H), 2.18 (s, 3H), 1.40 (s, 6H). MS(ESI$^+$): 430.1.

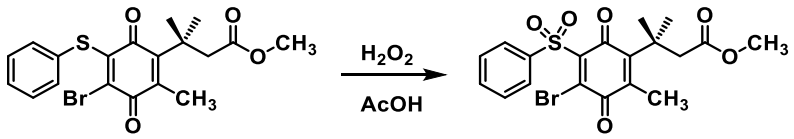

methyl 3-(4-bromo-2-methyl-3,6-dioxo-5-(phenylsulfonyl)cyclohexa-1,4-dien-1-yl)-3-methylbutanoate. (To a solution of thiophenolquinone (47.2 mg, 0.11 mmol) at 50 °C in 5 mL of glacial acetic acid was added 0.05 mL H_2O_2 (30% aq). The resulting solution was refluxed (110-115 °C) with addition of H_2O_2 as necessary until TLC indicated the reaction was complete. The mixture was concentrated and the resulting yellow residue was dissolved in water / ethyl acetate. The organic layer was washed with water, sodium bicarbonate, and brine before drying ($MgSO_4$) and filtering. Removing solvent gave 47.2 mg (93% yield) of the pure sulfone. ^{1}H NMR (600 MHz, Chloroform-*d*) δ 8.21 (dd, *J* = 8.1, 1.4 Hz, 2H), 7.65 (t, *J* = 7.4 Hz, 1H), 7.55 (t, *J* = 7.7 Hz, 2H), 3.68 (s, 3H), 2.86 (s, 2H), 2.17 (s, 3H), 1.41 (s, 6H). If not enough H_2O_2 is added, the sulfoxide is present in the crude product.

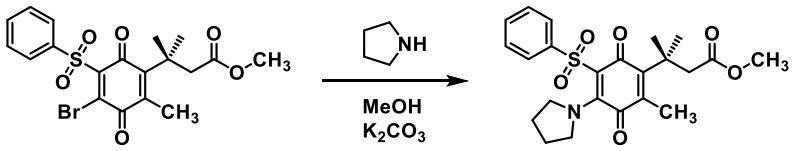

methyl 3-methyl-3-(2-methyl-3,6-dioxo-5-(phenylsulfonyl)-4-(pyrrolidin-1-yl)cyclohexa-1,4-dien-1-yl)butanoate (27). To a mixture of thiosulfonequinone (47.2 mg, 0.1 mmol) suspended in 20 mL of methanol at 0 °C was added pyrrolidine (0.0074 g, 0.1 mmol) as a solution in MeOH, and the resulting orange solution was stirred overnight over K_2CO_3 (27 mg, 0.2 mmol). When TLC indicated complete conversion of the sulfone, the reaction was concentrated. The residue was dissolved in dichloromethane, washed with aqueous bicarbonate and brine, then dried ($MgSO_4$), filtered and concentrated to give the product as an orange solid in quantitative yield. ^{1}H NMR (600 MHz, Chloroform-*d*) δ 7.91 (d, *J* = 7.2, 1.3 Hz, 2H), 7.45 (t, 1H), 7.41 (t, 2H), 4.10 – 3.88 (m, 4H), 3.47 (s, 3H), 2.90 (s, 2H), 2.09 (s, 3H), 1.99 (q, *J* = 4.6, 2.9 Hz, 4H), 1.30 (s, 6H). UV-vis: $\lambda_{max(vis)}$: 444 nm (1,900 $M^{-1}cm^{-1}$).

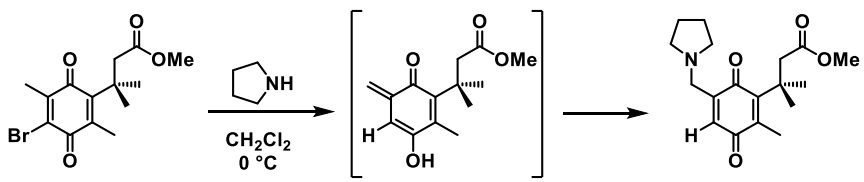

methyl 3-methyl-3-(2-methyl-3,6-dioxo-5-(pyrrolidin-1-ylmethyl)cyclohexa-1,4-dien-1-yl)butanoate (28). Prepared by action of pyrrolidine in dichloromethane. Orange-red product. ^{1}H NMR (600 MHz, Chloroform-*d*) δ 6.67 (t, *J* = 1.9 Hz, 1H), 3.57 (s, 3H), 3.44 (d, *J* = 1.9 Hz, 2H), 2.61 – 2.53 (m, 5H), 2.15 (s, 4H), 1.84 – 1.74 (m, 5H).

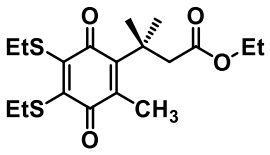

ethyl-3-(4,5-bis(ethylthio)-2-methyl-3,6-dioxocyclohexa-1,4-dien-1-yl)-3-methyl-butanoate (28). Prepared by action of excess thioethanol on 2-methoxyl-3-bromo-QTML derivative. ^{1}H NMR (600 MHz, Chloroform-*d*) δ 4.09 – 3.99 (m, 2H), 3.06 (q, *J* = 7.4 Hz, 2H), 2.98 (q, *J* = 7.5, Hz, 2H), 2.89 (s, 2H), 2.14 (s, 3H), 1.42 (s, 6H), 1.27 (t, *J* = 7.6 Hz, 3H), 1.25 (t, *J* = 7.3 Hz, 3H), 1.19 (t, *J* = 7.1 Hz, 2H). $\lambda_{max(vis)}$ =447 nm (4,000 $M^{-1}cm^{-1}$).

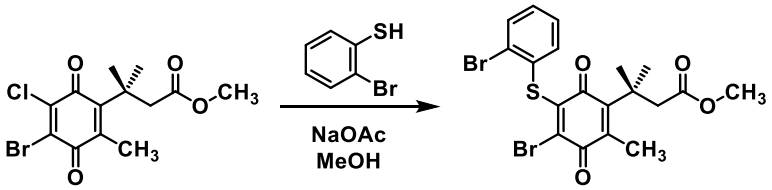

methyl 3-(4-bromo-5-((2-bromophenyl)thio)-2-methyl-3,6-dioxocyclohexa-1,4-dien-1-yl)-3-methylbutanoate. To a stirred solution of quinone (200 mg, 0.57 mmol) in MeOH at 0 °C was added 2-bromothiophenol (0.73 mL of a 10.6 % (v/v) methanol solution, 0.643 mmol) followed by dropwise addition of 5.2 mL 0.11 M NaOAc solution in MeOH (0.57 mmol) over 5-10 min. The pale yellow solution turned to deep yellow then orange-red. Removal of solvent and purification by flash chromatography (6.7% EtOac/Hexanes) collecting the yellow band gave 107 mg (37% isolated yield). A pale yellow compound (starting material) eluted first, and an orange compound (disubstituted) eluted after the desired mono-substituted product (yellow solid). ^{1}H NMR (600 MHz, Chloroform-*d*) δ 7.58 (td, *J* = 7.8, 1.6 Hz, 2H), 7.21 (td, *J* = 7.5, 1.5 Hz, 1H), 7.16 (td, *J* = 7.6, 1.7 Hz, 1H), 3.60 (s, 3H), 2.66 (s, 2H), 2.21 (s, 3H), 1.29 (s, 6H). MS (m/z$^+$) [M+Na$^+$]: 524.9 (100.0%), 522.9 (50%), 526.9 (50%).

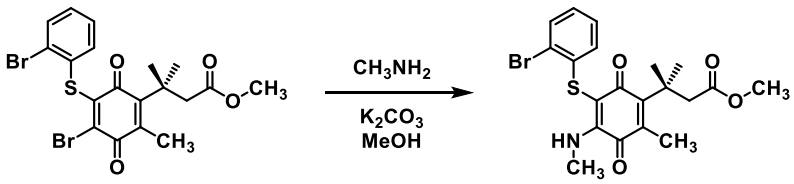

methyl 3-(5-((2-bromophenyl)thio)-2-methyl-4-(methylamino)-3,6-dioxocyclohexa-1,4-dien-1-yl)-3-methylbutanoate. To a stirred solution of bromoquinone (97.5 mg, 0.19 mmol) in methanol at 0 °C was added 40% methyl amine (0.22 mmol) followed by K_2CO_3 (28 mg, 0.2 mmol). The resulting solution was stirred, protected from light, until TLC indicated complete conversion. The solvent was evaporated and the residue purified by chromatography (10% EtOAc/Hexanes) collecting the red band to yield 33.8 mg (38%) of a red solid.

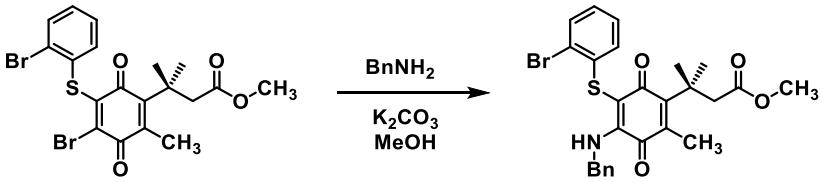

methyl 3-(4-(benzylamino)-5-((2-bromophenyl)thio)-2-methyl-3,6-dioxocyclohexa-1,4-dien-1-yl)-3-methylbutanoate. To a stirred solution of bromoquinone (161.6 mg, 0.32 mmol) in 30 mL methanol at 0 °C was added benzylamine (0.031 mL, 0.3 mmol) followed by K_2CO_3 (44.2 mg, 0.32 mmol). The resulting solution was stirred, protected from light, until TLC indicated complete conversion. The solvent was evaporated and the residue purified by chromatography (10% EtOAc/Hexanes) collecting the red band to yield 81.1 mg (48%) of a red solid.

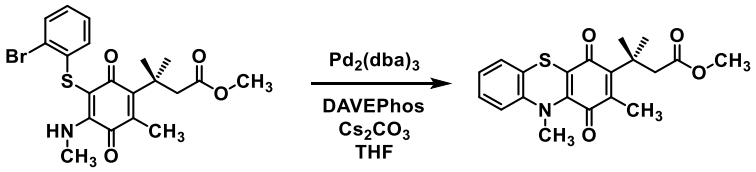

methyl-3-(2,10-dimethyl-1,4-dioxo-4,10-dihydro-1H-phenothiazin-3-yl)-3-methyl-butanoate (33). To a flask under argon was added quinone substrate (33.8 mg, 0.075 mmol), Cs_2CO_3 (26.2 mg, 0.08 mmol), $Pd_2(dba)_3$ (4.7 mg, 5×10^{-6} mol), DAVEPhos (4.8 mg, 1.2×10^{-5} mol), and 4 mL of THF. The resulting solution was refluxed in darkness under argon overnight. After cooling, solvent was removed and the residue was purified by chromatography (10% EtOAc / Hexanes). Collecting the blue band gave 8.6 mg of the phenothiazine (78 % based on 16.1 mg (48%) recovered starting material). UV-vis: $\lambda_{max(vis)}$ = 648 nm (1,900 $M^{-1}cm^{-1}$).

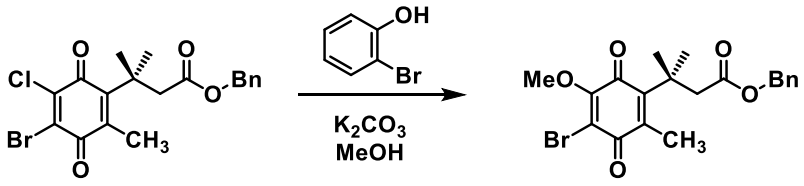

benzyl-3-(4-bromo-5-methoxy-2-methyl-3,6-dioxocyclohexa-1,4-dien-1-yl)-3-methyl-butanoate. Prepared according to the general method from 112.5 mg **10**, 28 μL 2-bromophenol, 37 mg K_2CO_3 in 10 mL MeOH. After the pale yellow solution turned darker yellow, solvent was removed and the residue flashed (10% EtOAc / Hexanes), collecting the yellow band. The undesired methoxy derivative was isolated as the major product, 87.2 mg (78% isolated yield). ^{1}H NMR (600 MHz, Chloroform-*d*) δ 7.37 – 7.28 (m, 3H), 7.28 – 7.23 (m, 2H), 5.05 (s, 2H), 3.88 (s, 3H), 3.00 (s, 2H), 2.15 (s, 3H), 1.43 (s, 6H).

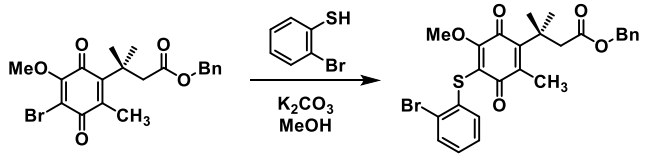

benzyl 3-(4-((2-bromophenyl)thio)-5-methoxy-2-methyl-3,6-dioxocyclohexa-1,4-dien-1-yl)-3-methylbutanoate. Treating methoxybromoquinone (87.2 mg) with 2-bromothiophenol (25 μL) in methanol with 1.9 mL of 0.11 M NaOAc solution in methanol gave the bromosubstituted product by LCMS.

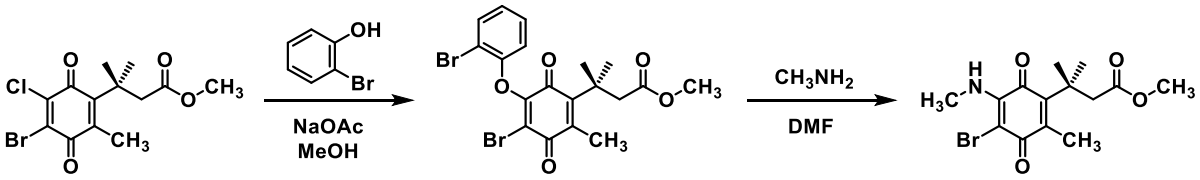

methyl-3-(4-bromo-2-methyl-5-(methylamino)-3,6-dioxocyclohexa-1,4-dien-1-yl)-3-methyl-butanoate. To a stirred solution of quinone (34.5 mg, 0.1 mmol) in 1.5 mL of dimethylformamide (DMF) was added a solution of 2-bromophenol (10 μL, 0.095 mmol) and Cs_2CO_3 (35 mg, 0.1 mmol) in 0.5 mL DMF. The major product by LCMS was the desired chloride substitution. Addition of 9 μL (1 equivalent) of 40% aqueous methylamine displaced the phenol by LCMS.

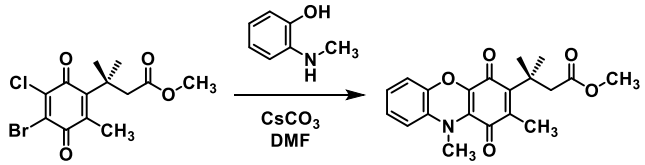

methyl-3-(2,10-dimethyl-1,4-dioxo-4,10-dihydro-1H-phenoxazin-3-yl)-3-methyl-butanoate (33). A flask under argon was loaded with 2-(methylamino)phenol (23.6 mg, 0.19

mmol), Cs_2CO_3 (123.2 mg, 0.38 mmol). Dimethylformamide (1 mL) was added, and the resulting mixture was stirred for 5 min before addition of quinone **10** in 4 mL DMF. The reaction was stirred, protected from light. After 1 h, the solution had turned blue, and after 6 h TLC indicated the reaction was complete. Aqueous workup and flash chromatography collecting the blue band afforded the phenoxazine. ^{1}H NMR (500 MHz, Chloroform-*d*) δ 6.80 (ddd, *J* = 7.9, 7.1, 2.0 Hz, 1H), 6.75 – 6.68 (m, 2H), 6.50 (dd, *J* = 7.8, 1.4 Hz, 1H), 3.64 (s, 3H), 3.02 (s, 3H), 2.92 (s, 2H), 2.12 (s, 3H), 1.43 (s, 8H).

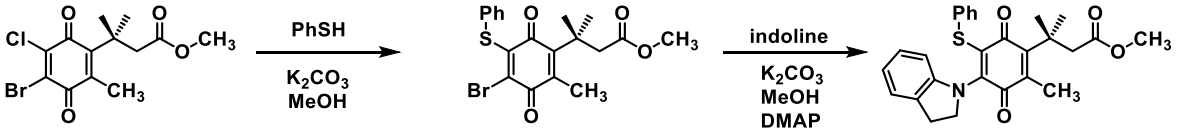

methyl 3-(4-(indolin-1-yl)-2-methyl-3,6-dioxo-5-(phenylthio)cyclohexa-1,4-dien-1-yl)-3-methylbutanoate (30). To 0.55 mmol **10** was sequentially added thiophenol (0.056 mL), and K_2CO_3 (79.4 mg, 0.57 mmol). When the reaction was complete by TLC, indoline (0.067 mL, 0.6 mmol) was added along with an additional equivalent of K_2CO_3 (75.5 mg, 0.55 mmol) and a catalytic amount of DMAP (5 mg, 5%). The resulting solution was stirred overnight, then concentrated and purified by flash chromatography. A mixture of diastereomers (rotation) or more likely regioisomers resulted. ^{1}H NMR (400 MHz, Chloroform-*d*) δ 7.20 – 6.74 (m, 13H), 6.47 (d, *J* = 7.9 Hz, 1H), 6.44 (d, *J* = 7.8 Hz, 2H), 3.96 (t, *J* = 8.1 Hz, 2H), 3.87 (t, *J* = 8.2 Hz, 4H), 3.68 (s, 5H), 3.63 (s, 3H), 3.04 (s, 2H), 2.96 (s, 4H), 2.32 (d, *J* = 8.2 Hz, 3H), 2.29 (s, 2H), 2.22 (s, 6H), 1.57 (s, 6H), 1.49 (s, 16H). UV-vis: $\lambda_{max(vis)}$: 560 nm.

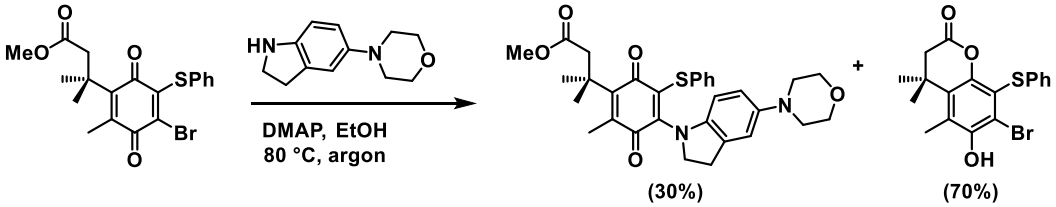

methyl 3-methyl-3-(2-methyl-4-(5-morpholinoindolin-1-yl)-3,6-dioxo-5-(phenylthio)-cyclohexa-1,4-dien-1-yl)butanoate (31). To a solution of bromoquinone (167.6 mg, 0.4 mmol) in degassed ethanol was added 4-(morpholinoino)indoline (154.1 mg, 0.75 mmol) and DMAP (10 mg). The solution was refluxed for 40 min, then $NaHCO_3$ was added and TLC indicated complete conversion. Evaporation of the solvent and purification of the residue by

column chromatography (SiO_2, 15% EtOAc / Hexanes), collecting the blue-green band, gave 81.5 mg (30%) of the desired product . ^{1}H NMR (400 MHz, Chloroform-*d*) δ 7.12 – 7.04 (m, 1H), 7.03 – 6.93 (m, 2H), 6.85 – 6.78 (m, 2H), 6.75 (dd, *J* = 8.6, 2.5 Hz, 1H), 6.61 – 6.54 (m, 1H), 6.48 (d, *J* = 8.6 Hz, 1H), 4.01 (t, *J* = 7.9 Hz, 2H), 3.96 – 3.78 (m, 4H), 3.62 (s, 3H), 3.16 – 3.08 (m, 4H), 3.06 (s, 2H), 2.24 (t, *J* = 7.9 Hz, 2H), 2.19 (s, 3H), 1.49 (s, 6H). ^{13}C NMR (101 MHz, $CDCl_3$) δ 185.40, 185.25, 173.04, 154.51, 146.90, 139.94, 136.70, 135.76, 135.24, 134.28, 129.85, 127.99, 126.75, 119.86, 116.40, 112.99, 112.73, 66.97, 54.25, 51.35, 50.73, 47.84, 38.83, 29.07, 14.31. UV-vis: $\lambda_{max(vis)}$ = 625 nm. The reduced and lactonized product was isolated in 70% yield. ^{1}H NMR (500 MHz, Chloroform-*d*) δ 7.24 – 7.08 (m, 4H), 5.77 (s, 1H), 2.48 (s, 2H), 2.47 (s, 3H), 1.47 (s, 6H). ^{13}C NMR (126 MHz, cdcl$_3$) δ 166.76, 148.20, 146.69, 135.96, 132.08, 128.94, 128.93, 128.09, 126.19, 125.54, 120.33, 117.66, 45.44, 36.16, 27.25, 15.73. MS(ESI$^+$): 393,391 (1:1).

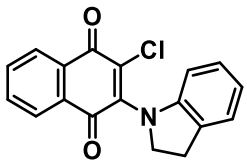

2-chloro-3-indolino-1,4-naphthoquinone. Indoline (5.6 mL, 50 mmol) and sodium acetate (2.50 g, 30.5 mmol) were added to a suspension of 2,3-dichloronaphthoquinone (5.6211 g, 25 mmol) in 50 mL ethanol. The mixture was heated to 78 °C for 45 min, then filtered hot to collect the purple precipitate in quantitative yield. ^{1}H NMR (500 MHz, Chloroform-*d*) δ 8.20 – 8.15 (m, 1H), 8.10 – 8.03 (m, 1H), 7.25 – 7.21 (m, 1H), 7.12 (dddt, *J* = 8.1, 7.5, 1.4, 0.7 Hz, 1H), 6.93 (td, *J* = 7.4, 1.0 Hz, 1H), 6.45 (ddd, *J* = 8.0, 1.0, 0.5 Hz, 1H), 4.41 (t, *J* = 7.9 Hz, 2H), 3.19 (t, *J* = 7.9 Hz, 2H). ^{13}C NMR (126 MHz, cdcl$_3$) δ 181.22, 177.71, 144.20, 144.04, 134.24, 133.42, 132.12, 131.81, 131.43, 127.02, 126.87, 126.28, 125.96, 124.82, 122.07, 114.98, 55.91, 30.07. UV-vis: $\lambda_{max(vis)}$ =558 nm.

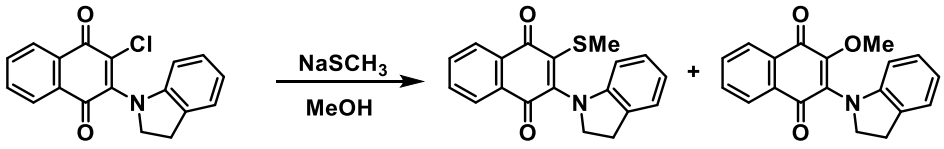

2-indolino-3-methanethiol-1,4-naphthoquinone. ^{1}H NMR (500 MHz, Chloroform-*d*) δ 8.16 – 8.12 (m, 1H), 8.12 – 8.07 (m, 1H), 7.76 – 7.71 (m, 2H), 7.27 (ddd, *J* = 7.3, 1.2, 0.6 Hz, 1H), 7.16 (dddt, *J* = 8.1, 7.4, 1.4, 0.7 Hz, 1H), 6.93 (td, *J* = 7.4, 1.0 Hz, 1H), 6.42 (ddd, *J* = 7.9, 1.0, 0.5 Hz, 1H), 4.43 (t, *J* = 8.3 Hz, 2H), 3.27 (t, *J* = 8.2 Hz, 2H), 2.12 (s, 3H).

2-indolino-3-methoxy-1,4-naphthoquinone. ^{1}H NMR (500 MHz, Chloroform-*d*) δ 8.12 – 8.06 (m, 1H), 8.06 – 7.99 (m, 1H), 7.73 – 7.64 (m, 2H), 7.18 (ddt, *J* = 7.2, 1.6, 1.0 Hz, 1H), 7.07 (tdd, *J* = 7.4, 1.3, 0.7 Hz, 1H), 6.83 (td, *J* = 7.4, 1.0 Hz, 1H), 6.40 (ddd, *J* = 8.1, 1.0, 0.5 Hz, 1H), 4.23 (t, *J* = 8.3 Hz, 2H), 3.80 (s, 3H), 3.20 (t, *J* = 8.2 Hz, 2H).

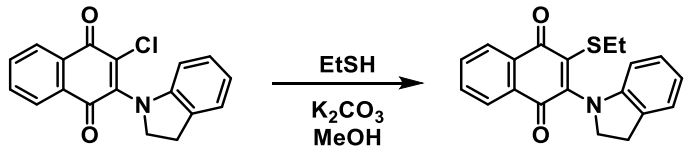

2-ethanethiol-3-indolino-1,4-naphthoquinone. To a solution of 2-chloro-3-indolino-1,4-naphthoquinone (511.5 mg, 1.65 mmol) in 20 mL methanol was added thioethanol (0.15 mL) and potassium carbonate (228.5 mg, 1.65 mmol). After quantitative conversion was observed by LCMS, the solvent was removed and the crude product purified by chromatography (10% EtOAc / Hexanes), collecting the blue-purple band. ^{1}H NMR (300 MHz, Chloroform-*d*) δ 8.14 – 8.08 (m, 1H), 8.08 – 8.01 (m, 1H), 7.79 – 7.58 (m, 2H), 7.25 – 7.17 (m, 1H), 7.10 (dddd, *J* = 8.4, 7.9, 1.6, 0.7 Hz, 1H), 6.88 (td, *J* = 7.4, 1.0 Hz, 1H), 6.38 (ddt, *J* = 8.0, 1.0, 0.5 Hz, 1H), 4.35 (t, *J* = 8.2 Hz, 2H), 3.21 (t, *J* = 8.1 Hz, 2H), 2.60 (q, *J* = 7.4 Hz, 2H), 1.19 – 1.02 (m, 3H). ^{13}C NMR (126 MHz, cdcl$_3$) δ 182.20, 180.81, 144.43, 143.84, 133.60, 133.26, 132.73, 132.05, 131.02, 126.63, 126.48, 126.47, 126.25, 124.70, 121.09, 113.10, 54.51, 29.72, 27.74, 14.25. $\lambda_{max(vis)}$ = 408 nm (thioquinone band), 582 nm (indolino band).

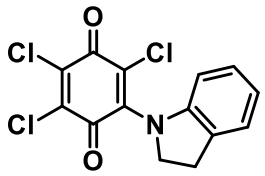

2-indolino-3,5,6-trichloro-1,4-benzoquinone was prepared by refluxing a mixture of chloranil (5.0725 g, 20.6 mmol), indoline (2.4 mL, 21.4 mmol), and sodium acetate (1.7850 g, 21.8 mmol) in 50 mL ethanol 1.5 h. After cooling, filtered solution, collecting solid, trituration with hot hexanes removed a purple impurity from the blue product. ^{1}H NMR (600 MHz, Chloroform-*d*) δ 7.25 (m, 1H), 7.15 (d, *J* = 8.2, 1H), 6.99 (t, *J* = 7.5, 1H), 6.44 (d, *J* = 8.0, Hz, 1H), 4.36 (t, *J* = 7.7 Hz, 2H), 3.18 (t, *J* = 7.7 Hz, 2H). $\lambda_{max(vis)}$ =640 nm.

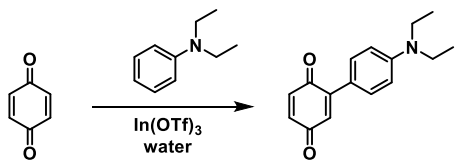

4'-(diethylamino)-[1,1'-biphenyl]-2,5-dione. A suspension of 1,4-benzoquinone (1.1214 g, 10.4 mmol) and N,N-diethylaniline (0.83 mL, 5.2 mmol) in 3 mL water was stirred with catalytic indium (III) triflate (30 mg, 5%). After 5 h the mixture was diluted with water and extracted with dichloromethane. The organic layers were washed with brine and dried over $MgSO_4$ before concentrating. The product was formed in < 3% yield by NMR and coeluted with starting material on silica gel. Purple fractions were collected and the benzoquinone starting material was sublimed out of the mixture leaving behind pure product. ^{1}H NMR (600 MHz, Chloroform-*d*) δ 7.55 – 7.39 (m, 1H), 6.82 – 6.72 (m, 2H), 6.72 – 6.63 (m, 1H), 3.41 (q, *J* = 7.1 Hz, 2H), 1.20 (t, *J* = 7.1 Hz, 3H). $\lambda_{max(vis)}$ = 595 nm ($CHCl_3$), 540 nm (hexanes), 500 nm (MeCN/water), 480 nm (MeOH), 470 nm (MeCN).

General Photolysis Procedure and Equipment: Approximately 5-20 mg of compound was dissolved in methanol (25-50 mL). The resulting solution was exposed to the focused output of a 455 nm, 900 mW mounted LED (M455L3) or a 565 nm, 880 mW mounted LED (M565L3) under ambient conditions with stirring. When the solution became colorless, the solvent was removed, and the crude NMR and LCMS taken. In almost all cases, the crude NMR and LCMS were pure product. The yield of released methanol and ethanol were inferred from that of the lactone products or observed directly in deuterated solvents.

The 455 nm and 565 nm LEDs were used for convenience, but a 300 W Hg arc lamp with long-pass filters >400 nm gave clean photolysis as a generic visible light source. The mounted LEDs and the LEDD1B T-Cube driver used to power them were purchased from Thor Labs. For the selective photolysis experiment, a >530 nm glass long-pass filter was required to remove the weak emission at 400-500 nm for the 565nm LED.

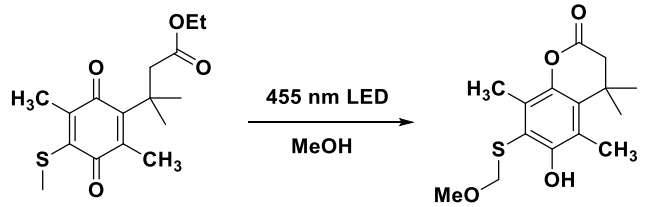

Photolysis of 6a. A dilute solution of **6a** in methanol was irradiated with a 455 nm LED until colorless. The solvent was removed to give the product, 6-hydroxy-7-((methoxymethyl)thio)-4,4,5,8-tetramethylchroman-2-one (**16a**), in quantitative yield by NMR. ^{1}H NMR (400 MHz, Chloroform-*d*) δ 7.17 (s, 1H), 4.69 (s, 2H), 3.48 (s, 3H), 2.55 (s, 2H), 2.50 – 2.42 (m, 3H), 2.41 – 2.35 (m, 3H), 1.46 (s, 6H). ^{13}C NMR (101 MHz, cdcl$_3$) δ 168.23, 152.64, 143.19, 132.95,

128.26, 119.73, 117.69, 79.56, 57.43, 45.75, 35.80, 27.43, 15.06, 15.02. HRMS (ESI) calculated for $C_{15}H_{19}O_4S$ $[M-H]^-$ 295.1010, Found 295.1009.

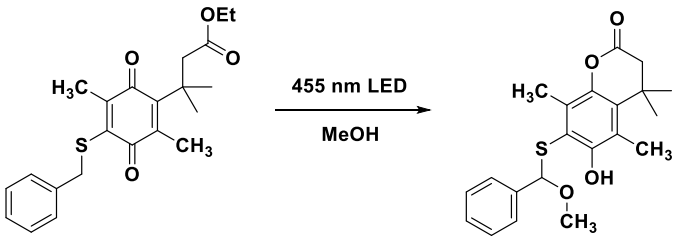

Photolysis of 6b. A dilute solution of **6b** in methanol was irradiated with a 455 nm LED until colorless. The solvent was removed to give the product, 6-hydroxy-7-((methoxy(phenyl)-methyl)thio)-4,4,5,8-tetramethylchroman-2-one (**16b**), in 85% yield by NMR. ^{1}H NMR (400 MHz, Chloroform-*d*) δ 7.44 (s, 1H), 7.35 – 7.15 (m, 5H), 5.47 (s, 1H), 3.44 (s, 3H), 2.54 (s, 2H), 2.34 (s, 3H), 2.27 (s, 3H), 1.46 (s, 6H). ^{13}C NMR (101 MHz, $CDCl_3$) δ 168.33, 153.63, 142.99, 137.78, 133.24, 129.10, 128.63, 128.34, 125.88, 119.64, 116.33, 92.23, 57.64, 45.81, 35.81, 27.56, 27.37, 15.01. HRMS (ESI) calculated for $C_{21}H_{23}O_4S$ $[M-H]^-$ 371.1323, Found 371.1327.

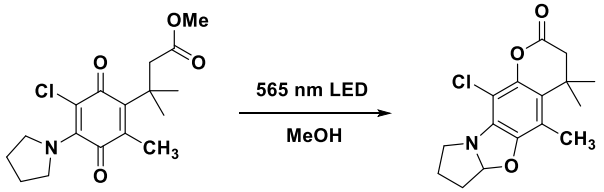

Photolysis of 11. A dilute solution of **11** in methanol was irradiated with a 565 nm LED until colorless. The solvent was removed to give the product, 11-chloro-4,4,5-trimethyl-3,4,6,7,8,9-hexahydro-2H-chromeno[7,6-d]pyrrolo[2,1-b]oxazol-2-one (**19**), in quantitative yield by NMR. ^{1}H NMR (500 MHz, Chloroform-*d*) δ 5.91 (dd, J = 5.0, 2.6 Hz, 1H), 3.45 (dt, J = 10.7, 7.1 Hz, 1H), 3.35 – 3.17 (m, 1H), 2.57 (d, J = 2.5 Hz, 2H), 2.27 (s, 4H), 1.94 – 1.83 (m, 2H), 1.43 (d, J = 10.4 Hz, 6H). ^{13}C NMR (126 MHz, $cdcl_3$) δ 167.38, 149.38, 141.61, 137.26, 125.51, 114.04, 107.42, 103.01, 54.62, 45.56, 35.93, 32.67, 27.75, 27.66, 23.76, 14.58. HRMS (ESI) calculated 308.1048 for $C_{16}H_{19}ClNO_3$ $[M+H]^+$, found 308.1049.

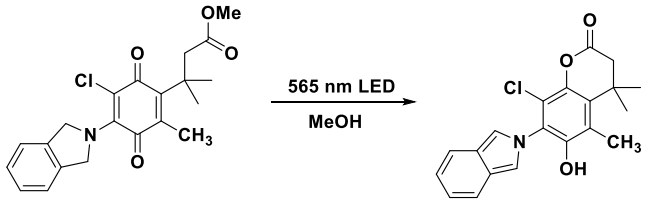

Photolysis of 12. A dilute solution of **12** in methanol was irradiated with a 565 nm LED until colorless. The solvent was removed to give the product, 8-chloro-6-hydroxy-7-(2H-isoindol-2-yl)-4,4,5-trimethylchroman-2-one (**20**), in quantitative yield by NMR. ^{1}H NMR (400 MHz, Chloroform-*d*) δ 7.72 – 7.44 (m, 2H), 7.11 (d, *J* = 0.5 Hz, 2H), 7.06 – 6.86 (m, 2H), 5.71 (s, 1H), 2.61 (s, 2H), 2.52 (s, 3H), 1.53 (s, 7H). ^{13}C NMR (101 MHz, $CDCl_3$) δ 166.11, 146.70, 141.26, 130.99, 124.44, 124.36, 121.35, 119.99, 117.31, 112.76, 53.43, 45.47, 36.21, 29.71, 27.51, 15.14. HRMS (ESI) calculated for $C_{20}H_{19}ClNO_3^+$ 356.1048, found 356.1030.

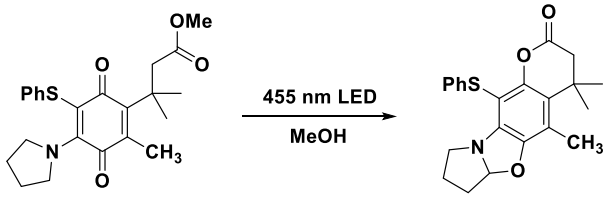

Photolysis of 13. A dilute solution of **13** in methanol was irradiated with a 455 nm LED until colorless. The solvent was removed to give the product, 4,4,5-trimethyl-11-(phenylthio)-3,4,6a,7,8,9-hexahydro-2H-chromeno[7,6-d]pyrrolo[2,1-b]oxazol-2-one (**21**), in quantitative yield by NMR. HRMS (ESI) calculated 382.1471 for $C_{22}H_{24}NO_3S$ $[M+H]^+$, found 382.1475.

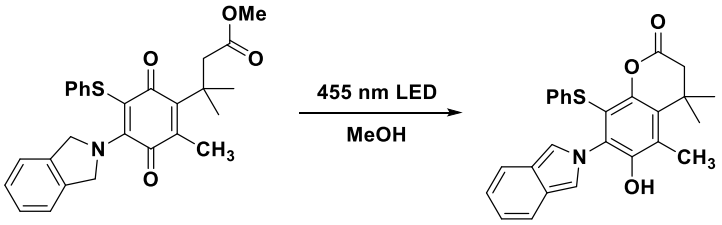

Photolysis of 14. A dilute solution of **14** in CD_3OD sparged with argon was irradiated with a 455 nm LED until colorless. When followed by NMR and LCMS in degassed solvents, the reaction was relatively clean and gave the expected product cleanly, but attempts at preparatory photolysis led to complex mixtures, presumably due to the photoproduct's instability. The proton spectrum was immediately taken to show two products, assigned to the hydroquinone intermediate and lactone final product. After 10 min in the dark the major species in solution was assigned as **22** and free methanol. ^{1}H NMR (600 MHz, methanol-d_4) δ 7.53 – 7.43 (m, 2H), 7.17 – 7.11 (m, 2H), 7.11 – 7.03 (m, 1H), 7.02 – 6.97 (m, 2H), 6.90 – 6.80 (m, 2H), 2.56 (s, 2H), 2.50 (s, 2H), 1.52 (s, 7H).

UV-vis Spectra: Photolysis was conducted with 3 mL of dilute methanol solution of compound under ambient conditions with an overhead LED inside the UV-vis cavity, scanning every 0.1 min for all compounds except **13**. Changes in absorbance over time are indicated by arrows.

Figure 2.5.1. Photolysis of **6a** in methanol

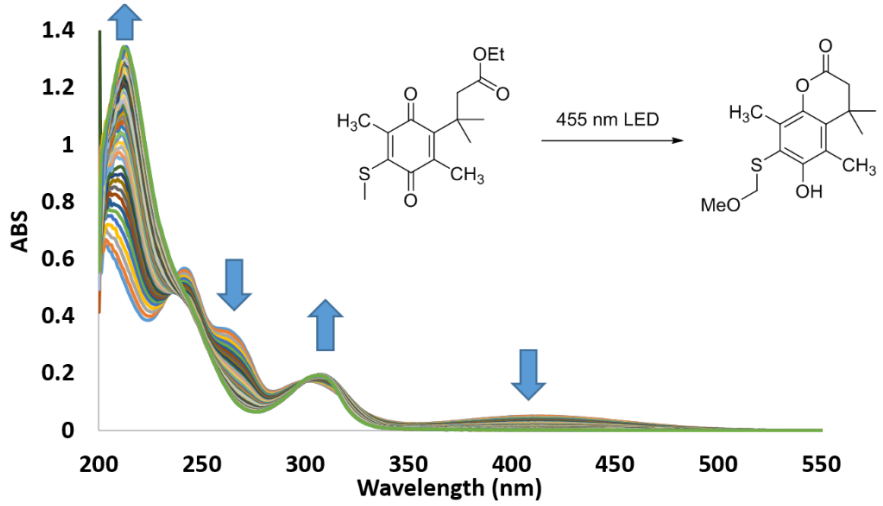

Figure 2.5.2 Photolysis of **6b** in methanol

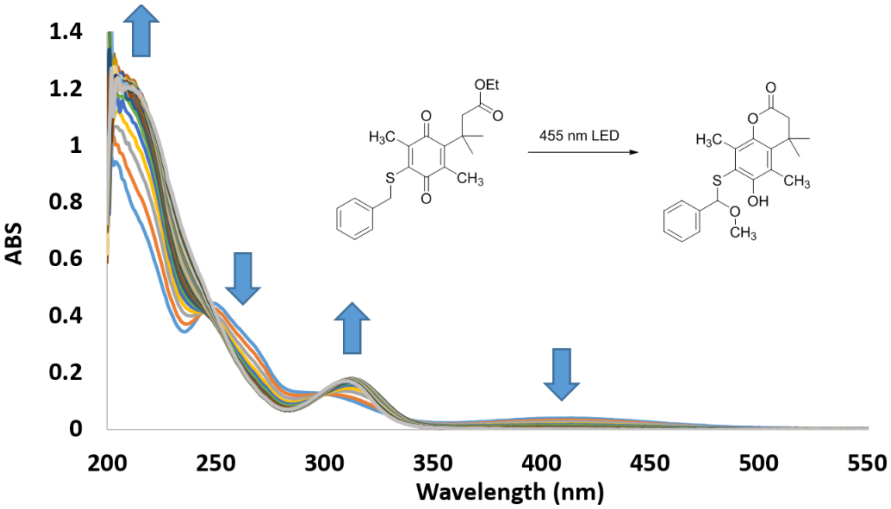

Figure 2.5.3 Photolysis of **11** in methanol

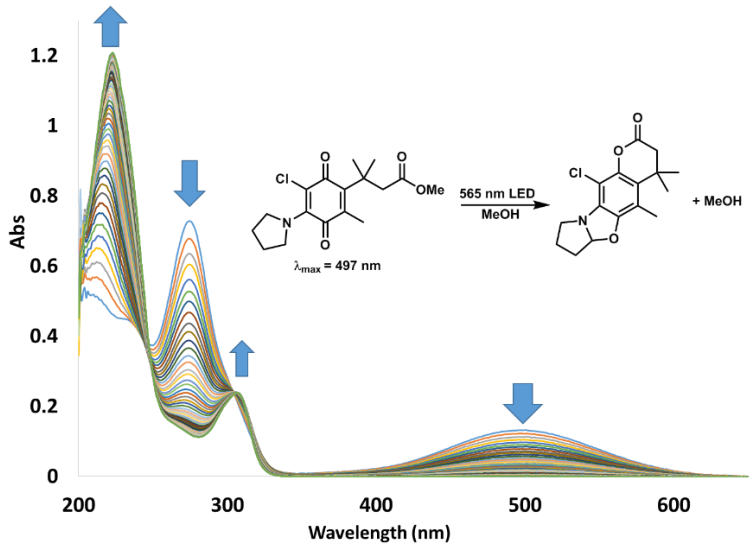

Figure 2.5.4 Photolysis of **12** in methanol

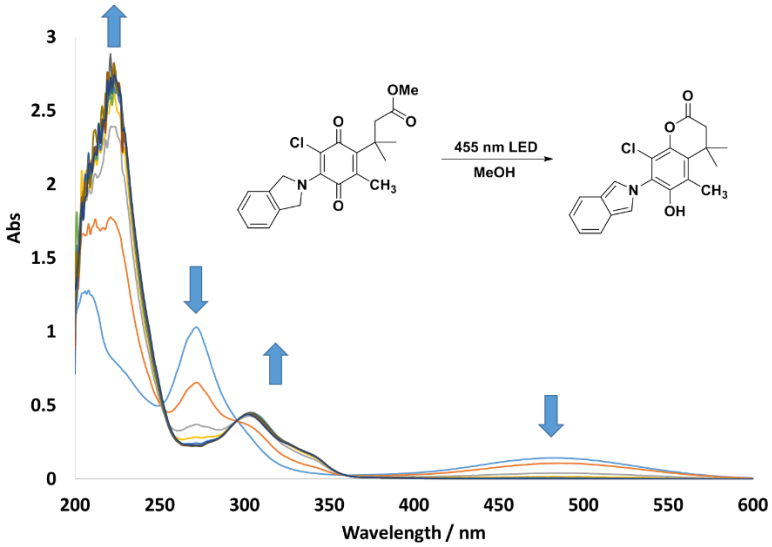

Figure 2.5.5 Photolysis of **13** in methanol. Due to a slow rate of photolysis, traces were >> 0.1 min apart and the sample was sparged and sealed to avoid evaporation.

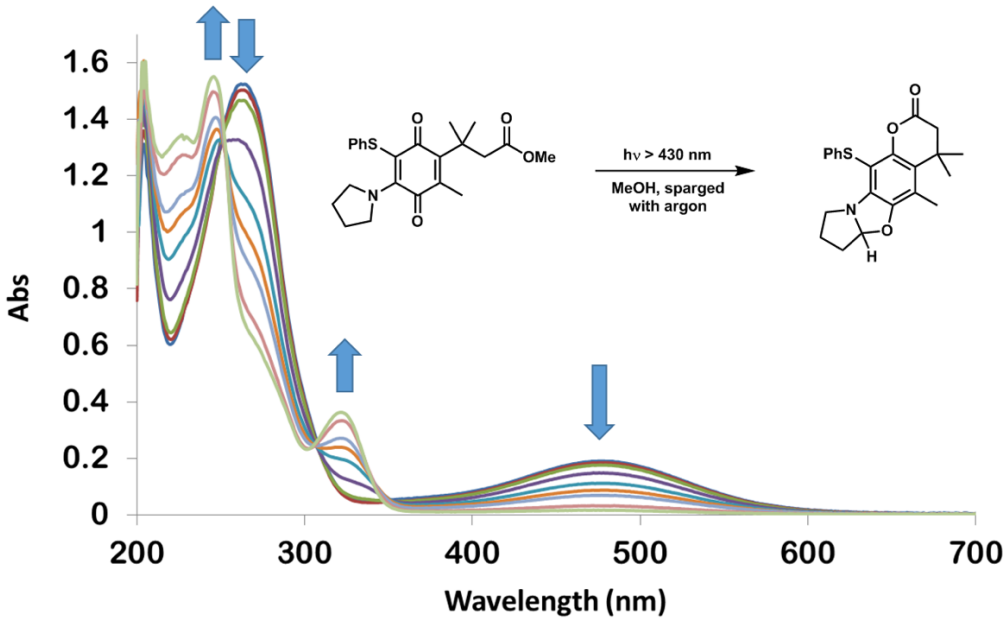

Figure 2.5.6 Photolysis of **14** in methanol

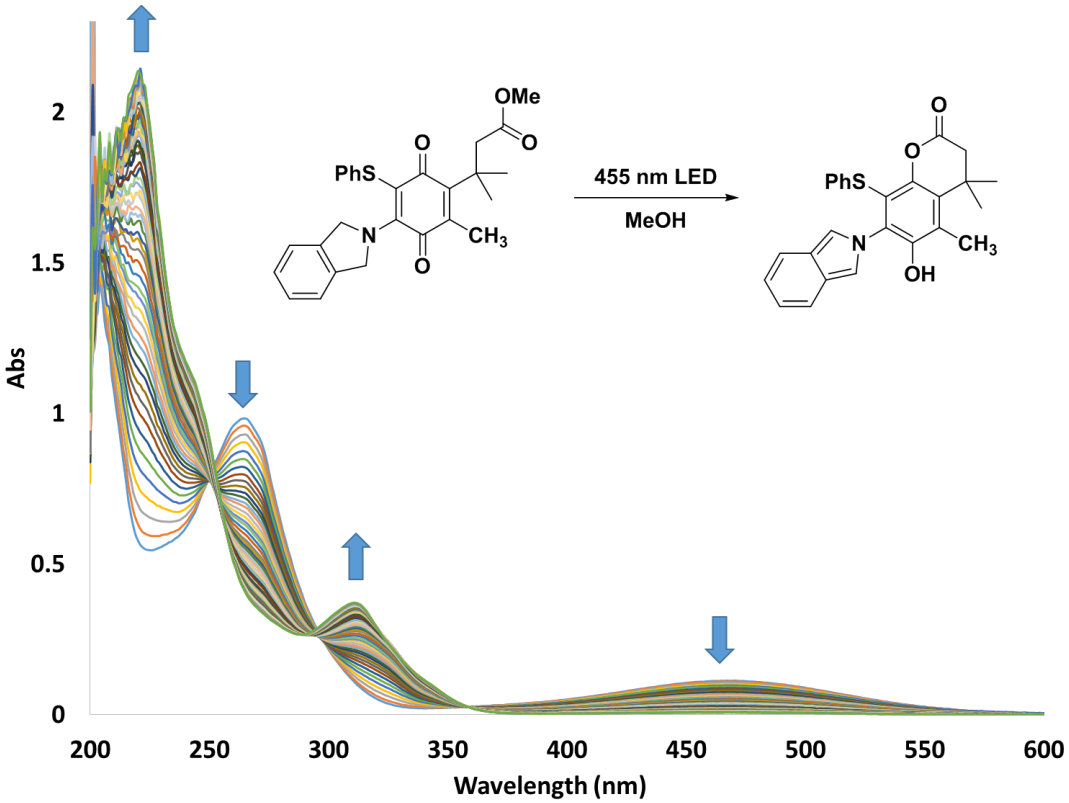

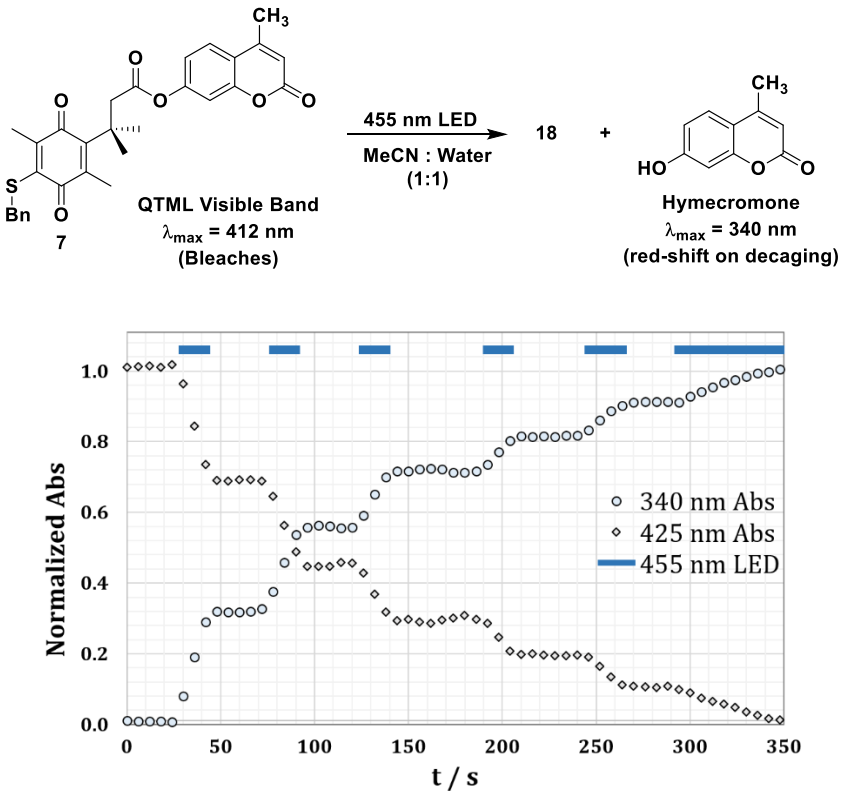

Figure 2.5.7 Stepped Release of Hymecromone Monitored by UV-vis. Normalized absorption vs. time for controlled release of Hymecromone from **7**. Release of the coumarin is complete during the photolysis cycles, with no dark release.

Photolysis of 12 in CD_3OD. Photolysis rapidly converted the starting material to a mixture of the hydroquinone intermediate and the final lactone product in only a few minutes (figure 8). The intermediate hydroquinoine is assigned based on an overall similarity to the starting material, disappearance of the isoindolino N-CH_2 that undergoes an H-shift (peak at 5.23 ppm), and only a slight shift in the methyl ester peak from 3.28 to 3.26 ppm. Although from preparatory photolysis studies we expected to see an isoindole peak for the hydroquinone and lactone, deuterium exchange occurred (figure 8), presumably due to equilibration with the oxazolidine isomer. The hydroquinone converted to lactone **20** in the dark, with concomitant release of methanol. The final spectrum shows quantitative chemical yield of both methanol and hydroquinone.

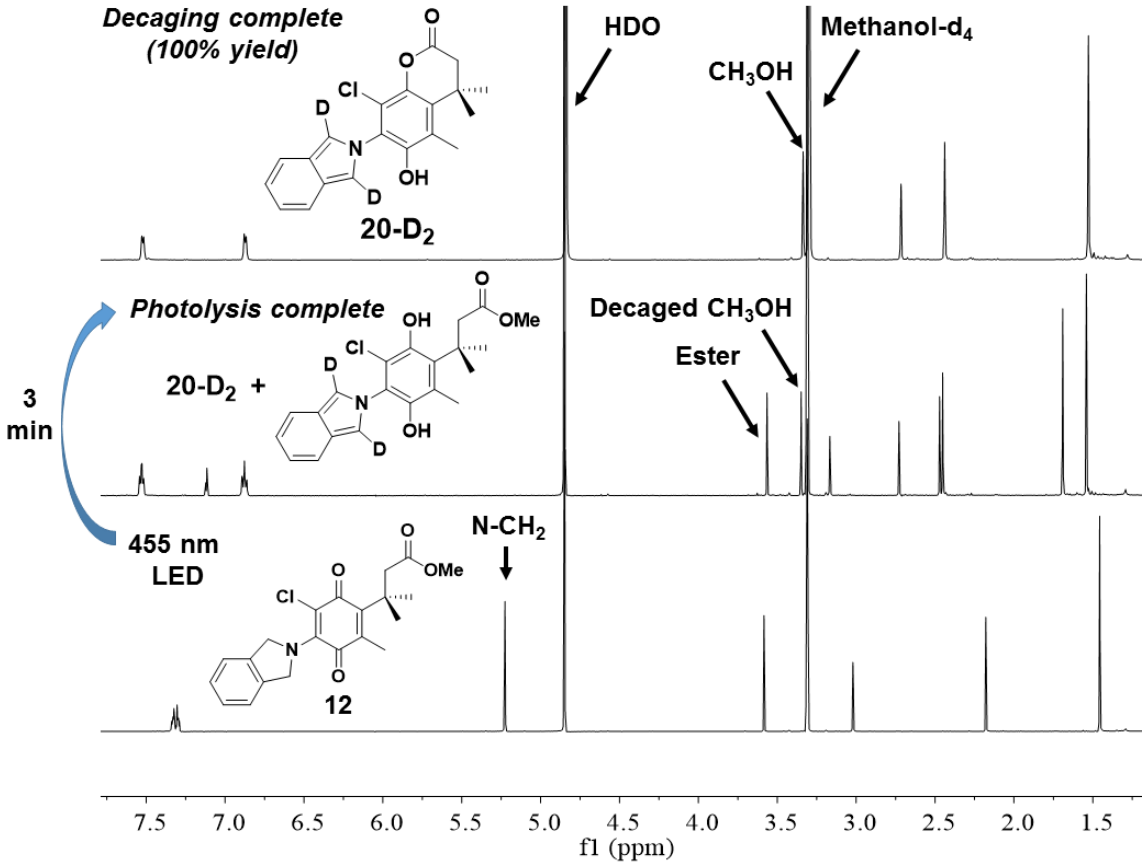

Figure 2.5.8 Photolysis of **12** in CD_3OD; the hydroquinone intermediate and subsequent methanol release are observable.

Oocyte Preparation, Injection and Electrophysiology

Xenopus laevis oocytes were harvested at stage V and VI according to standard protocols approved by the Caltech Institutional Animal Care and Use Committee (IACUC).[6] Oocytes were injected with 5 ng total mRNA as a 50 nL solution of $(\alpha_1)_2(\beta_{2s})_2(\gamma_{2s})_1$ = 2:2:1 mRNA ratio by weight before incubation at 18 °C for 24–48 hours.

Electrophysiology experiments were conducted with the two-electrode voltage clamp mode of an OpusXpress 6000A (Axon Instruments). A holding potential of 60 mV was used. HEPES-free ND96 medium was used for all experimental running/wash buffers (96 mM NaCl, 1.8 mM $CaCl_2$, 2 mM KCl, 1 mM MgCl2, 5 mM $NaHCO_3$ [pH 7.5], 190-240 mOsm). Three doses of EC_{50} concentration (GABA) of which the first dose was ignored were used to equilibrate the cell for testing. Reponses from the second and third doses were averaged together for comparison of the next step (Figure 9a). For photolysis experiments, an approximately 300 μM solution of **9** was applied to the cell and aspiration was paused for the duration of irradiation (Figure 9b). Electrical noise from the LED was filtered out with the ClampFit software. After washing the photolysis products off the cell, a dose of EC_{50} concentration (GABA) was applied to compare the level of signal recovery to pre-photolysis responses. For dose-response curves (Figure 9c), approximately 300 μM solutions of **9** in HEPES-free ND96 buffer were irradiated *ex-vivo* for various durations before the crude photolysis solutions were applied to cells. In control experiments, no response was observed for irradiation of the parent acid, **5a**, which releases water in place of GABA when irradiated.

Selective Photolysis Experimental Details. A solution of **11** (1.5 mL; A = 0.3) was mixed with a solution of **6a** (1.5 mL; A = 0.3) to give a mixture with the broad visible absorbace shown above. The sample was transferred to a screw-cap cuevette (to avoid evaporation) and irradiated with a 565 nm 1 watt LED with > 530 nm long-pass filter. UV-vis spectra were taken periodically until no change was detected. An aliquot was analyzed by LCMS to ensure no decaging of **6a** had occurred during the complete conversion of **11** (see below). The now yellow sample was then irradiated until colorless (blue traces). The sample was then analyzed by LCMS to ensure complete decaging of **6a**. Finally, a dark control sample showed no decaging without light when mixed. LCMS spectra are shown below (PES10A, 40-95% $MeCN_{(aq)}$).

LCMS Data for Selective Photolysis.

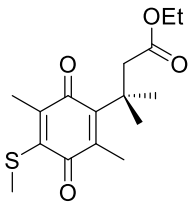

[M+Na]+: 333.11

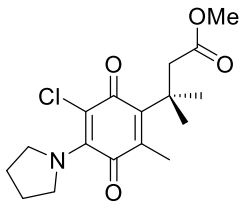

[M+H]+ = 340.13

```
Method Info      : PES10B: 5-95 ACN (8 min); 95-100 ACN (1 min); 100 ACN (1 min) 190 to 800
                   AMU

Sample Info      : Easy-Access Method: 'PES10A_40-95'
```

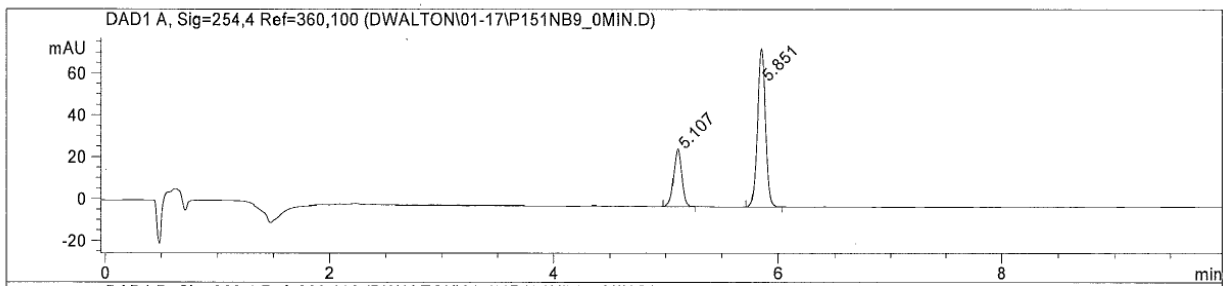

Retention Time (LC)	LC Area	Retention Time (MS)	MS Area	Mol. Weight or Ion
5.107	139	5.183	2349180	340.10 I
5.851	377	5.922	529823	265.00 I 227.00 I

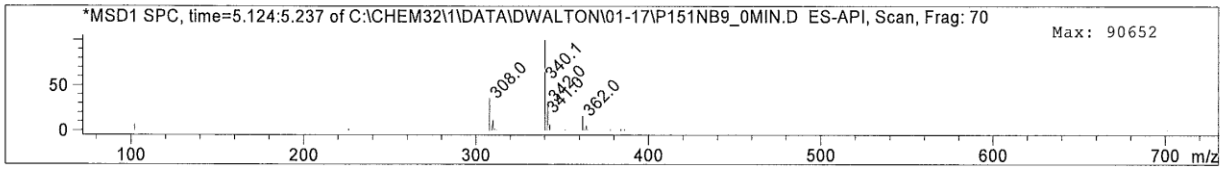

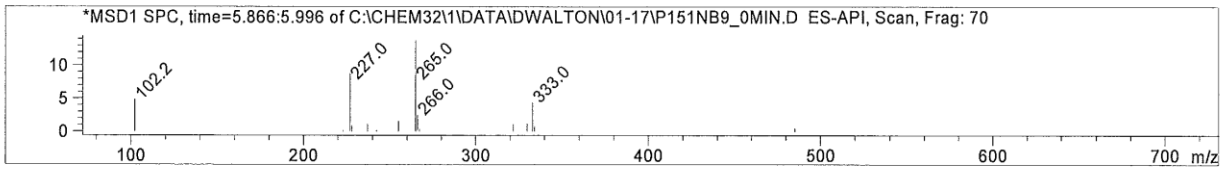

Figure 2.5.10 LCMS of mixture before any irradiation.

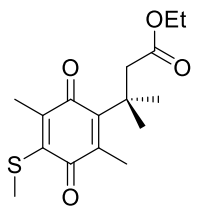

[M+Na]+: 333.11

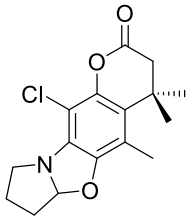

[M+H]+ = 308.10

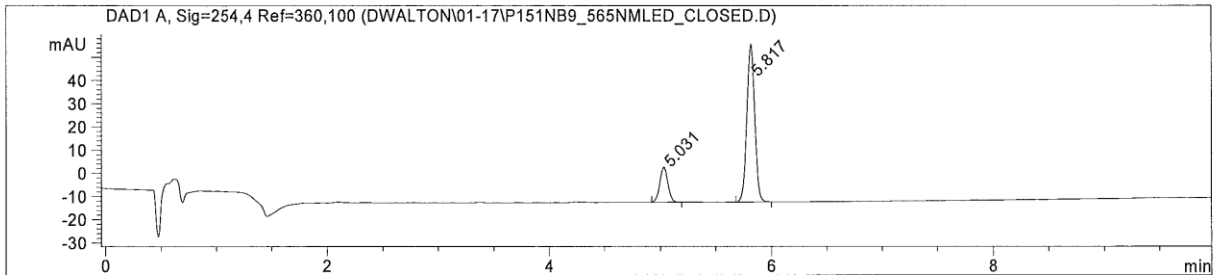

Retention Time (LC)	LC Area	Retention Time (MS)	MS Area	Mol. Weight or Ion
5.031	77	5.106	1587549	308.00 I
5.817	338	5.887	555454	265.05 I
				227.00 I

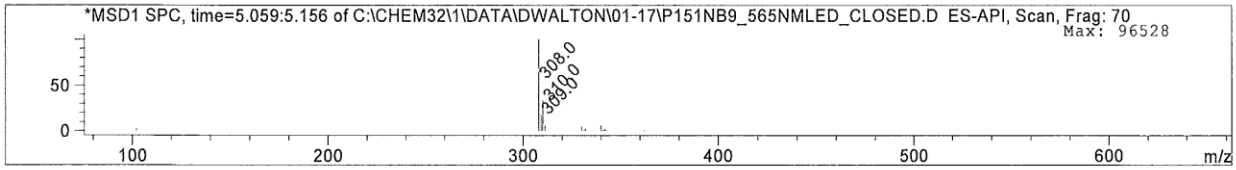

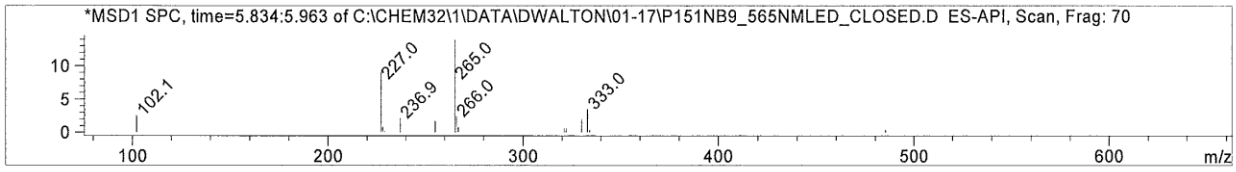

Figure 2.5.11 LCMS of mixture after irradiation with 565 nm LED (with >530 nm long-pass).

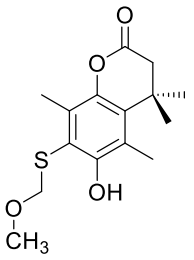

[M+H]+ = 297.12

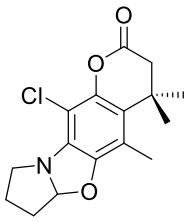

[M+H]+ = 308.10

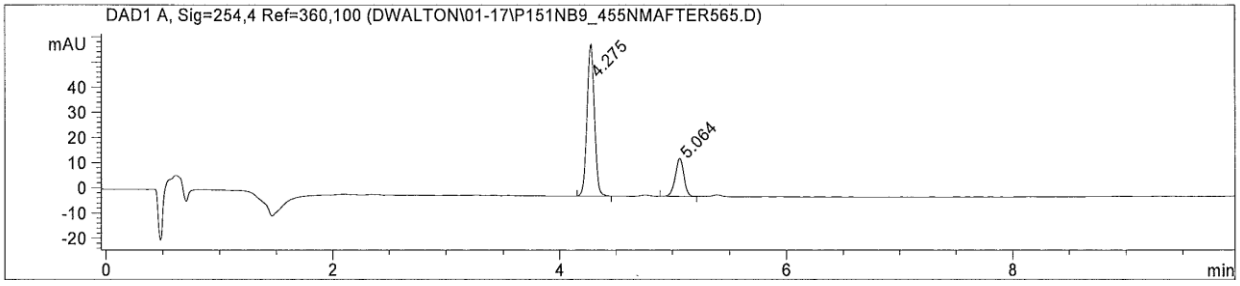

Retention Time (LC)	LC Area	Retention Time (MS)	MS Area	Mol. Weight or Ion
4.275	276	4.356	677740	297.00 I
5.064	79	5.139	1419220	308.00 I

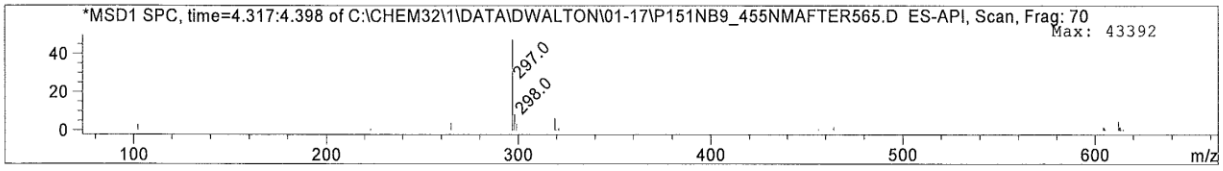

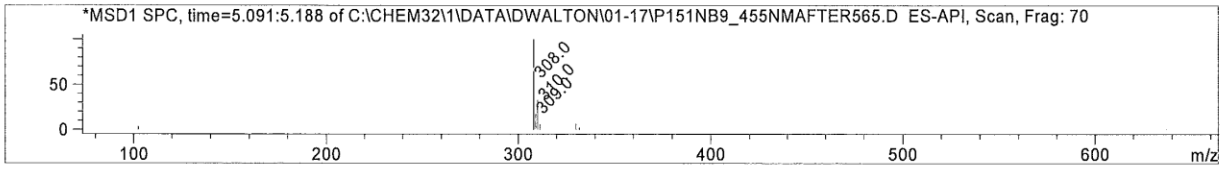

Figure 2.12 LCMS of mixture after irradiation with 565 nm LED, followed by 455 nm LED.

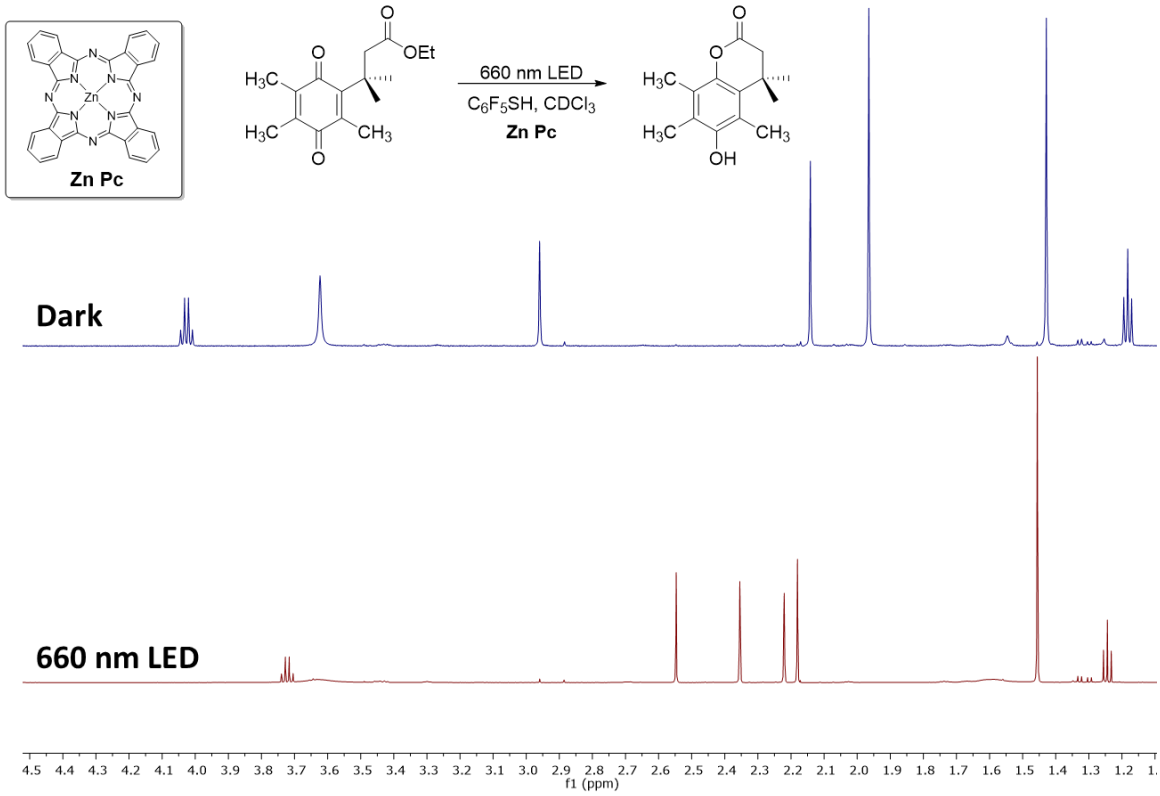

Figure 2.5.13 Sensitized photoreduction of a QTML. NMR spectra before and after 12 h of 660nm LED irradiation. Samples were degassed and flame sealed before irradiation. A saturated solution of Zn Pc was used. Pentafluorothiophenol in place of thiophenol simplifies reaction monitoring by NMR.

2.6 References

1. Levine, M. N.; Raines, R. T., Trimethyl lock: a trigger for molecular release in chemistry, biology, and pharmacology. *Chemical Science* **2012,** *3* (8), 2412-2420.
2. Carpino, L. A.; Triolo, S. A.; Berglund, R. A., Reductive lactonization of strategically methylated quinone propionic acid esters and amides. *The Journal of Organic Chemistry* **1989,** *54* (14), 3303-3310.
3. Amsberry, K. L.; Borchardt, R. T., Amine Prodrugs Which Utilize Hydroxy Amide Lactonization. I. A Potential Redox-Sensitive Amide Prodrug. *Pharm. Res.* **1991,** *8* (3), 323-330.
4. Best, Q. A.; Johnson, A. E.; Prasai, B.; Rouillere, A.; McCarley, R. L., Environmentally Robust Rhodamine Reporters for Probe-based Cellular Detection of the Cancer-linked Oxidoreductase hNQO1. *ACS Chemical Biology* **2016,** *11* (1), 231-240.
5. Borchardt, R. T.; Cohen, L. A., Stereopopulation control. III. Facilitation of intramolecular conjugate addition of the carboxyl group. *J. Am. Chem. Soc.* **1972,** *94* (26), 9175-9182.
6. Ciampi, S.; James, M.; Le Saux, G.; Gaus, K.; Justin Gooding, J., Electrochemical "Switching" of Si(100) Modular Assemblies. *J. Am. Chem. Soc.* **2012,** *134* (2), 844-847.

7. Hettiarachchi, S. U.; Prasai, B.; McCarley, R. L., Detection and Cellular Imaging of Human Cancer Enzyme Using a Turn-On, Wavelength-Shiftable, Self-Immolative Profluorophore. *J. Am. Chem. Soc.* **2014,** *136* (21), 7575-7578.
8. Huang, S.-T.; Lin, Y.-L., New Latent Fluorophore for DT Diaphorase. *Org. Lett.* **2006,** *8* (2), 265-268.
9. Ji, C.; Miller, P. A.; Miller, M. J., Syntheses and Antibacterial Activity of N-Acylated Ciprofloxacin Derivatives Based on the Trimethyl Lock. *ACS Medicinal Chemistry Letters* **2015,** *6* (6), 707-710.
10. Loew, M.; Forsythe, J. C.; McCarley, R. L., Lipid Nature and Their Influence on Opening of Redox-Active Liposomes. *Langmuir* **2013,** *29* (22), 6615-6623.
11. Milstien, S.; Cohen, L. A., Stereopopulation control. I. Rate enhancement in the lactonizations of o-hydroxyhydrocinnamic acids. *J. Am. Chem. Soc.* **1972,** *94* (26), 9158-9165.
12. Ong, W.; McCarley, R. L., Chemically and Electrochemically Mediated Release of Dendrimer End Groups. *Macromolecules* **2006,** *39* (21), 7295-7301.
13. Ong, W.; Yang, Y.; Cruciano, A. C.; McCarley, R. L., Redox-Triggered Contents Release from Liposomes. *J. Am. Chem. Soc.* **2008,** *130* (44), 14739-14744.
14. Prasai, B.; Silvers, W. C.; McCarley, R. L., Oxidoreductase-Facilitated Visualization and Detection of Human Cancer Cells. *Anal. Chem.* **2015,** *87* (12), 6411-6418.
15. Shin, W. S.; Han, J.; Verwilst, P.; Kumar, R.; Kim, J.-H.; Kim, J. S., Cancer Targeted Enzymatic Theranostic Prodrug: Precise Diagnosis and Chemotherapy. *Bioconjugate Chem.* **2016,** *27* (5), 1419-1426.
16. Silvers, W. C.; Payne, A. S.; McCarley, R. L., Shedding light by cancer redox-human NAD(P)H:quinone oxidoreductase 1 activation of a cloaked fluorescent dye. *Chem. Commun.* **2011,** *47* (40), 11264-11266.
17. Silvers, W. C.; Prasai, B.; Burk, D. H.; Brown, M. L.; McCarley, R. L., Profluorogenic Reductase Substrate for Rapid, Selective, and Sensitive Visualization and Detection of Human Cancer Cells that Overexpress NQO1. *J. Am. Chem. Soc.* **2013,** *135* (1), 309-314.
18. Zheng, A.; Shan, D.; Wang, B., A Redox-Sensitive Resin Linker for the Solid Phase Synthesis of C-Terminal Modified Peptides. *The Journal of Organic Chemistry* **1999,** *64* (1), 156-161.
19. Pelliccioli, A. P.; Wirz, J., Photoremovable protecting groups: reaction mechanisms and applications. *Photochemical & Photobiological Sciences* **2002,** *1* (7), 441-458.
20. Fournier, L.; Aujard, I.; Le Saux, T.; Maurin, S.; Beaupierre, S.; Baudin, J.-B.; Jullien, L., Coumarinylmethyl Caging Groups with Redshifted Absorption. *Chemistry – A European Journal* **2013,** *19* (51), 17494-17507.
21. Klán, P.; Šolomek, T.; Bochet, C. G.; Blanc, A.; Givens, R.; Rubina, M.; Popik, V.; Kostikov, A.; Wirz, J., Photoremovable Protecting Groups in Chemistry and Biology: Reaction Mechanisms and Efficacy. *Chem. Rev.* **2013,** *113* (1), 119-191.
22. Gorka, A. P.; Nani, R. R.; Zhu, J.; Mackem, S.; Schnermann, M. J., A Near-IR Uncaging Strategy Based on Cyanine Photochemistry. *J. Am. Chem. Soc.* **2014,** *136* (40), 14153-14159.
23. Denning, D. M.; Pedowitz, N. J.; Thum, M. D.; Falvey, D. E., Uncaging Alcohols Using UV or Visible Light Photoinduced Electron Transfer to 9-Phenyl-9-tritylone Ethers. *Org. Lett.* **2015,** *17* (24), 5986-5989.

24. Goswami, P. P.; Syed, A.; Beck, C. L.; Albright, T. R.; Mahoney, K. M.; Unash, R.; Smith, E. A.; Winter, A. H., BODIPY-Derived Photoremovable Protecting Groups Unmasked with Green Light. *J. Am. Chem. Soc.* **2015,** *137* (11), 3783-3786.
25. Hansen, M. J.; Velema, W. A.; Lerch, M. M.; Szymanski, W.; Feringa, B. L., Wavelength-selective cleavage of photoprotecting groups: strategies and applications in dynamic systems. *Chem. Soc. Rev.* **2015,** *44* (11), 3358-3377.
26. Kunsberg, D. J.; Kipping, A. H.; Falvey, D. E., Visible Light Photorelease of Carboxylic Acids via Charge-Transfer Excitation of N-Methylpyridinium Iodide Esters. *Org. Lett.* **2015,** *17* (14), 3454-3457.
27. Šolomek, T.; Wirz, J.; Klán, P., Searching for Improved Photoreleasing Abilities of Organic Molecules. *Acc. Chem. Res.* **2015,** *48* (12), 3064-3072.
28. Carling, C.-J.; Olejniczak, J.; Foucault-Collet, A.; Collet, G.; Viger, M. L.; Nguyen Huu, V. A.; Duggan, B. M.; Almutairi, A., Efficient red light photo-uncaging of active molecules in water upon assembly into nanoparticles. *Chemical Science* **2016,** *7* (3), 2392-2398.
29. Gandioso, A.; Cano, M.; Massaguer, A.; Marchán, V., A Green Light-Triggerable RGD Peptide for Photocontrolled Targeted Drug Delivery: Synthesis and Photolysis Studies. *The Journal of Organic Chemistry* **2016,** *81* (23), 11556-11564.
30. Bruce, J. M., Light-induced reactions of quinones. *Quarterly Reviews, Chemical Society* **1967,** *21* (3), 405-428.
31. Baxter, I.; Phillips, W. R., Reactions between 2,5-di-t-butyl-1,4-benzoquinone and certain primary aliphatic amines. *J. Chem. Soc., Perkin Trans. 1* **1973,** (0), 268-272.
32. Görner, H., Photoreduction of p-Benzoquinones: Effects of Alcohols and Amines on the Intermediates and Reactivities in Solution¶. *Photochem. Photobiol.* **2003,** *78* (5), 440-448.
33. Görner, H., Photoprocesses of p-Benzoquinones in Aqueous Solution. *The Journal of Physical Chemistry A* **2003,** *107* (51), 11587-11595.
34. Görner, H.; von Sonntag, C., Photoprocesses of Chloro-Substituted p-Benzoquinones. *The Journal of Physical Chemistry A* **2008,** *112* (41), 10257-10263.
35. Cameron, D. W.; Giles, R. G. F., A photochemical rearrangement involving aminated quinones. *Chem. Commun.* **1965,** (22), 573-574.
36. Cameron, D. W.; Giles, R. G. F., Photochemical formation of benzoxazoline derivatives from aminated quinones. *Journal of the Chemical Society C: Organic* **1968,** (0), 1461-1464.
37. Giles, R. G. F., The photochemistry of an aminated 1,4-benzoquinone. *Tetrahedron Lett.* **1972,** *13* (22), 2253-2254.
38. Maruyama, K.; Kozuka, T.; Otsuki, T., The Intramolecular Hydrogen Abstraction Reaction in the Photolysis of Aminated 1,4-Naphthoquinones. *Bull. Chem. Soc. Jpn.* **1977,** *50* (8), 2170-2173.
39. Jones; Qian, X., Photochemistry of Quinone-Bridged Amino Acids. Intramolecular Trapping of an Excited Charge-Transfer State. *The Journal of Physical Chemistry A* **1998,** *102* (15), 2555-2560.
40. Chen, Y.; Steinmetz, M. G., Photochemical Cyclization with Release of Carboxylic Acids and Phenol from Pyrrolidino-Substituted 1,4-Benzoquinones Using Visible Light. *Org. Lett.* **2005,** *7* (17), 3729-3732.
41. Chen, Y.; Steinmetz, M. G., Photoactivation of Amino-Substituted 1,4-Benzoquinones for Release of Carboxylate and Phenolate Leaving Groups Using Visible Light. *The Journal of Organic Chemistry* **2006,** *71* (16), 6053-6060.

42. Hidetoshi, I., Photoinduced Intramolecular Cyclization Reaction of 3-Substituted 2-Alkenoyl-1,4-benzoquinones. *Bull. Chem. Soc. Jpn.* **1989,** *62* (11), 3479-3487.
43. Iwamoto, H.; Takuwa, A., Photoinduced Intramolecular Cyclization Reaction of 2-(2-Alkenoyl)-3-isopropylthio-1,4-benzoquinones to Heterocyclic Compounds. *Bull. Chem. Soc. Jpn.* **1991,** *64* (2), 724-726.
44. Kallmayer, H.-J.; Fritzen, W., Photoreaktivität einiger 2-Alkylthio/Phenylthio-3, 5, 6-trichlor/brom-1, 4-benzochinone. *Pharmazie* **1994,** *49* (6), 412-415.
45. Regan, C. J.; Walton, D. P.; Shafaat, O. S.; Dougherty, D. A., Mechanistic Studies of the Photoinduced Quinone Trimethyl Lock Decaging Process. *J. Am. Chem. Soc.* **2017,** *139* (13), 4729-4736.
46. Yusa, M.; Nagata, T., Photoreduction of quinones by thiols sensitized by phthalocyanines. *Photochemical & Photobiological Sciences* **2017,** *16* (7), 1043-1048.
47. Greenwald, R. B.; Choe, Y. H.; Conover, C. D.; Shum, K.; Wu, D.; Royzen, M. *J. Med. Chem.* **2000**, *43*, 475.
48. *Sethna, S. M. Chem. Rev.*, **1951**, *49*, 91–101
49. Zeep, C., Gao, Y., U.S. Patent US 20120171229, July 5, 2012
50. Carpino, L. A.; Triolo, S. A.; Berglund, R. A. *J. Org. Chem.*, **1989**, *54*, 3303–3310.
51. Borchardt, R. T.; Cohen, L. A. *J. Am. Chem. Soc.*, **1972**, *94*, 9175–9182
52. Nowak, M., Gallivan, J.P., Silverman, S., Labarca, C.G., Dougherty, D.A., and Lester, H.A. *Methods Enzymol.* **1998**, *293*, 504–529.

(1)

Chapter 3. Mechanistic Studies of the Photoinduced Quinone Trimethyl Lock Decaging Process*‡

* Parts of this chapter are adapted with permission from: Regan, C. J.; Walton, D. P.; Shafaat, O. S.; Dougherty, D. A. Mechanistic Studies of the Photoinduced Quinone Trimethyl Lock Decaging Process. *J. Am. Chem. Soc.* **2017**, *139* (13), 4729–4736.

‡ Clint Regan (quantum yields, racemization, sensitization, and quenching studies) and Oliver Shafaat.(LFP, electrochemistry), Walton (synthesis, exploratory and preparatory photolysis) Dennis Dougherty (mechanistic interpretation, experimental design, calculations).

3.1 Abstract

Mechanistic studies of a general reaction that decages a wide range of substrates on exposure to visible light are described. The reaction involves a photochemically initiated reduction of a quinone mediated by an appended thioether. After reduction, a trimethyl lock system incorporated into the quinone leads to thermal decaging. The reaction could be viewed as an electron-transfer initiated reduction of the quinone or as a hydrogen abstraction – Norrish Type II – reaction. Product analysis, kinetic isotope effects, stereochemical labeling, radical clock, and transient absorption studies support the electron transfer mechanism. The differing reactivities of the singlet and triplet states are determined, and the ways in which this process deviates from typical quinone photochemistry are discussed. Comparisons to the longer wavelength amine appended quinones are discussed. The mechanism suggests strategies for extending the reaction to longer wavelengths that would be of interest for applications in chemical biology and in a therapeutic setting.

3.2 Introduction and Synthesis of Sulfide Quinones

We recently described a new class of compounds that undergo photochemical decaging of a wide range of substrates at wavelengths as long as 600 nm.[1] Such compounds could find use as chemical biology tools, and in a therapeutic setting, where longer wavelengths lead to deeper tissue penetration. In an effort to maximize decaging efficiency and to provide insights into possible strategies for extending the photoreactivity to longer wavelengths, we

have conducted extensive mechanistic studies of the photoreaction. Herein we describe those mechanistic studies and the design strategies they suggest.

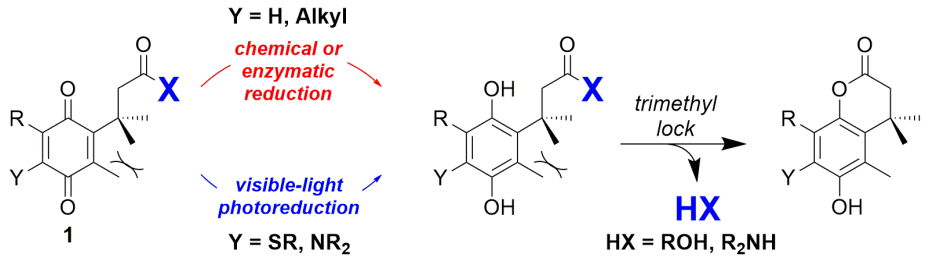

Figure 3.1. Variants of the trimethyl lock decaging process.

The initial approach sought to take a known *chemical* decaging process and design systems that could be phototriggered. Figure 1 shows two variants of the well-established trimethyl lock system.[2–4] Either reducing a quinone or revealing a phenol produces a nucleophile that can exploit the remarkable rate enhancements associated with the trimethyl lock system, releasing **HX** as a generic alcohol, amine, thiol, or phosphate. Of course, deprotection of the phenol can be accomplished photochemically using established caging groups,[5,6] but this approach does not lead naturally to longer wavelength systems.

Scheme 3.1. Products of photolysis of 1 at 420 nm.

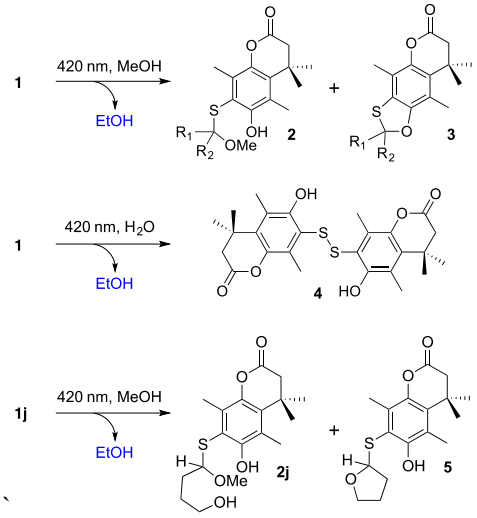

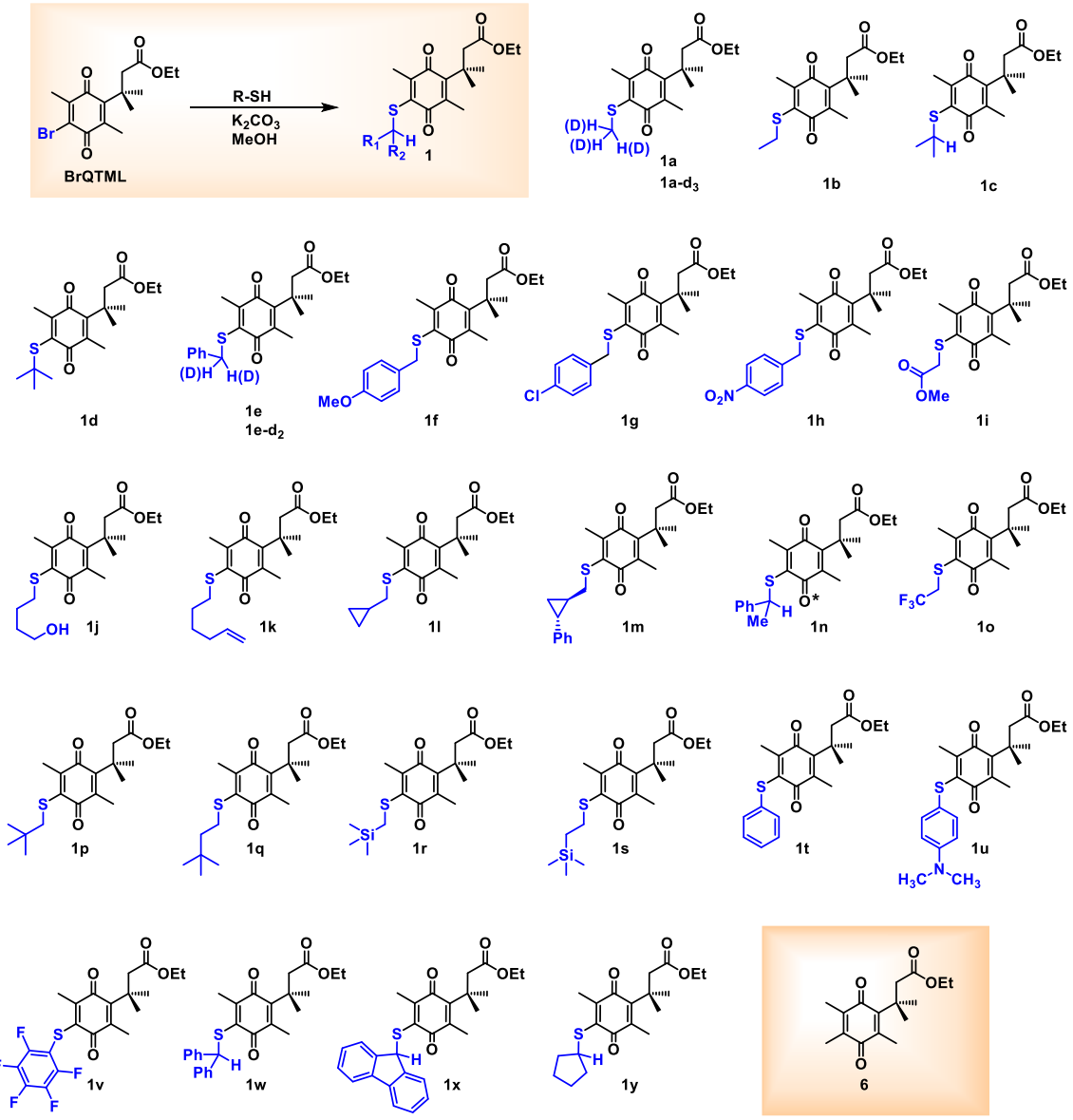

Figure 3.2 Photoinduced quinone trimethyl lock derivatives prepared.

With a goal of creating a photochemically triggered trimethyl lock system, we considered compound **1** (**Figure 3.2**). The bimolecular photoreduction of quinones by sulfides has been reported, but, in general, the reaction has not been extensively studied.[7,8] The process is believed to be initiated by an electron transfer (ET) followed by a crucial C-H

oxidation, similar to photoreduction by amines.[9–12] Intramolecular variants are known,[13,14] but for these reactions a direct hydrogen abstraction (Norrish Type II-like) process cannot be ruled out. For the present purposes, we sought to employ an ET mechanism, as this seemed better suited for longer wavelengths. Although most quinone photoreductions involve amines,[15–22] we chose a sulfide as the potential electron donor in our initial design. We anticipated a more facile synthesis of the desired systems, more favorable redox properties, and perhaps greater stability in air and in a biological system. The synthesis of **1** is efficient and permits a wide variety of sulfide substituents to be introduced in the last step (Figure 2). A representative UV/Vis spectrum is shown in **Figure 3** for the methyl derivative (**1a**). Notably, a broad absorption band is observed at approximately 413 nm; the relevant data for this band (λ_{max} and ε) for key substrates are reported in **Table 3.1**. We have been unable to observe luminescence from **1a**, either in fluid media at room temperature or at 77K in a frozen matrix, as is typical of quinones.[23–30]

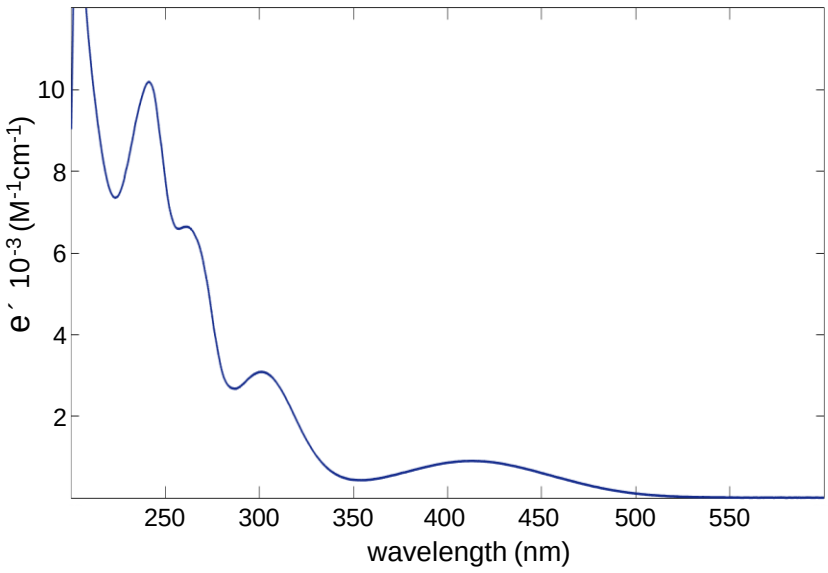

Figure 3.3 Absorbance spectrum of 1a in methanol.

Steady-State Photolysis

Photolysis of **1a** with, for example, a 420 or 455 nm LED, in air-equilibrated methanol leads to the clean formation of thioacetal **2a** (**Scheme 3.1**), as observed by ^{1}H NMR of the crude product. When the reaction is carried out in deuterated solvent, ethanol can also be detected in the reaction mixture as the exclusive byproduct. For some variants of **1**, other reaction products are observed in the crude and can be isolated by silica gel chromatography. Compound **3** is presumably produced by intramolecular capture of the species that is trapped by methanol. Photolysis in water (pure or buffered to pH 7.5) also releases the caged alcohol and produces the disulfide **4**, presumably via a thiohemiacetal intermediate. Both reactions are very clean; quantum yields will be discussed below. In other solvents such as acetonitrile, benzene, or hexane, the reaction is slower and produces a complex mixture of products.

Compound **1j** contains a tethered alcohol, and upon photolysis in methanol it cleanly produces both **2j** and the expected cyclic product **5** in a 1:4 ratio (**Scheme 3.1**). Photolysis of **1j** in acetonitrile or benzene does produce the cyclic product, but there are also other intractable products. It is clear that some of the decomposition products have not undergone trimethyl lock lactonization, suggesting that unmasking of the phenol has not occurred. Compounds **1d** and **1t-v** lack the necessary γ-hydrogen on sulfur and are found to be nonreactive to photolysis at 420 nm. Compounds **1h**, **1i,** and **1o**, all possessing electron-withdrawing groups, are peculiar in that they produce decomposition products upon photolysis in methanol and display visible absorption bands that are weak and blue-shifted (**Table 1**). By comparison, compound **6** (**Figure 2**) lacks a sulfur substituent altogether, and it is found to undergo γ-hydrogen abstraction from the trimethyl lock side chain. Similar processes have been reported previously.[7,31–37]

3.3 Mechanistic Studies

Most of our mechanistic studies have been conducted in methanol, where the reaction is clean and solubility is not an issue. We will examine the mechanism by working backwards from the final product. It is clear that the actual ring closure of the trimethyl lock and the release of the caged compound is the final and slowest step of the process. One could have imagined that an initial photochemical ET from the sulfide to the quinone would build enough

negative charge on the quinone oxygens such that a trimethyl lock closure could occur before further reduction of the quinone,[18] but that is not the case. In deuterated methanol, the hydroquinone (**7**, **Scheme 2**) can be directly observed by ^{1}H NMR prior to trimethyl lock ring closure. In aqueous systems the ring closure is rapid for an alcohol leaving group, but not for an amine leaving group, again allowing the hydroquinone to be observed prior to trimethyl lock closure.[38] These results could be anticipated based on known trimethyl lock rates.[2]

The mechanistic issue then becomes the conversion of quinone **1** to the methanol adduct hydroquinone, **7**. The requirement for a solvent capture step implicates zwitterion **8** as the likely precursor to **7**. Conceptually, the conversion of **1** to **8** then requires reduction of the quinone by two electrons and the shift of a proton from the carbon attached to the sulfur to the quinone oxygen. The matter in question is whether the reaction proceeds through ionic intermediates, similar to bimolecular photoreductions by sulfides and amines, or through a traditional radical mechanism similar to the Norrish II (**Scheme 3.2**). To keep the semantics straight, we will use the term hydrogen-shift as noncommittal regarding all steps in the process **1** → **8**.

Scheme 3.2. Potential intermediates and pathways in the photolysis of 1.

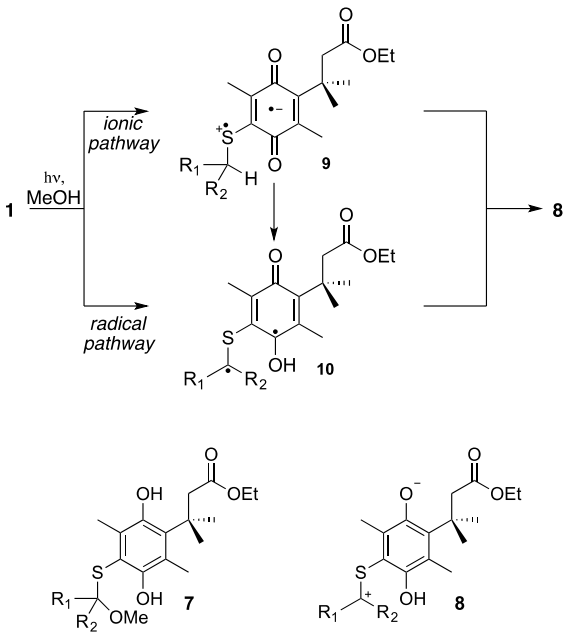

We have applied a number of mechanistic tools to this reaction. First, the influence of sulfide substituents on the quantum yield for product formation was probed. Using a ferrioxalate actinometer[39] we have determined the quantum yield (Φ) for the conversion of **1** in degassed methanol solutions, and the results are summarized in **Table 3.1**. The effect of added oxygen on the quantum yield is generally small and will be discussed further below. There is a trend of *i*-propyl (**1c**) > ethyl (**1b**) > methyl (**1a**) in relative quantum yield, although the effect is not large. A benzyl substituent (**1e**) shows the largest effect, with a > 5-fold increase in quantum yield. These trends would be consistent with either radical or cationic character building up on the substituted carbon. However, substituted benzyl compounds (**1f**,**1g**) do not follow a simple trend, and we note again that the *p*-nitrobenzyl substrate **1h** produces a complex mixture of products.

We next considered the role of the hydrogen shift on the overall process. There is an isotope effect (Φ_H/Φ_D) on the quantum yield for quinone disappearance. A value of 4.0 is obtained for the methyl compound (**1a** vs. **1a-d$_3$**), and 2.5 for the benzyl compound (**1e** vs. **1e-d$_2$**) (**Table 3.1**). These observations highlight the critical role of the hydrogen-shift in the overall process.

	λ_{max}[b]	ε[b]	Φ[c]	τ[d]	Φ^S[e]	Φ^T[e]	ϕ^1_{isc}[f]	ϕ^T_{rxn}[g]	k^T_{rxn}[h]
1	(nm)	($M^{-1}cm^{-1}$)	(%)	(ns)	(%)	(%)	(%)	(%)	(10^5 s^{-1})
1a	413	903	1.2	930	1.0	0.2	0.9	21	2.3
1a-d$_3$	413	923	0.3	1070	0.27	0.03	10	0.3	0.03
1b	414	1005	1.7	750	1.5	0.2	1.3	15	2.0
1c	411	927	2.2	543	1.6	0.6	2.8	21	3.9
1e	413	951	6.3	143	3.0	3.3	4.5	73	51
1e-d$_2$	412	944	2.5	577	1.0	1.5	3.5	42	7.3
1f	410	953	3.1	600	–	–	–	44	7.3
1g	409	832	5.2	180	–	–	–	89	49
1h	396	709	0.6	–	–	–	–	–	–
1i	394	604	0.6	–	–	–	–	–	–

Table 3.1 Spectroscopic and photolysis data for 1 in MeOH.[a]

[a]All quantum yields are reported at 420 nm relative to ferrioxalate actinometer with a standard deviation of < 10%. [b]Longest wavelength absorption band in air-equilibrated methanol. [c]Quantum yield for disappearance of **1**. [d]Lifetime of the transient observed at 480 nm upon pulsed laser irradiation at 355 nm in degassed methanol. [e]Quantum yield for disappearance of **1** through the singlet (S) and triplet (T) pathways; ref to Eq. 1. [f]Quantum efficiency of intersystem crossing for **1**. [g]Minimum value of the

quantum efficiency for disappearance of **1** from the sensitized state. [h]Rate constant for reaction from the sensitized state.

Either a radical or ionic mechanism could potentially generate biradical **10** (Scheme 2), with the former being a conventional Norrish II reaction. To probe for the intermediacy of **10**, we incorporated radical clocks into the system, preparing the 5-hexenyl (**1k**), cyclopropylmethyl (**1l**), and 2-phenylcyclopropylmethyl (**1m**) derivatives**.** These are standard probes that have been used successfully in conventional Norrish II reactions.[40–44] For both **1k** and **1l**, no radical rearrangement is seen; the products **2** and **3** are cleanly produced. The phenylcyclopropyl clock shows a very fast intrinsic ring opening rate of 10^{11} s^{-1}.[40,45] Photolysis of **1m** produces a 20% yield of the expected methanol-trapping product with the phenylcyclopropyl ring still intact. The remaining material is a mixture of products that has not been fully characterized. While it is likely true that the sulfur in our system perturbs the radical rearrangements studied here, it seems safe to conclude that if a biradical such as **10** is directly formed in this system, it has a very short lifetime – much shorter than a typical Norrish II biradical.[43]An especially telling probe of the role of the hydrogen shift was provided by a stereochemical test. Enantiomerically pure phenethyl derivative **1n** was prepared with >95% ee as determined by chiral HPLC (Supporting Information). Upon photolysis to 75% conversion, recovered starting material showed no racemization within the detection limits of the method. As such, we conclude that the hydrogen shift is effectively irreversible, and that nonproductive decay of the excited state occurs prior to the hydrogen shift, making the hydrogen shift a key mechanistic event.

Nanosecond Transient Absorption Studies

To provide further insight into possible mechanisms for this reaction, we have studied this system using nanosecond laser flash photolysis with transient absorption. Briefly, samples were excited at 355 nm with an 8 ns pulse at 10 Hz. On excitation of **1a**, a transient spectrum with an absorption λ_{max} of 480 nm is observed (**Figure 3.4**). The transient absorption signal decayed in a single exponential with a lifetime (τ) of 930 ns in degassed methanol. Similar transients are seen from a number of structures (**Table 3.1**).

In all cases we have observed that the products formed in the laser experiments are the same as in the steady-state photolysis. In air-equilibrated solutions, the same transient is observed, but in all cases the lifetime is in the 100 – 200 ns range, consistent with diffusional quenching by oxygen. The observed transient is also quenched by amine-based quenchers. Considering the parent, **1a**, in the presence of 10 mM triethylamine (TEA), an initial decay with a lifetime of 310 ns is seen, compared to 930 ns in the absence of TEA. As shown in **Table 3.1**, there is a considerable variation in lifetime (τ) for the 480 nm transient. For the simple hydrocarbon systems (methyl, ethyl, isopropyl, benzyl), the transient lifetime tracks the product quantum yield measured in bulk, with the benzyl transient being significantly shorter lived than the methyl. As in the bulk photolysis, a significant KIE is seen for the transient lifetime for the benzyl compound (**1e** vs. **1e-d$_2$**). However, a minimal KIE is seen for the methyl compound (**1a** vs. **1a-d$_3$**).

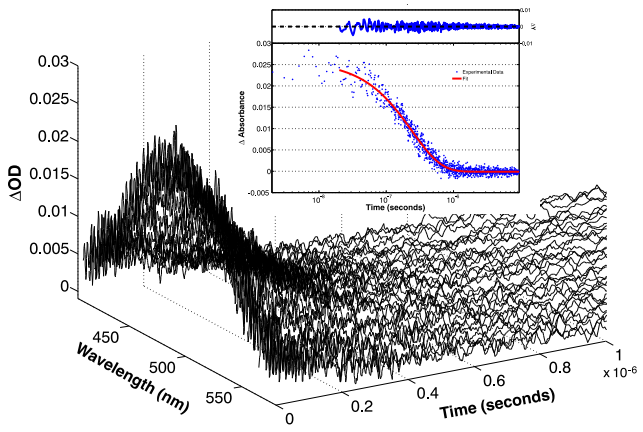

Figure 3.4 Transient absorption spectrum of 1a observed upon laser flash photolysis at 355 nm in aerated acetonitrile. Inset: single exponential fit (red) of transient decay at 480 nm.

Triplet Sensitization/Quenching Studies

Excitation of simple quinones typically produces a triplet state with near unit efficiency.[23,24] The present system, however, is significantly perturbed, electronically by the sulfur substituent and geometrically by the bulky trimethyl lock system. The long lifetime of the transient from the flash photolysis studies, and the fact that it is quenched efficiently by oxygen, suggest that the transient is a triplet. However, in steady-state photolysis studies,

oxygen has only a small effect on the quantum yield. We have undertaken several studies to probe the role and nature of the triplet state in the photoreaction.

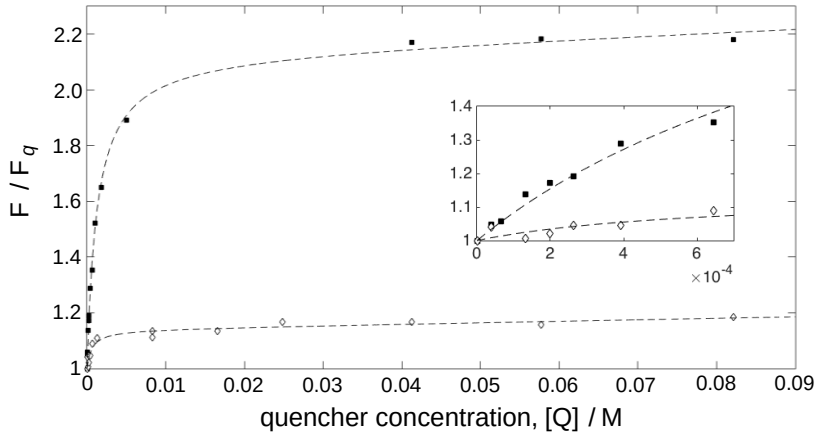

Figure 3.5 Stern-Volmer plot for the quenching of the quantum yield for disappearance of 1a (white diamonds) and 1e (black squares) by diethylaniline. Dotted curves are multivariable regression fits to Eq. 2. Inset is the low concentration region of the plot.

We initially considered the impact of triplet quenchers on the overall process, and obtained clean quenching with diethylaniline. Quenching by diethylaniline likely occurs through reversible electron transfer, as has been previously shown in similar systems.[46] Shown in **Figure 3.5** are Stern-Volmer (SV) plots for photoreaction of the methyl (**1a**) and benzyl (**1e**) compounds, where Φ_q is defined as the quantum yield in the presence of quencher. At low concentrations of diethylaniline (up to ~ 1 mM), roughly linear SV behavior is observed (Figure 5, inset). However, at higher concentrations (up to ~ 100 mM), the SV plot deviates from linearity and plateaus. This indicates that the photoreaction proceeds through two different pathways, one being much more efficiently quenched than the other. We have assigned the less and more quenchable portions of the photoreaction to those that occur through the singlet (Φ^S) and triplet (Φ^T) state, respectively. The sum of these pathways describes the overall quantum yield (Eq. 1).

$$\Phi = \Phi^S + \Phi^T \quad (1)$$

$$\frac{\Phi}{\Phi_q} = \frac{(1 + K_{SV}^S[Q])(1 + K_{SV}^T[Q])}{1 + \frac{K_{SV}^T[Q]}{1+(\Phi^T/\Phi^S)}} \quad (2)$$

Eq. 2 has been previously derived to describe the variation in quantum yield when there are two quenchable pathways.[39] The expression includes two SV quenching constants, K_{SV}^{S} and K_{SV}^{T}, for the singlet and triplet pathways, and the ratio of their quantum yields (Φ^{T}/Φ^{S}). A regression analysis of Eq. 2 results in the fits shown in **Figure 3.5**. This analysis has been performed for key substrates, producing values of Φ^{S} and Φ^{T} after insertion of the determined ratio Φ^{T}/Φ^{S} into Eq. 1 (**Table 3.1**). As expected, the triplet pathways of **1a** and **1e** are efficiently quenched, with similar K_{SV}^{T} values of 1,800 and 1,700 M^{-1}, respectively. In contrast, the singlet states are negligibly quenched with K_{SV}^{S} values of 0.45 and 0.52 M^{-1}. These two compounds are found to differ largely in their ratios of singlet to triplet reactivity, Φ^{T}/Φ^{S}. The calculated ratios reveal that, for **1a**, the reaction proceeds 88% through the singlet and 12% through the triplet. For **1e**, the corresponding singlet and triplet values are 47% and 53%. If we assume that the transient observed in laser flash photolysis is the triplet, we can use the transient lifetimes (τ) and K_{SV}^{T} values to obtain k_q, the second-order rate constant for quenching. We find k_q to be 10 x 10^9 $M^{-1}s^{-1}$ and 2 x 10^9 $M^{-1}s^{-1}$ for **1a** and **1e**, respectively, which are similar to diffusion-controlled values in methanol, where k_{diff} = 1.2 x 10^{10} $M^{-1}s^{-1}$.[47]

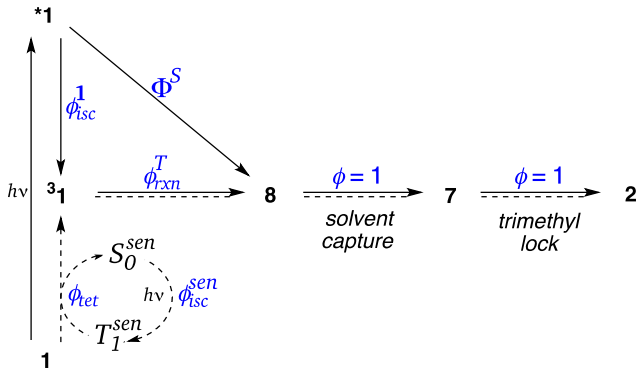

Figure 3.6 Processes that contribute to the direct (solid) and sensitized (dashed) quantum yields for the disappearance of 1 upon excitation at 420 nm. Nonproductive processes have been omitted for clarity.

The results from the quenching experiments reveal that the overall quantum yield (Φ, **Table 3.1**) measured in the steady-state photolysis has components from both the singlet (Φ^{S})

and triplet (Φ^T) pathways (Eq. 1). A minimal model describing the relevant steps that contribute to these pathways is shown in **Figure 3.6**, where nonproductive processes have been omitted for clarity. According to this model, the quantum yield from the singlet (Φ^S) due to direct photolysis of the quinone is defined by the pathway **1** → ***1** → **8** → **7** → **2**. The conversion of **8** → **7** → **2** occurs with unit efficiency, as evidenced by the clean formation of product and the irreversibility of the hydrogen-shift. Φ^S is therefore simply defined by the efficiency of ***1** → **8**.

Likewise, disappearance of quinone through the triplet state (Φ^T) upon direct photolysis is defined by the pathway **1** → *1 → ^{3}**1** → **8** → **7** → **2**. The quantum yield for this process, given by Eq. 3, is constructed as the product of the contributing efficiencies, namely $\phi_{isc}^{\mathbf{1}}$, the efficiency of triplet formation via intersystem crossing, and ϕ_{rxn}^{T}, conversion of triplet to zwitterion **8**.

$$\Phi^T = \phi_{isc}^{\mathbf{1}} \bullet \phi_{rxn}^{T} \qquad (3)$$

We sought to explore the nature of this triplet pathway in more detail through the use of triplet sensitizers. Many efforts to employ sensitizers were either ineffective (acetophenone, benzophenone, methylene blue) or produced undesired side products (biacetyl, naphthalene, anthracene, rose bengal). However, thioxanthone produced clean and consistent results. Also shown in **Figure 3.6** are processes that contribute to the sensitized quantum yield for the disappearance of **1**. The pathway begins with excitation and intersystem crossing of the sensitizer, $S_0^{sen} \rightarrow T_1^{sen}$, followed by bimolecular triplet energy transfer to the quinone, $T_1^{sen} + \mathbf{1} \rightarrow S_0^{sen} + {}^3\mathbf{1}$. Conversion of the triplet quinone to product then proceeds normally (^{3}**1** → **8** → **7** → **2**). The quantum yield for this pathway (Φ_{sen}) is given by the product shown in Eq. 4, where ϕ_{isc}^{sen} is the efficiency of intersystem crossing for the sensitizer, and ϕ_{tet} is the efficiency of triplet energy transfer. The efficiency of triplet energy transfer depends upon the concentration of quinone, [**1**], and is described by Eq. 5, where τ^{sen} is the intrinsic lifetime of the triplet sensitizer, and $k_{tet}[\mathbf{1}]$ and $k_{np}[\mathbf{1}]$ are pseudo-first order rate constants for deactivation of the sensitizer through productive and nonproductive collisions with quinone, respectively.

$$\Phi_{sen} = \phi_{isc}^{sen} \bullet \phi_{tet} \bullet \phi_{rxn}^{T} \quad (4)$$

$$\phi_{tet} = \frac{k_{tet}[\mathbf{1}]}{1/\tau^{sen} + k_{tet}[\mathbf{1}] + k_{np}[\mathbf{1}]} \quad (5)$$

Insertion of Eq. 5 into Eq. 4, and taking the inverse reveals a double-reciprocal linear relationship between the sensitized quantum yield (Φ_{sen}) and quinone concentration ([**1**]) (Eq. 6), where the product $k_{tet} \bullet \tau^{sen}$ is recognized as a Stern-Volmer constant K_{SV}^{tet} for the productive quenching of the triplet sensitizer by **1**. The reciprocal of the y-intercept in Eq. 6 is designated as Φ_{sen}^{lim} (Eq. 7) and describes the sensitized quantum yield for the disappearance of **1** in the limit where deactivation of the triplet sensitizer occurs exclusively through collisions with the quinone. Similar analyses have been presented previously.[48]

$$\frac{1}{\Phi_{sen}} = \frac{1}{\phi_{isc}^{sen} \bullet \phi_{rxn}^{T}} \left(\frac{1}{K_{SV}^{tet}} \bullet \frac{1}{[\mathbf{1}]} + \frac{k_{tet} + k_{np}}{k_{tet}} \right) \quad (6)$$

$$\Phi_{sen}^{lim} = \phi_{isc}^{sen} \bullet \phi_{rxn}^{T} \bullet \frac{k_{tet}}{k_{tet} + k_{np}} \quad (7)$$

Representative double-reciprocal plots are shown in **figure 3.7** for **1a**, **1e**, and the deuterated anologs **1a-d**$_3$ and **1e-d**$_2$. Determination of Φ_{sen}^{lim} from the fit is accomplished by averaging three independent samples. Although the standard deviation in Φ_{sen}^{lim} is consistently less than 10% (**Figure 3.7**, error bars), we note that the slope in the double-reciprocal plots is unexpectedly sensitive to the concentration of thioxanthone. This fact is demonstrated explicitly for **1a**, where three samples containing 1, 2, and 3 mM thioxanthone resulted in incremental shifts in the slope. The y-intercept, however, is clearly unaffected. This kind of behavior has been seen before,[48] and it was not probed further.

If we assume that each quenching event of the sensitizer leads to triplet energy transfer, then $k\_tet/(k\_tet + k\_np) = 1$. This, combined with the known efficiency of intersystem crossing for thioxanthone (ϕ_{isc}^{sen}) of 0.56,[49,50] allows the determination of ϕ_{rxn}^{T} values, which are reported in Table 1. These values represent lower limits, given the assumption above. In general, ϕ_{rxn}^{T} is much larger than Φ, suggesting that the triplet state is not efficiently generated by direct photolysis. Substitution of ϕ_{rxn}^{T} into Eq. 3 permits calculation of the efficiency for intersystem crossing by the quinone ($\phi_{isc}^{\mathbf{1}}$, Table 1). Although quinones typically

form triplets with high yields,[23] the efficiencies observed in this system do not exceed 10%, likely due to the electronic and steric effects of the sulfide and trimethyl-lock substituents, respectively.

The first-order rate constants for formation of **8** from the triplet state (k_{rxn}^{T}) can be calculated using Eq. 8 if we assume that the triplet considered here is the transient observed in laser flash photolysis. Although the results, collected in **Table 3.1**, reflect broad trends in bond dissociation energy (BDE) with the simple alkyl substituents **1a – 1c** reacting slower than benzylic substituent **1e**, the rates are clearly complicated by other factors. For instance, the fact that the methyl (**1a**) and isopropyl (**1c**) derivatives have essentially the same rate constant cannot be explained using simple BDE arguments alone.

$$\phi_{rxn}^{T} = k_{rxn}^{T} \bullet \tau \quad (8)$$

Significant isotope effects on the sensitized quantum yield (ϕ_{rxn}^{T}) are also observed in **Figure 7** and **Table 1**. For the **1e/1e-d$_2$** system, a magnitude of 1.7, given by the ratio ϕ_H/ϕ_D is similar to the magnitude of 2.5 observed in direct photolysis. Application of Eq. 8 to these data reveal a large normal KIE (k_H/k_D) of 7. A similar analysis shows that the methyl analogue, **1a**/**1a-d$_3$**, experiences a very large sensitized product isotope effect (ϕ_H/ϕ_D) of 70, compared to a direct photolysis isotope effect of 4. In particular, we find that the deuterated analog (**1a-d$_3$**) is very inefficient in the sensitized photolysis (Figure 7), with a quantum yield (ϕ_{rxn}^{T}) of 0.03, comparable to the efficiency for direct photolysis (Φ). Calculation of the KIE for **1a**/**1a-d$_3$** from the transient lifetimes and Eq. 8 yields a value (k_H/k_D) of 70.

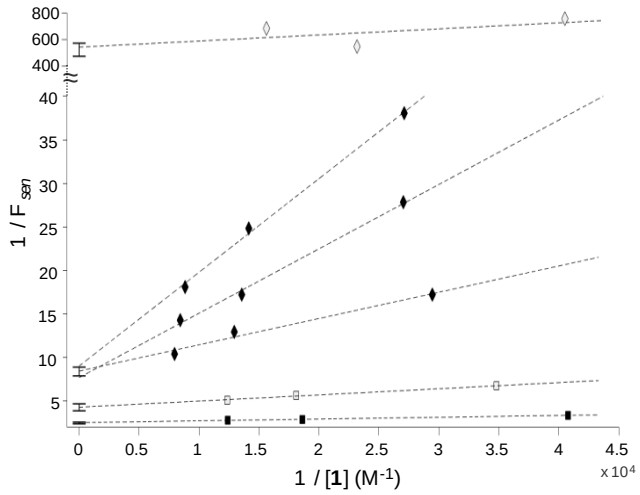

Figure 3.7 Double reciprocal plots for the sensitized photolysis of 1 by thioxanthone in degassed methanol. 1e (black squares), 1e-d_2 (white squares),1a (black diamonds), 1a-d_3 (white diamonds). Dotted lines are linear fits; error bars are the standard deviation in the y-int for three independent samples. Three samples of 1a using different concentrations of thioxanthone are shown to demonstrate that the slope, but not the y-intercept, is affected.

3.4 Mechanistic Interpretation

Based on the accumulated evidence, we argue that the most plausible mechanism is the one outlined in **Figure 8** (a more complete version of the ionic path in Scheme 2). The penultimate intermediate is the zwitterion **8**; once it is formed, product formation involves solvent capture and subsequent trimethyl lock ring closure. That **8** proceeds with high efficiency (>95%) to the final products is evidenced by the stereochemical labeling studies. Formation of **8** can occur in both the singlet and the triplet manifolds. For the simple alkyl substrates, product formation is dominated by the singlet pathway, as evidenced by a large contribution of Φ^S to the overall quantum yield, Φ (**Table 1**). The more efficient reaction for the benzylic substrates includes a more substantial contribution from the triplet pathway.

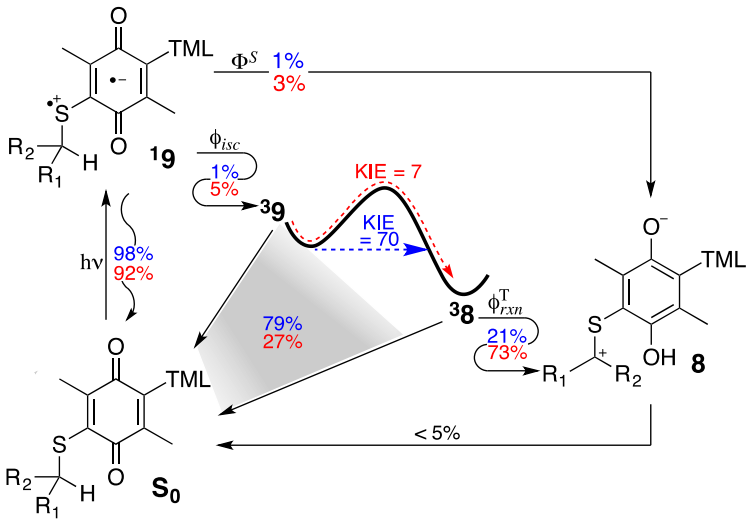

Figure 8. The overall photochemical transformation and efficiencies for the conversion of 1a (R = H; blue) and 1e (R = Ph; red) to the zwitterion 8. The ester side chain is abbreviated TML.

Based on several lines of evidence, we consider the initial excited state to be the charge transfer state, ^{1}**9**, as in Figure 8, rather than a simple n,π* state. The broad visible absorption band observed in these compounds (**Figure 3**) is common for benzoquinones bearing sulfide or amino groups, and is indicative of charge-transfer.[29] The dominant fate of ^{1}**9** is nonemissive return to the ground state (> 90% efficiency), again in contrast to simpler benzoquinones, which typically undergo intersystem crossing to the triplet with near unit efficiency.[23]

The triplet state does form with low efficiency, and again it is not like the triplet of a typical benzoquinone. Shown in Figure 9 are spin-density plots for relevant species computed using DFT M06/6-311++G**, where the trimethyl lock side chain is not displayed for clarity but is included in the calculation. The parent benzoquinone is a conventional n,π* triplet state (consistent with experiment),[51] demonstrated by significant spin density on the oxygen n-orbitals orthogonal to the π-system (**Figure 3.9A**). In sharp contrast, the triplet state of **1** is well-represented by the charge-transfer structure, ^{3}**9**, with no spin density on the oxygen n-orbitals, indicating that they are doubly-occupied. There is also significant spin-density on sulfur (Figure 9B).

Typically, when given the opportunity, excited states of simple benzoquinones will readily undergo γ-hydrogen abstraction.[36,37,52] The trimethyl lock unit of the present system possesses eight γ-hydrogens, but we see no products suggesting that hydrogen abstraction occurs from that unit. In contrast, compound **6**, lacking sulfur, undergoes efficient abstraction of the trimethyl lock hydrogens, but **1d**, possessing a t-butyl substituent on sulfur, is remarkably photostable. These observations suggest formation of a charge transfer excited state that, in both the singlet and triplet states, has a reactivity pattern that is significantly different from that of a simple benzoquinone. While the charge transfer excited state converts to products with low efficiency, apparently it also suppresses the typical reactivity of benzoquinones, and so product formation is very clean.

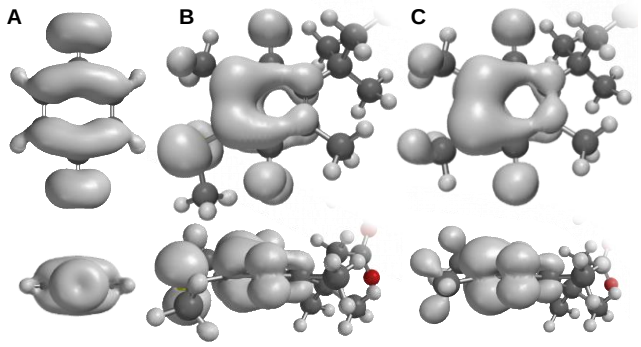

Figure 3.9. Spin-density plots for the triplet state of (A) benzoquinone,(B) 1a, and (C) 6 computed using M06/6-311++G**. The trimethyl lock side chain is not displayed for clarity.

We conclude that the transient observed in the laser flash photolysis experiments is the triplet state, ^{3}**9**. That the transient is a triplet is supported by quenching data for both oxygen and diethylaniline, and by its long lifetime.[53] That this triplet is on the reaction pathway is supported by several lines of evidence. Product formation is very clean in the transient absorption experiments. Additionally, a significant KIE for the transient lifetime indicates that the transient is a species that undergoes a hydrogen-shift reaction. Also, to a considerable extent, the lifetime of the transient tracks with the quantum yield of the bulk reaction (**Table 1**). We would not expect a perfect correlation, because both singlet and triplet paths are involved in the bulk photolysis. Based on its reactivity pattern and the computations noted

above, we conclude that this triplet has considerable charge transfer character, unlike a typical Norrish II triplet. Also, for the alkyl substrates, reaction from the triplet is unusually slow ($k_{rxn}^{T} \sim 10^5$ s^{-1}, Table 1) compared to typical γ-hydrogen shifts, which have rate constants greater than 10^7 s^{-1} for typical ketones[54] and simple benzoquinones.[52] We interpret this to reflect the decreased n,π* character in the triplet state of the structures studied here. Since γ-hydrogen shifts are typically initiated by the electrophilic oxygen that is characteristic of an n,π* state,[54] ^{3}**9** is expected to react more slowly through this type of mechanism. Electron-donating substituents are known to preferentially stabilize the lowest π,π* triplet state of quinones,[23,55] and the substituents of **1**, especially the sulfide, are likely to exhibit this effect in ^{3}**9**. The triplet state of **6**, lacking sulfur, is also predicted to possess a high degree of π,π* character (**Figure 3.9C**), suggesting that alkyl substituents alone may have a substantial effect on the electronics of the quinone. While this could be due to geometric distortion brought on by the trimethyl lock, some unstrained quinones bearing alkyl substituents are also known to have lowest π,π* triplet states.[51]

In the present system, strong electron-withdrawing groups, such as *p*-nitrobenzyl (**1h**), methyl acetate (**1i**), and 2,2,2-trifluoroethyl (**1o**) result in considerably lower quantum yields for quinone consumption and yield a complex mixture of photolysis products. Again, this is consistent with the presence of an ionic structure on the pathway, as it would be destabilized by electron withdrawing substituents due to the significant positive charge on the carbon attached to sulfur.

Although the triplet is formed in low yields, it proceeds to the product much more efficiently than the excited singlet. For benzylic derivatives, values of ϕ_{rxn}^{T} can approach unity. The effect of substitution on the triplet photoreaction as a whole is complicated. The *p*-chlorobenzyl derivative (**1g**) is more efficient than the benzyl derivative (**1e**) not because the hydrogen-shift is more favorable, but because the rate of nonproductive triplet decay is lessened. In **Figure 3.8** we show the triplet pathway as ^{3}**9** → ^{3}**8** → **8**. However, a direct conversion ^{3}**9** → **8** seems possible. As noted above, the reaction is slower than a typical hydrogen transfer. Additionally, since the triplet accounts for less than 10% of the excited

states, the stereochemical labeling studies do not establish whether nonproductive triplet decay occurs directly from ^{3}**9** or through reverse hydrogen shift from ^{3}**8**.

Another intriguing feature of this system is the collection of KIEs seen. The macroscopic quantum yield shows a moderate isotope effect. More interestingly, combining the transient absorption spectroscopy with the sensitized photolysis studies allows a determination of the true KIE, k_H/k_D, for the triplet. For the benzyl system, **1e**/**1e-d$_2$**, a value of 7 is observed, which is relatively large for a reaction of this sort. Remarkably, the parent methyl system, **1a**/**1a-d$_3$**, gives a k_H/k_D of 70 (**Table 1**). This effect is not evident in transient lifetime data because the dominant decay path for the **1a**/**1a-d$_3$** triplet is return to S_0. Such a large KIE strongly implies tunneling in the hydrogen shift for this system. While γ-hydrogen shifts by triplet ketones are generally understood to be activated processes, certain constrained systems have been designed to probe for tunneling at low temperature.[56,57] The tunneling rates observed in those systems by deuterium are found to be similar to k_{rxn}^{T} for **4a-d$_3$** ($\sim 10^3$ s^{-1}), indicating that nonclassical effects may be observable for this slow reaction even at room temperature.

Additional considerations

Although we believe the above mechanism accurately describes the intramolecular photoreduction of sulfide-containing quinones such as **1a-y**, compounds **1o-y** were omitted from detailed experimental work for clarity. Rather than contradict the proposed mechanism, it is likely that in these special cases, steric and electronic effects merely obfuscate the overall trends. The quantum yield of the triplet and singlet states were not determined for **1o**-**y**, therefore any conclusions concerning their relative reactivity in bulk photolysis and LFP data (**Table 3.2**) are to be taken as preliminary. The following is a brief description of these additional findings along with plausible explanations congruent with the mechanism.

Compound **1d** gives no transient, but is unable to react from the triplet state via a hydrogen shift. This has been interpreted as steric crowding leading to a fast deactivation from either the singlet or triplet excited state for **1d**, and therefore the triplet is not observed. Conversely, **1r** also lacks an observable transient, but undergoes efficient photolysis. The effect

on τ is not steric as neopentyl sulfide **1p** displays a typical transient and efficient reactivity. The TMS group is known to lower sulfide radical cation oxidation potentials (β-TMS effect),[58] and we believe the reactive state has significant charge transfer character. The lack of transient for **1r** is therefore attributed to a fast reaction facilitated by the electron donating TMS group, or a nonproductive electron transfer in addition to enhanced reactivity from either state.

Arylsulfides **1t** and **1v** give transients but also lack abstractable γ-hydrogens. The steric effect of phenylsulfide is likely different than *t*-butylsulfide, and therefore **1t** and **1v** lack the geometric constraints leading to fast deactivation as in **1d**. Additionally, arylsulfide oxidation potential correlates with lifetimes for **1t** and **1v**, with the electron withdrawing sulfide undergoing slower deactivation. This is especially interesting in the context of quinone trimethyl locks with thiophenol substituents such as **2.13** (below). The comparatively high oxidation potential of the 2,2,2-trifluoroethanyl sulfide in **1o** results in more significant blue-shifted absorbance than **1i**, yet it has a long-lived triplet and photolyzes slowly to a mixture of products. This suggests a continuum where reactivity at the sulfide substituent and the quinone itself are subject to the electron donating ability of sulfide substituents. Finally, the fluorenyl derivative **1x** might be expected to react the fastest of **1a-y** due to a weak C-H bond. Photolysis of **1x** is instead slow, indicating conformational or steric effects greatly inhibiting the hydrogen shift. Steric effects are otherwise understated in **1a-y**, but common for analogous aminoquinones. This is understandable as the photoreactive dialkylamines have twice the potential for steric interactions than a sulfide. The sulfide presumably has to be quite large for these effects, as it is for **1x**.

Compound	Sulfide (S-R)	Rate (sec^{-1})	τ (ns)
1t	Ph	1.79×10^7	56
1v	C_6F_6	1.54×10^6	650
1x	fluorenyl	1.47×10^6	680
1o	CF_3CH_2-	9.17×10^5	1091
1i	CH_2CO_2Me	4.85×10^5	206
1q	CH_2CMe_3	1.58×10^6	633
1r	CH_2SiMe_3	0	0
1d	*tert*-butyl	0	0

Table 3.2 Additional LFP data. Solvent is degassed methanol for all entries.

The mechanism proposed by Gritsan and Bazhin for photolysis of 2-amino-1,4-naphthoquinones is qualitatively very similar to our findings.[59,60] The authors suggest that the reactive state for aminoquinones has considerable charge transfer character and behaves differently than typical n,π* states of carbonyls. Oxygen has little effect on quantum yields, and the solvent trends are the opposite of what is expected for HAT reactions, with quantum yields decreasing with solvent polarity. In the context of the sulfide mechanism, we expect reactivity from both the singlet and triplet CT states of aminoquinones. Although LFP, sensitization, and quenching data would be necessary for the full picture, preliminary observations are outlined in **Scheme 3.3**. It appears that benzylic hydrogens improve the amine reaction (**12** vs **11**), but competing electron transfer (**2.13** vs. **2.27** vs. **2.11**) and constrained rotation (**12** vs. **13**) inhibit it. A moderate overall k_H/k_D = 1.8 was measured for 2-chloro-3-(N,N-dimethylamino)-1,4-naphthoquinone (**11**) in air equilibrated methanol, but one might expect the individual values for the triplet and singlet to vary greatly.

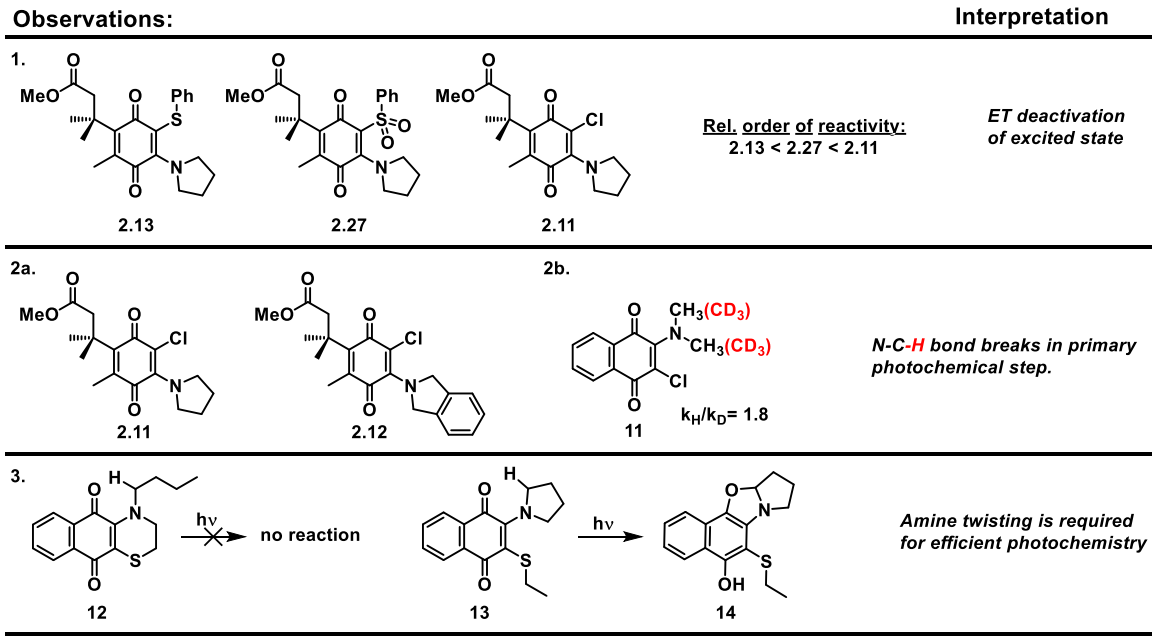

Scheme 3.3 Comparable photochemistry of amine substituted quinones

3.5 Conclusions

We describe mechanistic studies of a new reaction that allows rapid photochemical decaging of a wide range of structures using the well-established trimethyl lock lactonization process. Key to the development of this system was the discovery of an effective phototrigger based on an intramolecular redox reaction of benzoquinones bearing a sulfide substituent. Our results indicate that the process begins with photoinduced electron transfer, followed by a critical and irreversible hydrogen shift that ultimately results in two electron reduction to the hydroquinone. The nucleophilic hydroquinone oxygen is then capable of undergoing rapid, thermal trimethyl lock lactonization with release of the caged compound. Both singlet and triplet pathways are viable, with the latter proceeding to product much more efficiently.

Given our mechanistic conclusions, many strategies for extending the excitation wavelength can be envisioned, as photoinduced electron transfer is a heavily studied and well-understood process. Additionally, the mechanism detailed here appears applicable to aminoquinone-based photocages. Conclusions drawn from the now well understood sulfide system can be applied and tested in future designs, including aminoquinones. Also, the modular synthesis of these compounds allows the substituent on sulfur to be readily varied, allowing the introduction of groups that impact solubility, cell permeability, and biodistribution in general.

3.6 Materials and Methods

Unless otherwise stated, reactions were carried out under ambient conditions. Light sensitive compounds were protected from light using aluminum foil and under low ambient light, or with an appropriate safelight. Commercially available reagents were obtained from Sigma Aldrich, AK Scientific, Alfa Aesar, or Acros Organics and used without further purification. Solvents used for photolysis and UV-vis were EMD Millipore omnisolve grade. Other solvents were used as received or dried by elution through activated alumina where noted. If a photoproduct was found to be unstable to hydrolysis, methanol was distilled from magnesium. Thin-layer chromatography using EMD/Merck silica gel 60 F254 pre-coated plates

(0.25 mm) was used to monitor reactions. Silica gel chromatography was conducted as described by Still et al. (W. C. Still, M. Kahn, A. Mitra, *J. Org. Chem.* **1978**, *43*, 2923), with silica gel purchased from Alfa Aesar (60 Å, 230-400 mesh). NMR spectra were recorded on Varian (300, 400, 500, or 600 MHz), or Bruker (400 MHz) spectrometers. HRMS (ESI) were obtained with an Agilent 6200 Series TOF. UV-vis spectra were recorded on a Cary 60 spectrometer. Samples were irradiated with a M455L3 (455 nm, 900 mW), or a M565L3 (565 nm, 880 mW) mounted LED purchased from Thor Labs. Photolysis was conducted inside the UV-vis spectrometer cavity or side on through a glass flask or NMR tube in air-equilibrated methanol, methanol-d_4. Deuterated thiols were prepared from thiourea and the appropriate alkyl bromide or iodide following literature procedures (J.-F.; d'Orchymont, H. *J. Org. Chem.* **1982**, 47, 2882– 2886).

Preparative Procedures and Spectroscopic Data

Preparation of sulfide-substituted benzoquionones (1a-1n). Both procedures start from ethyl-3-(4-bromo-2,5-dimethyl-3,6-dioxocyclohexa-1,4-dien-1-yl)-3-methylbutanoate, prepared as previously reported.[1]

General Procedure A: In a 50 mL round bottom flask equipped with a magnetic stir bar and rotected from light was dissolved the bromoquinone (1 eq, 0.1 M) in methanol. To this solution is then sequentially added the thiol (1.1 eq) and K_2CO_3 (1.1 eq). The reaction was stirred until starting material was completely consumed as determined by TLC or LCMS (~ 15 mins), then 1 equivalent of acetic acid was added to neutralize the base, and the solvent was removed. The crude was taken up in a small amount of CH_2Cl_2, then diluted in hexanes and filtered through a cotton plug to remove inorganic salts before purification by flash column chromatography (SiO_2, 0 – 10% EtOAc in hexanes) to yield **1** as a yellow solid or oil in > 95% yield.

General Procedure B: In a 20 mL vial equipped with a magnetic stir bar and protected from light was dissolved the bromoquinone (1 eq, 0.1M) in 1:1 dichloromethane/water. To the biphasic mixture was added tetrabutylammonium bromide (0.05 eq) and either the thiol (2 eq) and

K_2CO_3 (2 eq) or the sodium salt of the thiolate (2 eq). The solution was stirred or shaken vigorously for 5 minutes, then diluted in water and extracted with dichloromethane (x 3). The combined organics are dried over $MgSO_4$ and concentrated *in vacuo*. The crude was purified by flash column chromatography (SiO_2, 0 – 10% EtOAc in hexanes) to yield **1** as a yellow solid or oil.

ethyl 3-[2,5-dimethyl-4-(methylsulfanyl)-3,6-dioxocyclohexa-1,4-dien-1-yl]-3-methylbutanoate (1a). Prepared according to *General Procedure B*. ^{1}H NMR (300 MHz, Chloroform-*d*) δ 4.03 (q, *J* = 7.1 Hz, 2H), 2.95 (s, 2H), 2.47 (s, 2H), 2.16 (s, 3H), 2.13 (s, 2H), 1.42 (s, 6H), 1.19 (t, *J* = 7.1 Hz, 2H). ^{13}C NMR (101 MHz, $CDCl_3$) δ 188.26, 183.32, 172.70, 152.99, 146.36, 141.61, 139.54, 60.26, 47.62, 38.12, 28.64, 17.09, 14.64, 14.51, 14.18. HRMS (ESI) calculated for $C_{16}H_23O_4S$ $[M+H]^+$ 311.1312, found 311.1316.

ethyl-3-{2,5-dimethyl-4-[($^2H_3$)methylsulfanyl]-3,6-dioxocyclohexa-1,4-dien-1-yl}-3-methylbutanoate (1a-d_3). Prepared according to *General Procedure A*. ^{1}H NMR (600 MHz, Chloroform-*d*) δ 4.03 (q, *J* = 7.1 Hz, 2H), 2.94 (s, 2H), 2.16 (s, 3H), 2.12 (s, 3H), 1.42 (s, 6H), 1.19 (t, *J* = 7.1 Hz, 3H). ^{13}C NMR (101 MHz, $CDCl_3$) δ 188.25, 183.34, 172.70, 152.99, 146.30, 141.60, 139.54, 77.23, 60.27, 47.63, 38.14, 28.65, 14.64, 14.52, 14.19. ESI-MS(+) calculated for $C_{16}H_{19}D_3NaO_4S$ $[M+Na]^+$ 336.1, found 336.0. HRMS (ESI) calculated for $C_{16}H_{20}D_3O_4S$ $[M+H]^+$ 314.1500, found 314.500.

ethyl 3-[4-(ethylsulfanyl)-2,5-dimethyl-3,6-dioxocyclohexa-1,4-dien-1-yl]-3-methylbutanoate (1b). Prepared according to *General Procedure A*. ^{1}H NMR (600 MHz, Chloroform-*d*) δ 4.02 (q, *J* = 7.1 Hz, 2H), 3.00 (d, *J* = 7.5 Hz, 2H), 2.94 (s, 2H), 2.16 (s, 3H), 2.14 (s, 3H), 1.42 (s, 6H), 1.23 (d, *J* = 7.4 Hz, 3H), 1.18 (t, *J* = 7.1 Hz, 3H). ^{13}C NMR (126 MHz, cdcl$_3$) δ 188.45, 183.64, 172.57, 153.11, 148.02, 140.31, 139.49, 60.24, 47.64, 38.20, 28.69, 28.11, 15.47, 14.93, 14.57, 14.19. HRMS (ESI) calculated for $C_{17}H_{25}O_4S$ $[M+H]^+$ 325.1468, found 325.1468.

ethyl 3-[2,5-dimethyl-3,6-dioxo-4-(propan-2-ylsulfanyl)cyclohexa-1,4-dien-1-yl]-3-methylbutanoate (1c). Prepared according to *General Procedure A*. ^{1}H NMR (400 MHz, Chloroform-*d*) δ 4.02 (q, *J* = 7.1 Hz, 2H), 3.77 (p, *J* = 6.7 Hz, 1H), 2.94 (s, 2H), 2.17 (d, *J* =

2.9 Hz, 6H), 1.44 (s, 6H), 1.25 (d, *J* = 6.7 Hz, 6H), 1.18 (t, *J* = 7.1 Hz, 3H). ^{13}C NMR (101 MHz, $CDCl_3$) δ 188.78, 183.92, 172.46, 153.26, 149.56, 140.00, 139.41, 60.22, 47.62, 38.21, 37.96, 28.69, 23.81, 15.19, 14.59, 14.19. HRMS (ESI) calculated for $C_{18}H_{27}O_4S$ $[M+H]^+$ 339.1625, found 339.1621.

ethyl 3-[4-(tert-butylsulfanyl)-2,5-dimethyl-3,6-dioxocyclohexa-1,4-dien-1-yl]-3-methylbutanoate (1d). Prepared according to *General Procedure A*. ^{1}H NMR (400 MHz, Chloroform-*d*) δ 4.03 (q, *J* = 7.1 Hz, 2H), 2.93 (s, 2H), 2.29 (s, 3H), 2.20 (s, 3H), 1.44 (s, 6H), 1.33 (s, 9H), 1.19 (t, *J* = 7.1 Hz, 3H). ^{13}C NMR (101 MHz, $CDCl_3$) δ 190.00, 184.92, 172.56, 156.68, 153.56, 139.13, 137.70, 60.22, 49.74, 47.39, 37.99, 31.94, 29.71, 28.45, 22.71, 16.59, 14.86, 14.21. HRMS (ESI) calculated for $C_{19}H_{29}O_4S$ $[M+H]^+$ 353.1781, found 353.1785.

ethyl 3-[4-(benzylsulfanyl)-2,5-dimethyl-3,6-dioxocyclohexa-1,4-dien-1-yl]-3-methylbutanoate (1e). Prepared according to *General Procedure A*. ^{1}H NMR (300 MHz, Chloroform-*d*) δ 7.36 – 7.14 (m, 5H), 4.18 (s, 2H), 3.98 (q, *J* = 7.1 Hz, 2H), 2.90 (s, 2H), 2.16 (s, 3H), 2.00 (s, 3H), 1.40 (s, 6H), 1.14 (t, *J* = 7.1 Hz, 3H). ^{13}C NMR (126 MHz, cdcl$_3$) δ 188.50, 183.71, 172.44, 153.14, 149.22, 139.47, 139.40, 137.76, 129.01, 128.52, 127.24, 60.21, 47.53, 38.19, 38.16, 28.62, 14.86, 14.59, 14.18. HRMS (ESI) calculated for $C_{22}H_{27}O_4S$ $[M+H]^+$ 387.1625, found 387.1632.

ethyl 3-(2,5-dimethyl-3,6-dioxo-4-{[phenyl(²H₂)methyl]sulfanyl}-cyclohexa-1,4-dien-1-yl)-3-methylbutanoate (1e-d₂). Prepared according to *General Procedure A*. ^{1}H NMR (400 MHz, Chloroform-*d*) δ 7.46 – 6.99 (m, 5H), 4.00 (q, *J* = 7.1 Hz, 2H), 2.92 (s, 2H), 2.18 (s, 3H), 2.03 (s, 3H), 1.42 (s, 6H), 1.16 (t, *J* = 7.1 Hz, 3H). ^{13}C NMR (101 MHz, $CDCl_3$) δ 188.48, 183.71, 172.44, 153.12, 149.13, 139.47, 139.38, 137.63, 128.98, 128.51, 127.24, 60.20, 47.51, 38.15, 37.61 (quintet, CD_2), 28.61, 14.84, 14.58, 14.17. HRMS (ESI) calculated for $C_{22}H_{25}D_2O_4S$ $[M+H]^+$ 389.1750, found 389.1751.

ethyl 3-(4-{[(4-methoxyphenyl)methyl]sulfanyl}-2,5-dimethyl-3,6-dioxocyclohexa-1,4-dien-1-yl)-3-methylbutanoate (1f). Prepared according to *General Procedure A*. ^{1}H NMR (300 MHz, Chloroform-*d*) δ 7.17 (d, *J* = 8.6 Hz, 2H), 6.80 (d, *J* = 8.6 Hz, 2H), 4.15 (s, 2H),

3.99 (q, *J* = 7.1 Hz, 2H), 3.77 (s, 3H), 2.91 (s, 2H), 2.16 (s, 3H), 2.02 (s, 3H), 1.41 (s, 6H), 1.19 – 1.10 (m, 3H). ^{13}C NMR (126 MHz, cdcl$_3$) δ 188.51, 183.74, 172.46, 158.79, 153.10, 148.84, 139.79, 139.40, 130.17, 129.72, 113.92, 77.27, 77.01, 76.76, 60.20, 55.23, 47.55, 38.16, 37.73, 28.64, 14.86, 14.60, 14.17, 0.01. HRMS (ESI) calculated for $C_{23}H_{29}O_5S$ $[M+H]^+$ 417.1730, found 421.417.1602.

ethyl 3-(4-{[(4-chlorophenyl)methyl]sulfanyl}-2,5-dimethyl-3,6-dioxocyclohexa-1,4-dien-1-yl)-3-methylbutanoate (1g). Prepared according to *General Procedure A*. ^{1}H NMR (300 MHz, Chloroform-*d*) δ 7.24 – 7.14 (m, 4H), 4.13 (s, 2H), 4.00 (q, *J* = 7.2 Hz, 2H), 2.90 (s, 2H), 2.15 (s, 3H), 2.01 (s, 3H), 1.40 (s, 6H), 1.16 (t, *J* = 7.1 Hz, 3H). ^{13}C NMR (126 MHz, cdcl$_3$) δ 188.47, 183.61, 172.47, 153.52, 149.81, 139.18, 138.79, 136.39, 133.01, 130.34, 128.69, 77.29, 77.03, 76.78, 60.24, 47.50, 38.11, 37.41, 28.53, 14.95, 14.57, 14.19. HRMS (ESI) calculated for calculated for $C_{22}H_{26}ClO_4S$ $[M+H]^+$ 421.1235, found 421.1180.

ethyl 3-(2,5-dimethyl-4-{[(4-nitrophenyl)methyl]sulfanyl}-3,6-dioxocyclohexa-1,4-dien-1-yl)-3-methylbutanoate (1h). Prepared according to *General Procedure A*. ^{1}H NMR (500 MHz, Chloroform-*d*) δ 8.23 – 8.10 (m, 2H), 7.43 – 7.32 (m, 2H), 4.21 (s, 2H), 3.99 (q, *J* = 7.1 Hz, 2H), 2.89 (s, 2H), 2.15 (s, 3H), 1.98 (s, 3H), 1.39 (s, 6H), 1.17 (t, *J* = 7.1 Hz, 3H). ^{13}C NMR (126 MHz, cdcl$_3$) δ 188.41, 183.41, 172.57, 154.21, 151.03, 146.99, 145.62, 138.82, 137.59, 129.75, 123.83, 60.25, 47.42, 37.96, 37.31, 28.32, 15.05, 14.56, 14.16. ESI-MS(+) calculated for $C_{22}H_{25}NNaO_6S$ [M+Na]+ 454.1, found 454.1.

ethyl 3-{4-[(2-methoxy-2-oxoethyl)sulfanyl]-2,5-dimethyl-3,6-dioxocyclohexa-1,4-dien-1-yl}-3-methylbutanoate (1i). Prepared according to *General Procedure A*. ^{1}H NMR (600 MHz, Chloroform-*d*) δ 4.02 (q, *J* = 7.4 Hz, 2H), 3.73 (s, 2H), 3.70 (s, 3H), 2.92 (s, 2H), 2.15 (s, 6H), 1.42 (q, *J* = 7.6 Hz, 6H), 1.18 (t, *J* = 7.0 Hz, 3H). ^{13}C NMR (126 MHz, cdcl$_3$) δ 188.26, 183.29, 172.55, 169.83, 153.33, 148.90, 139.55, 138.07, 60.28, 52.51, 47.55, 38.19, 34.65, 28.60, 14.92, 14.58, 14.19. ESI-MS(+) calculated for $[C_{18}H_{24}NaO_6S]^+$ ($[M+Na]^+$) 391.1, found 391.0. HRMS (ESI) calculated for $C_{18}H_{25}O_6S$ $[M+H]^+$ 369.1366, found 369.1385.

ethyl 3-{4-[(4-hydroxybutyl)sulfanyl]-2,5-dimethyl-3,6-dioxocyclohexa-1,4-dien-1-yl}-3-methylbutanoate (1j). Prepared according to *General Procedure B* in 43% yield. ^{1}H NMR (300 MHz, Chloroform-*d*) δ 4.02 (q, *J* = 7.2 Hz, 2H), 3.68 – 3.58 (m, 2H), 3.05 – 2.96 (m, 2H), 2.94 (s, 2H), 2.17 (s, 3H), 2.15 (s, 3H), 1.70 – 1.62 (m, 4H), 1.42 (s, 6H), 1.19 (t, *J* = 7.1 Hz, 3H). ^{13}C NMR (126 MHz, cdcl$_3$) δ 188.42, 183.54, 172.92, 153.45, 148.09, 140.45, 139.31, 62.29, 60.38, 47.65, 38.13, 33.41, 31.48, 28.58, 26.78, 14.91, 14.53, 14.16. ESI-MS(+) calculated for [$\mathbf{C_{19}H_{28}NaO_5S}$]$^+$ ([M+Na]$^+$) 391.1, found 391.1. HRMS (ESI) calculated for $C_{19}H_{29}O_5S$ [M+H]$^+$ 369.1730, found 369.1740.

ethyl 3-[4-(hex-5-en-1-ylsulfanyl)-2,5-dimethyl-3,6-dioxocyclohexa-1,4-dien-1-yl]-3-methylbutanoate (1k). Prepared according to *General Procedure A*. ^{1}H NMR (500 MHz, Chloroform-*d*) δ 5.76 (ddt, *J* = 16.9, 10.2, 6.7 Hz, 1H), 5.02 – 4.94 (m, 1H), 4.95 – 4.89 (m, 1H), 4.01 (q, *J* = 7.1 Hz, 2H), 2.97 (dd, *J* = 7.7, 6.8 Hz, 2H), 2.93 (s, 2H), 2.15 (s, 3H), 2.13 (s, 3H), 2.08 – 2.00 (m, 2H), 1.60 – 1.52 (m, 2H), 1.51 – 1.43 (m, 2H), 1.41 (s, 6H), 1.17 (t, *J* = 7.1 Hz, 3H). ^{13}C NMR (126 MHz, cdcl$_3$) δ 188.41, 183.59, 172.54, 153.11, 147.83, 140.53, 139.47, 138.35, 114.73, 60.21, 47.61, 38.18, 33.64, 33.20, 29.7s6, 28.67, 27.80, 14.93, 14.57, 14.19. ESI-MS(+) calculated for $C_{21}H_{30}NaO_4S^+$ ([M+Na]$^+$) 401.1, found 401.2. HRMS (ESI) calculated for $C_{21}H_{31}O_4S^+$ [M+H]$^+$ 379.1938, found 379.1948.

ethyl 3-{4-[(cyclopropylmethyl)sulfanyl]-2,5-dimethyl-3,6-dioxocyclohexa-1,4-dien-1-yl}-3-methylbutanoate (1l). Prepared according to *General Procedure A* in 54% yield. ^{1}H NMR (300 MHz, Chloroform-*d*) δ 3.99 (q, *J* = 7.1 Hz, 1H), 2.91 (s, 2H), 2.88 (d, *J* = 7.3 Hz, 2H), 2.14 (s, 6H), 1.40 (s, 6H), 1.15 (t, *J* = 7.2 Hz, 3H), 1.04 – 0.82 (m, 1H), 0.64 – 0.38 (m, 2H), 0.24 – 0.11 (m, 2H). ^{13}C NMR (126 MHz, cdcl$_3$) δ 188.52, 183.73, 172.57, 153.18, 147.88, 140.74, 139.43, 60.23, 47.62, 39.67, 38.17, 28.68, 14.95, 14.58, 14.19, 11.76, 5.59. ESI-MS(+) calculated for $C_{19}H_{26}NaO_4S$ [M+Na]$^+$ 373.1, found 373.1. HRMS (ESI) calculated for $C_{19}H_{27}O_4S$ [M+H]$^+$ 351.1625, found 351.1650.

ethyl 3-[2,5-dimethyl-3,6-dioxo-4-({[(1R,2R)-2-phenylcyclopropyl]methyl}sulfanyl)-cyclohexa-1,4-dien-1-yl]-3-methylbutanoate (1m). Prepared according to *General Procedure*

A. ^{1}H NMR (400 MHz, Chloroform-*d*) δ 7.22 (dd, *J* = 7.7, 7.2 Hz, 2H), 7.14 (t, *J* = 7.2 Hz, 1H), 7.02 (d, *J* = 7.7 Hz, 2H), 4.01 (q, *J* = 7.0 Hz, 2H), 3.21 – 3.00 (m, 2H), 2.93 (q, *J* = 16.1 Hz, 2H), 2.16 (s, 3H), 2.13 (s, 3H), 1.89 – 1.69 (m, 1H), 1.42 (d, *J* = 3.5 Hz, 6H), 1.36 – 1.23 (m, 1H), 1.18 (t, *J* = 7.0 Hz, 3H), 1.09 – 0.96 (m, 1H), 0.95 – 0.84 (m, 1H). ESI-MS(+) calculated for $C_{25}H_{30}NaO_4S$ $[M+Na]^+$ 449.1, found 449.2.

ethyl 3-{2,5-dimethyl-3,6-dioxo-4-[(1-phenylethyl)sulfanyl]cyclohexa-1,4-dien-1-yl}-3-methylbutanoate (1n). Prepared according to *General Procedure A*. ^{1}H NMR (300 MHz, Chloroform-*d*) δ 7.24 – 7.13 (m, 5H), 4.79 (q, *J* = 7.1 Hz, 1H), 4.04 – 3.87 (m, 2H), 2.86 (s, 2H), 2.11 (s, 3H), 2.01 (s, 3H), 1.61 (d, *J* = 7.0 Hz, 3H), 1.37 (d, *J* = 9.8 Hz, 6H), 1.13 (t, *J* = 7.1 Hz, 3H). ^{13}C NMR (126 MHz, cdcl$_3$) δ 188.78, 184.01, 172.26, 152.97, 150.17, 143.06, 139.47, 139.33, 128.42, 127.38, 127.26, 77.28, 77.03, 76.78, 60.15, 47.44, 46.46, 38.17, 28.65, 22.40, 14.98, 14.57, 14.21. ESI-MS(+) calculated for $C_{23}H_{28}NaO_4S$ $[M+Na]^+$ 423.1, found 423.0. HRMS (ESI) calculated for $C_{23}H_{29}O_4S^+$ $[M+H]^+$ 401.1781, found 401.1778.

ethyl 3-(2,5-dimethyl-3,6-dioxo-4-((2,2,2-trifluoroethyl)thio)cyclohexa-1,4-dien-1-yl)-3-methylbutanoate (1o). Prepared according to *General Procedure A*. ^{1}H NMR (500 MHz, Chloroform-*d*) δ 4.02 (q, *J* = 7.1 Hz, 2H), 3.61 (q, *J* = 9.7 Hz, 2H), 2.92 (s, 2H), 2.22 (s, 3H), 2.17 (s, 3H), 1.43 (s, 6H), 1.18 (t, *J* = 7.1 Hz, 3H). ^{13}C NMR (126 MHz, Chloroform-*d*) δ 188.30, 183.16, 172.50, 153.99, 151.50, 139.39, 136.08, 125.16 (q, *J* = 276.4 Hz), 60.35, 47.54, 38.22, 34.77 (q, *J* = 32.9 Hz), 28.51, 15.28, 14.54, 14.13. UV-vis λ_{max} = 378 nm (585 $M^{-1}cm^{-1}$).

ethyl 3-(2,5-dimethyl-4-(neopentylthio)-3,6-dioxocyclohexa-1,4-dien-1-yl)-3-methylbutanoate (1p). Prepared according to *General Procedure A*. ^{1}H NMR (500 MHz, Chloroform-*d*) δ 4.02 (q, *J* = 7.2 Hz, 2H), 2.94 (s, 2H), 2.91 (s, 2H), 2.18 (d, *J* = 5.7 Hz, 6H), 1.43 (s, 6H), 1.18 (t, *J* = 7.2 Hz, 3H), 1.00 (s, 9H).

ethyl 3-(4-((3,3-dimethylbutyl)thio)-2,5-dimethyl-3,6-dioxocyclohexa-1,4-dien-1-yl)-3-methylbutanoate (1q). Prepared according to *General Procedure A*. ^{1}H NMR (600 MHz, Chloroform-*d*) δ 4.03 (q, *J* = 7.1 Hz, 2H), 3.00 – 2.95 (m, 2H), 2.94 (s, 2H), 2.17 (s, 3H), 2.14

(s, 3H), 1.53 (s, 2H), 1.49 – 1.44 (m, 1H), 1.43 (s, 6H), 1.18 (t, *J* = 7.1 Hz, 3H), 0.89 (s, 9H). UV-vis: λ_{max} = 416 nm (1,045 $M^{-1}cm^{-1}$).

ethyl 3-(2,5-dimethyl-3,6-dioxo-4-(((trimethylsilyl)methyl)thio)cyclohexa-1,4-dien-1-yl)-3-methylbutanoate (1r).). Prepared according to *General Procedure A*. ^{1}H NMR (500 MHz, Chloroform-*d*) δ 4.02 (q, *J* = 7.1 Hz, 2H), 2.94 (s, 2H), 2.29 (s, 2H), 2.16 (s, 3H), 2.13 (s, 3H), 1.42 (s, 5H), 1.19 (t, *J* = 7.1 Hz, 3H), 0.12 (d, *J* = 0.7 Hz, 8H). ^{13}C NMR (126 MHz, $cdcl_3$) δ 188.37, 183.38, 172.59, 152.81, 145.94, 143.16, 139.66, 77.26, 77.01, 76.75, 60.21, 47.62, 38.11, 28.67, 19.64, 14.53, 14.47, 14.18, -1.86.

ethyl 3-(2,5-dimethyl-3,6-dioxo-4-((2-(trimethylsilyl)ethyl)thio)cyclohexa-1,4-dien-1-yl)-3-methylbutanoate (1s). Prepared according to *General Procedure A*. ^{1}H NMR (400 MHz, Chloroform-*d*) δ 4.03 (q, *J* = 7.1 Hz, 2H), 3.10 – 2.98 (m, 2H), 2.95 (s, 2H), 2.17 (s, 3H), 2.14 (s, 3H), 1.43 (s, 6H), 1.19 (t, *J* = 7.1 Hz, 3H), 0.98 – 0.65 (m, 2H), 0.02 (s, 9H). ^{13}C NMR (101 MHz, $CDCl_3$) δ 188.60, 183.86, 172.71, 153.11, 147.35, 141.18, 139.60, 60.35, 47.78, 38.32, 30.23, 28.84, 18.56, 14.99, 14.71, 14.33, -1.66. UV-vis: λ_{max} = 419 nm (1,072 $M^{-1}cm^{-1}$).

ethyl 3-(4-(benzhydrylthio)-2,5-dimethyl-3,6-dioxocyclohexa-1,4-dien-1-yl)-3-methylbutanoate (1w). Prepared according to *General Procedure A*. ^{1}H NMR (400 MHz, Chloroform-*d*) δ 7.47 – 7.34 (m, 2H), 7.34 – 7.24 (m, 2H), 7.24 – 7.15 (m, 1H), 6.11 (s, 0H), 3.97 (q, *J* = 7.1 Hz, 1H), 2.84 (s, 1H), 2.07 (s, 1H), 1.99 (s, 1H), 1.32 (s, 3H), 1.14 (t, *J* = 7.1 Hz, 1H). ^{13}C NMR (101 MHz, $CDCl_3$) δ 188.61, 183.89, 172.14, 152.64, 148.86, 140.55, 139.69, 139.30, 128.59, 128.52, 128.50, 127.33, 60.10, 55.37, 47.33, 38.09, 28.57, 14.78, 14.43, 14.23.

ethyl 3-(4-((9H-fluoren-9-yl)thio)-2,5-dimethyl-3,6-dioxocyclohexa-1,4-dien-1-yl)-3-methylbutanoate (1x). Prepared according to *General Procedure A*. ^{1}H ^{1}H NMR (400 MHz, Chloroform-*d*) δ 7.72 (dt, *J* = 7.7, 1.0 Hz, 2H), 7.59 (ddt, *J* = 7.5, 1.6, 0.7 Hz, 2H), 7.38 (tdd,

J = 7.4, 1.2, 0.6 Hz, 2H), 7.30 (td, *J* = 7.5, 1.2 Hz, 2H), 5.70 (s, 1H), 4.08 (q, *J* = 7.1 Hz, 2H), 2.96 (s, 2H), 2.22 (s, 3H), 2.00 (s, 3H), 1.48 (s, 6H), 1.22 (t, *J* = 7.1 Hz, 3H).

ethyl 3-(4-(cyclopentylthio)-2,5-dimethyl-3,6-dioxocyclohexa-1,4-dien-1-yl)-3-methyl-butanoate (1y). Prepared according to *General Procedure A*. (96%). ^{1}H NMR (500 MHz, Chloroform-*d*) δ 4.02 (q, *J* = 7.1 Hz, 2H), 3.99 – 3.91 (m, 1H), 2.94 (s, 2H), 2.17 (s, 3H), 2.15 (s, 3H), 2.00 – 1.86 (m, 2H), 1.77 (qdd, *J* = 6.5, 4.1, 1.7 Hz, 2H), 1.66 – 1.47 (m, 4H), 1.43 (s, 6H), 1.18 (t, *J* = 7.1 Hz, 3H). ^{13}C NMR (126 MHz, cdcl$_3$) δ 188.68, 172.47, 153.02, 148.44, 140.90, 139.50, 60.22, 47.65, 46.07, 38.24, 34.16, 28.74, 24.69, 15.02, 14.62, 14.19.

ethyl 3-(2,5-dimethyl-3,6-dioxo-4-(phenylthio)cyclohexa-1,4-dien-1-yl)-3-methyl-butanoate (1t). Prepared according to *General Procedure A*. ^{1}H NMR (300 MHz, Chloroform-*d*) δ 7.58 – 6.71 (m, 8H), 4.05 (q, *J* = 7.1 Hz, 2H), 2.94 (s, 3H), 2.15 (s, 3H), 2.12 (s, 3H), 1.44 (s, 8H), 1.20 (t, *J* = 7.1 Hz, 3H). UV-vis: λ_{max} = 415 nm (900 M^{-1}cm^{-1}).

ethyl 3-(4-((9H-fluoren-9-yl)thio)-2,5-dimethyl-3,6-dioxocyclohexa-1,4-dien-1-yl)-3-methylbutanoate (1u). ^{1}H NMR (400 MHz, Chloroform-*d*) δ 7.34 – 7.29 (m, 2H), 6.66 – 6.56 (m, 2H), 4.03 (q, *J* = 7.1 Hz, 2H), 2.94 (s, 6H), 2.93 (s, 2H), 2.10 (s, 3H), 2.09 (s, 3H), 1.42 (s, 6H), 1.18 (t, *J* = 7.1 Hz, 3H). ^{13}C NMR (101 MHz, cdcl$_3$) δ 189.13, 183.64, 172.45, 152.98, 150.03, 147.28, 141.04, 139.38, 134.21, 133.90, 118.08, 112.65, 112.47, 60.20, 47.62, 40.31, 38.23, 28.70, 14.85, 14.58, 14.23. UV-vis: λ_{max} = 426 nm (1,070 M^{-1}cm^{-1}), 500 nm (sh, 900 M^{-1}cm^{-1}).

3-methyl-3-(2,4,5-trimethyl-3,6-dioxocyclohexa-1,4-dien-1-yl)butanoic acid (6). 6-hydroxy-4,4,5,7,8-pentamethylchroman-2-one was prepared according to literature (*J. Am. Chem. Soc.*, **2006**, *128* (29), 9518–9525) procedure from 2,3,5-trimethylhydroquinone and 3,3-dimethylacrylic acid in 84% yield. ^{1}H NMR (500 MHz, Chloroform-*d*) δ 4.98 (s, 1H), 2.54 (s, 2H), 2.36 (s, 2H), 2.21 (s, 3H), 2.18 (s, 3H), 1.45 (s, 6H). ^{13}C NMR (126 MHz, cdcl$_3$) δ 169.09, 148.90, 143.42, 128.15, 123.37, 122.05, 119.11, 46.04, 35.45, 27.70, 27.69, 14.51, 12.55, 12.33.The crude lactone was oxidized with N-bromosuccinamide in acetonitrile / water to

yield the quinone acid as a yellow solid in 88% yield. ^{1}H NMR (500 MHz, Chloroform-*d*) δ 3.01 (s, 2H), 2.14 (s, 3H), 1.95 (q, *J* = 1.1 Hz, 3H), 1.92 (q, *J* = 1.1 Hz, 3H), 1.43 (s, 6H). ^{13}C NMR (126 MHz, cdcl$_3$) δ 190.85, 187.42, 178.84, 152.02, 142.97, 139.00, 138.37, 47.28, 37.91, 28.77, 14.31, 12.50, 12.11.

ethyl 3-methyl-3-(2,4,5-trimethyl-3,6-dioxocyclohexa-1,4-dien-1-yl)butanoate (6). 3-methyl-3-(2,4,5-trimethyl-3,6-dioxocyclohexa-1,4-dien-1-yl)butanoic acid (2.6 g, 10 mmol) and ethanol (12 mL, 205 mmol) were dissolved in CH_2Cl_2 (25 mL) and the resulting solution was cooled to 0 °C. N-(3-Dimethylaminopropyl)-N'-ethylcarbodiimide hydrochloride (2.36 g, 12.3 mmol) and 4-(Dimethylamino)pyridine (195 mg, 1.6 mmol) were added in one portion, and the solution was stirred for 15 min at to 0 °C before allowing to warm to room temperature. The solvent was then removed, and the crude product was purified on silica (SiO_2, 10% EtOAc / hexanes). ^{1}H NMR (400 MHz, Chloroform-*d*) δ 4.03 (q, *J* = 7.1 Hz, 2H), 2.96 (s, 2H), 2.14 (s, 3H), 1.97 (s, 6H), 1.43 (s, 6H), 1.18 (t, *J* = 7.1 Hz, 3H). ^{13}C NMR (101 MHz, $CDCl_3$) δ 190.90, 187.47, 172.78, 152.75, 143.11, 138.52, 138.30, 60.20, 47.68, 38.13, 28.74, 14.27, 14.17, 12.65, 12.14. HRMS (ESI) calculated for $C_{16}H_{23}O_4$ $[M+H]^+$ 279.1591, found 279.1593.

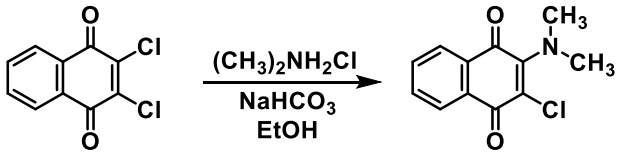

2-(bis(methyl)amino)-3-chloronaphthalene-1,4-dione. A suspension of N,N-dimethylamine hydrochloride (6.394 g, 81 mmol), $NaHCO_3$ (6.979 mg, 83 mmol), and 2,3-dichloro-1,4-naphthoquinone (6.395 mg, 28 mmol) was heated at 80 °C until a deep red solution formed. After cooling, the mixture was diluted with water and the product collected by filtration to give 4 g of the product as a red solid (60%). An analytical sample was prepared by flash column chromatography (10% EtOAc / Hexanes), collecting the red band. ^{1}H NMR (400 MHz, Chloroform-*d*) δ 8.22 – 8.05 (m, 1H), 8.05 – 7.93 (m, 1H), 7.69 (td, *J* = 7.4, 1.6 Hz, 1H), 7.64 (td, *J* = 7.4, 1.5 Hz, 1H), 3.25 (s, 6H). ^{13}C NMR (101 MHz,

$CDCl_3$) δ 182.19, 177.93, 150.95, 134.01, 132.80, 131.70, 131.35, 126.76, 126.39, 120.09, 44.42 (N-CH_3). ESI-MS(+): 242.1 (100%), 243.1 (30%).

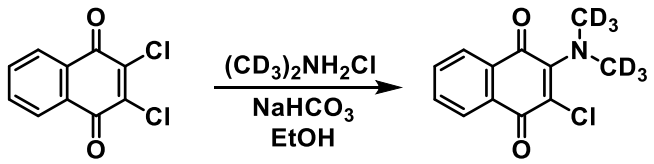

2-(bis(methyl-d3)amino)-3-chloronaphthalene-1,4-dione. A suspension of $(CD_3)_2NH_2Cl$ (144 mg, 1.6 mmol), $NaHCO_3$ (191 mg, 2.3 mmol), and 2,3-dichloro-1,4-naphthoquinone (194 mg, 0.8 mmol) was heated at 80 °C until a deep red solution formed. After cooling, the mixture was diluted with water and extracted with ethyl acetate. The combined organic layers were washed with brine and dried ($MgSO_4$) before concentrating. Purification via silica gel chromatography afforded 120 mg (58%) of the product as a red solid (>99% isotopically pure by NMR). ^{1}H NMR (400 MHz, Chloroform-*d*) δ 8.16 – 8.04 (m, 1H), 8.05 – 7.91 (m, 1H), 7.69 (td, *J* = 7.5, 1.6 Hz, 1H), 7.64 (td, *J* = 7.5, 1.5 Hz, 1H). ^{13}C NMR (101 MHz, $CDCl_3$) δ 182.22, 177.92, 150.95, 134.02, 132.78, 131.72, 131.35, 126.75, 126.39, 119.84, 43.57 (t, N-CD_3). ESI-MS(+): 236.05.

Preparative-Scale Photolysis

In a round-bottom flask equipped with a magnetic stir bar was dissolved **1a** (10-15 mg) in air-equilibrated dry methanol (20 mL). The solution was irradiated with focused light from a 420 nm LED until the solution was colorless or the starting material was completely consumed determined by TLC analysis. The sample was then concentrated *in vacuo* to yield the products **2, 3,** or **4**, unless otherwise stated. If a mixture was obtained, the crude was purified by flash column chromatography (SiO_2, 10%-25% EtOAc in hexanes) to yield the isolated products. All reported yields are based on integration of the crude NMR spectrum.

6-hydroxy-7-[(6-hydroxy-4,4,5,8-tetramethyl-2-oxo-3,4-dihydro-2H-1-benzopyran-7-yl)disulfanyl]-4,4,5,8-tetramethyl-3,4-dihydro-2H-1-benzopyran-2-one (4). ^{1}H NMR (300 MHz, Chloroform-*d*) δ 6.46 (s, 2H), 2.56 (s, 4H), 2.31 (s, 6H), 2.13 (s, 6H), 1.47 (s, 12H).

^{13}C NMR (101 MHz, $CDCl_3$) δ 167.83, 152.80, 143.26, 135.37, 128.73, 120.10, 118.08, 45.58, 36.00, 27.39, 14.87, 14.40**.** HRMS (ESI) calculated for $C_{26}H_{29}O_6S_2$ $[M-H]^-$ 501.1411, found 501.1408.

6-hydroxy-7-((methoxymethyl)thio)-4,4,5,8-tetramethylchroman-2-one (2a). Photolysis of **1a** produces **2a** (99%). ^{1}H NMR (400 MHz, Chloroform-*d*) δ 7.17 (s, 1H), 4.69 (s, 2H), 3.48 (s, 3H), 2.55 (s, 2H), 2.50 – 2.42 (m, 3H), 2.41 – 2.35 (m, 3H), 1.46 (s, 6H). ^{13}C NMR (101 MHz, cdcl$_3$) δ 168.23, 152.64, 143.19, 132.95, 128.26, 119.73, 117.69, 79.56, 57.43, 45.75, 35.80, 27.43, 15.06, 15.02. HRMS (ESI) calculated for $C_{15}H_{19}O_4S$ $[M-H]^-$ 295.1010, Found 295.1009.

6-hydroxy-7-((methoxymethyl-d2)thio)-4,4,5,8-tetramethylchroman-2-one (2a-d$_2$). Photolysis of **1a-d$_2$** produced **2a-d$_2$** quantitatively. ^{1}H NMR (400 MHz, Chloroform-*d*) δ 7.18 (s, 1H), 3.48 (s, 3H), 2.56 (s, 2H), 2.45 (d, J = 0.7 Hz, 3H), 2.40 – 2.37 (m, 3H), 1.46 (s, 6H). ^{13}C NMR (101 MHz, $CDCl_3$) δ 168.29, 152.64, 143.20, 132.95, 128.29, 119.73, 117.62, 57.35, 45.75, 35.81, 27.44, 15.10, 15.05. HRMS (ESI) calculated for $C_{15}H_{17}D_2O_4S$ $[M-H]^-$ 297.1135, found 297.1136.

6-hydroxy-7-[(1-methoxyethyl)sulfanyl]-4,4,5,8-tetramethyl-3,4-dihydro-2H-1-benzopyran-2-one (2b). Photolysis of **1b** produces **2b** quantitatively. ^{1}H NMR (500 MHz, Chloroform-*d*) δ 7.38 (s, 1H), 4.68 (q, J = 6.2 Hz, 1H), 3.52 (s, 3H), 2.58 (s, 2H), 2.45 (d, J = 0.7 Hz, 3H), 2.40 (d, J = 0.7 Hz, 3H), 1.48 (d, J = 2.0 Hz, 6H), 1.44 (d, J = 6.2 Hz, 3H). ^{13}C NMR (126 MHz, cdcl$_3$) δ 168.30, 153.25, 143.23, 132.95, 128.93, 119.62, 115.48, 87.50, 56.74, 45.81, 35.83, 27.57, 27.42, 21.80, 15.31, 15.07. HRMS (ESI) calculated for $C_{16}H_{21}O_4S$ $[M-H]^-$ 309.1166, found 309.1171.

6-hydroxy-7-[(2-methoxypropan-2-yl)sulfanyl]-4,4,5,8-tetramethyl-3,4-dihydro-2H-1-benzopyran-2-one (2c). Photolysis of **1c** produces **2c** quantitatively, however hydrolysis of **5c** to **7** was observed if the solvent was not removed immediately after completion of photolysis. ^{1}H NMR (400 MHz, Chloroform-*d*) δ 7.57 (s, 1H), 3.49 (s, 3H), 2.56 (s, 2H), 2.42

(s, 3H), 2.38 (s, 3H), 1.52 (s, 6H), 1.47 (s, 6H). ^{13}C NMR (101 MHz, $CDCl_3$) δ 168.37, 153.59, 143.12, 132.91, 129.17, 119.56, 116.81, 91.75, 51.05, 45.81, 35.80, 27.65, 27.48, 15.46, 15.05. HRMS (ESI) calculated for $C_{17}H_{23}O_4S$ $[M-H]^-$ 323.1323, found 323.1324.

6-hydroxy-7-{[methoxy(phenyl)methyl]sulfanyl}-4,4,5,8-tetramethyl-3,4-dihydro-2H-1-benzopyran-2-one (2e). Photolysis of **1e** produces **2e** (85%). ^{1}H NMR (400 MHz, Chloroform-*d*) δ 7.44 (s, 1H), 7.35 – 7.15 (m, 5H), 5.47 (s, 1H), 3.44 (s, 3H), 2.54 (s, 2H), 2.34 (s, 3H), 2.27 (s, 3H), 1.46 (s, 6H). ^{13}C NMR (101 MHz, $CDCl_3$) δ 168.33, 153.63, 142.99, 137.78, 133.24, 129.10, 128.63, 128.34, 125.88, 119.64, 116.33, 92.23, 57.64, 45.81, 35.81, 27.56, 27.37, 15.01. HRMS (ESI) calculated for $C_{21}H_{23}O_4S$ $[M-H]^-$ 371.1323, found 371.1327.

6-hydroxy-7-((methoxy(phenyl)methyl-d)thio)-4,4,5,8-tetramethylchroman-2-one (2e-d_2). Photolysis of **1e-d_2** produces **2e-d_2** (85%). ^{1}H NMR (400 MHz, Chloroform-*d*) δ 7.43 (s, 1H), 7.32 – 7.27 (m, 3H), 7.26 – 7.19 (m, 2H), 3.44 (s, 3H), 2.54 (s, 2H), 2.42 – 2.30 (m, 3H), 2.27 (d, J = 0.7 Hz, 3H), 1.46 (s, 6H). ^{13}C NMR (101 MHz, $CDCl_3$) δ 168.33, 153.63, 142.98, 137.72, 133.24, 129.09, 128.63, 128.34, 125.87, 119.63, 116.30, 57.59, 45.81, 35.81, 27.56, 27.37, 15.01. HRMS (ESI) calculated for $C_{21}H_{22}DO_4S$ $[M-H]^-$ 372.1385, found 372.1390.

Photolysis of **1f** produces **6f** (64%) and **7** (36%). **5-(4-methoxyphenyl)-2,8,13,13-tetramethyl-4,10-dioxa-6-thiatricyclo[7.4.0.0^{3,7}]trideca-1(9),2,7-trien-11-one (6f)**. ^{1}H NMR (300 MHz, Chloroform-*d*) δ 7.54 (d, J = 8.7 Hz, 2H), 7.06 – 6.78 (m, 3H), 3.83 (s, 3H), 2.55 (s, 2H), 2.32 (s, 3H), 2.18 (s, 3H), 1.43 (s, 6H).

Photolysis of **1j** produces **2j** and **6** in a ratio of 17:83. **6-hydroxy-4,4,5,8-tetramethyl-7-(oxolan-2-ylsulfanyl)-3,4-dihydro-2H-1-benzopyran-2-one (6).** ^{1}H NMR (500 MHz, Chloroform-*d*) δ 7.56 (s, 1H), 5.29 (dd, J = 6.9, 4.3 Hz, 1H), 4.09 – 4.00 (m, 1H), 3.99 – 3.91 (m, 1H), 2.55 (d, J = 1.3 Hz, 2H), 2.45 (d, J = 0.6 Hz, 3H), 2.39 (d, J = 0.7 Hz, 3H), 2.38 – 2.31 (m, 1H), 2.12 – 1.98 (m, 2H), 1.96 – 1.85 (m, 1H), 1.46 (d, J = 4.9 Hz, 6H). ^{13}C NMR (126 MHz, Chloroform-*d*) δ 168.37, 153.22, 143.15, 132.97, 128.57, 119.83, 117.21, 88.55, 68.19, 45.81, 35.84, 32.75, 27.57, 27.37, 25.13, 15.13, 15.07. Although an analytically pure

sample of **2j** could not be obtained due to decomposition while carrying out standard purification techniques, the yield was estimated by integration of diagnostic peaks in the ^{1}H-NMR spectrum (R(OC**H**$_3$)SC-**H**) and the identity established by LC-MS analysis of the crude reaction mixture. **6-hydroxy-7-[(4-hydroxy-1-methoxybutyl)sulfanyl]-4,4,5,8-tetramethyl-3,4-dihydro-2H-1-benzopyran-2-one (2j)**. ^{1}H NMR (300 MHz, Chloroform-*d*) δ 4.52 (t, *J* = 6.1 Hz, 1H), 3.51 (s, 3H). ESI-MS(+) calculated for $C_{18}H_{26}NaO_5S$ $[M+Na]^+$ 377.1, found 377.1.

6-hydroxy-7-[(1-methoxyhex-5-en-1-yl)sulfanyl]-4,4,5,8-tetramethyl-3,4-dihydro-2H-1-benzopyran-2-one (2k). Photolysis of **1k** produces **2k.** ^{1}H NMR (400 MHz, Chloroform-*d*) δ 7.43 (s, 1H), 5.74 (ddt, *J* = 16.9, 10.2, 6.7 Hz, 1H), 5.05 – 4.89 (m, 2H), 4.48 (dd, *J* = 7.6, 5.2 Hz, 1H), 3.49 (s, 3H), 2.56 (s, 2H), 2.44 (s, 3H), 2.38 (s, 3H), 2.10 – 1.96 (m, 2H), 1.83 – 1.62 (m, 2H), 1.56 – 1.49 (m, 2H), 1.47 (s, 6H). ^{13}C NMR (101 MHz, $CDCl_3$) δ 168.32, 153.10, 143.21, 137.99, 132.77, 128.56, 119.65, 116.06, 115.03, 91.76, 57.01, 45.80, 35.81, 35.04, 33.11, 27.53, 27.44, 25.20, 15.26, 15.06.

Photolysis of **1l** produces **2l**. **7-{[cyclopropyl(methoxy)methyl]sulfanyl}-6-hydroxy-4,4,5,8-tetramethyl-3,4-dihydro-2H-1-benzopyran-2-one (2l).** ^{1}H NMR (400 MHz, Chloroform-*d*) δ 7.43 (s, 1H), 3.94 (d, *J* = 8.0 Hz, 1H), 3.50 (s, 3H), 2.56 (s, 2H), 2.47 (s, 3H), 2.38 (s, 3H), 1.46 (d, *J* = 1.7 Hz, 6H), 1.18 – 1.02 (m, 1H), 0.69 – 0.54 (m, 2H), 0.53 – 0.44 (m, 1H), 0.40 – 0.32 (m, 1H). ^{13}C NMR (101 MHz, $CDCl_3$) δ 168.35, 153.38, 143.12, 132.87, 129.01, 119.40, 116.12, 94.99, 56.82, 45.81, 35.81, 27.54, 27.44, 15.98, 15.33, 15.06, 5.41, 3.91. Note: NMR of **5l** contains **7** as an impurity as a result of thermal decomposition after purification.

Photolysis of **1m** produces the diastereomers **6-hydroxy-7-((1-methoxy-2-phenylcyclopropyl)thio)-4,4,5,8-tetramethylchroman-2-one (4m)** in a 3:2 ratio, along with other uncharacterized byproducts. Although isolation proved difficult due to decomposition, assignment has been made primarily based on clear ^{1}H-NMR resonances for the cyclopropane -CH, oxidized methylene -CH, methyl ether -OCH_3, aryl -CH_3, and the lactone methylene -CH_2

protons. **4m:** ^{1}H NMR (400 MHz, Chloroform-*d*) δ 4.41 (d, *J* = 5.8 Hz, 1H), 3.53 (s, 3H), 2.47 (s, 2H), 2.42 (s, 3H), 2.29 (s, 3H). Second product: ^{1}H NMR (400 MHz, Chloroform-*d*) δ 4.31 (d, *J* = 7.0 Hz, 1H), 3.55 (s, 3H), 2.51 (s, 2H), 2.39 (s, 3H), 2.26 (s, 3H).

Photolysis of **1o** produces **2o**. **6-hydroxy-7-((methoxy(trimethylsilyl)methyl)thio)-4,4,5,8-tetramethylchroman-2-one (2o).** ^{1}H NMR (500 MHz, Chloroform-*d*) δ 7.66 (s, 1H), 4.33 (s, 1H), 3.40 (s, 3H), 2.56 (s, 2H), 2.45 (d, *J* = 0.6 Hz, 3H), 2.38 (d, *J* = 0.7 Hz, 3H), 1.47 (s, 3H), 1.46 (s, 3H), 0.13 (s, 9H). ^{13}C NMR (126 MHz, cdcl$_3$) δ 168.55, 152.84, 143.25, 132.41, 127.44, 120.51, 120.02, 87.09, 59.33, 46.00, 35.91, 27.75, 27.61, 15.17, 15.14, -2.77. LCMS (M/Z-) = 367.1.

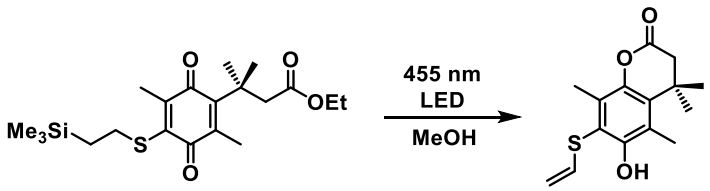

Photolysis of **1s** produces **2s**. **6-hydroxy-7-((methoxy(trimethylsilyl)methyl)thio)-4,4,5,8-tetramethylchroman-2-one (15).** ^{1}H NMR (300 MHz, Chloroform-*d*) δ 6.68 (s, 1H), 6.17 (dd, *J* = 16.4, 9.6 Hz, 1H), 5.25 (dd, *J* = 9.6, 0.5 Hz, 1H), 4.88 (dd, *J* = 16.4, 0.5 Hz, 1H), 2.58 (s, 2H), 2.46 – 2.34 (m, 6H), 1.48 (s, 6H). MS (ESI-) = 277.1

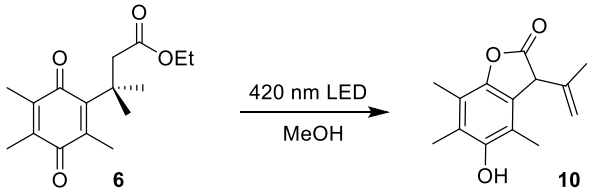

Photolysis of 6. An approximately 1.5 mM solution of **6** was irradiated with a focused 420 nm LED in methanol with continuous argon sparging until complete consumption of starting material was observed by TLC. The solvent was removed under reduced pressure to yield, by NMR analysis, a mixture of products resulting from H-atom abstraction from the *t*-butyl group followed by a known rearrangement. An illustrative compound, **5-hydroxy-4,6,7-trimethyl-3-(prop-1-en-2-yl)benzofuran-2(3H)-one (10)**, was isolated from the mixture by silica gel chromatography followed by recrystallization, and fully characterized. ^{1}H NMR (600 MHz, Chloroform-*d*) δ 5.13 (p, *J* = 1.5 Hz, 1H), 5.03 (q, *J* = 0.9 Hz, 1H), 4.45 (s, 1H), 4.30 (s, 1H),

2.22 (s, 3H), 2.20 (s, 3H), 2.10 (s, 3H), 1.69 (dd, J = 1.5, 0.8 Hz, 3H). ^{13}C NMR (126 MHz, cdcl$_3$) δ 175.70, 148.62, 146.32, 138.73, 123.28, 121.51, 118.45, 117.63, 116.90, 52.97, 19.66, 12.29, 12.07, 11.73. HRMS (ESI) calculated for $C_{14}H_{15}O_3$ [M-H]$^-$ 231.1027, found 231.1018.

Quantum Yield Measurements

Materials and Methods

All chemicals and solvents were purchased in the highest grade available. Spectral grade methanol was distilled prior to use for quantum yield measurements. Thioxanthone was purified by preparative HPLC using a 5-95% acetonitrile-water gradient, and pure fractions were used for measurement of sensitized quantum yields. Diethylaniline was distilled under vacuum immediately prior to use. Samples were prepared in eight-inch NMR tubes (Wilmad WG-1000) and photolyzed in a custom-made merry-go-round apparatus rotating at 20 rpm using diffuse light from a 1 watt LED centered at 420 nm (Thorlabs M420L3), powered with approximately 1 amp. All procedures were carried out in darkness with a red safety-light. Data were collected on an Agilent 1260 HPLC equipped with a diode-array detector using a 60% isocratic acetonitrile-water (+ 0.1% AcOH) elution. Absorbance spectra were recorded on a Cary 60 using cuvettes with a 10 mm path-length.

Preparation of Potassium Ferrioxalate

The following procedure[61] is taken from *Photochemistry of Organic Compounds* by Klan & Wirz and is performed in a dark room with a red safety-light. In an Erlenmeyer flask with magnetic stir-bar is mixed 1.5 M potassium oxalate monohydrate (300 mL) and 1.5 M ferric chloride hexahydrate (100 mL). The mixture is stirred 10 minutes then filtered using a Büchner funnel. The collected solid is recrystallized three times from warm water, filtered, and dried over a current of warm air overnight to provide crystalline potassium ferrioxalate trihydrate, which is stored at room temperature in the dark.

General procedure for Ferrioxalate actinometry

Solutions of potassium ferrioxalate and 1,10-phenanthroline are always made fresh when measuring quantum yields. Solid potassium ferrioxalate trihydrate (60 mg) is weighed into a tared 20 mL vial to which is then added 0.05 M H_2SO_4 (20 mL). The mixture is thoroughly shaken to ensure a homogenous solution is formed. Additionally, a solution of 1,10-phenanthroline (40 mg) in 1M sodium acetate buffer (20 mL; prepared by adding 82 g of $NaOAc•3H_2O$ and 10 mL H_2SO_4 to 1 L of water) is prepared, and again thoroughly shaken until the solid is completely dissolved.

Using a 1 mL gas-tight syringe fitted with a four-inch needle, 500 □ L of actinometer solution is transferred to the bottom of an NMR tube and capped. The solution is irradiated at 420 nm in the merry-go-round apparatus. Upon completion, 100 □ L of the photolysate is transferred to a 2 mL volumetric flask (the syringe is initially flushed three times with a small volume of photolysate). 800 □ L of buffered phenanthroline solution is added and the flask is diluted with deionized water to the mark. The solution is allowed to develop for 15 minutes, then transferred via pipette to a clean dry cuvette and the UV/Vis spectrum recorded.

General procedures for photolysis quantum yields

Sample preparation for direct photolysis. Into an amber HPLC vial is transferred 1 mL of a solution of **1** in methanol that is adjusted to a concentration such that the 10 mm absorbance at 420 nm is between 0.05 – 0.1. Using a 1 mL gas-tight syringe fitted with a four-inch needle, 500 μL of the solution is transferred to the bottom of an eight-inch NMR tube, freeze-pump-thawed three times, then flame-sealed while frozen under vacuum. The remaining 500 μL is capped for HPLC analysis.

Sample preparation for sensitized photolysis. A stock solution of thioxanthone in methanol is initially prepared with a 10 mm absorbance at 420 nm between 0.05 – 0.1 and a total volume of 10 mL. To 5 mL of this solution is added a calculated amount of **1** such that the 10 mm absorbance of **1** would be 0.1 at 420 nm (determined by HPLC calibration curve). Using a 1 mL gas-tight syringe, samples with different concentrations of **1** are prepared in amber HPLC vials (1 mL total) by mixing the two stock solutions at different ratios (up to a

10x dilution of **1**). Using a 1 mL gas-tight syringe fitted with a four-inch needle, 500 μL of each solution is transferred to the bottom of an eight-inch NMR tube, freeze-pump-thawed three times, then flame-sealed under vacuum. The remaining 500 μL is capped for HPLC analysis. In some cases, the thioxanthone precipitates from the freeze-pump-thawed solution in which case gentle agitation results in dissolution.

Sample preparation for direct photolysis in the presence of quencher. A stock solution of **1** in methanol is initially prepared with a 10 mm absorbance at 420 nm between 0.05 – 0.1 and a total volume of 10 mL. To 5 mL of this solution is added N,N-diethylaniline (80 μL) to create a second stock solution with a 0.1 M quencher concentration. Using a 1 mL gas-tight syringe, samples with different quencher concentrations (0 – 100 mM) are prepared in amber HPLC vials (1 mL total) by mixing the two stock solutions at different ratios. Using a 1 mL gas-tight syringe fitted with a four-inch needle, 500 μL of each solution is transferred to the bottom of an eight-inch NMR tube, freeze-pump-thawed three times, then flame-sealed under vacuum. The remaining 500 μL is capped for HPLC analysis.

Photolysis. The prepared samples are irradiated in a well-ventilated space using a 420 nm LED and merry-go-round apparatus that spins at approximately 20 rpm. Both components (the LED and merry-go-round) are mounted on an optical rail to ensure consistency in light exposure. In some cases, the intensity of the LED is adjusted such that total photolysis time is at least 5 minutes, which ensures an adequate number of revolutions on the merry-go-round. Upon completion, the NMR tubes are scored near the surface of the liquid, cracked, poured into amber HPLC vials, and capped for analysis.

Data collection. In general, quantitative analysis for the photolysis of **1** was performed by HPLC using an isocratic elution of 60% acetonitrile in water and integration of the peak corresponding to **1** in the 254 nm absorbance trace. Quantitative analysis for photolysis of ferrioxalate was performed by UV/Vis spectroscopy using a glass cuvette (10

mm path length), blanked with water, and by measurement of the absorbance at 510 nm corresponding to the Fe^{2+}-phenanthroline complex.

Calculation of the quantum yield. The quantum yield for disappearance of **1** (Φ) due to direct photolysis is given by Eq. 1a.

$$\Phi = \frac{n_4}{p_4} \quad (1a)$$

where n_4 is the number of moles of **1** consumed, and p_4 is the number moles of photons absorbed by **1.** n_4 is further given by Eq. 1b, the difference between the number of moles pre- and post-photolysis, which are calculated from the integrations in the HPLC (I_4), the use of a calibration function (f), and the volume of the photolysis sample (V).

$$n_4 = (f(I_4^{pre}) - f(I_4^{post})) \bullet V \quad (1b)$$

The value for p_4 is calculated using Eq. 1c, where $(1 - 10^{-Abs_4})$ represents the fraction of the LED output absorbed by **1**, $(1 - 10^{-Abs_{Fe3+}})$ is that absorbed by potassium ferrioxalate, Φ_{Fe2+} is the quantum yield for Fe^{2+} production (1.115[61]), and n_{Fe2+} is the number of moles of Fe^{2+} produced. The latter is given by the absorbance of the Fe^{2+}-phenanthroline complex measured at 510 nm (see general procedure above), the known extinction coefficient (11100 $M^{-1}cm^{-1}$), and the photolysis volume. The fraction of photons absorbed by **1** is given by a calibration function (g) between $(1 - 10^{-Abs_4})$ and I_4, which is more convenient than measuring the actual absorbance spectrum of the photolysis solution. For the fraction of photons absorbed by the ferrioxalate solution, the absorbance must be measured directly before and after photolysis.

$$p_4 = \frac{(1-10^{-Abs_4})}{(1-10^{-Abs_{Fe3+}})} \bullet \frac{\Phi_{Fe2+}}{n_{Fe2+}} = \frac{g(I_4)}{(1-10^{-Abs_{Fe3+}})} \bullet \frac{\Phi_{Fe2+}}{n_{Fe2+}} \quad (1c)$$

For calculation of the sensitized quantum yield, $(1 - 10^{-Abs_4})$ is replaced with the fraction of photons absorbed by the sensitizer, which is again given by a calibration function between the integration of the thioxanthone peak in the HPLC trace and its UV/Vis absorption spectrum. In some cases, a small amount of direct photolysis occurs during sensitization experiments. To correct for this, the amount of **1** consumed (n_4) due to direct photolysis is subtracted from the total using the known quantum yield (Φ_4) before calculation of the

sensitized quantum yield is performed. In most cases, this amount accounted for less than 10% of the total consumption of **1**.

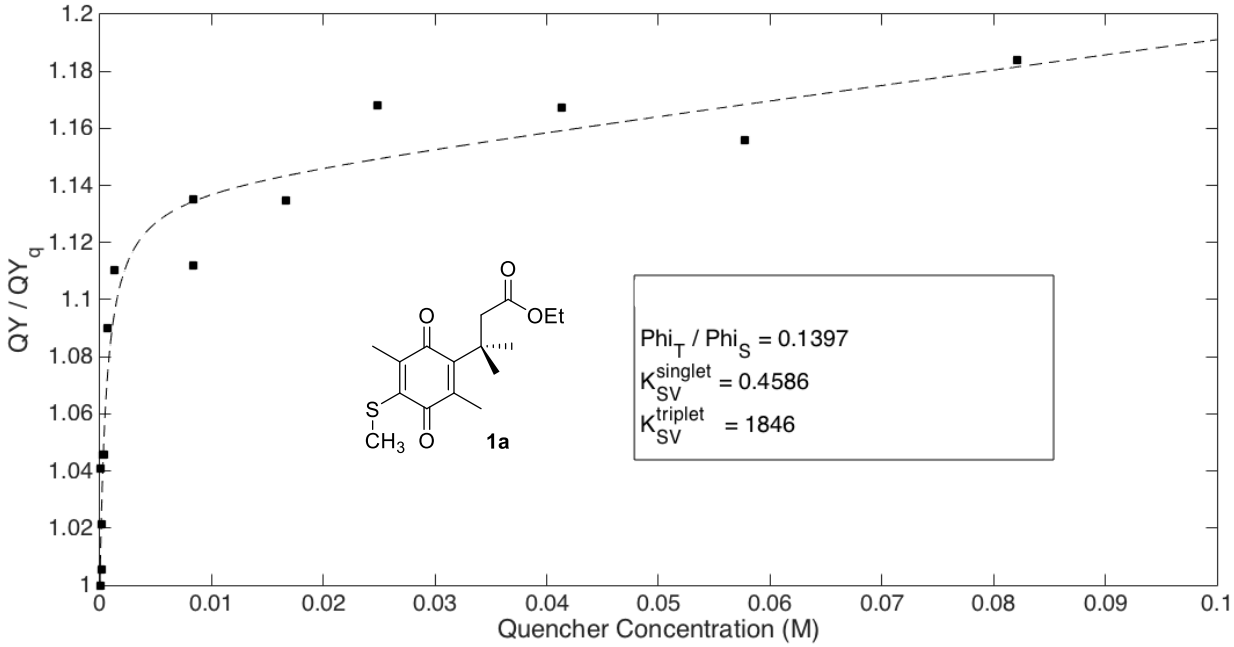

Figure 3.10. Stern-Volmer quenching of the photolysis of **1a** by diethylaniline.

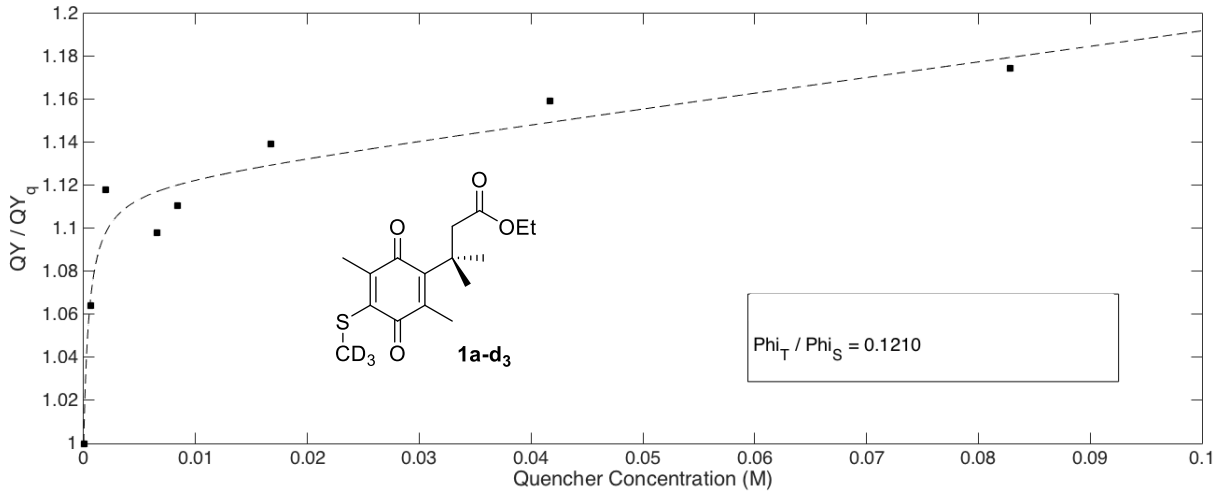

Figure 3.11. Stern-Volmer quenching of the photolysis of **1a-d3** by diethylaniline.

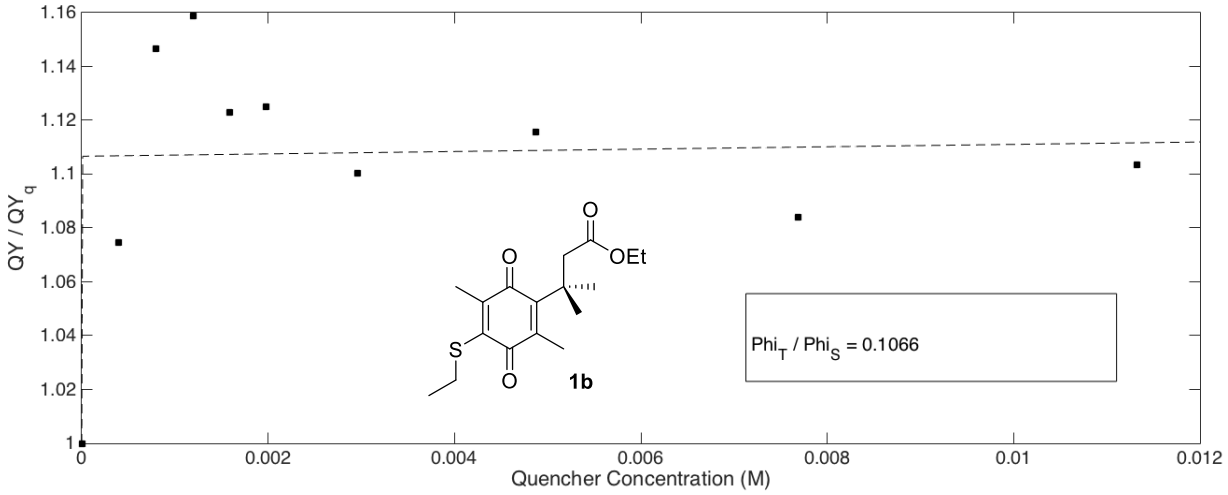

Figure 3.12. Stern-Volmer quenching of the photolysis of **1b** by diethylaniline.

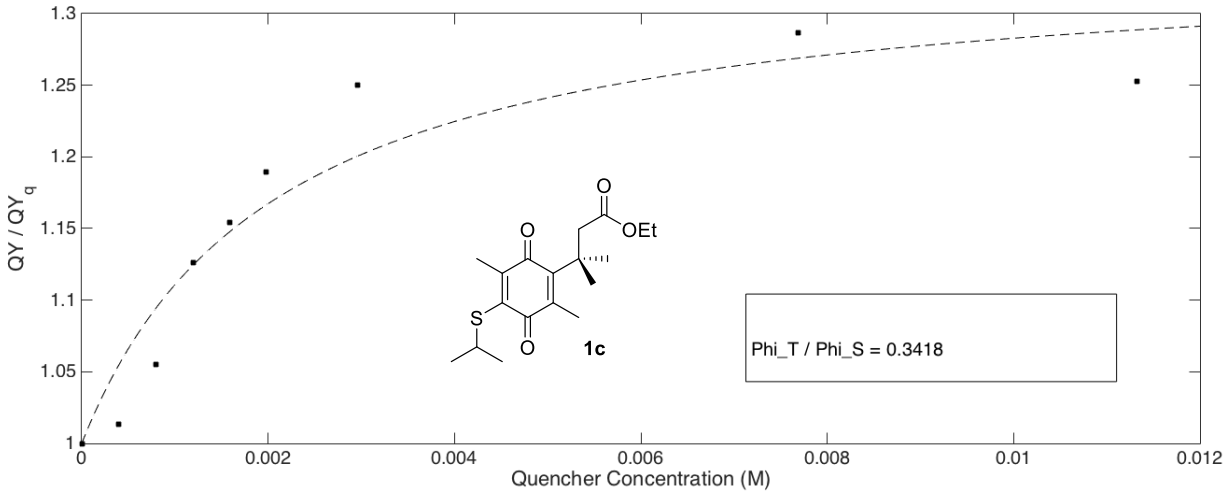

Figure 3.13. Stern-Volmer quenching of the photolysis of **1c** by diethylaniline.

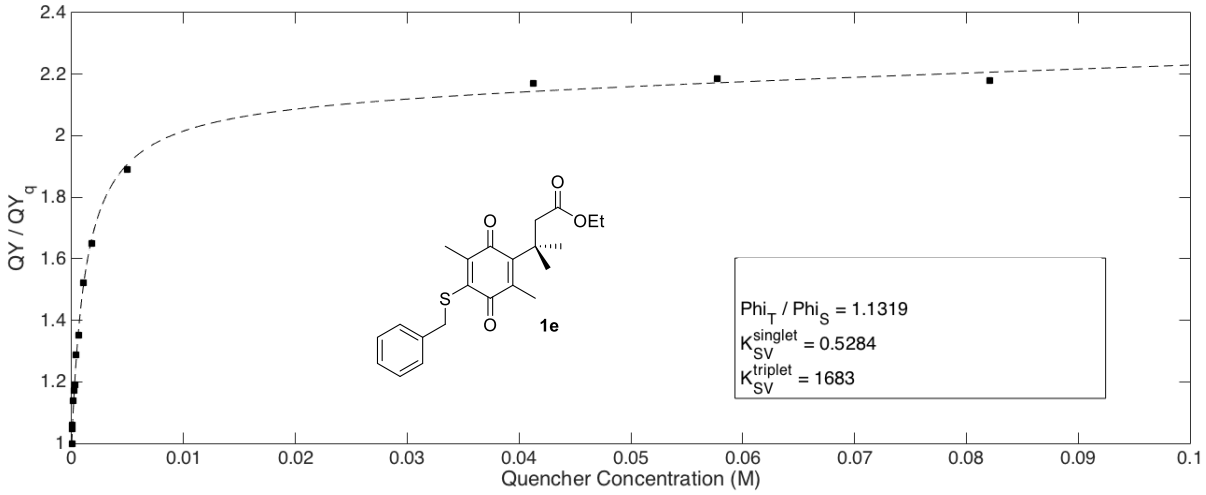

Figure 3.14. Stern-Volmer quenching of the photolysis of **1e** by diethylaniline.

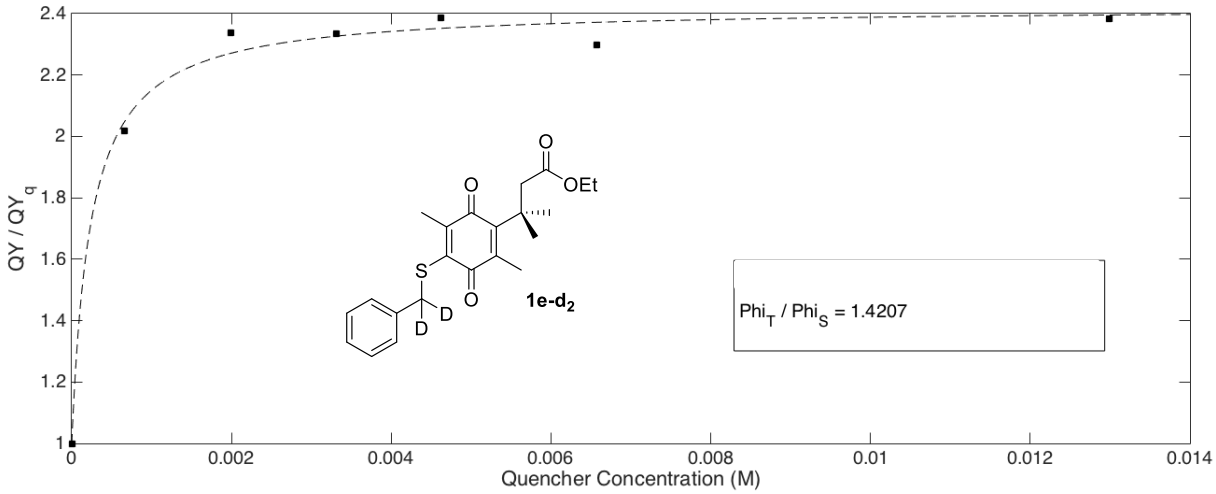

Figure 3.15. Stern-Volmer quenching of the photolysis of **1e-d$_2$** by diethylaniline.

Transient Absorption Spectroscopy. Compounds for study were dissolved in the indicated solvent, then diluted to a concentration such that $A_{355} < 0.4$. The sample was placed in a four sided quartz cuvette (Starna Cells) with a stir bar. This cuvette was open to air for the oxygen-saturated samples. Air-free samples were subjected to freeze-pump-thaw cycles to remove oxygen, before backfilling with argon. A custom cuvette with an auxiliary bulb for freezing, connections for Schlenk line maniuplations, and Teflon valve (Kontes) for sealing under high-vacuum was used for samples void of oxygen.

The third harmonic from a Q-switched Nd:YAG laser (SpectraPhysics, Quanta-Ray PRO Series) provided 355 nm pulses, 8 ns, at 10 Hz for excitation. A 75 W Xe arc-lamp operated in continuous or pulsed mode was passed through the sample colinearly with the excitation pulse for single-wavelength transient absorption experiments. A double monochromator selected probe wavelengths. Stray light was removed with appropriate short-pass and long-pass filter, while intensity was modulated with a neutral density filter. A photomultiplier tube (Hamamatsu R928), and amplified using a 200 MHz wideband voltage amplifier (FEMTO, DHPVA-200) was used to detect light. Approximately 150 shots were collected at each wavelength, and the data were log-compressed and then fit with custom scripts in MATLAB (Mathworks). The same laser system was used for full-spectrum transient absorption with the modifications of a nanosecond flash lamp and diode detector as described elsewhere (Dempsey, J. L.; Winkler, J. R.; Gray, H. B. *Journal of the American Chemical Society* **2010**, 132, 1060–1065).

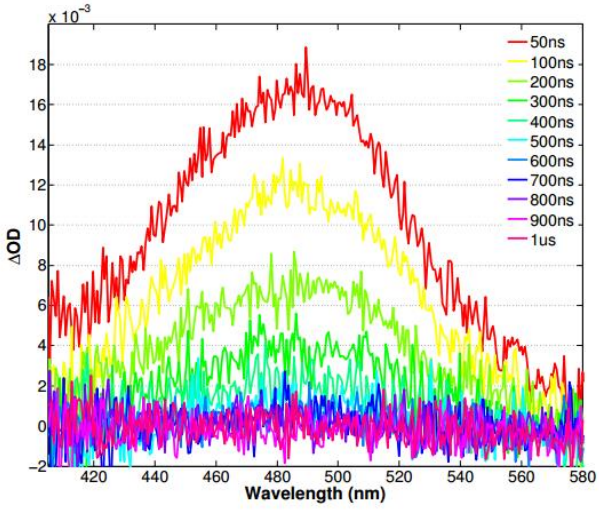

Figure 3.16. Full-spectrum transient absorption trace **1a** in air-equilibrated acetonitrile.

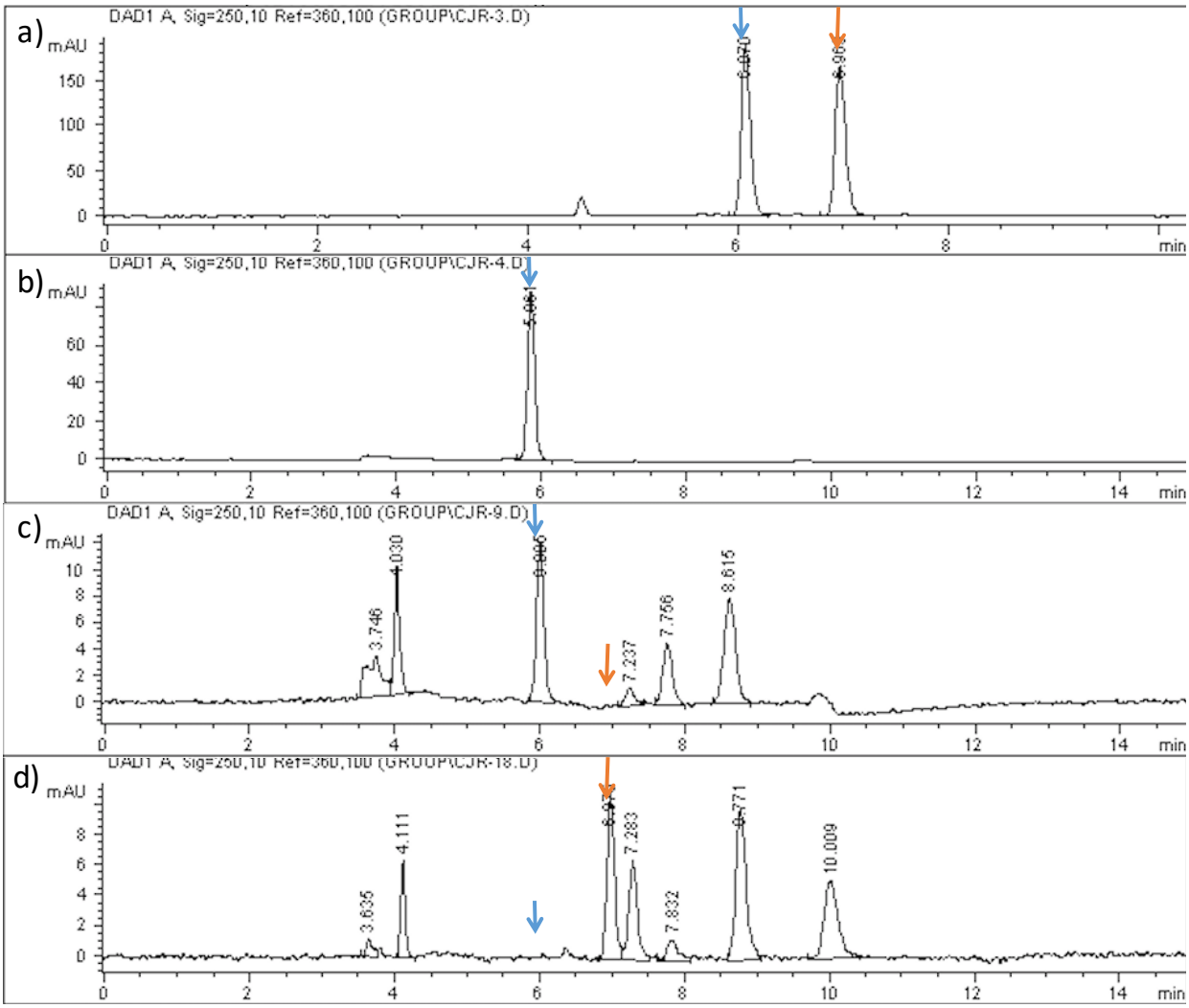

Figure 3.17. Chiral HPLC traces for the photolysis of enantioenriched **1n** where arrows indicate the peaks for each enantiomer. **a)** Racemic mixture of **1n**. **b)** Single enantiomer isolated by HPLC **c)** Photolysis of the enantiomer indicated by blue arrow to 75% conversion. **d)** photolysis of the enantiomer indicated by the orange arrow to 75% conversion.

3.7 References

1. Walton, D. P.; Dougherty, D. A. A General Strategy for Visible-Light Decaging Based on the Quinone Trimethyl Lock. *J. Am. Chem. Soc.* **2017**, *139* (13), 4655–4658. https://doi.org/10.1021/jacs.7b01548.
2. Levine, M. N.; Raines, R. T. Trimethyl Lock: A Trigger for Molecular Release in Chemistry, Biology, and Pharmacology. *Chem Sci* **2012**, *3* (8), 2412–2420. https://doi.org/10.1039/C2SC20536J.
3. Greenwald, R. B.; Choe, Y. H.; Conover, C. D.; Shum, K.; Wu, D.; Royzen, M. Drug Delivery Systems Based on Trimethyl Lock Lactonization: Poly(Ethylene Glycol) Prodrugs of Amino-Containing Compounds. *J. Med. Chem.* **2000**, *43* (3), 475–487. https://doi.org/10.1021/jm990498j.
4. Gomes, P.; Vale, N.; Moreira, R. Cyclization-Activated Prodrugs. *Molecules* **2007**, *12* (11), 2484–2506. https://doi.org/10.3390/12112484.
5. Pelliccioli, A. P.; Wirz, J. Photoremovable Protecting Groups: Reaction Mechanisms and Applications. *Photochem. Photobiol. Sci.* **2002**, *1* (7), 441–458. https://doi.org/10.1039/B200777K.
6. Klán, P.; Šolomek, T.; Bochet, C. G.; Blanc, A.; Givens, R.; Rubina, M.; Popik, V.; Kostikov, A.; Wirz, J. Photoremovable Protecting Groups in Chemistry and Biology: Reaction Mechanisms and Efficacy. *Chem. Rev.* **2013**, *113* (1), 119–191. https://doi.org/10.1021/cr300177k.
7. Görner, H. Photoreactions of P-Quinones with Dimethyl Sulfide and Dimethyl Sulfoxide in Aqueous Acetonitrile†. *Photochem. Photobiol.* **2006**, *82* (1), 71–77. https://doi.org/10.1562/2005-05-25-RA-540.
8. Kavarnos, G. J.; Turro, N. J. Photosensitization by Reversible Electron Transfer: Theories, Experimental Evidence, and Examples. *Chem. Rev.* **1986**, *86* (2), 401–449. https://doi.org/10.1021/cr00072a005.
9. Görner, H. Photoreduction of P-Benzoquinones: Effects of Alcohols and Amines on the Intermediates and Reactivities in Solution¶. *Photochemistry and Photobiology* **2003**, *78* (5), 440–448. https://doi.org/10.1562/0031-8655(2003)0780440POPEOA2.0.CO2.
10. Scheerer, R.; Graetzel, M. Laser Photolysis Studies of Duroquinone Triplet State Electron Transfer Reactions. *J. Am. Chem. Soc.* **1977**, *99* (3), 865–871. https://doi.org/10.1021/ja00445a032.
11. Baxter, I.; Phillips, W. R. Reactions between 2,5-Di-t-Butyl-1,4-Benzoquinone and Certain Primary Aliphatic Amines. *J. Chem. Soc., Perkin Trans. 1* **1973**, No. 0, 268–272. https://doi.org/10.1039/P19730000268.
12. Bruce, J. M. Light-Induced Reactions of Quinones. *Q. Rev. Chem. Soc.* **1967**, *21* (3), 405–428. https://doi.org/10.1039/QR9672100405.
13. Iwamoto, H.; Takuwa, A.; Hamada, K.; Fujiwara, R. Intra- and Intermolecular Photocyclization of Vinylbenzo-1,4-Quinones. *J. Chem. Soc., Perkin Trans. 1* **1999**, No. 5, 575–582. https://doi.org/10.1039/A809530B.
14. Kallmayer, H.-J.; Fritzen, W. Photoreactivity of Some 2-Alkylthio/Phenylthio-3,5,6-Trichloro/Bromo-1, 4-Benzoquinones. *Pharmazie* **1994**, *49* (6), 412–415.
15. Shi, M.; Yang, W.-G.; Wu, S. Wavelength-Dependent Photolyses of 2,5-Dichloro-3,6-Bis(Dialkylamino)-[1,4]Benzoquinone. *Journal of Photochemistry and Photobiology A:*

Chemistry **2007**, *185* (2–3), 140–143. https://doi.org/10.1016/j.jphotochem.2006.05.019.

16. Chen, Y.; Steinmetz, M. G. Photoactivation of Amino-Substituted 1,4-Benzoquinones for Release of Carboxylate and Phenolate Leaving Groups Using Visible Light. *J. Org. Chem.* **2006**, *71* (16), 6053–6060. https://doi.org/10.1021/jo060790g.
17. Chen, Y.; Steinmetz, M. G. Photochemical Cyclization with Release of Carboxylic Acids and Phenol from Pyrrolidino-Substituted 1,4-Benzoquinones Using Visible Light. *Org. Lett.* **2005**, *7* (17), 3729–3732. https://doi.org/10.1021/ol051362k.
18. Jones; Qian, X. Photochemistry of Quinone-Bridged Amino Acids. Intramolecular Trapping of an Excited Charge-Transfer State1. *J. Phys. Chem. A* **1998**, *102* (15), 2555–2560. https://doi.org/10.1021/jp972325g.
19. Falci, K. J.; Franck, R. W.; Smith, G. P. Approaches to the Mitomycins. Photochemistry of Aminoquinones. *J. Org. Chem.* **1977**, *42* (20), 3317–3319. https://doi.org/10.1021/jo00440a033.
20. Giles, R. G. F. The Photochemistry of an Aminated 1,4-Benzoquinone. *Tetrahedron Letters* **1972**, *13* (22), 2253–2254. https://doi.org/10.1016/S0040-4039(01)84819-X.
21. Cameron, D. W.; Giles, R. G. F. Photochemical Formation of Benzoxazoline Derivatives from Aminated Quinones. *J. Chem. Soc. C* **1968**, No. 0, 1461–1464. https://doi.org/10.1039/J39680001461.
22. Cameron, D. W.; Giles, R. G. F. A Photochemical Rearrangement Involving Aminated Quinones. *Chem. Commun. (London)* **1965**, No. 22, 573–574. https://doi.org/10.1039/C19650000573.
23. Barbafina, A.; Latterini, L.; Carlotti, B.; Elisei, F. Characterization of Excited States of Quinones and Identification of Their Deactivation Pathways. *J. Phys. Chem. A* **2010**, *114* (19), 5980–5984. https://doi.org/10.1021/jp911734x.
24. Hubig, S. M.; Bockman, T. M.; Kochi, J. K. Identification of Photoexcited Singlet Quinones and Their Ultrafast Electron-Transfer vs Intersystem-Crossing Rates. *J. Am. Chem. Soc.* **1997**, *119* (12), 2926–2935. https://doi.org/10.1021/ja963907z.
25. Trommsdorff, H. P. Electronic States and Spectra of P- Benzoquinone. *The Journal of Chemical Physics* **1972**, *56* (11), 5358–5372. https://doi.org/10.1063/1.1677047.
26. Asundi, R. K.; Singh, R. S. Absorption Spectrum of Benzoquinone. *Nature* **1955**, *176* (4495), 1223–1224. https://doi.org/10.1038/1761223a0.
27. Bridge, N. K.; Porter, G. Primary Photoprocesses in Quinones and Dyes. I. Spectroscopic Detection of Intermediates. *Proceedings of the Royal Society of London A: Mathematical, Physical and Engineering Sciences* **1958**, *244* (1237), 259–275. https://doi.org/10.1098/rspa.1958.0040.
28. Orgel, L. E. The Electronic Structures and Spectra of P-Benzoquinone and Its Derivatives. *Trans. Faraday Soc.* **1956**, *52*, 1172–1175. https://doi.org/10.1039/TF9565201172.
29. Braude, E. A. 127. Studies in Light Absorption. Part I. p-Benzoquinones. *J. Chem. Soc.* **1945**, No. 0, 490–497. https://doi.org/10.1039/JR9450000490.
30. Bridge, N. K.; Porter, G. Primary Photoprocesses in Quinones and Dyes. II. Kinetic Studies. *Proceedings of the Royal Society of London A: Mathematical, Physical and Engineering Sciences* **1958**, *244* (1237), 276–288. https://doi.org/10.1098/rspa.1958.0041.

31. Orlando, C. M.; Bose, A. K. Photorearrangement of Di-t-Butyl-p-Benzoquinones. *J. Am. Chem. Soc.* **1965**, *87* (16), 3782–3783. https://doi.org/10.1021/ja01094a051.
32. Orlando, C. M.; Mark, H.; Bose, A. K.; Manhas, M. S. Photoreactions. IV. Photolysis of Tert-Butyl-Substituted p-Benzoquinones. *J. Am. Chem. Soc.* **1967**, *89* (25), 6527–6532. https://doi.org/10.1021/ja01001a027.
33. Orlando, C. M.; Mark, H.; Bose, A. K.; Manhas, M. S. Photoreactions. V. Mechanism of the Photorearrangement of Alkyl-p-Benzoquinones. *J. Org. Chem.* **1968**, *33* (6), 2512–2516. https://doi.org/10.1021/jo01270a076.
34. Baxter, I.; Mensah, I. A. Photolysis of T-Butyl-Substituted p-Benzoquinone Mono- and Di-Imine Derivatives. *J. Chem. Soc. C* **1970**, No. 18, 2604–2608. https://doi.org/10.1039/J39700002604.
35. King, T. J.; Forrester, A. R.; Ogilvy, M. M.; Thomson, R. H. Photolysis of 2,6-Di-t-Butyl-1,4-Benzoquinone: A New Rearrangement. *J. Chem. Soc., Chem. Commun.* **1973**, No. 21, 844–844. https://doi.org/10.1039/C39730000844.
36. Kraus, G. A.; Wu, Y. 1,5- and 1,9-Hydrogen Atom Abstractions. Photochemical Strategies for Radical Cyclizations. *J. Am. Chem. Soc.* **1992**, *114* (22), 8705–8707. https://doi.org/10.1021/ja00048a057.
37. Görner, H. Photoreactions of 2,5-Dibromo-3-Methyl-6-Isopropyl-1,4-Benzoquinone. *Journal of Photochemistry and Photobiology A: Chemistry* **2005**, *175* (2–3), 138–145. https://doi.org/10.1016/j.jphotochem.2005.03.028.
38. Walton, D.; Regan, C.; Dougherty, D. A Strategy for Long-Wavelength Decaging of Bioactive Molecules.
39. Klán, P.; Wirz, J. Techniques and Methods. In *Photochemistry of Organic Compounds*; John Wiley & Sons, Ltd, 2009; pp 73–135.
40. Hu, S.; Neckers, D. C. Lifetime of the 1,4-Biradical Derived from Alkyl Phenylglyoxylate Triplets: An Estimation Using the Cyclopropylmethyl Radical Clock. *J. Org. Chem.* **1997**, *62* (3), 755–757. https://doi.org/10.1021/jo961659j.
41. Griller, D.; Ingold, K. U. Free-Radical Clocks. *Acc. Chem. Res.* **1980**, *13* (9), 317–323. https://doi.org/10.1021/ar50153a004.
42. Wagner, P. J.; Liu, K. C. Photorearrangement of .Alpha.-Allylbutyrophenone to 2-Phenyl-2-Norbornanol. Determination of 1,4-Diradical Lifetimes. *J. Am. Chem. Soc.* **1974**, *96* (18), 5952–5953. https://doi.org/10.1021/ja00825a052.
43. Small, R. D.; Scaiano, J. C. Photochemistry of Phenyl Alkyl Ketones. The Lifetime of the Intermediate Biradicals. *J. Phys. Chem.* **1977**, *81* (22), 2126–2131. https://doi.org/10.1021/j100537a018.
44. Engel, P. S.; Keys, D. E. Estimation of a Cyclic 1,4-Biradical Lifetime Using the Cyclopropylcarbinyl Rearrangement. *J. Am. Chem. Soc.* **1982**, *104* (24), 6860–6861. https://doi.org/10.1021/ja00388a100.
45. Castellino, A. J.; Bruice, T. C. Intermediates in the Epoxidation of Alkenes by Cytochrome P-450 Models. 2. Use of the Trans-2,Trans-3-Diphenylcyclopropyl Substituent in a Search for Radical Intermediates. *J. Am. Chem. Soc.* **1988**, *110* (22), 7512–7519. https://doi.org/10.1021/ja00230a039.
46. Amouyal, E.; Bensasson, R. Interaction of Duroquinone Lowest Triplet with Amines. *J. Chem. Soc., Faraday Trans. 1* **1977**, *73* (0), 1561–1568. https://doi.org/10.1039/F19777301561.

47. Klán, P.; Wirz, J. Information Sources, Tables. In *Photochemistry of Organic Compounds*; John Wiley & Sons, Ltd, 2009; pp 467–470.
48. Balzani, V.; Ballardini, R.; Gandolfi, M. T.; Moggi, L. Sensitized Photolysis and Luminescence of the Tris(Ethylenediamine)Chromium(III) Ion in Aqueous Solution. *J. Am. Chem. Soc.* **1971**, *93* (2), 339–345. https://doi.org/10.1021/ja00731a008.
49. Allonas, X.; Ley, C.; Bibaut, C.; Jacques, P.; Fouassier, J. P. Investigation of the Triplet Quantum Yield of Thioxanthone by Time-Resolved Thermal Lens Spectroscopy: Solvent and Population Lens Effects. *Chemical Physics Letters* **2000**, *322* (6), 483–490. https://doi.org/10.1016/S0009-2614(00)00462-0.
50. Burget, D.; Jacques, P. Dramatic Solvent Effects on Thioxanthone Fluorescence Lifetime. *Journal of Luminescence* **1992**, *54* (3), 177–181. https://doi.org/10.1016/0022-2313(92)90006-U.
51. Kemp, D. R.; Porter, G. Photochemistry of Methylated P-Benzoquinones. *Proceedings of the Royal Society of London A: Mathematical, Physical and Engineering Sciences* **1971**, *326* (1564), 117–130. https://doi.org/10.1098/rspa.1971.0195.
52. Görner, H. Photoreactions of 2-Methyl-5-Isopropyl-1,4-Benzoquinone. *Journal of Photochemistry and Photobiology A: Chemistry* **2004**, *165* (1–3), 215–222. https://doi.org/10.1016/j.jphotochem.2004.03.020.
53. Barbafina, A.; Elisei, F.; Latterini, L.; Milano, F.; Agostiano, A.; Trotta, M. Photophysical Properties of Quinones and Their Interaction with the Photosynthetic Reaction Centre. *Photochem. Photobiol. Sci.* **2008**, *7* (8), 973–978. https://doi.org/10.1039/B805897K.
54. Wagner, P. J. Type II Photoelimination and Photocyclization of Ketones. *Acc. Chem. Res.* **1971**, *4* (5), 168–177. https://doi.org/10.1021/ar50041a002.
55. Amouyal, E.; Bensasson, R.; Land, E. J. Triplet States of Ubiquinone Analogs Studied by Ultraviolet and Electron Nanosecond Irradiation. *Photochemistry and Photobiology* **1974**, *20* (5), 415–422. https://doi.org/10.1111/j.1751-1097.1974.tb06596.x.
56. Garcia-Garibay, M. A.; Gamarnik, A.; Bise, R.; Pang, L.; Jenks, W. S. Primary Isotope Effects on Excited State Hydrogen Atom Transfer Reactions. Activated and Tunneling Mechanisms in an Ortho-Methylanthrone. *J. Am. Chem. Soc.* **1995**, *117* (41), 10264–10275. https://doi.org/10.1021/ja00146a011.
57. Johnson, B. A.; Kleinman, M. H.; Turro, N. J.; Garcia-Garibay, M. A. Hydrogen Atom Tunneling in Triplet O-Methylbenzocycloalkanones: Effects of Structure on Reaction Geometry and Excited State Configuration. *J. Org. Chem.* **2002**, *67* (20), 6944–6953. https://doi.org/10.1021/jo016210r.
58. Nyulászi, L.; Veszprémi, T.; Réffy, J. Photoelectron Spectrum and Reactivity of Silylalkyl Sulphides. Stabilization of Radical Cations by the β-Silyl Effect. *Journal of Organometallic Chemistry* **1993**, *445* (1–2), 29–34. https://doi.org/10.1016/0022-328X(93)80182-B.
59. Gritsan, N. P.; Bazhin, N. M. The Mechanism of Photolysis of 2-Amino-1,4-Naphthoquinone Derivatives. *Russ Chem Bull* **1981**, *30* (2), 210–214. https://doi.org/10.1007/BF00953566.
60. Gritsan, N. P.; Bazhin, N. M. Nature and Properties of the Reaction State in the Photolysis of 2-Amino-1,4-Naphthoquinone Derivatives. *Russ Chem Bull* **1980**, *29* (6), 897–902. https://doi.org/10.1007/BF00958803.
61. Klán, P.; Wirz, J. Techniques and Methods. In *Photochemistry of Organic Compounds*; John Wiley & Sons, Ltd, 2009; pp 73–135.

Chapter 4. A General Strategy for Visible-Light Decaging Based on the Quinone Cis-Alkenyl Lock

4.1 Abstract

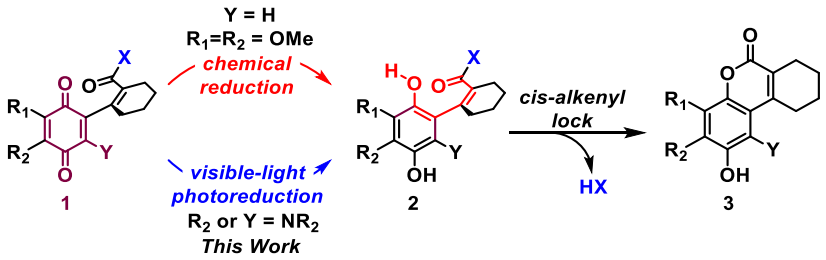

Combining the fast thermal cyclization of *o*-coumaric acid derivatives with the intramolecular photoreduction of quinones gives new visible-light photoremovable protecting groups for alcohols and amines absorbing well above 450 nm. The cis-alkenyl group is applicable to both benzoquinone and naphthoquinone cores, greatly expanding the potential for long-wavelength derivatives. The synthesis and photolysis of aminoquinones **1** in air equilibrated methanol proceeded smoothly (Φ_{565nm} = 0.01-0.04) to quantitatively release alcohols.

4.2 Introduction

Photoremovable protecting groups, or photocages, allow precise spatiotemporal control over the release of compounds into a system.[1] The ubiquitous nitrobenzyl protecting groups undergo a hydrogen atom abstraction as the key photochemical step. This high energy reaction requires biologically harmful UV light that penetrates tissue only to limited depths, and the photolysis byproducts are toxic to cells. Despite these drawbacks, nitrobenzyl protecting groups are still in widespread use. In recent years, several groups have developed photoremovable protecting groups that use biologically safe visible to near-infrared light, which has the added benefit of deeper tissue penetration. Coumarins[2–6], BODIPY[7–11], and cyanine[12–15] dyes have shown promise in this regard. Coumarins and BODIPY dyes rely on heterolysis to release their cargo, which can lead to leaving group-dependent quantum yields. The cyanine dyes instead use the low energy process of singlet oxygen generation, but have so far required extensive irradiation times and potentially cause collateral oxidative stress.

Quinones have been relatively less studied as photoremovable protecting groups[1,16–21] despite their rich photochemistry.[22–35] The intramolecular photoreduction of aminated quinones first reported by Cameron and Giles[36] has proven useful in the development of light activated *ortho*-quinone methides[16] and quinone trimethyl locks.[18] Although performing well at 450-650 nm, application of the system reported by Chen and Steinmetz in biological settings is limited by the reactivity of the photolysis byproduct and low quantum yield in polar solvents (**Scheme 4.1**).[16,17] Carling et al. used water-dispersible nanoparticles to encapsulate the same aminated quinones, allowing fast release in water.[20]

We sought to combine quinone photoreduction with a less reactive thermal step in general. Our first approach was to utilize photoreduction to launch the well-known quinone trimethyl lock lactonization (QTML) reaction, which precludes reactive *ortho*-quinone methide byproducts (**Scheme 4.1**).[18] We found that sulfide substituents absorb at shorter wavelengths than amines (400-600nm), and benzylic heteroatom substituents increase photolysis efficiency.[18,19] Sulfide and amine QTMLs photolyzed cleanly to release alcohols and amines in quantitative yield. Wang and Kalow also noted[21] the enhanced reactivity of isoindoline vs. pyrrolidine substituents when updating the photocages developed[16] by Chen and Steinmetz.

Despite similar aminated 1,4-benzoquinone structures, the QTMLs are blue shifted compared to simpler amine substituted quinones by at least 50 nm.[17,18] The blue shift presumably stems from a distorted quinone core imparted by the trimethyl lock's 3,3-dimethylpropionic acid side chain. While the quinone trimethyl lock system is robust, we encountered two synthetic limitations for extending the wavelength of absorption. These are the steric bulk of the 3,3-dimethyl propionic acid chain and the requirement that the intramolecular photoreduction occur *para* to the trimethyl lock group with few exceptions. This last constraint limits direct extension to 1,4-naphthoquinone systems, which are common for near-infrared absorbing quinone dyes.

As progress towards longer wavelengths of absorption, we now describe an alternative quinone based photocage where a less sterically demanding cis-alkenyl group replaces the trimethyl lock (**Scheme 4.1a)**. The fast cyclization[37–40] of *o*-coumaric esters when photoisomerized to the *cis* confirmation with UV light is an effective protecting group

(Scheme 4.1b).[41–47] Tremblay and Salmes protected the phenol as a quinone carbonyl and locked the alkene in a *cis* conformation as a cyclohexene ring, allowing the chemical reduction of the quinone to result in fast lactonization (**Scheme 4.1c**).[48] We predicted that addition of an amine substituent would render these quinones[16–18,23,24,36,49] and the analogous naphthoquinones[29,50] activatable by visible light while allowing more synthetic flexibility. Additionally, the photolysis byproduct is a UV-absorbing coumarin which can be used as a fluorescent turn on probe concomitant with release of substrate.

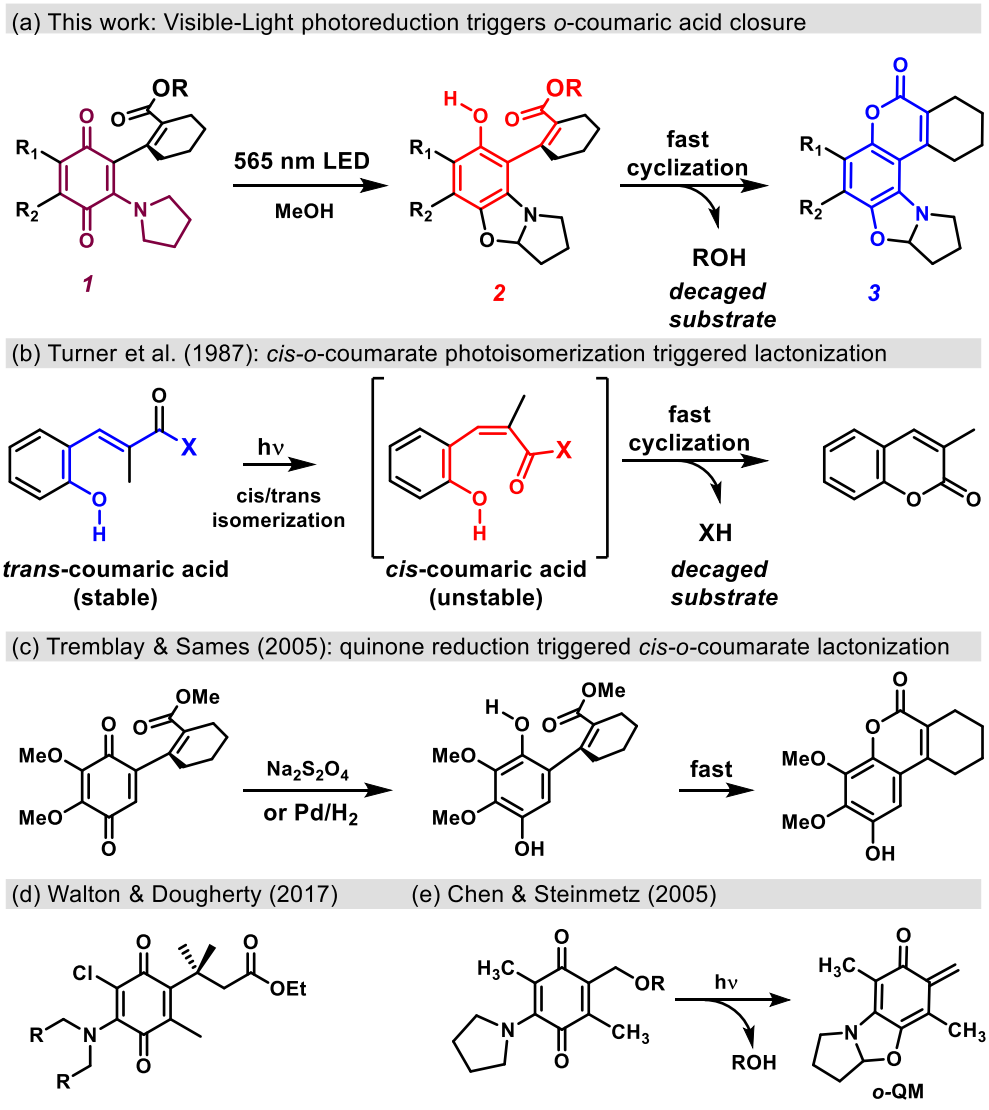

Scheme 4.1. Coumaric acids and quinone based protecting groups.

4.3 Results and Discussion

Our initial route to cis-alkenyl lock quinone photocages such as **1** is shown in **Scheme 4.2** and is adapted from the published procedure[48] to allow amine addition. Bromoquinones **4** were reduced and methylated to give 1,4-dimethoxy arenes **6.** Boronic acids **7** were prepared via lithium halogen exchange or purchased (**7a**). Suzuki coupling of arylbornic acids **7** and ethyl 2-bromocyclohex-1-ene-1-carboxylate (**8**) gave **9**. Alternatively, Pechmann condensation[51] of hydroquinones (**11a,c**) with ethyl 2-oxocyclohexane-1-carboxylate (**12**) in methanesulfonic acid followed by methylative hydrolysis of the coumarin gave **9a,c**. Oxidative demethylation of 1,4-dimethoxyarenes **9** with ceric ammonium nitrate (CAN) formed the cis-alkenyl quinones **10**, which underwent conjugate addition / oxidation in acetonitrile to give **1**. Solvent choice is important here to slow the lactonization of intermediate hydroquinones formed from conjugate addition enough to allow aerobic oxidation. Conjugate addition yields were particularly low for **1d**, and the reaction proceeds slowly for both **1c** and **1d**.

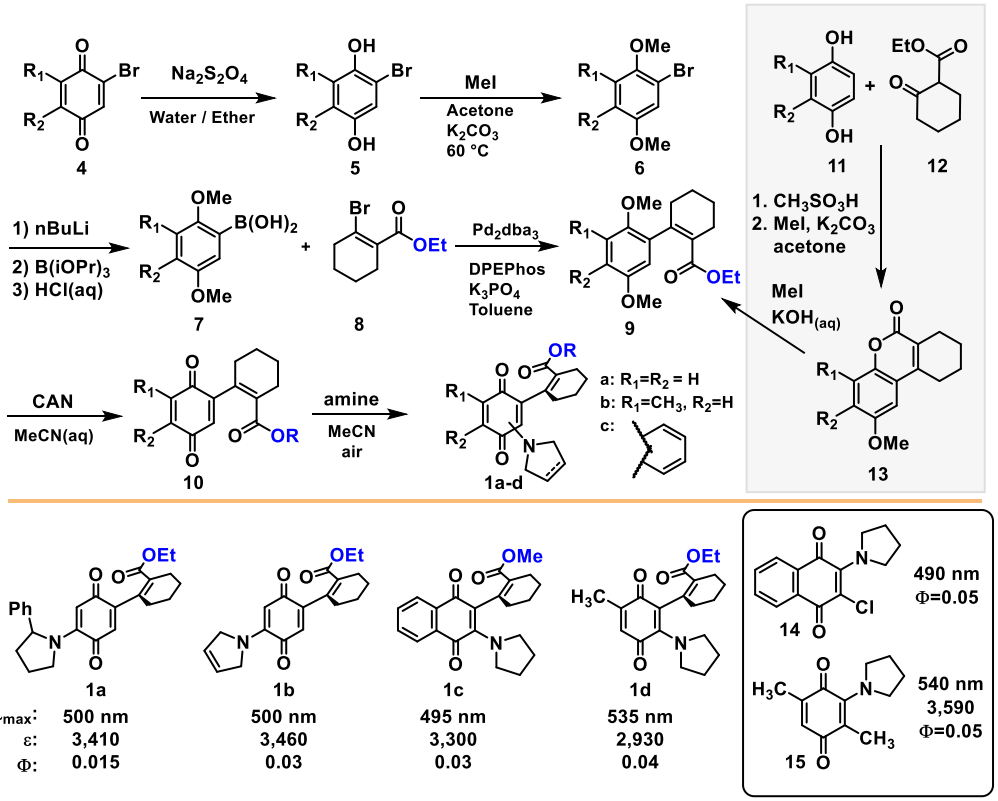

Scheme 4.2 Quinone Cis-Alkenyl Lock (QCAL) Compounds **1a-d.** UV-vis data (λ_{max}, vis (nm), ε ($M^{-1}cm^{-1}$)) and quantum yields (Φ(565nm), Ref. = **14** and **15**) were measured in air equilibrated methanol.

Aminated quinones **1** display broad charge transfer bands in methanol (λ_{max} = 495-535 nm, ε ≈ 3,000 M^{-1} cm^{-1}) (**Figure 4.1**). Naphthoquinone derivative **1c** absorbs at shorter

wavelengths than the benzoquinone derivatives as expected.[52] Benzoquinone **1d** is red-shifted by nearly 40 nm compared to pyrrolidino trimethyl lock compounds,[18] absorbing out to 650nm. Photolysis of **1d** was possible by irradiation above > 600 nm in 30% aqueous acetonitrile (see SI).

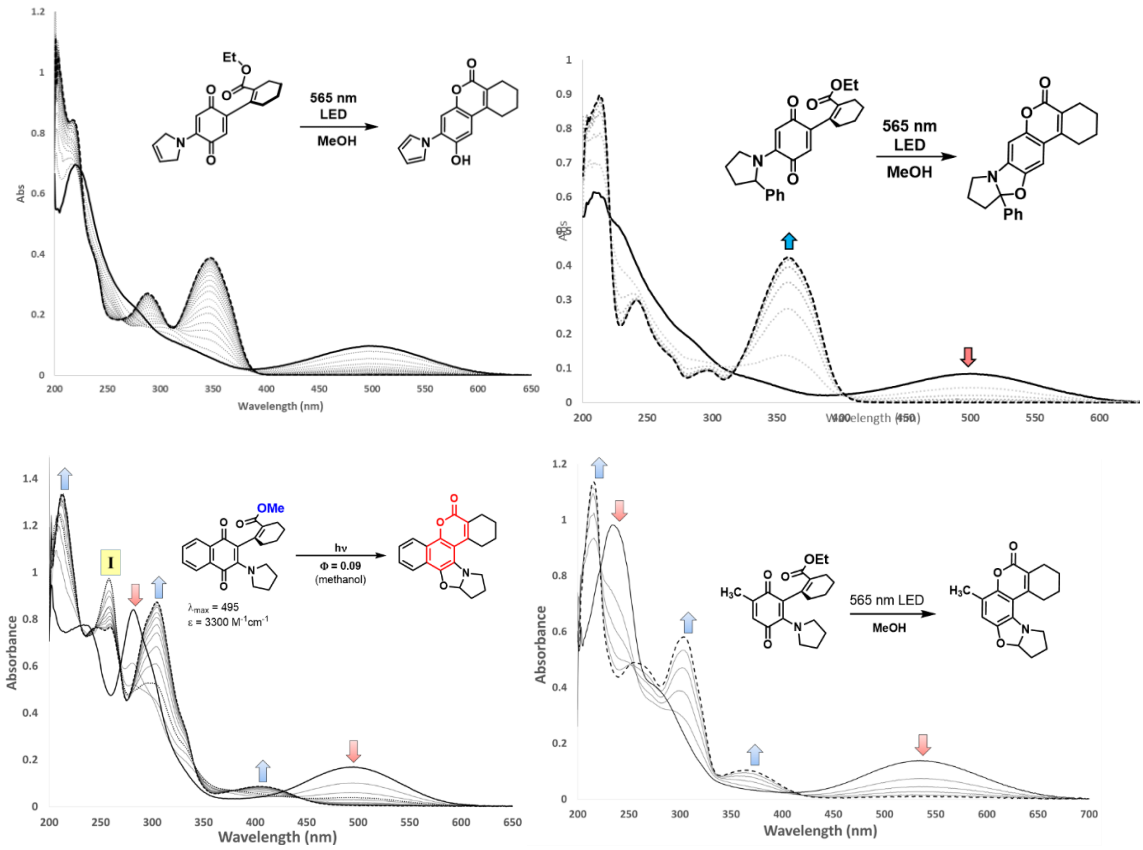

Figure 4.1. UV-vis spectra of **1a-d** during photolysis with a 880 mW 565 nm LED in air saturated methanol. Photolysis was complete < 5min (traces are 0.3 min apart for **1c** and 0.5 min apart for **1d**).

The timecourses of photoreduction of compounds **1a-d** in air saturated methanol with an 880 mW 565 nm LED are shown in **Figure 4.1**. Photolysis occurs efficiently in methanol with Φ = 0.015-0.04 (**Table 4.1**) to quantitatively give coumarins **3** and decaged alcohol (**Scheme 4.3**). Notably, the photolysis byproducts are transparent at the irradiation wavelength and inert, allowing high chemical yields and simplified product analysis. The

immediate product of photolysis is benzoxazoline **2**, which undergoes the typical fast *cis*-coumaric acid cyclization ($t_{1/2}$ ~ sec) to coumarin **3**. A characteristic coumarin absorbance at 375 nm for benzoquinones **1a,b,d** and 405 nm for naphthoquinone **1c** is indicative of conversion from **2** →**3**. In non-polar aprotic solvents where cyclization is slow, **2** is observable by NMR and UV-vis (**I** in **Figure 4.1**). Lactonization of hydroquinones **2** are all fast, and the relative order is **1a ≈ 1b > 1c ≈ 1d**, as expected from substituent effects on coumarin cyclizations.[40] Solvent effects were therefore as expected for photolysis[17] and coumarin formation.[48] Although photolysis is more efficient in nonpolar solvents, coumarin formation is drastically slowed. Methanol was chosen as a compromise to allow efficient photolysis and alcohol release.

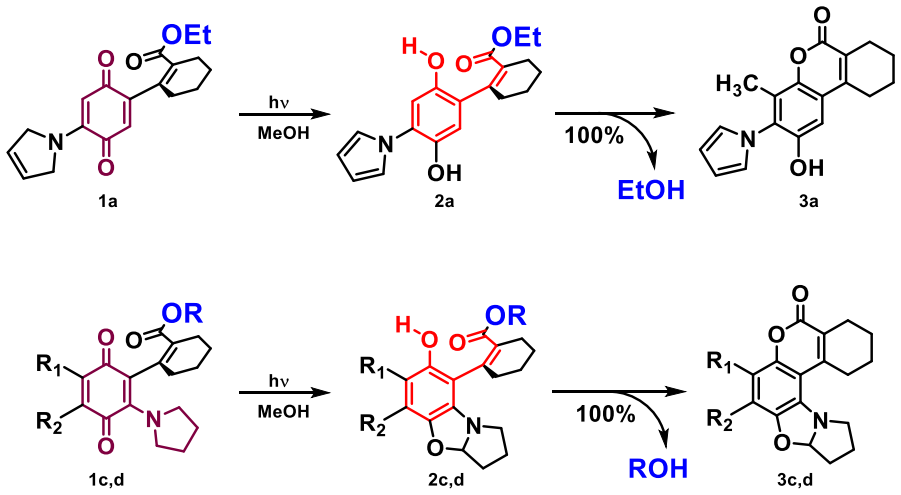

Scheme 4.3 Photolysis of 1a and 1c,d

	1a	1b	1c	1d	14	15	14(CH_2Cl_2)*	15 (PhMe)*
λmax (nm)	500	500	495	535	540	490	540	490
ε ($M^{-1}cm^{-1}$)	3410	3460	3300	2930	3590	----	3,380	4,900
Φ	0.015	0.03	0.03	0.04	0.05	0.05	0.09	0.19

Table. 4.1 Quantum yields of **1a-d** and measured relative to **14** and **15**.

The amine substituents of **1a-d** were chosen to optimize photolysis and cyclization rates. For **1a,b** which lack an *ortho*-substituent to the amine, weak C-H bonds were required

for efficient photolysis. Although we had previously used isoindoline,[18] we were concerned about the reactivity of the isoindole analogue of **2** formed on photolysis.[53] 3-Pyrroline[54] and 2-phenyl-pyrrolidine were therefore chosen for **1a,b**. In practice, **1b** was less reactive and gave a mixture of photolysis byproducts, presumably from hydrolysis of the benzoxaline. In the case of **1c** and **1d**, pyrrolidine derivatives were expected[33] to undergo efficient photoreduction and were preferred for the tied-back structure of the benzoxaline **2** to limit interference with subsequent lactonization.[4,13]

4.4 Conclusions

We believe the cis-lock strategy laid out above offers a complementary approach to our earlier work with the trimethyl lock, along with several potential benefits. In both cases, the light and thermal steps are energetically decoupled, allowing the photochemistry to be optimized separately at longer wavelengths. Importantly for biological applications, both coumarin and trimethyl lock lactone formation preclude generation of reactive *ortho*-quinonemethides, photolysis byproducts possible with aminated benzoquinones. While the trimethyl lock is a robust system operating in the 400-600 nm range, there are some substituent limitations imposed by the prerequisite adjacent methyl group to the dimethylpropionic acid chain. In the cis lock variation, the photoreducing moiety can be attached at the *ortho* position, leaving the entire distal side of a 2,3-substituted-1,4-benzoquinone available for modification. This is required for 1,4-naphthoquinone derivatives, and therefore **1c** has the additional benefit of being a model system for 1,4-napthoquinone based near-infrared dyes.[55]

4.5 Experimental

Unless otherwise stated, reactions were carried out under ambient conditions. Light sensitive compounds were protected from light using aluminum foil and under low ambient light, or with an appropriate safelight. Commercially available reagents were obtained from Sigma Aldrich, AK Scientific, Alfa Aesar, or Acros Organics and used without further purification. Solvents used for photolysis, HPLC, and UV-vis were omnisolve grade. Other solvents were used as received or dried by elution through activated alumina where noted. If a

photoproduct was found to be unstable to hydrolysis, methanol was distilled from magnesium. Thin-layer chromatography using EMD/Merck silica gel 60 F254 pre-coated plates (0.25 mm) was used to monitor reactions. Silica gel chromatography was conducted as described by Still et al. (W. C. Still, M. Kahn, A. Mitra, *J. Org. Chem.* **1978**, *43*, 2923), with silica gel purchased from AK Scientific (60 Å, 230-400 mesh). NMR spectra were recorded on Varian (300, 400, 500, or 600 MHz), or Bruker (400 MHz) spectrometers. HRMS (ESI) were obtained with an Agilent 6200 Series TOF. UV-vis spectra were recorded on a Cary 60 spectrometer. Samples were irradiated with a M565L3 (565 nm, 880 mW) mounted LED purchased from Thor Labs. Photolysis was conducted inside the UV-vis spectrometer cavity or side on through a glass flask or NMR tube in air-equilibrated methanol, methanol-d_4. (2,5-dimethoxyphenyl)boronic acid was purchased from AK Scientific and used without purification.

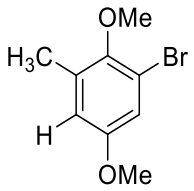

1-bromo-2,5-dimethoxy-3-methylbenzene: To a vigorously stirred mixture of 2-bromo-6-methyl-1,4-benzoquinone (5.692 g, 28 mmol) in ether, methanol, and water (2:1:2) was added sodium borohydride (5.3 g, 140 mmol, excess). The biphasic mixture turned from yellow to colorless and was allowed to stir for 15 minutes before extraction with ether three times. The combined organic phase was washed with brine and dried ($MgSO_4$) before removing solvent. The crude hydroquinone was immediately dissolved in acetone, cesium carbonate (18.45 g, 57 mmol) and methyl iodide (4.4 mL, 57 mmol) were added, and the mixture was refluxed under argon. Once conversion was complete by TLC, the mixture was cooled, filtered, and concentrated to yield 4.6466 g of 1-bromo-2,5-dimethoxy-3-methylbenzene (71% yield over two steps). An analytically pure sample was prepared by flash chromatography. ^{1}H NMR (500 MHz, Chloroform-*d*) δ 6.90 (dd, J = 3.1, 0.6 Hz, 1H), 6.66 (dq, J = 3.1, 0.7 Hz, 1H), 3.75 (d, J = 5.1 Hz, 6H), 2.30 (t, J = 0.7 Hz, 3H).

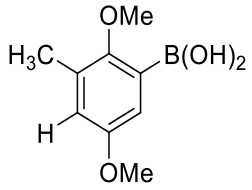

(2,5-dimethoxy-3-methylphenyl)boronic acid. To a solution of aryl bromide (3.5 g, 15 mmol) in 60 mL of dry THF at -76 °C was added dropwise 6.7 mL of *n*-butyl lithium (2.5 M in hexanes). The resulting mixture was stirred at -76 °C under argon for 1 hour before 9 mL of triisopropyl borate was added. After 30 minutes, the mixture was allowed to warm to ambient temperature. The crude borate ester was hydrolyzed with aqueous HCl, then extracted into ether, washed with brine and dried ($MgSO_4$). The solvent was removed and the crude was recrystallized to yield 2.1339 g of the boronic acid in 72% yield as a white solid. ^{1}H NMR (500 MHz, Chloroform-*d*) δ 7.15 (d, *J* = 3.1 Hz, 1H), 6.84 (dq, *J* = 3.4, 0.7 Hz, 1H), 6.16 (s, 2H), 3.77 (d, *J* = 20.1 Hz, 6H), 2.29 (d, *J* = 0.6 Hz, 3H).

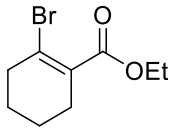

ethyl 2-bromocyclohex-1-ene-1-carboxylate. To a solution of bromocyclohex-1-ene-1-carboxylic acid (1.1025 g, 5.4 mmol) in dichloromethane was added excess oxalyl chloride (1.5 mL), followed by a drop of DMF. The mixture was stirred until bubbling ceased, then the solvent was removed to give the acid chloride as a yellow solid. The solid was dissolved in absolute ethanol, then 5 mg DMAP and 1 equivalent triethyl amine was added. The solvent was removed with heating. The resulting oil was dissolved in dichloromethane and washed with dilute HCl $_{(aq)}$, $NaHCO_{3(aq)}$, and brine before drying ($MgSO_4$). Evaporation of the organic layer yielded ethyl bromocyclohex-1-ene-1-carboxylate as a colorless oil (1.085 g, 86%) without further purification. ^{1}H NMR (500 MHz, Chloroform-*d*) δ 4.24 (q, *J* = 7.1 Hz, 2H), 2.68 – 2.48 (m, 2H), 2.48 – 2.31 (m, 2H), 1.80 – 1.63 (m, 4H), 1.32 (t, *J* = 7.1 Hz, 3H). ^{13}C NMR (126 MHz, cdcl$_3$) δ 167.98, 131.21, 125.35, 61.02, 36.95, 28.75, 23.98, 21.32, 21.31, 14.14.

ethyl 2-bromocyclohex-1-ene-1-carboxylate (alternative preparation). To a solution of 2-bromocyclohex-1-ene-1-carboxylic acid (1.9215 g, 9.3 mmol) in dichloromethane was added 10 mL ethanol, followed by EDCI·HCl (2.2 g, 11.5 mmol), DMAP (176 mg, 1.5 mmol). The solution was stirred until conversion was complete by TLC (less than 1 hour). The solvent was removed, and the crude was taken up in CH_2Cl_2 and loaded onto a column with an equal volume of hexanes, then flashed (10% Ethyl acetate / hexanes) to yield 1.003 g of a colorless oil (46% yield).

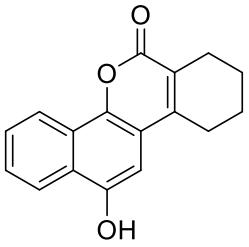

12-hydroxy-7,8,9,10-tetrahydro-6H-dibenzo[c,h]chromen-6-one. ^{1}H NMR (500 MHz, DMSO-d_6) δ 10.37 (s, 1H), 8.28 (ddd, J = 8.3, 1.4, 0.7 Hz, 1H), 8.18 (ddd, J = 8.2, 1.4, 0.7 Hz, 1H), 7.68 (ddd, J = 8.3, 6.8, 1.4 Hz, 1H), 7.64 (ddd, J = 8.2, 6.9, 1.4 Hz, 1H), 6.97 (s, 1H), 2.82 – 2.71 (m, 2H), 2.49 – 2.38 (m, 2H), 1.89 – 1.77 (m, 2H), 1.77 – 1.70 (m, 2H).

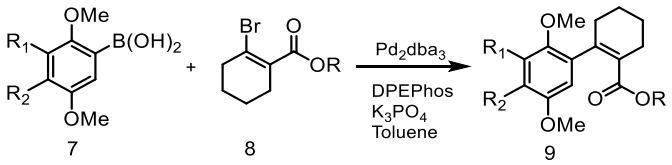

General conditions for coupling reaction:

Suzuki couplings were carried out according to the published procedure[48] for derivatives of **7**. To a flask under argon is added 2 equivalents of boronic acid, 3 equivalents powdered K_3PO_4, 10 % Pd_2dba_3, 10% DPEPhos. 1 equivalent of vinyl bromide is then added with toluene and mol sieves. The resulting mixture is refluxed over night or until TLC indicates completion.

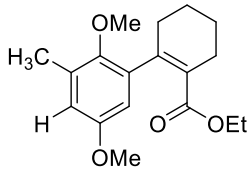

ethyl 2',5'-dimethoxy-3'-methyl-3,4,5,6-tetrahydro-[1,1'-biphenyl]-2-carboxylate. To a solution of ethyl 2-bromocyclohex-1-ene-1-carboxylate (360 mg) and (2,5-Dimethoxy-3-methylphenyl)boronic acid (660 mg) in degassed toluene (25 mL), was added K_3PO_4 (1.04 g), Pd_2dba_3 (200 mg), and DPEPhos (100 mg). The resulting mixture was heated overnight at 80 °C, then diluted with ether and filtered through celite before purification by flash chromatography (10% ethyl acetate / hexanes) to give 320 mg of a yellow oil (1:1 mixture of dba and product) which was carried on to the next step.

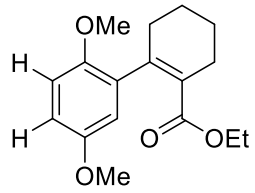

ethyl 2',5'-dimethoxy-3,4,5,6-tetrahydro-[1,1'-biphenyl]-2-carboxylate (9a). ^{1}H NMR (500 MHz, Chloroform-*d*) δ 6.78 (d, *J* = 8.9 Hz, 1H), 6.74 (dd, *J* = 8.9, 3.0 Hz, 1H), 6.55 (d, *J* = 2.9 Hz, 1H), 3.86 (q, *J* = 7.2 Hz, 2H), 3.75 (s, 3H), 3.73 (s, 2H), 2.39 (d, *J* = 52.9 Hz, 4H), 1.73 (t, *J* = 4.1 Hz, 4H), 0.84 (t, *J* = 7.1 Hz, 3H).

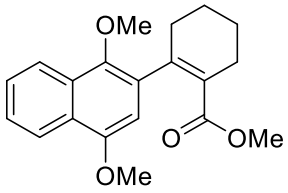

methyl 2-(1,4-dimethoxynaphthalen-2-yl)cyclohex-1-ene-1-carboxylate: To a suspension of **13c** (613 mg, 2.2 mmol) in 50% aqueous acetone was added NaOH (12 g, 300 mmol). Catalytic tetrabutylammonium bromide was added and the mixture was violently stirred at reflux until all solids dissolved. The solution was cooled to 60 °C, and methyl iodide (1 mL) was added. Heating and hourly addition of methyl iodide (1 mL) was continued until NMR aliquots showed complete conversion to **9c** (4 h, 4 mL total MeI). The acid is prepared in the same way, only with less methyl iodide. The reaction was cooled, diluted with water, and extracted with ether. The combined organic layers were washed with brine, dried ($MgSO_4$), filtered and concentrated to give the pure **9c**. ^{1}H NMR (500 MHz, Chloroform-*d*) δ 8.20 (ddd, *J* = 8.3, 1.3, 0.7 Hz, 1H), 8.06 (ddd, *J* = 8.4, 1.3, 0.7 Hz, 1H),

7.51 (ddd, *J* = 8.3, 6.8, 1.4 Hz, 1H), 7.45 (ddd, *J* = 8.2, 6.8, 1.3 Hz, 1H), 6.45 (s, 1H), 3.94 (s, 3H), 3.83 (s, 3H), 3.40 (s, 3H), 2.88 – 2.19 (m, 4H), 1.80 (t, *J* = 3.6 Hz, 4H). ^{13}C NMR (126 MHz, cdcl$_3$) δ 169.56, 151.39, 145.11, 145.06, 131.37, 128.74, 128.25, 126.40, 125.69, 125.13, 122.14, 121.98, 104.53, 61.53, 55.69, 51.24, 31.94, 26.58, 22.56, 22.14.

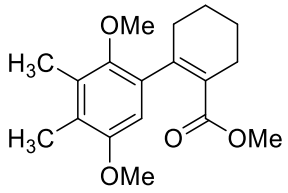

Methyl 2',5'-dimethoxy-3',4'-dimethyl-3,4,5,6-tetrahydro-[1,1'-biphenyl]-2-carboxylate. Prepared in the same manner as **9c**. ^{1}H NMR (400 MHz, Chloroform-*d*) δ 6.35 (s, 2H), 3.74 (s, 6H), 3.62 (s, 6H), 3.47 (s, 6H), 2.82 – 2.28 (m, 4H), 2.18 (s, 6H), 2.12 (s, 6H), 1.84 – 1.63 (m, 8H). ^{13}C NMR (101 MHz, CDCl$_3$) δ 169.74, 153.35, 148.39, 145.10, 133.74, 130.75, 127.69, 125.16, 107.90, 60.51, 55.82, 51.18, 32.14, 26.54, 22.57, 22.15, 12.66, 12.12.

Procedure for ceric (IV) ammonium nitrate oxidations: A dilute solution of quinone (1 equivalent) in 30% aqueous acetonitrile is degassed with house vacuum / sonication 10 times, then cooled to 0 °C under argon. A similarly degassed solution of CAN in 30% aqueous acetonitrile is added slowly with rapid stirring. After 5-15 min, the now yellow solution is diluted with water and extracted with ethyl acetate. The combined organic layers were washed with brine, dried over $MgSO_4$, filtered, and concentrated. Flash chromatography and collecting the yellow band afforded the quinone **10**. A common contaminant requiring additional purification was dibenzylideneacetone from the coupling.

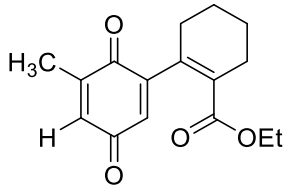

ethyl 5'-methyl-3',6'-dioxo-[1,1'-bi(cyclohexane)]-1,1',4'-triene-2-carboxylate. To a degassed solution of ethyl 2',5'-dimethoxy-3'-methyl-3,4,5,6-tetrahydro-[1,1'-biphenyl]-2-carboxylate (311.4 mg) in 30 mL of acetonitrile / water (2:1) at 0 °C was added 1.4734 g CAN as a solution in 10 mL of acetonitrile/water (1:1). After TLC indicated the reaction was

complete (< 30 min), water was added, and the mixture was extracted with ethyl acetate (3 x 50 mL). The combined organic layers were washed with brine, dried ($MgSO_4$) and concentrated. Purification by flash chromatography gave the product as a yellow oil (73 mg). ^{1}H NMR (400 MHz, Chloroform-*d*) δ 6.59 (dq, *J* = 3.1, 1.6 Hz, 1H), 6.33 (d, *J* = 2.6 Hz, 1H), 3.61 (s, 3H), 2.49 – 2.33 (m, 2H), 2.30 – 2.19 (m, 2H), 2.09 (d, *J* = 1.6 Hz, 3H), 1.79 – 1.66 (m, 4H). ^{13}C NMR (101 MHz, $CDCl_3$) δ 187.44, 185.82, 167.27, 152.31, 146.33, 142.68, 133.27, 129.39, 128.81, 51.72, 32.55, 25.39, 21.69, 21.65, 16.15.

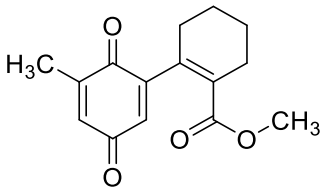

methyl 5'-methyl-3',6'-dioxo-[1,1'-bi(cyclohexane)]-1,1',4'-triene-2-carboxylate. ^{1}H NMR (400 MHz, Chloroform-*d*) δ 6.59 (dq, *J* = 3.1, 1.6 Hz, 1H), 6.33 (d, *J* = 2.6 Hz, 1H), 3.61 (s, 3H), 2.49 – 2.33 (m, 2H), 2.30 – 2.19 (m, 2H), 2.09 (d, *J* = 1.6 Hz, 3H), 1.79 – 1.66 (m, 4H). ^{13}C NMR (101 MHz, $CDCl_3$) δ 187.44, 185.82, 167.27, 152.31, 146.33, 142.68, 133.27, 129.39, 128.81, 51.72, 32.55, 25.39, 21.69, 21.65, 16.15.

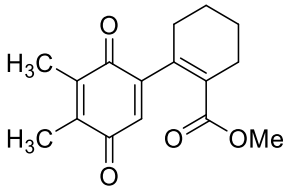

methyl 2',5'-dimethoxy-3,4,5,6-tetrahydro-[1,1'-biphenyl]-2-carboxylate (9a). ^{1}H NMR (400 MHz, Chloroform-*d*) δ 6.78 (d, *J* = 8.9 Hz, 1H), 6.74 (dd, *J* = 8.9, 2.9 Hz, 1H), 6.55 (d, *J* = 2.9, 0.5 Hz, 1H), 3.87 (q, *J* = 7.1 Hz, 2H), 3.75 (s, 3H), 3.73 (s, 3H), 2.87 – 1.90 (m, 4H), 1.90 – 1.63 (m, 4H), 0.84 (t, *J* = 7.1 Hz, 3H). ^{13}C NMR (101 MHz, $CDCl_3$) δ 169.11, 153.44, 150.14, 144.46, 133.92, 128.16, 114.23, 112.44, 111.81, 59.76, 56.30, 55.73, 31.88, 26.20, 22.34, 22.07, 13.57.

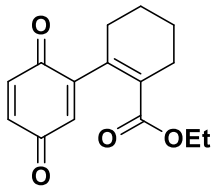

ethyl 3',6'-dioxo-[1,1'-bi(cyclohexane)]-1,1',4'-triene-2-carboxylate (**10a**). ^{1}H NMR (500 MHz, Chloroform-*d*) δ 6.81 (d, *J* = 10.1 Hz, 1H), 6.75 (dd, *J* = 10.1, 2.5 Hz, 1H), 6.41 (d, *J* = 2.5 Hz, 1H), 4.06 (q, *J* = 7.1 Hz, 2H), 2.43 (tt, *J* = 3.8, 2.0 Hz, 2H), 2.29 – 2.20 (m, 2H), 1.73 (h, *J* = 3.1 Hz, 4H), 1.19 (t, *J* = 7.1 Hz, 3H). ^{13}C NMR (126 MHz, cdcl$_3$) δ 187.43, 185.18, 166.83, 152.22, 141.51, 137.01, 136.47, 130.15, 128.96, 60.69, 32.48, 25.43, 21.71, 21.62, 14.10.

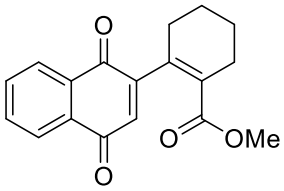

Ethyl 2-(1,4-dioxo-1,4-dihydronaphthalen-2-yl)cyclohex-1-ene-1-carboxylate. ^{1}H NMR (400 MHz, Chloroform-*d*) δ 8.16 – 7.98 (m, 2H), 7.89 – 7.64 (m, 2H), 6.62 (s, 1H), 3.56 (s, 3H), 2.47 (dd, *J* = 4.4, 2.2 Hz, 2H), 2.39 – 2.20 (m, 2H), 1.93 – 1.67 (m, 4H). ^{13}C NMR (101 MHz, $CDCl_3$) δ 185.02, 183.27, 167.26, 154.26, 142.77, 133.67, 133.64, 132.46, 132.18, 131.26, 129.49, 126.81, 126.08, 51.71, 32.61, 25.43, 21.75, 21.70.

General conditions for amine addition to quinones 10. 2.2 equivalents of amine are added to a solution of quinone **10** in dry acetonitrile at 0 °C under air. Dichloromethane and benzene are also suitable solvents, but methanol gives the coumarin product (cyclization is faster than aerobic aminoquinone oxidation in methanol). The solution is stirred, protected from light, until TLC indicates complete conversion (1-48 h). If excess amine is used, starting material is not recovered and yields do not improve. Removal of solvent and purification by column chromatography (SiO_2, 5-30% EtOAc / hexanes), and collecting the red or red-purple bands gave the product. Further purification by prep-HPLC was required for **1a** and **1d**.

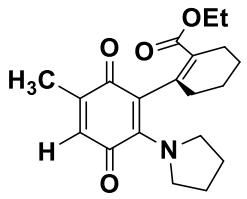

ethyl 5'-methyl-3',6'-dioxo-2'-(pyrrolidin-1-yl)-[1,1'-bi(cyclohexane)]-1,1',4'-triene-2-carboxylate (1d). To a solution of quinone (34.7 mg), ethyl 5'-methyl-3',6'-dioxo-[1,1'-bi(cyclohexane)]-1,1',4'-triene-2-carboxylate) in acetonitrile was added excess pyrrolidine (2-4 equivalents) until a purple band was noted by TLC. The solution was diluted with dilute HCl and extracted with dichloromethane (3 x 50 mL). The combined organic layers were washed with brine, dried ($MgSO_4$), and concentrated. Flash chromatography gave the product as a purple solid (10.4 mg). ^{1}H NMR (400 MHz, Chloroform-*d*) δ 6.30 (q, *J* = 1.5 Hz, 1H), 4.03 (qd, *J* = 7.2, 1.1 Hz, 2H), 3.76 – 3.61 (m, 2H), 3.58 – 3.43 (m, 2H), 2.66 – 2.46 (m, 1H), 2.45 – 2.24 (m, 2H), 2.03 (s, 1H), 2.00 (d, *J* = 1.6 Hz, 3H), 1.94 – 1.48 (m, 8H), 1.14 (t, *J* = 7.2 Hz, 3H). ^{13}C NMR (101 MHz, $CDCl_3$) δ 186.87, 183.08, 168.56, 147.32, 145.29, 142.38, 130.27, 129.84, 118.11, 59.99, 52.24, 32.80, 26.21, 25.73, 21.92, 21.82, 16.17, 14.11.

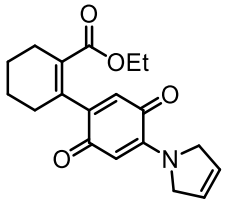

ethyl 4'-(2,5-dihydro-1H-pyrrol-1-yl)-3',6'-dioxo-[1,1'-bi(cyclohexane)]-1,1',4'-triene-2-carboxylate (^{1}H NMR (500 MHz, Chloroform-*d*) δ 6.21 (s, 1H), 5.92 (s, 2H), 5.51 (s, 1H), 4.63-4.11 (broad coalescing peaks) 4H, 4.09 (q, 2H), 4.37 2.54 – 2.32 (m, 2H), 2.34 – 2.12 (m, 3H), 1.72 (m, Hz, 4H), 1.19 (t, *J* = 7.1 Hz, 3H).

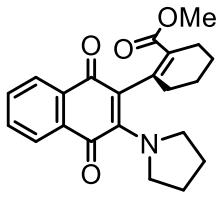

methyl 2-(1,4-dioxo-3-(pyrrolidin-1-yl)-1,4-dihydronaphthalen-2-yl)cyclohex-1-ene-1-carboxylate (1c). ^{1}H NMR (400 MHz, Chloroform-*d*) δ 8.00 (dd, *J* = 7.7, 0.9 Hz, 1H), 7.90 (dd,

J = 7.6, 0.9 Hz, 1H), 7.63 (td, *J* = 7.5, 1.4 Hz, 1H), 7.55 (td, *J* = 7.5, 1.4 Hz, 1H), 3.92 – 3.72 (m, 2H), 3.69 – 3.59 (m, 2H), 3.58 (s, 3H), 2.73 – 2.61 (m, 1H), 2.44 – 2.24 (m, 2H), 2.22 – 2.05 (m, 1H), 2.03 – 1.68 (m, 7H), 1.68 – 1.60 (m, 1H).

Preparatory photolysis. A dilute solution of aminoquinone was irradiated in methanol until UV-vis indicated the reaction was complete. The solvent was removed and the crude product's NMR was taken.

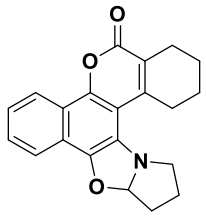

1,2,3,4,11a,12,13,14-octahydro-5H-dibenzo[3,4:7,8]chromeno[5,6-d]pyrrolo[2,1-b]-oxazol-5-one (3d). ^{1}H NMR (400 MHz, Chloroform-*d*) δ 8.49 (ddd, *J* = 8.4, 1.3, 0.7 Hz, 1H), 7.82 (ddd, *J* = 8.3, 1.4, 0.7 Hz, 1H), 7.48 (ddd, *J* = 8.2, 6.8, 1.4 Hz, 1H), 6.05 (d, *J* = 4.1 Hz, 1H), 3.73 – 3.51 (m, 1H), 3.46 – 3.27 (m, 1H), 3.09 – 2.93 (m, 1H), 2.81 (dd, *J* = 17.7, 4.3 Hz, 1H), 2.66 – 2.46 (m, 2H), 2.10 – 2.01 (m, 1H), 2.01 – 1.83 (m, 1H), 1.75 – 1.52 (m, 6H). ^{13}C NMR (101 MHz, $CDCl_3$) δ 161.62, 148.05, 144.56, 130.62, 127.67, 125.51, 123.32, 122.90, 120.99, 120.76, 119.87, 104.09, 59.09, 31.97, 29.71, 27.38, 24.46, 23.61, 21.94, 21.52.

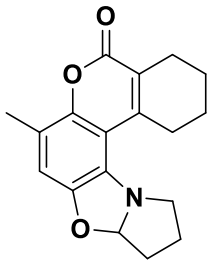

7-methyl-1,2,3,4,9a,10,11,12-octahydro-5H-benzo[3,4]chromeno[5,6-d]pyrrolo[2,1-b]oxazol-5-one (1d). ^{1}H NMR (400 MHz, Chloroform-*d*) δ 6.41 (t, *J* = 0.6 Hz, 1H), 5.79 (dd, *J* = 5.0, 2.5 Hz, 1H), 4.04 (q, *J* = 7.1 Hz, 2H), 3.09 (dt, *J* = 10.3, 7.1 Hz, 1H), 3.00 – 2.80 (m, 1H), 2.73 (d, *J* = 18.8 Hz, 1H), 2.46 (s, 0H), 2.31 – 1.95 (m, 4H), 1.94 – 1.58 (m, 4H).

UV-vis spectra.

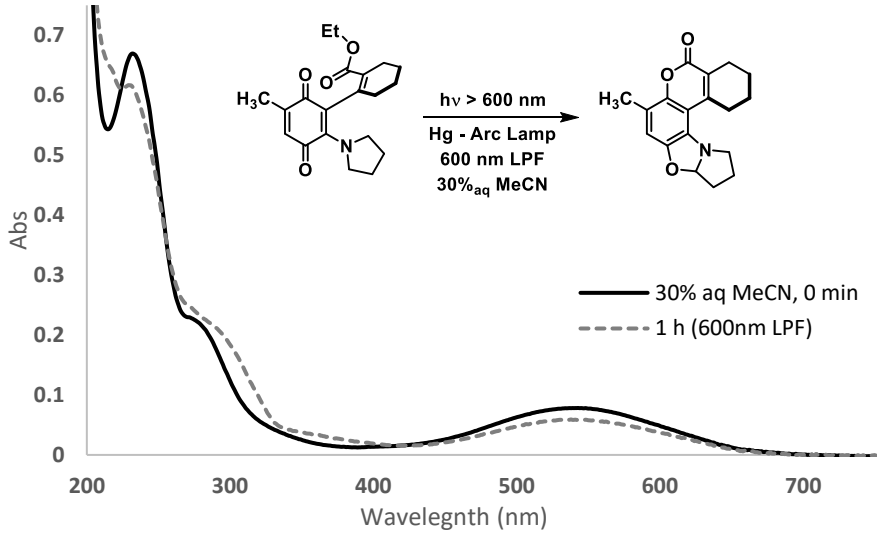

Figure 4.2 30% aqueous acetonitrile photolysis of **1d** with > 600 nm light (600 nm LPF on arc lamp)

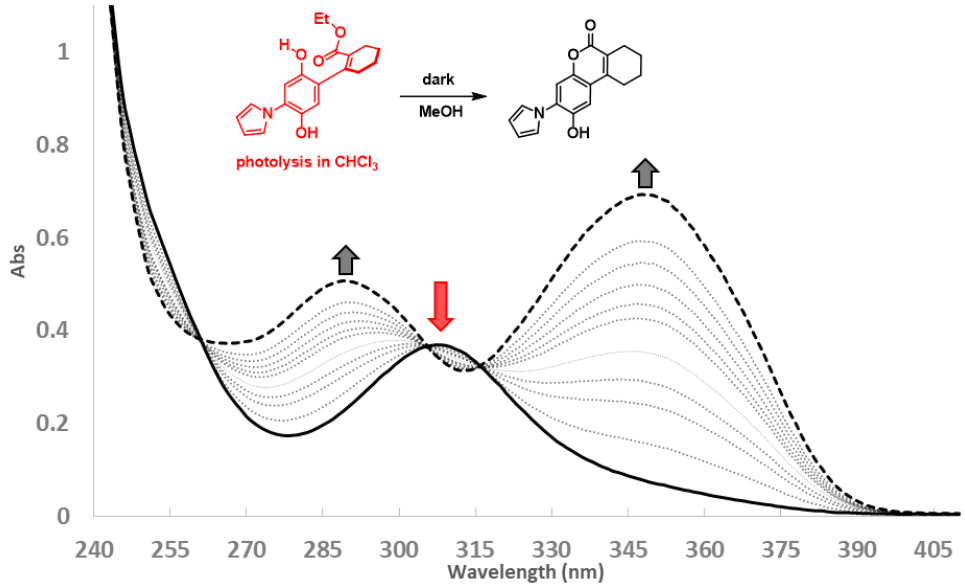

Figure 4.3 Addition of methanol to photolyzed chloroform solution of **1a** initiates the cis-lock closure.

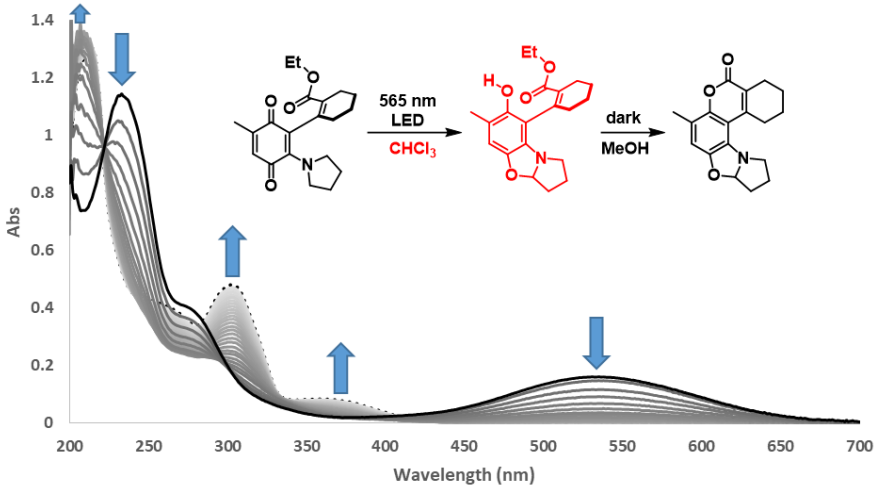

Figure 4.4 Addition of methanol to photolyzed chloroform solution of **1d** initiates the cis-lock closure.

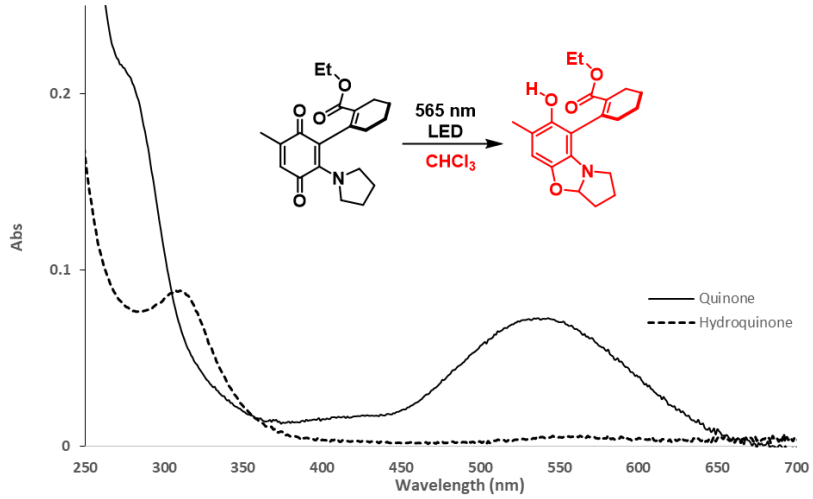

Figure 4.5 Before and after photolysis of **1d** in chloroform. Coumarin bands near 375 nm are notably absent in the hydoquinone.

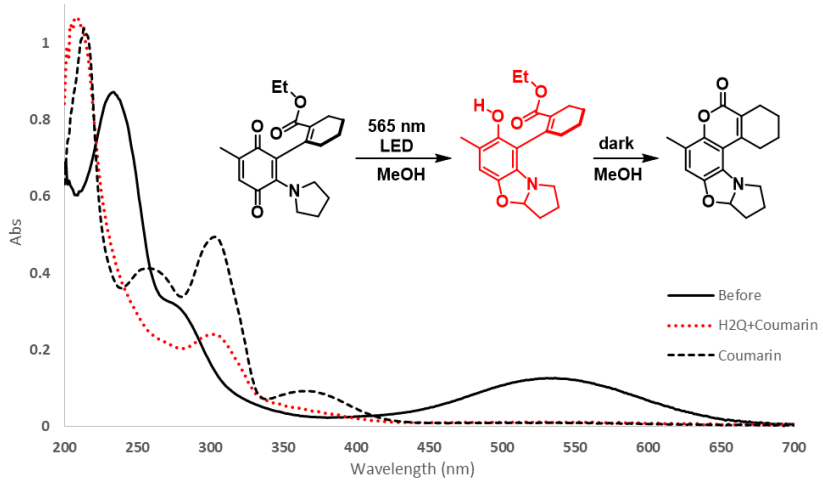

Figure 4.6 Before and after photolysis of **1d** in chloroform. Coumarin bands near 375 nm are notably absent in the hydoquinone.

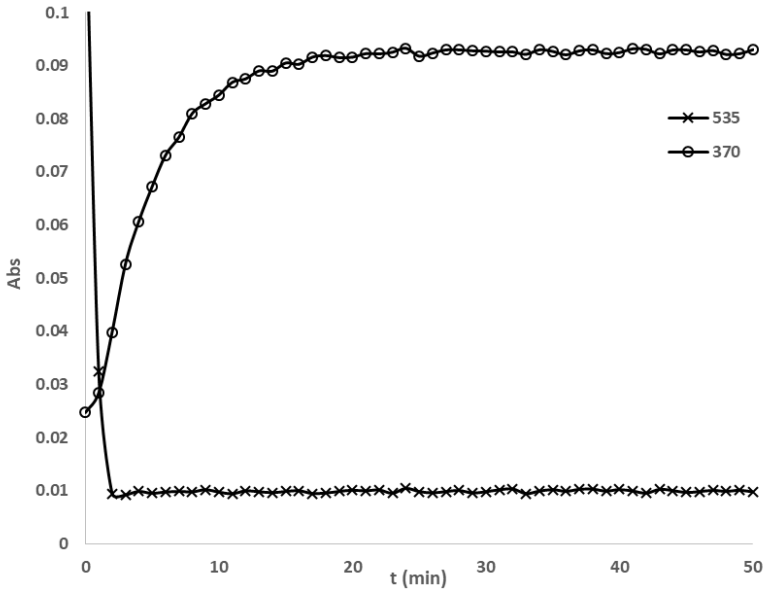

Figure 4.7 Absorbance at 535 nm (quinone) and 370 nm (coumarin) vs. time. Irradiation stopped when A(535 nm) = 0.01. The coumarin grows in over time, indicating lactonization in methanol is complete after 10-20 minutes in the dark for **1d**. The coumarin is immediately formed in methanol for **1a**,**b**.

4.6 References

1. Klán, P.; Šolomek, T.; Bochet, C. G.; Blanc, A.; Givens, R.; Rubina, M.; Popik, V.; Kostikov, A.; Wirz, J. Photoremovable Protecting Groups in Chemistry and Biology: Reaction Mechanisms and Efficacy. *Chem. Rev.* **2013**, *113* (1), 119–191. https://doi.org/10.1021/cr300177k.
2. Fournier, L.; Gauron, C.; Xu, L.; Aujard, I.; Le Saux, T.; Gagey-Eilstein, N.; Maurin, S.; Dubruille, S.; Baudin, J.-B.; Bensimon, D.; et al. A Blue-Absorbing Photolabile Protecting Group for in Vivo Chromatically Orthogonal Photoactivation. *ACS Chem. Biol.* **2013**, *8* (7), 1528–1536. https://doi.org/10.1021/cb400178m.
3. Fournier, L.; Aujard, I.; Le Saux, T.; Maurin, S.; Beaupierre, S.; Baudin, J.-B.; Jullien, L. Coumarinylmethyl Caging Groups with Redshifted Absorption. *Chem. Eur. J.* **2013**, *19* (51), 17494–17507. https://doi.org/10.1002/chem.201302630.
4. Amatrudo, J. M.; Olson, J. P.; Lur, G.; Chiu, C. Q.; Higley, M. J.; Ellis-Davies, G. C. R. Wavelength-Selective One- and Two-Photon Uncaging of GABA. *ACS Chem. Neurosci.* **2014**, *5* (1), 64–70. https://doi.org/10.1021/cn400185r.
5. Hansen, M. J.; Velema, W. A.; Lerch, M. M.; Szymanski, W.; Feringa, B. L. Wavelength-Selective Cleavage of Photoprotecting Groups: Strategies and Applications in Dynamic Systems. *Chem. Soc. Rev.* **2015**, *44* (11), 3358–3377. https://doi.org/10.1039/C5CS00118H.
6. Lin, Q.; Yang, L.; Wang, Z.; Hua, Y.; Zhang, D.; Bao, B.; Bao, C.; Gong, X.; Zhu, L. Coumarin Photocaging Groups Modified with an Electron-Rich Styryl Moiety at the 3-Position: Long-Wavelength Excitation, Rapid Photolysis, and Photobleaching. *Angewandte Chemie International Edition* **2018**, *57* (14), 3722–3726. https://doi.org/10.1002/anie.201800713.
7. Goswami, P. P.; Syed, A.; Beck, C. L.; Albright, T. R.; Mahoney, K. M.; Unash, R.; Smith, E. A.; Winter, A. H. BODIPY-Derived Photoremovable Protecting Groups Unmasked with Green Light. *J. Am. Chem. Soc.* **2015**, *137* (11), 3783–3786. https://doi.org/10.1021/jacs.5b01297.
8. Palao, E.; Slanina, T.; Muchová, L.; Šolomek, T.; Vítek, L.; Klán, P. Transition-Metal-Free CO-Releasing BODIPY Derivatives Activatable by Visible to NIR Light as Promising Bioactive Molecules. *J. Am. Chem. Soc.* **2016**, *138* (1), 126–133. https://doi.org/10.1021/jacs.5b10800.
9. Slanina, T.; Shrestha, P.; Palao, E.; Kand, D.; Peterson, J. A.; Dutton, A. S.; Rubinstein, N.; Weinstain, R.; Winter, A. H.; Klán, P. In Search of the Perfect Photocage: Structure–Reactivity Relationships in Meso-Methyl BODIPY Photoremovable Protecting Groups. *J. Am. Chem. Soc.* **2017**, *139* (42), 15168–15175. https://doi.org/10.1021/jacs.7b08532.
10. Šťacko, P.; Muchová, L.; Vítek, L.; Klán, P. Visible to NIR Light Photoactivation of Hydrogen Sulfide for Biological Targeting. *Org. Lett.* **2018**, *20* (16), 4907–4911. https://doi.org/10.1021/acs.orglett.8b02043.
11. Peterson, J. A.; Wijesooriya, C.; Gehrmann, E. J.; Mahoney, K. M.; Goswami, P. P.; Albright, T. R.; Syed, A.; Dutton, A. S.; Smith, E. A.; Winter, A. H. Family of BODIPY Photocages Cleaved by Single Photons of Visible/Near-Infrared Light. *J. Am. Chem. Soc.* **2018**, *140* (23), 7343–7346. https://doi.org/10.1021/jacs.8b04040.

12. Gorka, A. P.; Nani, R. R.; Zhu, J.; Mackem, S.; Schnermann, M. J. A Near-IR Uncaging Strategy Based on Cyanine Photochemistry. *J. Am. Chem. Soc.* **2014**. https://doi.org/10.1021/ja5065203.
13. Nani, R. R.; Gorka, A. P.; Nagaya, T.; Kobayashi, H.; Schnermann, M. J. Near-IR Light-Mediated Cleavage of Antibody–Drug Conjugates Using Cyanine Photocages. *Angewandte Chemie International Edition* **2015**, *54* (46), 13635–13638. https://doi.org/10.1002/anie.201507391.
14. Nani, R. R.; Gorka, A. P.; Nagaya, T.; Yamamoto, T.; Ivanic, J.; Kobayashi, H.; Schnermann, M. J. In Vivo Activation of Duocarmycin–Antibody Conjugates by Near-Infrared Light. *ACS Cent. Sci.* **2017**. https://doi.org/10.1021/acscentsci.7b00026.
15. Gorka, A. P.; Nani, R. R.; Schnermann, M. J. Harnessing Cyanine Reactivity for Optical Imaging and Drug Delivery. *Acc. Chem. Res.* **2018**, *51* (12), 3226–3235. https://doi.org/10.1021/acs.accounts.8b00384.
16. Chen, Y.; Steinmetz, M. G. Photochemical Cyclization with Release of Carboxylic Acids and Phenol from 1 , 4-Benzoquinones Using Visible Light. *Organic Letters* **2005**, *7*, 3729–3732.
17. Chen, Y.; Steinmetz, M. G. Photoactivation of Amino-Substituted 1,4-Benzoquinones for Release of Carboxylate and Phenolate Leaving Groups Using Visible Light. *J. Org. Chem.* **2006**, *71* (16), 6053–6060. https://doi.org/10.1021/jo060790g.
18. Walton, D. P.; Dougherty, D. A. A General Strategy for Visible-Light Decaging Based on the Quinone Trimethyl Lock. *J. Am. Chem. Soc.* **2017**, *139* (13), 4655–4658. https://doi.org/10.1021/jacs.7b01548.
19. Regan, C. J.; Walton, D. P.; Shafaat, O. S.; Dougherty, D. A. Mechanistic Studies of the Photoinduced Quinone Trimethyl Lock Decaging Process. *J. Am. Chem. Soc.* **2017**, *139* (13), 4729–4736. https://doi.org/10.1021/jacs.6b12007.
20. Carling, C.-J.; Olejniczak, J.; Foucault-Collet, A.; Collet, G.; Viger, M. L.; Huu, V. A. N.; Duggan, B. M.; Almutairi, A. Efficient Red Light Photo-Uncaging of Active Molecules in Water upon Assembly into Nanoparticles. *Chem. Sci.* **2016**, *7* (3), 2392–2398. https://doi.org/10.1039/C5SC03717D.
21. Wang, X.; Kalow, J. A. Rapid Aqueous Photouncaging by Red Light. *Org. Lett.* **2018**, *20* (7), 1716–1719. https://doi.org/10.1021/acs.orglett.8b00100.
22. Bruce, J. M. Light-Induced Reactions of Quinones. *Q. Rev. Chem. Soc.* **1967**, *21* (3), 405–428. https://doi.org/10.1039/QR9672100405.
23. Cameron, D. W.; Giles, R. G. F. Photochemical Formation of Benzoxazoline Derivatives from Aminated Quinones. *J. Chem. Soc. C* **1968**, No. 0, 1461–1464. https://doi.org/10.1039/J39680001461.
24. Giles, R. G. F.; Mitchell, P. R. K.; Roos, G. H. P.; Baxter, I. A Photochemical Reaction of 2-Acetyl-3-Alkylamino-1,4-Benzoquinones: Formation of Benzoxazoles. *J. Chem. Soc., Perkin Trans. 1* **1973**, No. 0, 493–496. https://doi.org/10.1039/P19730000493.
25. Iwamoto, H. Photoinduced Intramolecular Cyclization Reaction of 3-Substituted 2-Alkenoyl-1,4-Benzoquinones. *Bulletin of the Chemical Society of Japan* **1989**, *62* (11), 3479–3487. https://doi.org/10.1246/bcsj.62.3479.
26. Blankespoor, R. L.; De Jong, R. L.; Dykstra, R.; Hamstra, D. A.; Rozema, D. B.; VanMeurs, D. P.; Vink, P. Photochemistry of 1-Alkoxy- and 1-(Benzyloxy)-9,10-Anthraquinones in Methanol: A .Delta.-Hydrogen Atom Abstraction Process That

Exhibits a Captodative Effect. *J. Am. Chem. Soc.* **1991**, *113* (9), 3507–3513. https://doi.org/10.1021/ja00009a042.

27. Iwamoto, H.; Takuwa, A. Photoinduced Intramolecular Cyclization Reaction of 2-(2-Alkenoyl)-3-Isopropylthio-1,4-Benzoquinones to Heterocyclic Compounds. *Bulletin of the Chemical Society of Japan* **1991**, *64* (2), 724–726. https://doi.org/10.1246/bcsj.64.724.
28. Sakurai, H.; Abe, J.; Sakamoto, K. Photochemistry of Aryldisilanes and Disilanylquinones: Novel Photochemical Process from Intramolecular Charge-Transfer States. *Journal of Photochemistry and Photobiology A: Chemistry* **1992**, *65* (1–2), 111–120. https://doi.org/10.1016/1010-6030(92)85036-T.
29. Shishkina, R. P.; Berezhnaya, V. N. Photochemistry of 2-Dialkylamino-1,4-Naphthoquinones. *Russ. Chem. Rev.* **1994**, *63* (2), 139. https://doi.org/10.1070/RC1994v063n02ABEH000076.
30. Kallmayer, H.-J.; Fritzen, W. Photoreaktivität einiger 2-Alkylthio/Phenylthio-3,5,6-trichlor/brom-1,4-benzochinone. *Pharmazie* **1994**, *49* (6), 412–415.
31. Kallmayer, H.; Tappe, C. Chinon-Amin-Reaktionen, 21. Mitt.1) Photoreaktivität einiger 2-Amino-3-halogen-1.4-naphthochinone. *Archiv der Pharmazie* **1986**, *319* (9), 791–798. https://doi.org/10.1002/ardp.19863190905.
32. Iwamoto, H.; Takuwa, A.; Hamada, K.; Fujiwara, R. Intra- and Intermolecular Photocyclization of Vinylbenzo-1,4-Quinones. *J. Chem. Soc., Perkin Trans. 1* **1999**, No. 5, 575–582. https://doi.org/10.1039/A809530B.
33. Aponick, A.; Dietz, A. L.; Pearson, W. H. 2-(3-Pyrrolin-1-Yl)-1,4-Naphthoquinones: Photoactivated Alkylating Agents. *Eur. J. Org. Chem.* **2008**, *2008* (25), 4264–4276. https://doi.org/10.1002/ejoc.200800482.
34. Porhun, V. I.; Rakhimov, A. I. Mechanism of the Photochemical Reactions of Substituted Benzoquinones. *Russ J Gen Chem* **2011**, *81* (5), 890–912. https://doi.org/10.1134/S1070363211050112.
35. Ando, Y.; Suzuki, K. Photoredox Reactions of Quinones. *Chemistry – A European Journal* **2018**, *24* (60), 15955–15964. https://doi.org/10.1002/chem.201801064.
36. Cameron, D. W.; Giles, R. G. F. A Photochemical Rearrangement Involving Aminated Quinones. *Chem. Commun. (London)* **1965**, No. 22, 573–574. https://doi.org/10.1039/C19650000573.
37. Garrett, E. R.; Lippold, B. C.; Mielck, J. B. Kinetics and Mechanisms of Lactonization of Coumarinic Acids and Hydrolysis of Coumarins I. *Journal of Pharmaceutical Sciences* **1971**, *60* (3), 396–405. https://doi.org/10.1002/jps.2600600312.
38. Lippold, B. C.; Garrett, E. R. Kinetics and Mechanisms of Lactonization of Coumarinic Acids and Hydrolysis of Coumarins II. *Journal of Pharmaceutical Sciences* **1971**, *60* (7), 1019–1027. https://doi.org/10.1002/jps.2600600704.
39. Hershfield, R.; Schmir, G. L. Lactonization of Ring-Substituted Coumarinic Acids. Structural Effects on the Partitioning of Tetrahedral Intermediates in Esterification. *Journal of the American Chemical Society* **1973**, *95* (22), 7359–7369. https://doi.org/10.1021/ja00803a025.
40. Hershfield, R.; Schmir, G. L. Lactonization of Coumarinic Acids. Kinetic Evidence for Three Species of the Tetrahedral Intermediate. *Journal of the American Chemical Society* **1973**, *95* (24), 8032–8040. https://doi.org/10.1021/ja00805a014.

41. Turner, A. D.; Pizzo, S. V.; Rozakis, G. W.; Porter, N. A. Photochemical Activation of Acylated .Alpha.-Thrombin. *J. Am. Chem. Soc.* **1987**, *109* (4), 1274–1275. https://doi.org/10.1021/ja00238a062.
42. Turner, A. D.; Pizzo, S. V.; Rozakis, G.; Porter, N. A. Photoreactivation of Irreversibly Inhibited Serine Proteinases. *J. Am. Chem. Soc.* **1988**, *110* (1), 244–250. https://doi.org/10.1021/ja00209a040.
43. Porter, N. A.; Bruhnke, J. D. Acyl Thrombin Photochemistry: Kinetics for Deacylation of Enzyme Cinnamate Geometric Isomers. *J. Am. Chem. Soc.* **1989**, *111* (19), 7616–7618. https://doi.org/10.1021/ja00201a054.
44. Wang, B.; Zheng, A. A Photo-Sensitive Protecting Group for Amines Based on Coumarin Chemistry. *Chem. Pharm. Bull.* **1997**, *45* (4), 715–718. https://doi.org/10.1248/cpb.45.715.
45. Gagey, N.; Neveu, P.; Benbrahim, C.; Goetz, B.; Aujard, I.; Baudin, J.-B.; Jullien, L. Two-Photon Uncaging with Fluorescence Reporting: Evaluation of the o-Hydroxycinnamic Platform. *J. Am. Chem. Soc.* **2007**, *129* (32), 9986–9998. https://doi.org/10.1021/ja0722022.
46. Duan, X.-Y.; Zhai, B.-C.; Song, Q.-H. Water-Soluble o-Hydroxycinnamate as an Efficient Photoremovable Protecting Group of Alcohols with Fluorescence Reporting. *Photochem. Photobiol. Sci.* **2012**, *11* (3), 593–598. https://doi.org/10.1039/C2PP05309H.
47. Venkatesh, Y.; Srivastava, H. K.; Bhattacharya, S.; Mehra, M.; Datta, P. K.; Bandyopadhyay, S.; Singh, N. D. P. One- and Two-Photon Uncaging: Carbazole Fused *o* -Hydroxycinnamate Platform for Dual Release of Alcohols (Same or Different) with Real-Time Monitoring. *Organic Letters* **2018**, *20* (8), 2241–2244. https://doi.org/10.1021/acs.orglett.8b00090.
48. Tremblay, M. S.; Sames, D. A New Fluorogenic Transformation: Development of an Optical Probe for Coenzyme Q. *Org. Lett.* **2005**, *7* (12), 2417–2420. https://doi.org/10.1021/ol0507569.
49. Giles, R. G. F. The Photochemistry of an Aminated 1,4-Benzoquinone. *Tetrahedron Letters* **1972**, *13* (22), 2253–2254. https://doi.org/10.1016/S0040-4039(01)84819-X.
50. Stavitskaya, T. A.; Bukhtoyarova, A. D.; Shishkina, R. P.; Berezhnaya, V. N.; Shchegoleva, L. N.; Eroshkin, V. I. Influence of the Structure of 2-Dialkyl(Cycloalkyl)Amino-1,4-Naphthoquinones on Their Photochemical Activity. *Khimiya Vysokikh Energii* **1991**, *25* (3), 262–267.
51. Calvin, J. R.; Frederick, M. O.; Laird, D. L. T.; Remacle, J. R.; May, S. A. Rhodium-Catalyzed and Zinc(II)-Triflate-Promoted Asymmetric Hydrogenation of Tetrasubstituted α,β-Unsaturated Ketones. *Org. Lett.* **2012**, *14* (4), 1038–1041. https://doi.org/10.1021/ol203264a.
52. Russkikh, V. V. Synthesis and Photolysis of 2-Dialkylamino-1,4-Benzoquinones and 2-Dialkylamino-1,4-Anthraquinones. *Russian journal of organic chemistry : a translation of Zhurnal organicheskoi khimii* **1995**, *31* (3), 343–347.
53. Maruyama, K.; Kozuka, T.; Otsuki, T.; Naruta, Y. A TRANSIENT FORMATION OF N-SUBSTITUTED ISOINDOLE BY MEANS OF PHOTOCHEMICAL INTRAMOLECULAR HYDROGEN ABSTRACTION. *Chemistry Letters* **1977**, No. 9, 1125–1126. https://doi.org/10.1246/cl.1977.1125.

54. Maruyama, K.; Kozuka, T.; Otsuki, T. The Intramolecular Hydrogen Abstraction Reaction in the Photolysis of Aminated 1,4-Naphthoquinones. *Bulletin of the Chemical Society of Japan* **1977**, *50* (8), 2170–2173. https://doi.org/10.1246/bcsj.50.2170.
55. Fabian, J.; Nakazumi, H.; Matsuoka, M. Near-Infrared Absorbing Dyes. *Chem. Rev.* **1992**, *92* (6), 1197–1226. https://doi.org/10.1021/cr00014a003.

Chapter 5. Progress Towards Excited State Proton Transfer Mediated Photolabile Protecting Groups

5.1 Abstract

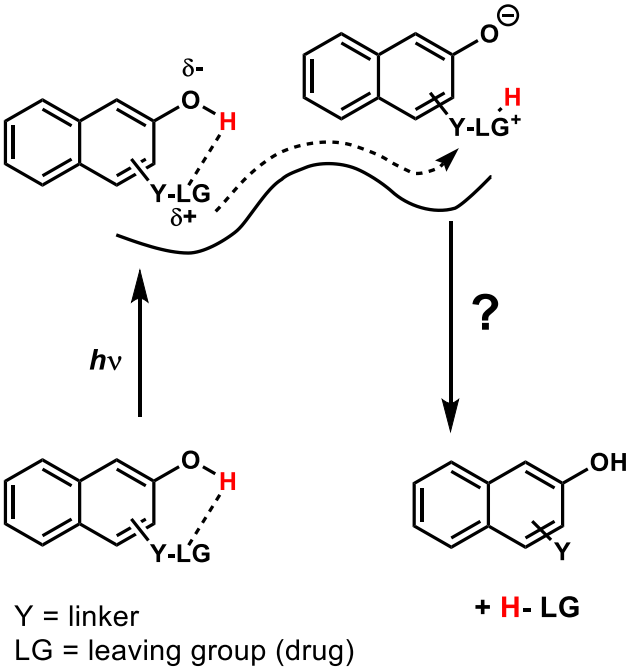

The ability of the photoacid 2-naphthol to undergo intramolecular excited state proton transfer resulting in deprotection of acid labile groups was investigated. Photoacid mediated cleavage of tetrahydropyranyl ethers was potentially observed, while *tert*-butyl esters were mostly stable to photolysis. The photochemical and ground-state reactivity observed provides a clear route to more reactive compounds for future designs.

5.2 Introduction to Photoacidity

The initial reports of excited state proton transfer (ESPT) were made by Förster (1949) and Weller (1955), based on large bathochromic shifts in fluorescence spectra of amino- and hydroxyaromatics. Since then, the field has been intensely researched, and ESPT has been the

subject of many reviews.[1,2] ESPT is observed for molecules that become strong acids on photoexcitation (typically S_1), and these molecules are therefore referred to as photoacids. Hydroxyarenes are the predominantly studied photoacids and can display substantially enhanced acidities of 5-12 pK_a units in the electronically excited states. ESPT from a photoacid is a reversible adiabatic process, and is therefore distinct from the photoacid generators (PAG) common to lithography, which produce a ground-state acid irreversibly on photolysis.[1-5]

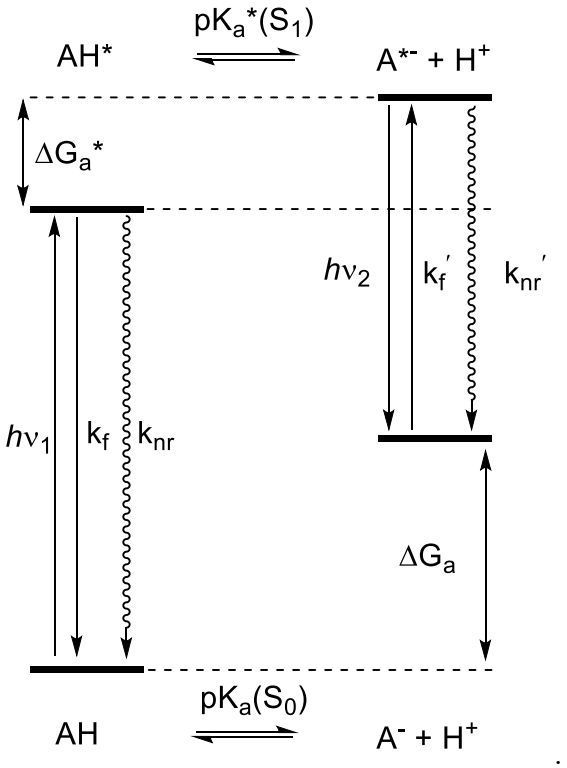

Figure 5.1 Förster cycle photoacidity

$$pK_a{}^* = pK_a - \frac{(h\nu_1 - h\nu_2)}{2.3RT} = pK_a - \frac{\Delta E_{0,0}}{2.3RT} \quad (1)$$

The Förster cycle is a model of photoacidity first proposed by Förster, who used it to approximate excited state acidity constants.[1,2] Photoacidity is thermodynamically treated as a change in the relative free energies of the acid and conjugate base in the excited state.[1-3]

Following the Kasha rule that internal conversion outcompetes direct relaxation from S_n, the Förster cycle only considers the S_0 – S_1 electronic transition energies ($E_{0,0}$) of the acid and conjugate base. $E_{0,0}$ values are typically estimated by averaging the S_0-S_1 and S_1-S_0 transition band energies taken at their maxima in the absorbance and fluorescence spectra of both the acid and conjugate base.[2] A Förster cycle diagram is depicted in **Figure 5.1**, where $h\nu_1$ is $E_{0,0}$ for the acid, $h\nu_2$ is $E_{0,0}$ for the conjugate base, h is Planck's constant, pK_a ($pK_a^*(S_1)$) is the acidity constant in the ground (excited S_1) state, ΔG_a (ΔG_a^*) is the difference in free energies between the acid and conjugate base in the ground (excited) state. Fluorescence and non-radiative decay are in competition with photoacidity, and are represented as their respective rates, k_f and k_{nr}. Depending on the photoacid, other quenching processes exist, such as proton-quenching.[3]

The excited state pK_a, pK_a^*, is then calculated using the Förster equation (eq 1), where the pK_a is obtained from ground state data, $(h\nu_1 - h\nu_2) = \Delta E_{0,0} = \Delta G_a - \Delta G_a^*$ for the photoacid and conjugate base, R is the gas constant, and T is temperature.[3] Estimated pK_a^*s derived this way are typically within one pK_a unit of those obtained by the more accurate, but experimentally challenging, methods that measure the protonation and deprotonation rates directly.[2]

Origins of Photoacidity

Pines argues that an electronic rearrangement on excitation results in preferential stabilization of the conjugate base in S_1. The stabilization of the excited conjugate base accounts for its diminished proton affinity, and a more thermodynamically favorable reaction.[2] Agmon et al. support this notion with the observation of solvatochromatic shifts for 2-naphthol derivatives. The authors found that in the S_1 state, 2-naphthol becomes a stronger hydrogen-bond donor while the 2-naphtholate anion becomes a weaker hydrogen-bond acceptor. These observations are consistent with both destabilization of the photoacid and stabilization of its conjugate base in the excited state, and through comparison to the methyl ether, the authors conclude that both the excited acid and base contribute to the pK_a^*.[6,7]

Tolbert et al. reason that photoacidity of hydroxyaromatics in the first excited state is best explained by Hückel molecular orbital theory. The authors describe the photoacid conjugate base as an odd-alternate hydrocarbon anion, with a non-bonding molecular orbital (NBMO) that has a large coefficient on the oxygen. Excitation of an electron from this NBMO to the lowest unoccupied molecular orbital (LUMO) delocalizes the charge on oxygen as the LUMO is more diffuse. The resulting intramolecular charge transfer (ICT) state leads to enhanced acidity in S_1.[3]

The same argument for ICT can be made by comparison of the L_a and L_b spectroscopic states of 1-naphthol and 2-naphthol.[4,8] Hydroxyl group substitution to give either of the naphthol isomers breaks the degeneracy of napthalene's two spectroscopic states, L_a and L_b. For 1-naphthol, the L_a is lower in energy than L_b, and the converse is true for 2-naphthol. Since the L_a state is more polarized than the L_b state, a greater transfer of charge from oxygen to the distal ring is possible for 1-naphthol. The relative populations of the L_a and L_b states of 1-naphthol (1N) and 2-naphthol (2N) manifests itself in a lower pK_a^* by nearly 3 pK units for 1-naphthol. Proton quenching also occurs at carbons 5 and 8 of 1-naphthol, where the negative charge localizes in the excited state, but not for 2-naphthol. The proton quenching of 1-naphthol suggests that negative charge localizes on C_5 and C_8 in the excited state.[8]

Tolbert et al. prepared a series of "super" photoacids with $pK_a^* < 0$ by stabilization of the conjugate base with electron withdrawing cyano substituents. The cyano-naphthols investigated by the authors and the measured pK_a and pK_a^* values are shown in table 1. Remarkably, the 5,8-dicyano-2-naphthol (DC2N) derivative has a pK_a^* of - 4.5, while the ground state pK_a is less affected (DC2N pK_a = 7.8 compared to 9.6 for 2N).[8,9]

	1N	**5CN1N**	**2N**	**5C2N**	**6C2N**	**7C2N**	**8C2N**	**5,8DC2N**
[a]**pK_a**	9.4	8.5	9.45	8.75	8.40	8.75	8.35	7.8
[b]**pK_a^***	- 0.2	- 2.8	2.8	- 1.2	0.2	- 1.3	- 0.4	- 4.5

Table 5.1. Acidity constants of cyano napthols in the ground and excited states[a]

[a]Abbreviations are as follows: 1-naphthol (1N), 5-cyano-1-naphthol (5C1N), 2-naphthol (2N), 5-cyano-2-naphthol (5C2N), 6-cyano-2-naphthol (6C2N), 7-cyano-2-naphthol (7C2N), 8-cyano-2-naphthol (8C2N), 5,8-dicyano-2-naphthol (5,8C2N). [a]Ground state pK_a values measured via absorption titration. [b]Calculated Förster pK_a^* values.

In a related work, Agmon et al. calculated the ground and excited state charge distributions for the cyano-2-naphthol derivatives with good correlations to experimental data. The Mulliken charges calculated decrease on carbons 1 and 6, and increase on carbons 3, 5, and 8 on excitation of 2-naphtholate. The effective shift in Mulliken charges is qualitatively shown in **Figure 5.2**, and the effect is larger for the naphtholate anions. These calculations complement the findings of Tolbert et al. that cyano substituents at C_5 and C_8 of 2-naphthol give stronger photoacids and that C_5 substitution has a smaller effect on ground state pK_a than at C_8.[8,10]

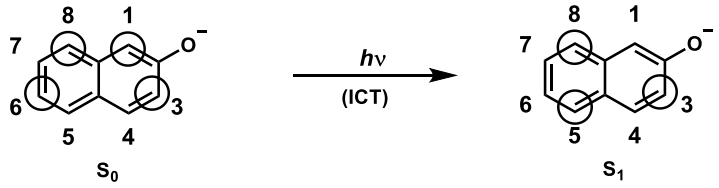

Figure 5.2 Localization of negative charge in the naphtholate ring in the ground and excited states.

The origin of photoacidity in the case of 2-naphthol and its cyano derivatives therefore appears to be migration of charge from the oxygen to the aromatic ring.[1-3,6-10] The resulting intramolecular charge transfer (ICT) character in the S_1 state is larger for the excited 2-naphtholate anion than the parent photoacid.[10] Stabilization of the excited conjugate base, therefore, predominately induces the large pK_a shift in the S_1 state for 2-naphthol derivatives.[10]

Agmon et al. argue that the underlying cause for increased ICT character of the excited anion arises from the reversal of Hückel's rules for aromaticity in S_1.[10] In the ground state, (4n+2) π electrons is aromatic and 4n π electrons is antiaromatic by Hückel's rules. In the T_1 and S_1 excited states, the reverse is true by Baird's rules.[11,12] 2-Naphthol has 10 π-electrons and is aromatic by the criteria of a large singlet-triplet gap and its similar geometry to the aromatic parent, naphthalene. In the ground state, the stabilizing delocalization of oxygen's charge into the aromatic ring comes at the cost of some aromatic character (12 π electron system). The excited anion enjoys a reduction in the antiaromatic character, if any, gained by delocalization of charge into the ring to create a 12 π electron system. ICT is therefore more favorable in the

excited state, where the stabilizing delocalization of charge contributes to aromatic character of the anion.[10]

While Tobert et al. had only investigated electron withdrawing groups in the distal ring of 2-naphthol (5,6,7, or 8- substitution)[8,9], Agmon et al. calculated that the most electronegative naphtholate carbon is actually C_3, followed by C_5, and then C_8.[10] Since 8- and 5-cyano-2-naphthol are strong photoacids[8,9], Agmon et al. suggest that 3-cyano-2-naphthol would also be a strong photoacid (perhaps the strongest mono-substituted cyanonaphthol), and that 3,5,8-dicyano-2-naphthol would be a very strong photoacid with a reasonable ground-state pK_a.[10] The pK_a* of 3-cyano-2-naphthol has still not been reported.

The 2-naphthol derivatives discussed above are informative examples of the processes driving photoacidity in hydroxyarenes. These and other common photoacids are shown (**Figure 5.3**) with acidity constants for the ground and excited states. For consistency, the pK_a and pK_a* values are taken from the same source,[2] however, discrepancies between sources are common.

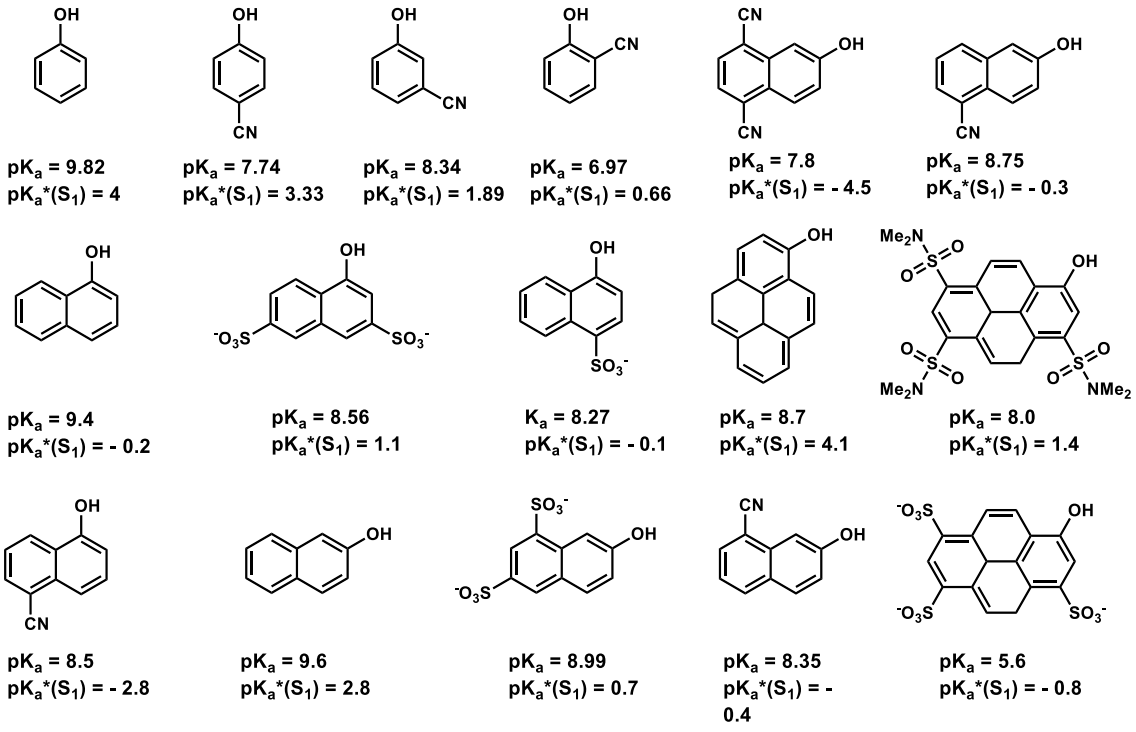

Figure 5.3 Ground state (pK_a) and excited state pK_a*(S_1) of Common Photoacids

Applications of Photoacidity and Excited State Proton Transfer (ESPT)

Photochemical excited state acid-base chemistry has been reviewed.[12] pH and pOH jump experiments resulting from intermolecular ESPT have applications in photolithography and proton hydration dynamics as mechanistic tools and in probing the micro-environments of micelles, proteins, cyclodextrins, and films. Intramolecular ESPT reactions have been used for chemical lasers, data and energy storage systems, polymer stabilizers, and radiation detectors.[1]

One relatively unexplored application for photoacids is their utility in conjunction with photolabile protecting groups, which comprise a growing field with many important biological applications. The photolabile starting compound is referred to as a caged molecule, and decaging is therefore photochemical release of the protected compound. Established photochemical decaging reactions involving the heterolytic or homolytic cleavage of C-R (R = H, C, O, N, halogen) bonds potentially require energies corresponding to UV-light, thus limiting the wavelength at which one-photon reactions of this type can occur.[13,14]

One attractive aspect of photoacidity is the potential for acid-base reactions caused by irradiation at long wavelengths. The Förster cycle predicts a pK_a shift in the excited state as only the difference in relative free energies of the excited acid and conjugate base. As an example, a generous pK_a shift of 10 units is calculated to only require a $\Delta E_{0,0}$ of 13.6 kcal/mol by equation 1. Thermodynamically, a significant enhancement of acidity is therefore associated with a relatively small energetic perturbation. The relatively large excess excitation energy in UV-absorbing photoacids is released as fluorescence from the excited conjugate base. One can imagine a system where the S_0-S_1 gap is small relative to $\Delta E_{0,0}$ for photoacid and conjugate base. Such a system would theoretically maintain photoacidity at long wavelengths. To our knowledge, excited state proton transfer as the photochemical process resulting in release of a caged molecule at any wavelength, has not been reported. We have therefore chosen 2-naphthol as a starting point to develop photoacid-mediated release of labile caged molecules at short wavelengths, with the goal of long wavelength application in the delivery of pharmaceuticals.

Rationale for Initial Design

The appropriate substrate design for an excited state proton transfer reaction is expected to be essential for an efficient reaction. Excited state lifetimes of 2-naphthol and its derivatives

are short, and a bulk pH change is not expected since geminate recombination of the acid and conjugate base occurs quickly.[1,3] In most cases, the photoacid proton is not expected to diffuse far into solution, if at all.[15] The large effective concentrations displayed in intramolecular acid catalysis were therefore desired.[16] A ground-state intramolecular hydrogen bond to the photoacid would also mitigate these challenges by directing the proton transfer to the appropriate position to immediately affect the acid-catalyzed reaction. We therefore envisioned the photochemical reaction as intramolecular ESPT from 2-naphthol to a closely tethered acid-labile group. ESPT along the hydrogen bond coordinate to give departure of the protonated leaving group yields the generalized products shown in **Figure 5.4.**

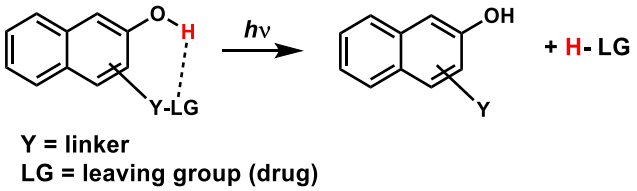

Figure 5.4 General design of a photoacid mediated photocage

The first photocage designs investigated (**1a, 1b, 2,** and **3**; figure 5) consisted of a *tert*-butyl ester moiety capable of making an intramolecular hydrogen bond to the hydroxyl group of 2-naphthol. The rationale behind this design was the low ring-strain of a 10-membered ring favoring ground state hydrogen bond (HB) formation[16] coupled with the known acid lability of *tert*-butyl esters.[17] The *tert*-butyl ester-like moiety was constructed by acylation of a tertiary alcohol on the side chain. This design also incorporates geminal methyl groups that enforce a favorable conformation for hydrogen bonding through angle compression in the side chain (Thorpe-Ingold effect).[18] The aryl ether of **1a,b** was incorporated for both synthetic utility and the heteroatom effect[16] expected to promote the 10-membered HB ring.

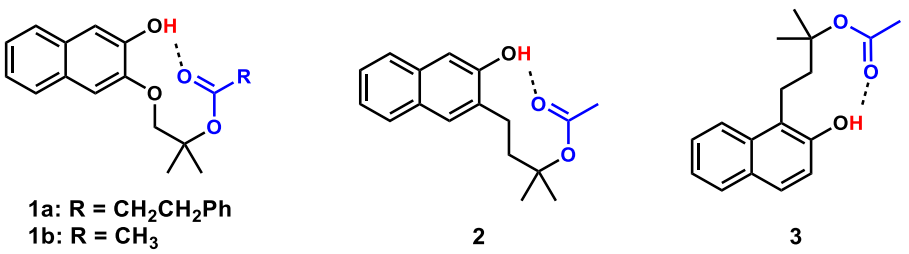

Figure 5.5 First generation photocage designs involving *tert*-butyl esters

5.3 Results and Discussion

Despite the facile synthesis of **1a,b** (**Scheme 5.6**), the aryl ether is problematic. Compound **1a** predominantly underwent photo-induced oxidation on irradiation in both degassed and air-saturated acetonitrile, water/methanol, water/acetonitrile, and methanol (**Scheme 5.7a**). This reaction is known for 1-naphthol, with relatively low quantum yields for the neutral compound (Φ_{max} = 0.02-0.03), and naphtholate anion (Φ_{max} = 0.09 – 0.12).[19] The naphthoxyl radical, superoxide radical anion (formed from solvated electrons), and singlet oxygen are all thought to be plausible reactants leading to the formation of intermediates such as **8**, to give the naphthoquinone **9** and water.[19,20] The structure of **9** is corroborated by irradiation of 3-methoxy-2-naphthol under identical conditions to give 3-methoxy-1,2-naphthoquinone (**10**), which was identified by comparison to its published NMR spectra (**Scheme 5.7b**).[21]

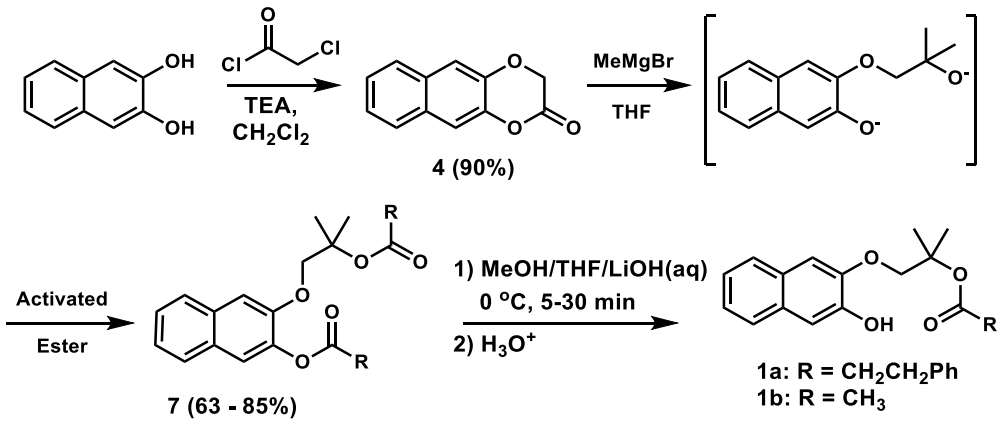

Scheme 5.6 Synthesis of **1a, 1b**

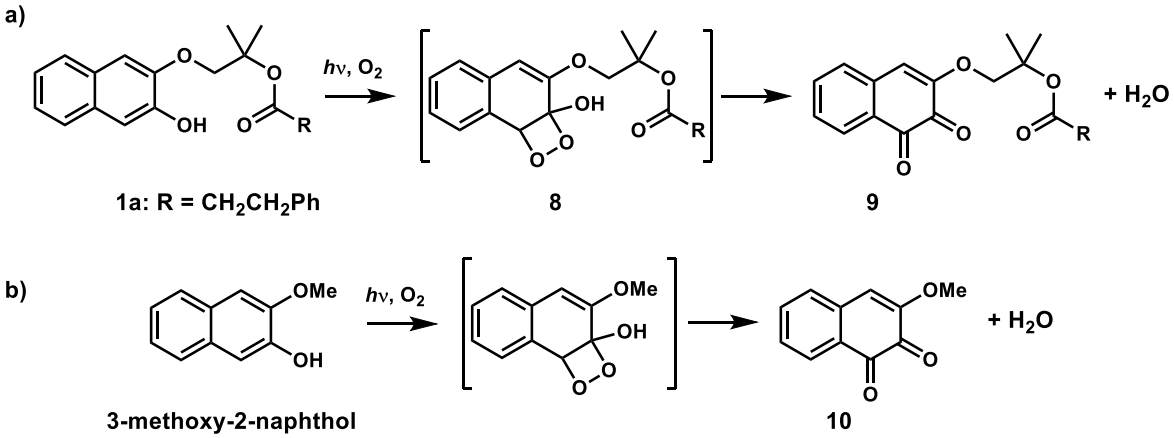

Scheme 5.7 Photo-initiated oxidation of **1a** and 3-methoxy-2-naphthol to the respective 1,2-naphthoquinones **9** and **10**.

Deprotection of the ester **1a** was observed only in low yields with quartz-filtered UV-irradiation. The weak acid lability of the substituted *tert*-butyl esters **1a**,**b** was a possible cause for the low yield of the decaged product, since the aryl ether oxygen could potentially destabilize positive charge built up in the transition state of the cleavage reaction. The ease of ground-state acid-catalyzed deprotection of **1a** and **1b** was therefore investigated. The standard trifluoracetic acid in dichloromethane (TFA/CH_2Cl_2) deprotection protocol for *tert*-butyl esters[17] was ineffectual (**Scheme 5.8a**). The commercially available alkyl-substituted *tert*-butyl acetate **11** quantitatively reacted under the same conditions to give the tertiary alcohol **12** (**Scheme 5.8b**). The relevant structural differences between **1a,b** and **11** are the aryl ether and phenolic hydroxyl group. The phenolic hydroxyl group is expected to accelerate the reaction through intramolecular trapping of the carbocation formed from cleavage of the ester O-$C(Me)_2R$ bond. This notion is supported by the addition of phenols as cation scavengers in TFA/CH_2Cl_2 deprotections.[17] Multiple products from **1a** are observed to form slowly in 50% $TFA/CDCl_3$ (or CH_2Cl_2), and conversion is complete in three days. In contrast, deprotection of **11** in TFA / $CDCl_3$ in the presence of 2-naphthol rapidly gave the acyclic naphthyl ether **13** from the analogous intermolecular reaction (**Scheme 5.9**). This result confirms the expectation that the phenolic group of **1a,b** was not the cause for the acid stability of **1a,b**. The aryl ether was

therefore proposed to be the cause of low-reactivity for **1a,b**, though it is not clear whether an inductive destabilization of the forming carbocation, non-productive protonation of the aryl ether, or both are the cause of stability to TFA/CH_2Cl_2.

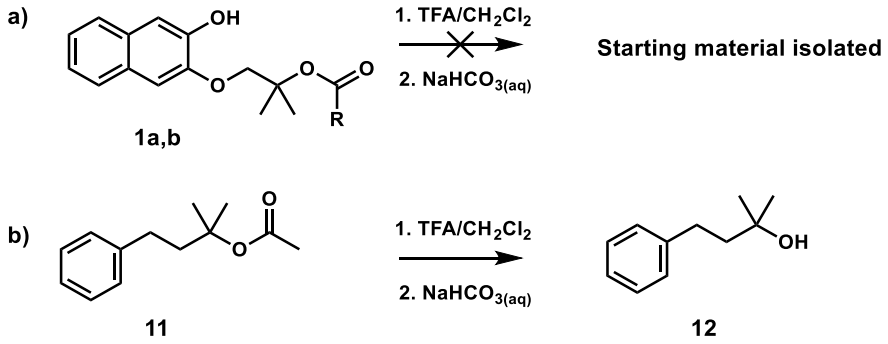

Scheme 5.8 Comparison of ground-state acid deprotection of **1a**,**b** and **12** after 3.5 hours

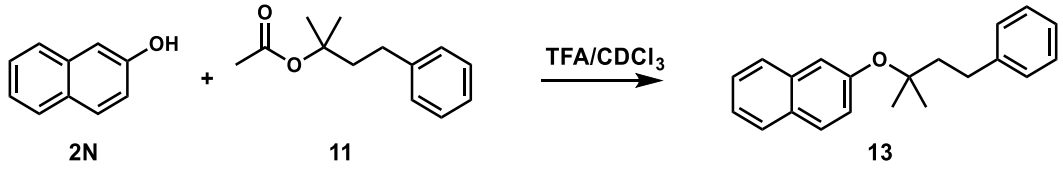

Scheme 5.9 Deprotection of **11** in the presence of 2-naphthol (2N) to give the naphthyl ether

In order to make the direct comparison of reactivity, compound **2** was synthesized as the ether-less analogue of **1a,b**. The synthesis of **2** is shown in **Scheme 5.10**, and begins with adapted procedures.[22-23] Overall, the synthesis is straightforward and relatively high-yielding until the last step, where Pd-C catalyzed hydrogenation proved troublesome for benzyl ether **20**.

In contrast to the aryl ethers **1a** and **1b**, 50% TFA/CH_2Cl_2 deprotection of **2** was complete within minutes to give the cyclic ether **21** and acetic acid as the only products (**Scheme 5.11**). The facile deprotection of **2**, and relative stability of **1b** towards standard[17] TFA/CH_2Cl_2 conditions is convincing evidence that the aryl ether of **1a,b** should be removed from future designs. Unfortunately, the improved acid-lability of **2** over **1a,b** did not lead to photoacid-mediated deprotection; no reactivity (oxidation or cleavage) was observed on irradiation of **2** in degassed aqueous methanol mixtures. The investigation of other structural details that might lead to photochemical reactivity, such as linker length and ring substituents, is necessary.

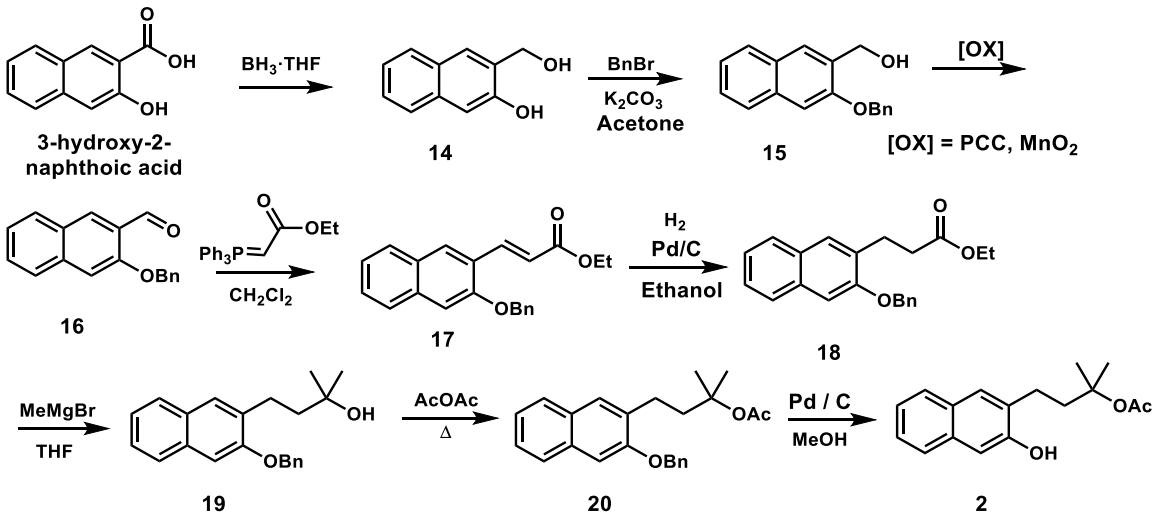

Scheme 5.10 Synthesis of compound **2**

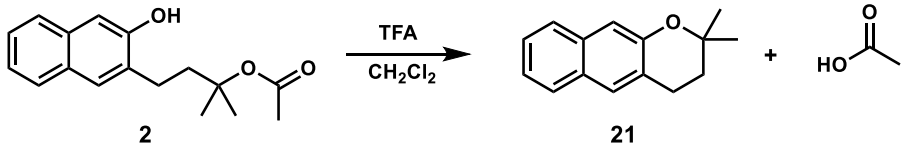

Scheme 5.11 TFA/CH_2Cl_2 deprotection of **2** giving cyclic ether **21** and acetic acid

The synthesis of **2** is more elaborate than for **1a,b** or **3**, partly because electrophilic substitution reactions occur at the 1-position, rather than the 3-position of the 2-naphthol. Various 1-substituted 2-napthols such as **3** are accessible through treatment of 2-naphthol with the appropriate electrophile under acidic and basic conditions (**Scheme 5.12**).[23-24] Substitution at the 3-position of 2-naphthol derivatives requires *ortho*-lithiation[25], purchase of 3-hydroxy-2-naphthoic acid derivatives, or a more involved synthesis.

Compound **2** was necessary for direct comparison of its acid lability to **1a,b**. The original choice for 2,3-substitution, however, was based on 2,3-dihydroxy-naphthalene, and not an integral part of the design. 2,3-Substitution was therefore abandoned in favor of the synthetically accessible 1,2-substitution. This modification has the added benefit of a steric clash between

the distal ring of 2-naphthol and the side-chain on C_1, potentially favoring a conformation that can form a 10-membered ring through an intramolecular hydrogen bond.

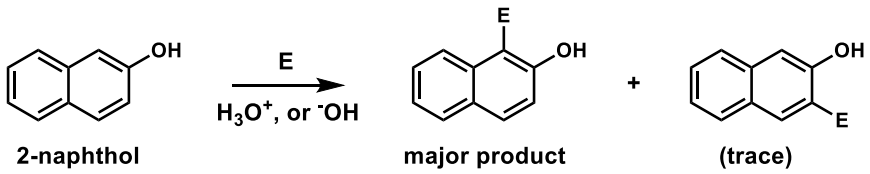

Scheme 5.12. Electrophilic substitution reactions of 2-naphthol: preference for reaction at C_1

Synthesis and Reactivity of a 1-(cage)-2-naphthol Derivative

Compound **3,** the 1,2-substituted analogue of **2**, was prepared in just four high-yielding steps from 2-naphthol (**Scheme 5.13**). The synthesis of **3** begins with the known[22-23] preparation of the dihydro-naphthocourmarin **22**, and avoids the troublesome deprotection step found for benzyl ether **20**. The synthesis of **3** is generally applicable to other side chains, and provides access to leaving groups other than acetate directly from diol **23**.

TFA/CH_2Cl_2 deprotection of **3** is quantitative, and rapidly gives the cyclic ether **25** (**Scheme 5.14**). ^{1}H NMR kinetic data measured in 16% TFA : 84% $CDCl_3$ for **3** follows pseudo-first-order kinetics with $t_{1/2}$ < 5 minutes. Ester **3**, however, failed to cleave photochemically upon glass-filtered irradiation in degassed aqueous methanol or acetonitrile, though no oxidation of the 1,2-naphthoquinone was observed.

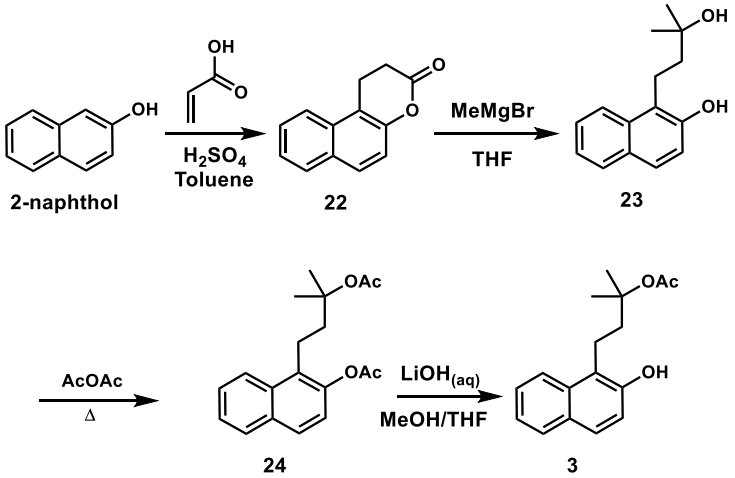

Scheme 5.13 Synthesis of compound **3**

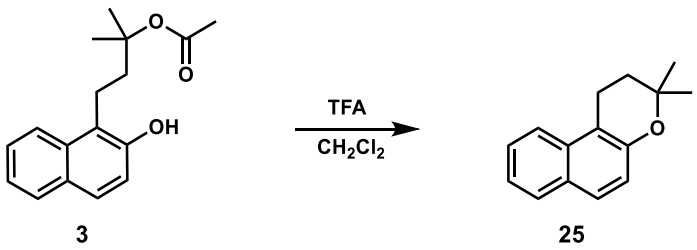

Scheme 5.14 Ground-state deprotection of tert-butyl ester **3**

Synthesis and Reactivity of a Caged Tetrahydropyranyl Ethers

The initial design involving release of an ester appears to be inefficient. Since the *tert*-butyl acetates **2** and **3** readily cleaved under the harsh TFA/CH_2Cl_2 conditions (pK_a = 0.5 for TFA), but not on irradiation (pK_a^* = 2.8 for 2-naphthol), a more labile protecting group was sought. Acetals are more acid-labile than *tert*-butyl esters[17], and the tetrahydropyranyl (THP) ether **28** was synthesized from diol **23** (**Scheme 5.15**) as a potentially more reactive derivative of **3**.

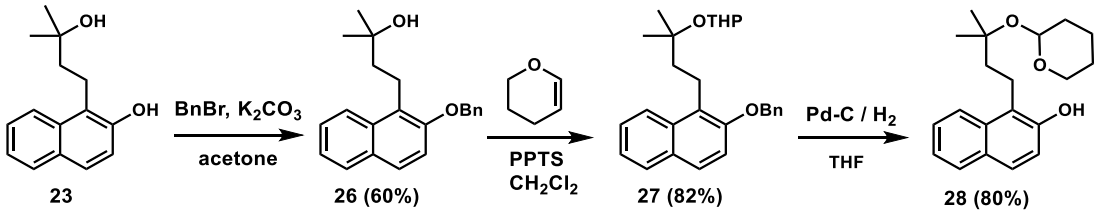

Scheme 5.15. Synthesis of THP ether **28**

Irradiation of **28** at 280-360 nm for one hour in acetonitrile gave the diol **23** and dihydropyran (DHP) as determined by comparison to ^{1}H NMR spectra of authentic samples (**Scheme 5.16**). Deprotection is quantitative and clean, with diol **24** as the only aromatic product observed by LCMS and ^{1}H NMR. At least one unidentified aliphatic product from the leaving

group, THP, is also formed. The THP ether **28** did not cleave on heating at 50º C in the dark for 24 hours in acetonitrile-d_3, indicating that the reaction is photochemically induced. After initial irradiation to give 50% conversion, however, the reaction continued to completion in the dark. The dark reaction gave the same products, indicative of photo-induced latent acid formation as the cause for reactivity.

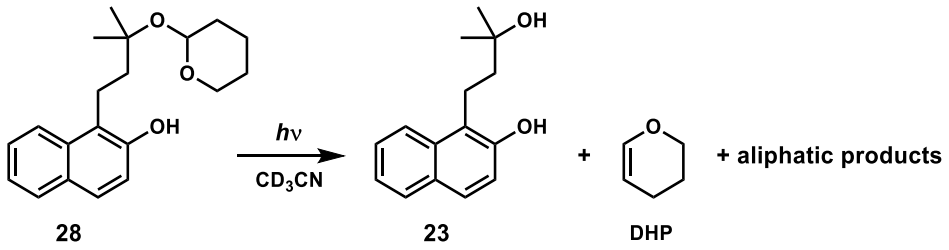

Scheme 5.16. Photo-induced deprotection of **28**

Characterization of Intramolecular Hydrogen Bonding

Intramolecular hydrogen bonding is observable in solution at room temperature by ^{1}H NMR for **28**, unlike the *tert*-butyl esters **1-3**. 2D Nuclear Overhauser Effect Spectroscopy (2D NOESY) correlations consistent with the structure shown in **Scheme 5.17** are found in chloroform-d, carbon tetrachloride, acetonitrile-d_3, and benzene-d_6 solutions. The relevant 2D NOESY spectra regions for **28** in benzene-d_6 and acetonitrile-d_3 showing the phenolic proton (H_1) correlations to protons H_2 and H_3 of C_6 in the THP ring are shown. The phenolic proton has a larger NOE associated with proton H_4 than proton H_5, and the converse is true for the aromatic proton H_8, indicative of a rigid conformation with limited rotation about the Ar-C bond of the linker. Protons H_6 and H_7 overlap in the ^{1}H NMR region of the other THP ring protons, complicating further analysis.

Certainly, the THP ether **28** has more hydrogens in various orientations and distances from the hydroxyl proton of 2-naphthol than esters **1-3**, and this could be a major factor in detecting correlations for **28** and not **1-3**. Evidence for intramolecular hydrogen bonding in esters **1-3** would more likely come from infrared (IR) spectroscopy of dilute CCl_4 solutions, where a shift in ν(CO) from that of a free ester would be indicative of the hydrogen bond.

Intermolecular (or intramolecular) hydrogen bonding in the solid state is evident for **3**, which has a shifted carbonyl absorption of ν(CO) = 1690 cm^{-1}. This is a significant shift from substituted *tert*-butyl acetate **11**, which absorbs at ν(CO) = 1730 cm^{-1} in the solid state and is incapable of hydrogen bonding. Attempts to obtain a CCl_4 solution IR spectrum for **3**, however, were limited by its low solubility. A longer path length solution IR cell will be used to obtain this data in future studies.

The observed hydrogen bond is formed to the wrong THP ether oxygen for efficient cleavage. In general, protonation of the endocyclic THP ether oxygen results in cleavage that is reversible via an intramolecular reaction, making hydrolysis less efficient. Protonation of the exocyclic THP ether oxygen, however, leads to cleavage that is reversible via a bimolecular process, which results in an entropically favorable forward reaction (**Scheme 5.17**).[26] The 6-31G** optimized structure with a 10-membered hydrogen bond is only ca. 1 kcal/mol lower in energy than the next best structure, which has an 8-membered hydrogen bond to the exocyclic oxygen of the THP ether. In solution, we expect both conformations to be sampled, with the most stable conformer dominating the spectra.

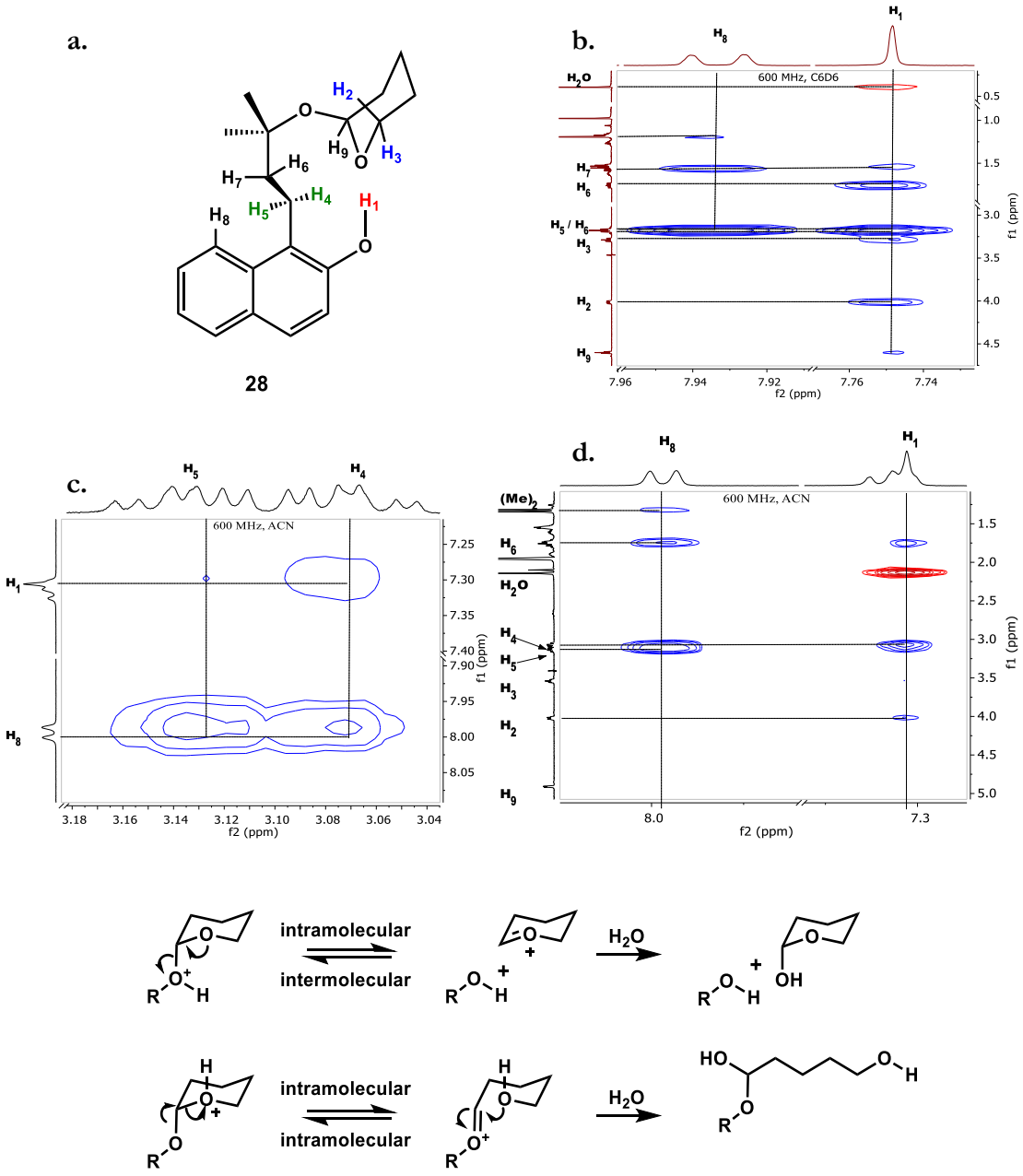

Scheme 5.17. Comparison of the site of protonation for THP ethers and Proposed conformation of 28 (a), NOESY correlations for **28** in C_6D_6 (b), and ACN-d_3 (c,d) at room temperature, 600 MHz.

Geometry optimization calculations at the 6-31G** level suggest that shortening the side-chain by one carbon to give the putative compound **29** would promote hydrogen bonding to the exocyclic THP ether oxygen (**Figure 5.6**). Given these calculations and the observed hydrogen bonding in **28**, it is reasonable to expect the decaging process to occur an order of

magnitude faster for **29**.[26] The synthesis of **29** is underway to investigate both the preferred intramolecular hydrogen bond and reactivity.

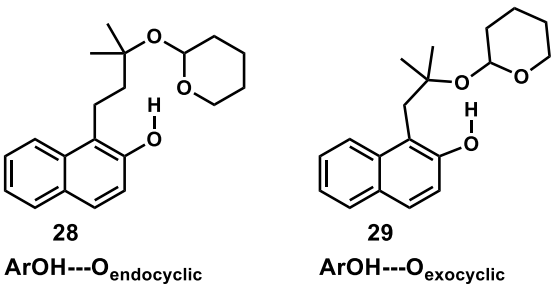

Figure 5.6 Comparison of intramolecular hydrogen bonding in **28** and **29**

Synthesis and Photochemical Reactivity of a Phenolic Caged THP Ether

The phenolic THP ether **30** was synthesized from 2,3-dihydroxynaphthalene by reaction with dihydropyran (DHP) and PPTS in dichloromethane. Irradiation at 280-360 nm in degassed acetonitrile, and acetonitrile/water mixtures gives 2,3-dihydroxynaphthalene. ^{1}H NMR spectra identify DHP and at least one unidentified aliphatic product as the fate of the leaving group (**Scheme 5.18**).

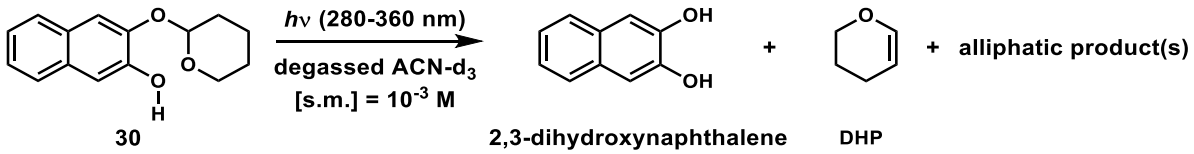

Scheme 5.18 Deprotection of THP ether **30** in degassed acetonitrile-d_3

The observed reactivity of **30** may be the result of an excited-state proton transfer to the exocyclic THP ether. ESPT resulting in heterolytic cleavage of the ArO-C bond followed by deprotonation of the generated carbocation to form DHP is plausible, and trapping of the

carbocation by water or other nucleophiles gives an avenue for the as yet unidentified aliphatic products. The suggested ESPT mechanism is depicted in **Scheme 5.7** below.

A radical mechanism is also likely for this reaction. The ArO-R bond is expected to be a weak bond, with a bond dissociation energy comparable to and likely lower in energy than *o*-hydroxy anisole (56 kcal/mol).[27] Homolytic cleavage of the ArO-R bond as in **scheme 5.8**, followed by hydrogen atom abstraction from the THP radical gives the products observed. Radical couplings or other hydrogen atom abstractions may account for the products not yet identified. The radical mechanism is supported by reports of homolysis of aryl ethers to give the photo-Fries rearrangement products.[28,29] The independently synthesized photo-Fries product **31**, however, was not detected in the product mixture by ^{1}H NMR. Alternatively, homolytic ArO-C bond cleavage followed by electron transfer generates the initial ion pair of the ESPT mechanism, potentially making the two mechanisms indistinguishable.

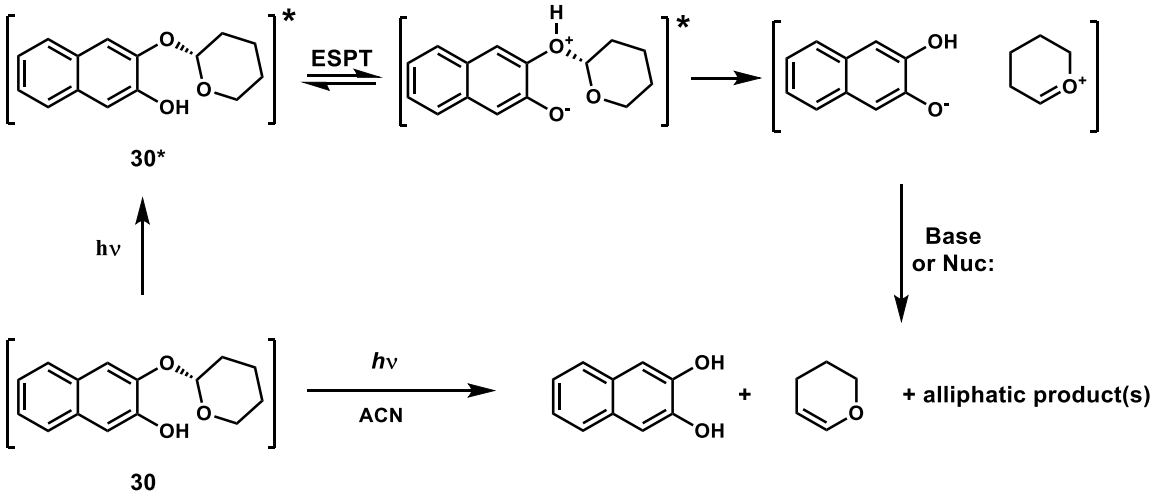

Figure 5.7. Suggested excited-state proton transfer mechanism for deprotection of **30**

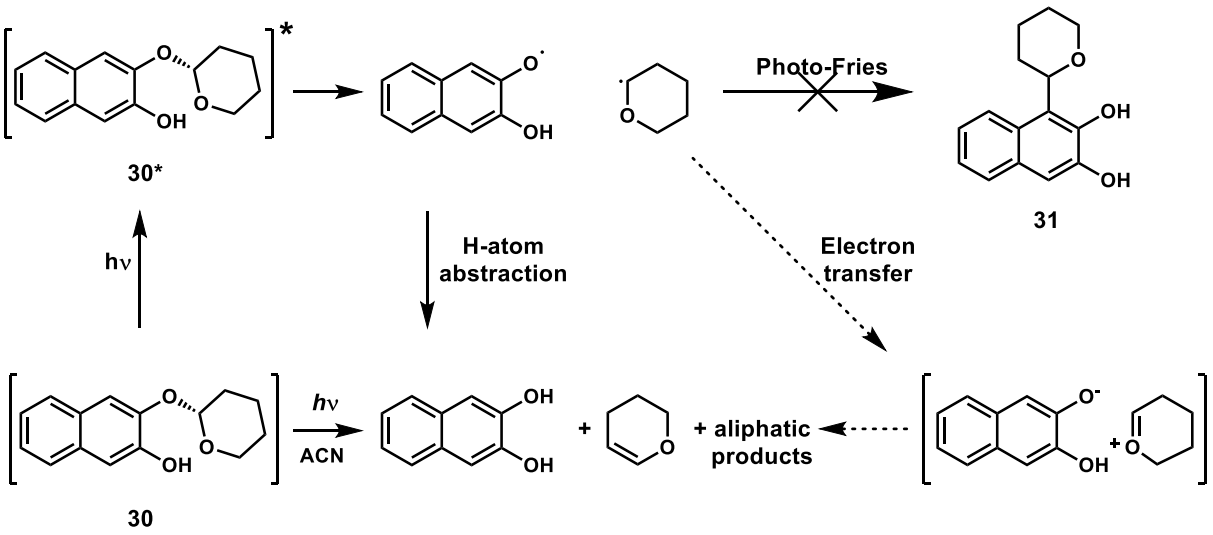

Figure 5.8. Suggested radical mechanism for deprotection of **30**

5.4 Conclusions and Future Work

The aryl ether of compound **1a,b** was identified as the cause for its low reactivity towards TFA/CH_2Cl_2 deprotection by comparison to the ether-less analogue **2** and related compound **11**. Furthermore, **1a** was observed to undergo oxidation to the 1,2-naphthoquinone derivative **9**, a reaction with a low quantum yield that is presumably facilitated by the electron-donating aryl-ether substituent. Similar aryl-ethers are therefore a design feature that should be avoided for the acid cleavage of esters. The alkyl-substituted *tert*-butyl esters **2** and **3** were stable to photolysis trials, but were acid labile. For synthetic accessibility, 1-substituted 2-naphthols such as **3** are desired over their 3-substituted counterparts such as **2**.

Photo-initiated deprotection of THP ether **28** was achieved in acetonitrile, although a dark reaction indicative of latent acid formation was also observed. Deprotection of the phenolic THP ether **30** on irradiation in acetonitrile and aqueous acetonitrile was also achieved, but a radical mechanism is also possible. These two reactions are encouraging candidates for ESPT, and will be investigated further after identification of the unknown aliphatic products.

An intramolecular hydrogen bond between the endocyclic THP oxygen and the photoacidic hydrogen of **28** was observed by 2D NOESY spectra in solution at room

temperature for various solvents. Calculations suggest that modification of the sidechain to give compound **29** may accelerate any ESPT-mediated reaction. Synthesis of **29** is underway, and its putative intramolecular hydrogen bond will be characterized, along with its photolysis products.

IR spectra of dilute CCl_4 solutions of **1-3** are needed to characterize hydrogen bonding in solution. Shifted ν(CO) adsorptions for esters **1-3** indicative of hydrogen bonding, however, were observed in the solid state. Irradiation of a thin layer of solid **3**, where an intra- or intermolecular hydrogen bond is clearly formed, might facilitate an ESPT reaction.

Future Direction of Project

Progress towards a photoacid-mediated reaction has so far involved improvement of the linker and choice of leaving group. It would also be prudent to modify the photoacid moiety to increase reactivity. A challenge we were aware of at the onset of this project that might render those modifications ineffectual, however, is the transiency of photoacids. Although 2-naphthol is thermodynamically acidic enough in the S_1 state to potentially effect an acid-catalyzed reaction ($pK_a^*(S_1)$ = 2.8 for 2N), the S_1 state is short-lived and only moderately acidic compared to conventional ground-state acids used for hydrolysis. We initially thought that since ESPT is exceedingly fast, preformation of an intramolecular hydrogen bond would allow acid-catalyzed reactions to compete with deactivation rates.[1-3] This does not seem to be the case for the caged esters, which are a more general leaving group than THP ethers that did cleave.

The next generation of photoacid cages will therefore involve features that increase the lifetime and excited state acidity of the photoacid. Incorporating a leaving group for which proton transfer is part of the rate-determining step would presumably help mediate the transiency of the excited state acid as well. The protection of orthoesters and other compounds where proton transfer is involved in the rate-limiting step for hydrolysis will be investigated.[26]

The cyanonaphthols are known 2-naphthol derivatives that increase the acidity of the excited state ($pKa^* \leq 0$). Although a known compound and a promising photoacid, the pK_a^* of 3-cyano-2-naphthol has not been determined to our knowledge. Due to ease of synthesis, 3-cyano-2-naphthol will be prepared and its pK_a^* will be estimated by Förster analysis. If shown

to be a strong photoacid, 3-cyano-2-naphthol appears to be a facile modification to the current photocage design, compared to 5- or 8-cyano-2-naphthol.[3,10]

Long-lived 1-(2-nitroethyl)-2-naphthol derivatives[30] are other apparent options for future designs. In these cases, the pK_a* of 2-naphthol should be sufficient as the conjugate base of 1-(2-nitroethyl)-2-naphthol becomes the carbanion on the 2-nitroethyl group after initial ESPT. Since photolysis of 1-(2-nitroethyl)-2-naphthol is known to generate a bulk pH change of 1-2 pK_a units, this is a promising design.[30] A series of leaving groups with a broad range of relative hydrolysis rates would be informative as to the effective acid concentration on irradiation.

5.5 Experimental

General. All reagents were purchased from Aldrich, Fisher, or TCI. Unless otherwise stated, all reactions were conducted under argon in oven-dried glassware (when anhydrous solvents are used). Photochemical reactions were carried out on an optical bench with a high pressure Hg-Xe arc lamp, with the wavelength of irradiation selected by glass filters. All NMR spectra were recorded on Varian spectrometers (MHz as noted). Varian's data reduction software was used for determination of concentrations by NMR integrals with the experimental conditions of 1 scan, a set gain level, and long acquisition time (example: nt=1, gain=20, at=15), to ensure accurate integrals (pre-equilibrium).

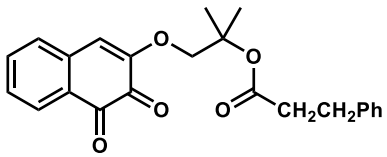

Photochemical oxidation of 1a to 9: A 200 mL quartz round bottom flask containing 0.08 mM solution of **1a** in 1:1 MeOH/H_2O (75 mL) was irradiated at $\lambda > 320$ nm for 19 h. The solvent was evaporated, and **9** was separated from the crude mixture by HPLC. The discernable NMR data is given for DMSO-d_6 and $CDCl_3$, due to overlapping solvent signals. In small trials under the same conditions, **9** was the only product by LCMS. ^{1}H NMR (300 MHz, DMSO-d_6) δ 7.81 (d, J = 7.6 Hz, 1H), 7.62 (t, J = 7.4 Hz, 1H), 7.40 (d, J = 7.7 Hz, 1H), 7.34 (t, J = 7.6 Hz, 1H), 7.29 – 7.12 (m, 6H), 6.84 (s, 1H), 4.07 (s, 2H), 1.46 (s, 6H). ^{1}H NMR (300 MHz,

Chloroform-*d*) δ 7.99 (d, *J* = 7.9 Hz, 1H), 7.58 – 7.49 (m, 1H), 6.41 (s, 1H), 4.10 (s, 2H), 2.91 (t, *J* = 7.7 Hz, 1H), 2.60 (t, *J* = 7.8 Hz, 1H).

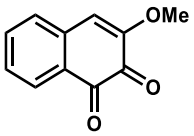

Photochemical oxidation of 3-methoxy-2-naphthol to 10. A 200 mL quartz round bottom flask containing 0.46 mM methanolic solution (100 mL) of 3-methoxy-2-naphthol was irradiated at 275-375 nm for 15 h. The solvent was evaporated, and **10** was separated from the crude mixture by HPLC. In small trials under the same conditions, **10** was the only product by LCMS. ^{1}H NMR (600 MHz, DMSO-d_6) δ 7.80 (d, *J* = 7.6 Hz, 1H), 7.61 (t, *J* = 7.5 Hz, 1H), 7.40 (d, *J* = 7.6 Hz, 1H), 7.32 (t, *J* = 7.5 Hz, 1H), 6.77 (s, 1H), 3.74 (s, 3H).

Protocol for TFA deprotection: The acid labile compound is dissolved in the deuterated solvent (CD_2Cl_2 or $CDCl_3$), and 16-50% by volume of TFA is layered on top of the solution. The layers are then rapidly mixed by shaking at t=0 min, and the reaction progress is monitored by ^{1}H NMR. The whole process is conducted quickly such that it is assumed only a small amount of reaction occurs at the interface before shaking. On the preparatory scale, a round bottom flask is used and the reaction is monitored by LCMS.

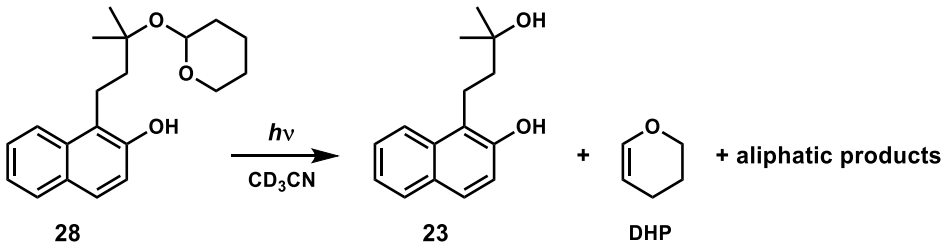

Photolysis of 28. THP protected 2-naphthol **28** was dissolved in CD_3CN to give an approximately 10^{-3} – 10^{-4} mM solution in a quartz J. Young tube. The solution underwent three freeze/pump/thaw cycles before backfilling with Ar. Concentration was then determined by ^{1}H NMR to be 1.6 mM. Irradiation at 280-360 nm for 40 min gave 50% conversion of starting material, after which the NMR tube was kept in the dark while the reaction completed.

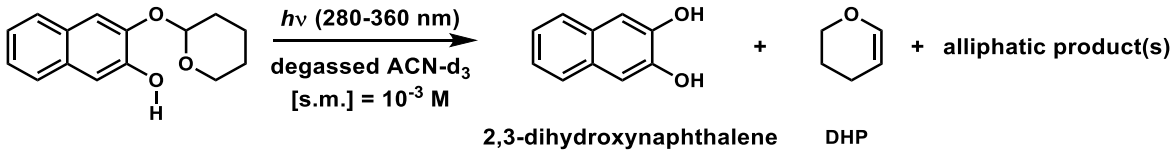

Photolysis of 3-((tetrahydro-2H-pyran-2-yl)oxy)naphthalen-2-ol (30). THP protected catechol **30** was dissolved in CD_3CN to give an approximately $10^{-3} – 10^{-4}$ mM solution in a quartz J. Young tube. The solution underwent three freeze/pump/thaw cycles before backfilling with Ar. Concentration was then determined by ^{1}H NMR to be 2 mM. Irradiation at 280-360 nm for 10 min gave 25-50% conversion of starting material, after which the NMR tube was kept in the dark where the reaction completed.

Synthesis of 1-3. The synthesis of compounds **1a** and **1b** was adapted from the notebook of Clinton Regan, who first prepared compound **1a** in the Dougherty lab. Unless otherwise stated, all procedures were conducted under an atmosphere of argon. Due to the simplicity of the intermediates, characterization was achieved with ^{1}H NMR and LCMS, where necessary, ambiguous 1D assignments were resolved by 2D NMR spectra. NMR spectra were recorded on Varian spectrometers (MHz as indicated).

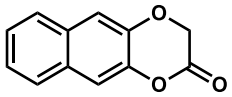

Lactone 4. To a 250 mL round bottom flask equipped with a reflux condenser is added 2,3-dihydroxynaphthalene (10.0 g, 62.4 mmol). The solid is dissolved in dry dichloromethane (62 mL) to form a 0.1 M solution, and cooled to 0 ºC. Trimethyl amine (19 mL, 136 mmol) is added, followed by dropwise addition of chloroacetyl chloride (5.6 mL, 70 mmol). The solution was allowed to warm to room temperature before refluxing for 2 h under argon. Volatiles were removed *in vacuo* to give 90% yield of lactone **4**, which was useable without further purification. Recrystalization from boiling ether proved effective where further purification was desired. ^{1}H NMR: (^{1}H NMR (500 MHz, Chloroform-*d*) δ 7.84 – 7.68 (m, 2H), 7.54 (d, *J* = 0.7 Hz, 1H), 7.51 – 7.37 (m, 3H), 7.26 (s, 1H), 4.77 (s, 2H).

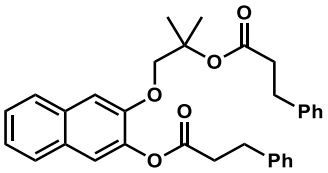

Diester 7a. A solution of lactone **4** (1.33 g, 6.6 mmol) in THF (66 mL) was cooled to 0 ºC before dropwise addition of MeMgBr (4.85 mL, 14.5 mmol). The reaction was monitored by TLC until complete conversion to the alkoxide, whereupon excess hydrocinnamoyl chloride was added (3.8 mL, 25 mmol). After stirring overnight, the reaction was quenched with $NaHCO_{3(aq)}$, and extracted with EtOAc. Flash chromatography (85% Hexanes/EtOAc) afforded diester **7a** (2.06 g, 63 % yield). ^{1}H NMR (500 MHz, Chloroform-*d*) δ 7.75 – 7.67 (m, 2H), 7.46 – 7.40 (m, 2H), 7.39 – 7.33 (m, 1H), 7.34 – 7.29 (m, 1H), 7.25 – 7.21 (m, 2H), 7.19 (s, 1H), 7.15 (m, 2H), 4.23 (s, 2H), 3.10 (dd, *J* = 9.1, 6.9 Hz, 2H), 2.98 – 2.84 (m, 4H), 2.57 (dd, *J* = 8.6, 7.2 Hz, 2H), 1.54 (s, 6H).

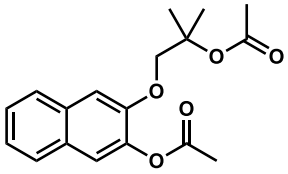

Diester 7b. To a stirred THF solution of lactone **4** (0.7550 g, 3.8 mmol) under argon, was added MeMgBr (3.4 mL, 0.10 mmol). TLC of worked-up aliquots showed complete conversion after 2 h, whereupon acetic anhydride (3 mL, 32 mmol) was added. The solution was stirred overnight. DI water was added, and the pH was adjusted to 7 with $NaHCO_{3(aq)}$ before extraction with ethyl acetate (3x50mL). The combined organic layers were washed with brine, dried over $MgSO_{4(s)}$, filtered, and evaporated to an oil. Flash chromatography (15% hexanes/EtOAc) afforded the diester **7b** as white solid (0.477 g, 40% yield). Alternatively, diester **7b** is prepared by aqueous workup of the Grignard reaction, followed by heating in neat acetic anhydride to give 100% yield. ^{1}H NMR (500 MHz, Chloroform-*d*) δ 7.75 – 7.64 (m, 2H), 7.47 (s, 1H), 7.40 (dd, *J* = 8.2, 6.7 Hz, 1H), 7.33 (t, *J* = 7.4 Hz, 1H), 7.18 (s, 1H), 4.24 (s, 2H), 2.34 (d, *J* = 1.2 Hz, 3H), 2.01 (d, *J* = 1.2 Hz, 3H), 1.57 (d, *J* = 1.3 Hz, 6H).

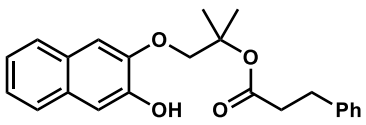

Ester 1a. A 100 mL rbf was charged with diester **7a** (0.218 g, 0.44 mmol) and 3 mL THF/MeOH (1:1), followed by dropwise addition of $LiOH_{(aq)}$ (1.5 mL, 1 M). The solution was maintained at 0 ºC during the reaction, which was essential for selectivity. After stirring for 30 min, the LiOH was neutralized with citric acid (1 M solution), and the solution was diluted with brine and extracted with ethyl acetate. The combined organic layers were washed with brine before drying over $MgSO_{4(s)}$. The concentrated filtrate was recrystallized to give **1a** (0.160 g, 75% yield). Product was identified by NMR and LCMS.

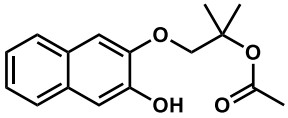

Ester 1b. Saponification of diester **7b** (0.209 g, 0.66 mmol) was carried out in 4.3 mL THF/MeOH (1:1) solution by addition of 2.15 mL $LiOH_{(aq)}$ at -10 ºC. The reaction was complete in less than 10 min. The reaction was quenched with citric acid, extracted with ethyl acetate, and purified via flash chromatography (70% Hexanes/EtOAc) to give ester **1b** (0.135 g, 78% yield). Product was identified by NMR and LCMS.

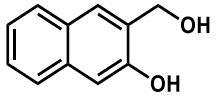

3-(hydroxymethyl)naphthalen-2-ol (14). To an oven-dried flask under argon was added 3-hydroxy-2-naphthoic acid (4.436 g, 23.6 mmol). The vessel was cooled to 0 ºC before the dropwise addition of $BH_3 \cdot THF$ (40 mL, 1 M solution, 40 mmol). After gas evolution had ceased, the mixture was allowed to stir at room temperature for 17.5 h before quenching with water to hydrolyze the boron adduct. The pH was adjusted to 8 with bicarbonate, and the solution was diluted with brine, then extracted with ethyl acetate to give (4.31 g, 100 % crude yield of acceptable purity). Recrystallization from boiling methanol removed the minor borate impurity, but resulted in low recovered yields. ^{1}H NMR (300 MHz, DMSO-d_6) δ 9.82 (s, 1H), 7.89 – 7.70 (m, 2H), 7.64 (d, J = 8.1 Hz, 1H), 7.41 – 7.28 (m, 1H), 7.28 – 7.17 (m, 1H), 7.09 (s, 1H), 4.63 (s, 2H), 3.37 (s, 1H).

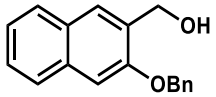

(3-(benzyloxy)naphthalen-2-yl)methanol (15). Diol **14** (0.2850 g, 1.6 mmol) was dissolved in distilled acetone (25 mL). Potassium carbonate (0.4557 g, 3.3 mmol), and benzyl bromide (0.195 mL, 1.6 mmol) were added, and the solution was brought to reflux for 4 h. The solution was cooled and diluted with water before extraction with ethyl acetate at pH 9-10. Flash chromatography afforded compound **15** in > 90% yield. ^{1}H NMR (300 MHz, DMSO-d_6) δ 7.89 (s, 1H), 7.84 (dd, J = 8.2, 1.2 Hz, 1H), 7.80 – 7.74 (m, 1H), 7.58 – 7.48 (m, 2H), 7.48 – 7.27 (m, 6H), 5.33 – 5.16 (m, 3H), 3.34 (d, J = 0.4 Hz, 2H).

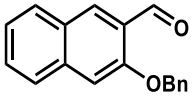

3-(Benzyloxy)-2-naphthaldehyde (16). A dry methylene chloride (0.9 mL) solution of **15** (0.020 g, 0.08 mmol) was stirred with MnO_2 (0.0649 g, 0.75 mmol) overnight. The solution was filtered through celite to remove MnO_2, and evaporated to give aldehyde **16** (0.020g, 95% yield). The product was characterized by ^{1}H NMR and LCMS.

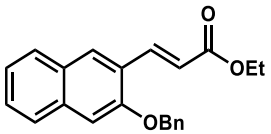

Ethyl (E)-3-(3-(benzyloxy)naphthalen-2-yl)acrylate (17). Aldehyde **16** (0.102 g, 0.4 mmol) and (Carbethoxymethylene)triphenylphosphorane (0.151 g, 0.43 mmol) were dissolved in a minimal amount of CH_2Cl_2 and immediately concentrated on the rotovap at 50 ºC to yield a film. Although the reaction is reported to be complete at this point, this process was repeated two more times. Flash chromatography (87.5 % Hexanes/EtOAc) gave **17** as a mixture of E/Z isomers (0.119 g, 93% yield).

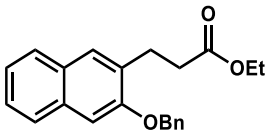

Ethyl 3-(3-(benzyloxy)naphthalen-2-yl)propanoate (18). In a round bottom flask equipped with a large stirbar is added **17** (0.147 g, 0.44 mmol) and 10% Pd on carbon (0.016 g). Ethanol (50 mL) was added, and the vessel was purged / backfilled with H_2 three times, then stirred under H_2 for 4 h. The catalyst was removed by filtration, and the concentrated filtrate was flashed (12.5 % EtOAc/Hexanes) to give **18** (0.127 g, 86% yield). ^{1}H NMR (300 MHz,

Chloroform-*d*) δ 7.71 (m, 7.4, Hz, 2H), 7.64 (s, 1H), 7.55 – 7.47 (m, 2H), 7.47 – 7.29 (m, 6H), 7.18 (s, 1H), 5.22 (s, 2H), 4.12 (q, *J* = 7.1 Hz, 2H), 3.18 (t, *J* = 8 Hz, 2H), 2.74 (t, *J* = 8, 7.1 Hz, 2H), 1.22 (t, *J* = 7.1 Hz, 3H).

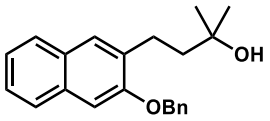

4-(3-(Benzyloxy)naphthalen-2-yl)-2-methylbutan-2-ol (19). To a dry THF (6 mL) solution of **18** (0.127 g, 0.38mmol), was added MeMgBr (0.4 mL, 3 M Et_2O solution, 1.2 mmol). The resulting solution was heated at 50 ºC for 9.5 h, cooled to room temperature, and quenched with dilute $HCl_{(aq)}$. The aqueous solution was extracted with ethyl acetate to give **19** (75% yield by NMR) and starting material (25% by ^{1}H NMR).

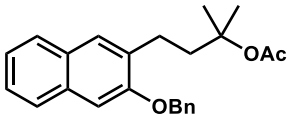

4-(3-(Benzyloxy)naphthalen-2-yl)-2-methylbutan-2-yl acetate (20). Alcohol **19** (0.045 g, 0.14 mmol) was dissolved in acetic anhydride, and the resulting solution was sparging with argon before heating at 95 ºC for 24 h. Acetic anhydride was removed *in vacuo*, and the concentrated mixture was purified by flash chromatography (12.5 % EtOAc/Hexanes) to afford **20** (0.040 g, 78% yield). ^{1}H NMR (300 MHz, Chloroform-*d*) δ 7.78 – 7.64 (m, 2H), 7.61 (s, 1H), 7.51 (m, 2H), 7.37 (m, 5 H), 7.18 (s, 1H), 5.20 (s, 2H), 2.98 – 2.71 (m, 2H), 2.21 – 2.02 (m, 2H), 1.93 (s, 3H), 1.48 (s, 6H).

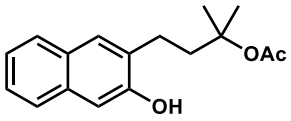

Deprotection of 20. In a 100 mL round bottom flask equipped with large stir bar, **20** (0.091 g, 0.34 mmol) was dissolved in ethanol (15 mL). 10% Pd on carbon (0.059 g) was added, and the solution was sparged with H_2, before purging and backfilling the headspace three times with H_2. The resulting mixture was allowed to stir vigorously overnight (17 h). The mixture was filtered to remove Pd/C, and **2** (75% yield by LCMS, < 0.053 g, < 57%) was isolated from the filtrate by flash chromatography (25% EtOAc/Hexanes) in low purified yields. ^{1}H NMR (600 MHz, Chloroform-*d*) δ 7.74 – 7.63 (m, 2H), 7.59 (s, 1H), 7.49 (d, 2H), 7.43 – 7.34 (m, 3H), 7.34

– 7.27 (m, 2H), 7.16 (s, 1H), 5.18 (s, 2H), 2.90 – 2.74 (m, 2H), 2.15 – 2.04 (m, 2H), 1.91 (s, 3H), 1.46 (s, 6H).

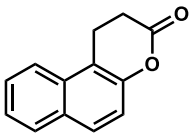

Lactone 22. A solution of 2-Naphthol (1.024 g, 7.1 mmol), acrylic acid (1 mL, 14.6 mmol), and sulfuric acid (1 mL) in a minimal amount of toluene was refluxed for 6 h. Sulfuric acid was neutralized with $NaHCO_{3(aq)}$, and the resulting mixture was extracted with ethyl acetate. The combined organic layers were washed with brine and dried over $MgSO_4$. Lactone **22** (0.890 g, 63% yield) was isolated by flash chromatography (30% EtOAc/Hexanes). IR (cm^{-1}): ν(CO) = 1771 (O-conjugated lactone). ^{1}H NMR (600 MHz, Chloroform-*d*) δ 7.90 (d, *J* = 8.6 Hz, 1 H), 7.86 (d, *J* = 8.3 Hz, 1H), 7.78 (d, *J* = 8.8 Hz, 1H), 7.62 – 7.54 (m, 1H), 7.52 – 7.44 (m, 1H), 7.24 (dd, *J* = 8.8, 1.1 Hz, 1H), 3.38 (t, *J* = 7.5 Hz, 2H), 2.93 (td, *J* = 7.4, 1.2 Hz, 2H).

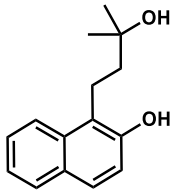

Diol 23. MeMgBr (3 mL, 3 M (Et_2O), 9 mmol) was added slowly to a solution of lactone **22** (0.890 g, 4.5 mmol) in dry THF (30 mL), and the solution was allowed to stir at room temperature overnight. The reaction was quenched with aqueous acid, and the resulting mixture was extracted with ethyl acetate. The combined organic layers were washed with brine and dried over $MgSO_{4(s)}$. Volatiles were removed *in vacuo* to quantitatively give diol **23**. ^{1}H NMR (500 MHz, Chloroform-*d*) δ 7.89 (dq, *J* = 8.6, 0.9 Hz, 1H), 7.78 (ddt, *J* = 8.1, 1.3, 0.6 Hz, 1H), 7.65 (d, *J* = 8.8 Hz, 1H), 7.48 (ddd, *J* = 8.4, 6.8, 1.4 Hz, 1H), 7.33 (ddd, *J* = 8.0, 6.8, 1.1 Hz, 1H), 7.15 (d, *J* = 8.8 Hz, 1H), 3.15 (t, *J* = 7.0 Hz, 2H), 1.93 (t, *J* = 7.0 Hz, 2H), 1.77 (s, 1H), 1.34 (s, 6H).

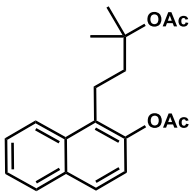

Diacetate 24. Diol **23** (1.06 g, 4.6 mmol) was heated (90-100 ºC) in acetic anhydride overnight. Acetic anhydride was removed *in vacuo*, and the concentrated crude was separated by flash chromatography (23% EtOAc/Hexanes) to give diacetate **24** (0.735 g, 51% yield). ^{1}H NMR (300 MHz, Chloroform-*d*) δ 8.06 – 7.96 (m, 1H), 7.85 (dd, *J* = 8.2, 1.4 Hz, 1H), 7.73 (d, *J* = 8.8 Hz, 1H), 7.55 (ddd, *J* = 8.5, 6.9, 1.5 Hz, 1H), 7.47 (ddd, *J* = 8.1, 6.8, 1.3 Hz, 1H), 7.17 (d, *J* = 8.8 Hz, 1H), 3.09 – 2.95 (m, 2H), 2.40 (s, 3H), 2.07 (d, *J* = 0.4 Hz, 3H), 2.06 – 1.96 (m, 2H), 1.57 (s, 6H).

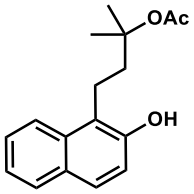

Saponification of 24. To a cooled (0 ºC) THF/MeOH (1:1, 32 mL) solution of diacetate **24** (0.735 g, 2.3 mmol) was added $LiOH_{(aq)}$ (12.5 mL, 1 M). The resulting solution was stirred for 10 min, before quenching with aqueous citric acid. Aqueous workup and flash chromatography (25% EtOAc/Hexanes) afforded **3**, which was recrystallized as needed for further experiments. ^{1}H NMR (600 MHz, Chloroform-*d*) δ 7.89 (d, *J* = 8.5 Hz, 1H), 7.78 (dd, *J* = 8.3, 1.2 Hz, 1H), 7.64 (d, *J* = 8.7 Hz, 1H), 7.55 – 7.44 (m, 1H), 7.38 – 7.29 (m, 1H), 7.11 (d, *J* = 8.7 Hz, 1H), 5.67 – 5.47 (m, 1H), 3.23 – 2.86 (m, 2H), 2.12 (s, 3H), 2.12 – 2.08 (m, 2H), 1.58 (s, 6H).

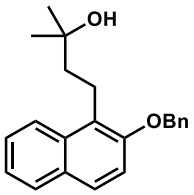

Benzyl ether 26. To a solution of **23** in 50 mL of distilled acetone, was added K_2CO_3 (1.035 g, 7.5 mmol) and benzyl bromide (0.45 mL, 3.8 mmol). The resulting mixture was refluxed for 3 d. Once cooled, the solution was diluted with brine and extracted with ethyl acetate. Flash chromatography (35% EtOAc/Hexanes) gave **26** (0.719 g, 60%). ^{1}H NMR (500 MHz, Chloroform-*d*) δ 7.98 (dq, *J* = 8.6, 0.9 Hz, 1H), 7.79 (ddt, *J* = 8.2, 1.3, 0.6 Hz, 1H), 7.71 (d, *J* = 8.9 Hz, 1H), 7.54 – 7.44 (m, 3H), 7.42 – 7.29 (m, 5H), 5.23 (s, 2H), 3.31 – 3.12 (m, 2H), 1.87 – 1.70 (m, 2H), 1.45 (s, 1H), 1.31 (s, 6H).

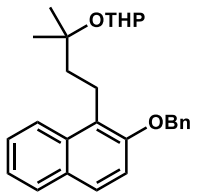

27. A dry methylene chloride (6 mL) solution of benzyl ether **26** (0.4486 g, 1.4 mmol), PPTS (0.07 g, 20%), and dihydropyran (0.16 mL, 1.7 mmol) was stirred for 45 h. The reaction was quenched with $NaHCO_{3(aq)}$, and the resulting mixture was extracted with methylene chloride. The combined organic layers were dried ($MgSO_4$) and concentrated *in vacuo*. Flash chromatography (10% EtOAc/Hexanes) was performed with silica gel washed first with TEA (7% EtOAc/3% TEA/Hexanes) to give **27** (0.467 g, 82% yield). ^{1}H NMR (500 MHz, Chloroform-*d*) δ 8.07 (dd, *J* = 8.6, 1.0 Hz, 1H), 7.82 – 7.74 (m, 1H), 7.69 (d, *J* = 9.0 Hz, 1H), 7.52 – 7.43 (m, 3H), 7.42 – 7.28 (m, 5H), 5.22 (s, 2H), 4.84 (dd, *J* = 5.7, 2.8 Hz, 1H), 4.13 – 3.95 (m, 1H), 3.48 (dt, *J* = 11.3, 5.5 Hz, 1H), 3.29 – 3.15 (m, 2H), 2.00 – 1.83 (m, 1H), 1.83 – 1.75 (m, 2H), 1.71 (ddd, *J* = 15.3, 7.1, 3.5 Hz, 1H), 1.65 – 1.46 (m, 3H), 1.36 (s, 3H), 1.31 (s, 3H).

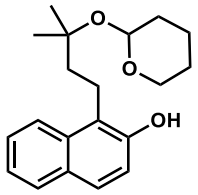

THP cage 28. Benzyl ether **27** (0.467 g, 1.5 mmol) was dissolved in 10 mL EtOAc in a 100 mL round bottom flask equipped with stir bar and 10% Pd on carbon (20% loading). The vessel was purged and backfilled with H_2 three times before stirring under H_2 for 38.5 h. The mixture was filtered to remove catalyst and concentrated to give **28** (80% by LCMS). **28** was purified as needed by HPLC. ^{1}H NMR (600 MHz, Acetonitrile-d_3) δ 7.98 (d, *J* = 8.6 Hz, 1H), 7.77 (d, *J* = 8.1 Hz, 1H), 7.63 (d, *J* = 8.8 Hz, 1H), 7.46 (ddd, *J* = 8.3, 6.7, 1.4 Hz, 1H), 7.35 – 7.24 (m, 2H), 7.11 (d, *J* = 8.8 Hz, 1H), 4.90 (dd, *J* = 6.4, 2.7 Hz, 1H), 4.01 (dt, *J* = 12.2, 4.9 Hz, 1H), 3.53 (ddd, *J* = 11.4, 7.2, 4.3 Hz, 1H), 3.22 – 2.94 (m, 2H), 1.92 – 1.84 (m, 1H), 1.81 – 1.67 (m, 3H), 1.67 – 1.46 (m, 4H), 1.33 (s, 3H), 1.31 (s, 3H).

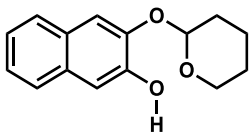

3-((tetrahydro-2H-pyran-2-yl)oxy)naphthalen-2-ol (30). A dry CH_2Cl_2 (10 mL) solution of 2,3-Dihydroxynaphthalene (0.544 g, 3.4 mmol), PPTS (170 mg), and DHP (0.20 mL, 2.2 mmol) was stirred overnight. $NaHCO_{3(aq)}$ was added, and the mixture was extracted with CH_2Cl_2 and dried over $Na_2SO_{4(s)}$. Evaporation of the solvent and flash chromatography gave **30** (0.131 g, 16%). ^{1}H NMR (300 MHz, DMSO-d_6) δ 9.44 (s, 1H), 7.71 – 7.56 (m, 2H), 7.42 (s, 1H), 7.33 – 7.16 (m, 2H), 7.17 (s, 1H), 5.63 – 5.54 (m, 1H), 3.85 (ddd, J = 11.7, 8.8, 3.5 Hz, 1H), 3.65 – 3.52 (m, 1H), 2.11 – 1.95 (m, 1H), 1.84 (ddd, J = 8.8, 5.8, 3.5 Hz, 2H), 1.68 – 1.46 (m, 3H).

5.6 References

1. Arnaut, L. G.; Formosinho, S. J. *J. Photochem. Photobiol. A Chem.* **1993**, *75*, 1
2. Pines, E. UV-visible spectra and photoacidity of phenols, naphthols and pyrenols. In *The Chemistry of Phenols;* Rappoport, Z., Ed.; John Wiley & Sons: Hoboken, NJ, **2003**; p 491-528
3. Tolbert, L. M.; Solntsev, K. M. *Acc. Chem. Res.* **2002**, *35*, 19
4. Hynes, J. T.; Tran-Thi, T.-H.; Granucci, G. *J. Photochem. Photobiol. A Chem.* **2002**, *154*,
5. Wallraff, G. M.; Hinsberg, W. D. *Chem. Rev.* **1999**, *99*, 1801.
6. Solntsev, K. M.; Huppert, D.; Tolbert, L. M.; Agmon, N. *J. Am. Chem. Soc.* **1998**, *120*, 7981-7982
7. Solntsev, K. M.; Huppert, D.; Agmon, N. *J. Phys. Chem. A* **1998**, *102*, 9599-9606
8. Tolbert, L. M.; Haubricht, J. E. *J. Am. Chem. Soc.* **1994**, *116*, 10593-10600
9. Tolbert, L. M.; Haubrich, J. E. *J. Am. Chem. Soc.* **1990**, *112*, 8163
10. Agmon, N.; Rettig, W.; Groth, C. *J. Am. Chem. Soc.* **2002**, *124*, 1089.
11. Ottosson, H. *Nat. Chem.* **2012**, *4*, 969
12. Wan, P.; Shukla, D. *Chem. Rev.* **1993**, *93*, 571-584
13. Pelliccioli, A. P.; Wirz, J. *Photochem. Photobiol. Sci.* **2002**, *1*, 441.
14. Klán, P.; Šolomek, T.; Bochet, C. G.; Blanc, A.; Givens, R.; Rubina, M.; Popik, V.; Kostikov, A.; Wirz, J.; Kla, P. *Chem. Rev.* **2013**, *113*, 119.
15. Agmon, N. *J. Phys. Chem. A* **2005**, *109*, 13.
16. Anslyn, Eric V., and Dennis A. Dougherty *Modern Physical Organic Chemistry*. Sausalito, CA: University Science, 2006
17. Green, T. W.; Wuts, P. G. M. *Protecting Groups in Organic Synthesis*; John Wiley & Sons: New York, 1999; pp 65-67 and 404-408
18. Jung, M. E.; Gervay, J. *J. Am. Chem. Soc.* **1991**, *113*, 224
19. Olegemöller, M.; Mattay, J.; Helmut, G. *J. Phys. Chem. A* **2011**, *115*, 280
20. Madhavan, D.; Pitchumani, K. *J. Photochem. Photobiol. A Chem.* **2002**, *153*, 205
21. Chang, C. W. J.; Moore, R. E.; Scheuer, P. J. *J. Chem. Soc.* **1967**, 840.

22. Posakony, J.; Hirao, M.; Stevens, S.; Simon, J.; Bedalov, A. *J. Med. Chem.* **2004**, *47*, 2635
23. Neugebauer, R. C.; Uchiechowska, U.; Meier, R.; Hruby, H.; Valkov, V.; Verdin, E.; Sippl, W.; Jung, M. *J. Med. Chem.* **2008**, *51*, 1203
24. Kito, T.; Yoshinaga, K.; Yamaye, M.; Mizpbe, H. *J. Org. Chem.* **1991**, *10*, 3336.
25. Coll, G.; Morey, J.; Costa, A.; Saá, J. M. *J. Org. Chem.* **1988**, *53*, 5345
26. Deslongchamps, P.; Dory, Y. L.; Li, S. *Tetrahedron* **2000**, *56*, 3533
27. Himo, F.; Eriksson, L. A.; Margareta, R. A.; Siegbahn, P. E. R. E. M. *Int. J. Quantum Chem.* **2000**, *76*, 714
28. DeCosta, D. P.; Bennett, A.; Pincock, A. L.; Pincock, J.; Stefanova, R. *J. Org. Chem.* **2000**, *65*, 4162
29. Pincock, A. L.; Pincock, J. a; Stefanova, R. *J. Am. Chem. Soc.* **2002**, *124*, 9768
30. Nunes, R. M. D.; Pineiro, M.; Arnaut, L. G. *J. Am. Chem. Soc.* **2009**, *131*, 9456